The interaction of CtIP with DNA damage response proteins.

Iga Agnieszka Abramowicz

A thesis submitted to the

University of Birmingham

for the degree of

DOCTOR OF PHILOSOPHY

School of Cancer Sciences

CRUK Institute for Cancer Studies

The Medical School

University of Birmingham

January 2010

ABSTRACT

In the course of this study it was established that CtIP associates *in vivo* with, and directly binds to, the DNA damage mediator proteins containing BRCT domains: 53BP1, MDC1, TopBP1 and NBS1. The binding sites on all of these proteins have been mapped establishing which regions of CtIP interact directly with 53BP1, MDC1, TopBP1 and NBS1 and *vice versa*. This implies that CtIP is involved in the DNA damage response on many levels interacting with proteins that mediate different aspects of DNA damage sensing and signalling.

CtIP's nuclear localization before and after DNA damage was determined and its co-localization with the other DNA damage responsive proteins examined. It was found that CtIP associates *in vivo* with DNA damage sensor proteins such as the MRN complex (Mre11, Rad50 and NBS1) and RPA70, signal transducer proteins such as the PIKK kinases ATM, ATR and SMG1 and the mediator proteins 53BP1 and MDC1. All of those proteins are involved in detecting and repairing double stranded or single stranded lesions.

Moreover CtIP has a major influence on phosphorylation events induced during repair processes and thus could be an inducer of kinase activity. The deletion of CtIP causes impairment of phosphorylation of important proteins that take part in the DNA damage response pathways such as NBS1, ATM, 53BP1, Chk1 and RPA70. However, impaired phosphorylation only occurs in response to single stranded DNA lesions or the collapse of replication forks. This implies that it is the ATR pathway that is malfunctioning in CtIP depleted cells.

CtIP was previously reported to be phosphorylated on Ser664 and Ser745 by the ATM kinase in response to the DNA double stranded breaks. I have established two possible new phosphorylation sites: Ser506 and Ser555. They could be potentially involved in CtIP's redistribution to the DNA damage sites but this remains to be elucidated.

'I was a normal duck once, but YOU KNOW, those scientists…'

Andrzej Mleczko

'Festina lente!'

Julius Caesar

'Everything should be made as simple as possible, but not one bit simpler.'

Albert Einstein

'For myself I am an optimist - it does not seem to be much use being anything else.'

Sir Winston Churchill

AKNOWLEGMENTS

I would like to thank many people for their help and support with this thesis. I am particularly grateful for the support of both my supervisors, namely, Dr Roger Grand and Dr Andy Turnell. I especially want to thank Roger for being a constant source of biochemical knowledge and for his patience with the use of 'a' and 'the'. Moreover, I appreciate him reminding me that 'you're nearly there'; which was a crucial in the final steps of my write-up.

I would also like to acknowledge my mum and dad for supporting me in the worst and the best moments of my stay in Birmingham. Their patience and persistence were of great help to me in facing what were many hurdles. This has paid off, as I am now completing the acknowledgments for my PhD thesis. My brother and his newly wedded wife also deserve a line in here as being with them always cheers me up.

Marcus has also had a great input in my final year trying to organise and 'formalise' my English; a task he has put much effort in. This work is still in progress. I will also never forget the Specials concert and 'the oyster'; the latter nearly shortening my lifespan.

The former Adeno group will always have a prominent place in my memories connected to the Institute: 'Lairy' Gary and all of his wisdom and reagents for molecular biology as well as Sarah, Natalie, Anoushka and Rakesh for brightening up the days in the lab. I would also like to express gratitude to Rachel for helping me at the beginning of the project and to Phil, without whom I would never clone my last two 53BP1 and MDC1 constructs.

Finally, I would want to thank all the 'good souls' in the Institute for lending and 'acquiring' reagents for me, namely Ania, Ed, Kelly, Grant, Esther, Katerzina, Gouri and others whom were kind enough to 'spare a smudge' for an experiment.

TABLE OF CONTENTS

LIST OF FIGURES

LIST OF TABLES

53BP1	p53 binding protein
9-1-1	Rad9-Hus1-Rad1
APS	ammonium persulfate solution
ATLD	ataxia telangiectasia-like disorder
ATM	ataxia telangiectasia mutated
ATP	adenosine triphosphate
ATR	ataxia telangiectasia and Rad3-related
ATRIP	ART interacting protein
BLM	Bloom's syndrome mutated
BRCA1	breast cancer type 1 susceptibility protein
BRCA2	breast cancer type 2 susceptibility protein
BRCT	BRCA1 C-terminal
BS	Bloom's syndrome
Chk1	checkpoint 1
CPT	camptothecin
CtIP	C-terminal binding protein interacting protein
DAPI	4',6'-diamidino-2-phenylindole
DNA	deoxyribonucletic acid
DNA-PK	DNA protein kinase
DSB	double strand break
DSBR	double strand break repair
dsDNA	double-stranded DNA
E. coli	*Escherichia coli*
EDTA	ethylenediaminetetraacetic acid
FCS	foetal calf serum
G1	cell cycle gap 1
G2	cell cycle gap 2
GST	gluthathione S-transferase
H2AX	histone 2A variant X
γ H2AX	phosphorylated histone 2A variant X
HR	homologous recombination
HU	hydroxyurea
IP	immunoprecipitation

IR	ionising radiation
IPTG	isopropyl β-D-1-thiogalactopyranoside
Kb	kilobase
kDa	kilodalton
LB	Luria broth
LCL	lymphoblastoid cell line
M	mitosis
MDC1	mediator of DNA damage checkpoint 1
NMD	nonsense mediated mRNA decay
MMEJ	microhomology-mediated end-joining
Mre11	meiotic recombination 11
MRN	Mre11-Rad50-NBS1 complex
MSI	microsatellite instability
NBS1	Nijmegen breakage syndrome 1
NHEJ	non-homologous end-joining
NLS	nuclear localisation signal
PIKK	phosphoinositide 3-kinase (PI3K)-related kinase
Rad50	DNA repair protein Rad50
Rb	retinoblastoma
RPA	replication protein A
S	cell cycle DNA synthesis phase
SCE	Sister Chromatid Exchange
SDS	sodium dodecyl sulphate
SDS-PAGE	sodium dodecyl sulphate-polyacrylamide gel electrophoresis
SMC1	structural maintenance of chromosomes 1, *Homo sapiens* (cohesin complex subunit SMC1, *Drosophila melanogaster*)
SMG1	suppressor with morfogenetic effect on genitalia 1
SS	Seckel syndrome
SSB	single stranded break
ssDNA	single- stranded DNA
TBE	Tris, boric acid and EDTA

TEMED	(N,N,N',N'-tetramethyl-ethylenediamine)
TopBP1	topoisomerase IIβ binding protein 1
UV	ultra-violet light

CHAPTER I

INTRODUCTION

1.1. The concept of cancer: a historical perspective.

Cancer is a Latin word meaning a crab, an invertebrate classified in the *Cancridae* family; with the Greek translation *καρκινος /karkinos/.* The term was first used by Hippocrates (460 b.c.–370 b.c.) to describe hard tumours and was proposed by a Persian doctor, Ibn Sina aka Avicenna (980–1037), to describe features of mammary carcinoma. A picture of a crab published by the French surgeon Ambroise Paré (1516–1590) in his works has become the symbol of Oncology.

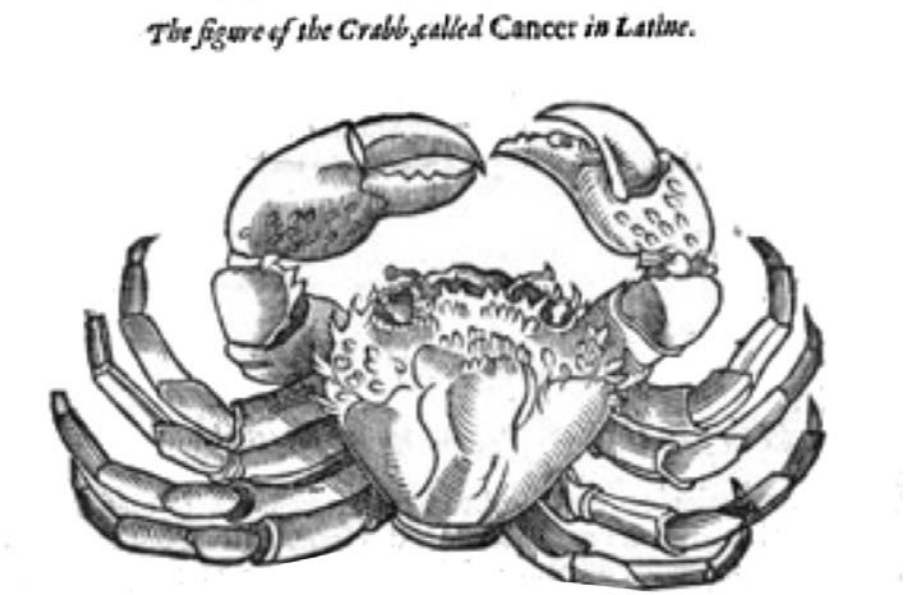

Figure.1.1. Picture of a crab from Ambroise Paré works, that has become the symbol of Oncology.

A new concept of cancer as a disease was proposed in 1865 by a German surgeon Karl Thiersch (1822–1895). While working with a German pathologist Heinrichem Wilhelmem von Waldeyer-Hartzem (1836–1921) he established that the solid tumour consists of two parts: a malignant part which originates from epithelium and the non-malignant part that originates from connective tissue. The concept of an *incipient carcinoma (carcinoma incipiens)* was established in 1910 by an American pathologist J. C. Rubin who used as an example tissue derived from cervical carcinoma. A modern definition of preinvasive carcinoma (*carcinoma praeinvasivum*) was established in 1928

by an Austrian-American gynecologist Walter Schiller (1887-1960) as an atypical growth without invasion through epithelial basement membrane, using squamous cervical carcinoma as an example. The American pathologist Albert Compton-Broders (1885–1964), in 1932, used the term '*carcinoma in situ'* to describe skin cancers and it became the most widely used term in medical publications. It is also known by the acronym SIL. However in the TNM Classification of Malignant Tumours (TNM) devised by Pierre Denoix between 1943 and 1952, using the size and extension of the primary tumour, its lymphatic involvement and the presence of metastases to classify the progression of cancer, it is described as *"pTis"*. The TNM was further developed by the International Union Against Cancer (UICC) to achieve a consensus in describing the extent of the tumour spread.

Cancer is a genetic disease which is characterized by unrestrained proliferation of a body's own cells. In normal circumstances cell division is a strictly controlled process that is governed by homeostasis of multiple signalling pathways. Simplistically, in the instance of network failure the cell escapes its normal growth and proliferation control and becomes cancerous.

The multi-stage theory of cancer development and progression was first developed by Armitage & Doll in 1954 (Armitage & Doll, 1954). Over the years it has been established that cancer is a disease that involves dynamic changes in the genome. A key finding was the recognition of tumour suppressor genes, with recessive loss of function phenotype, and dominant gain of function by mutations in genes described as oncogenes (Weinberg, 2006). Proteins involved in the DNA damage response are classed as tumour supressors, as the loss of function gives rise to cancerous growth such as in the case of the BRCA1 gene in breast cancer (Fearon, 1999). The current view considers cancer as a consequence of multiple genetic alterations that accumulate before the actual disease arises.

The process of changing from normal growth into an oncogenic one involves a number of cellular changes. The physiology of the cell has to change and the series of events have been divided into six groups: self-sufficiency in growth signals, insensitivity to antigrowth signals, bypassing apoptosis, unlimited proliferation potential, sustained angiogenesis, and tissue invasion leading to metastasis (Figure.1.2.; Hanahan & Weinberg, 2000). The set of changes described above can occur in all tumours cells although not all the cells have to undergo all of those changes to become carcinogenic. Most tumour tissues are heterogenous in nature such that the individual cells of the tumour may have slightly different genotypes due to constant mutations in a rapidly proliferating population (Heppner, 1984). From this observation a 'cancer stem cell' model has been derived whereby a 'cancer stem cell' possesses an ability to proliferate indefinitely. As cancer stem cells and tissue-specific stem cells share common properties such as the capability to self-renew and differentiate, it has been hypothesised that cancers are caused by mutations that have occurred in tissue-specific stem cells (Li et al., 2007; Pohl et al., 2008; Reya et al., 2001). This gives rise to a population of cells with an ability to metastasise and perform angiogenesis, and each generation may possess different genetic qualities (Martinez-Climent , Andreu & Prosper, 2006; Pathak, 2002).

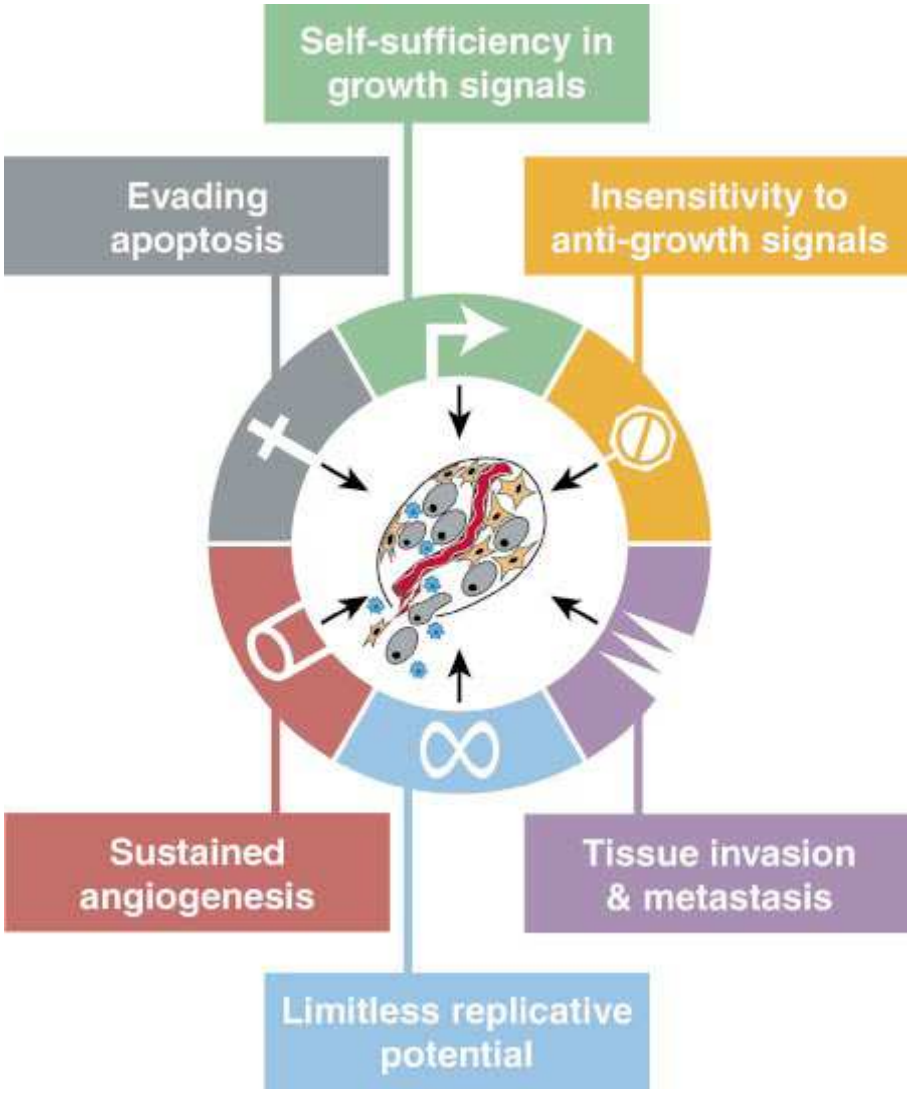

Figure.1.2. The six changes in cell's physiology that occur in the process of becoming cancerogenic. The set of changes depicted above can occur in all tumours cells; however not all the cells have to undergo all of these changes to become carcinogenic. (adapted from Hanahan & Weinberg, 2000).

1.2. Genetic disorders involving mutations in proteins taking part in the DNA damage response.

Cancer-prone genetic disorders in DNA damage response pathways mainly involve proteins that take part in homologous recombination (HR) such as ATM - Ataxia telangiectasia (A-T; Shiloh, 1997), NBS1 - Nijmegen breakage syndrome (NBS; Shiloh, 1997) and BLM – Bloom syndrome (BS; German, 1993). Other proteins involved in HR are connected with tumour suppression like BRCA1 or BRCA2 (Venkitaraman, 2002). Seckel's syndrome patients carry a mutation in the ATR gene (Faivre et al., 2002), the product of which is involved in DNA single stranded break (SSB) repair. Ataxia telangiectasia-like disorder (ATLD; Taylor et al., 2004) patients carry a mutation in the Mre11 gene again involved in HR and DNA damage response. In this section I will consider some of those disorders in slightly more detail.

1.2.1. Ataxia telangiectasia (A-T).

Ataxia telangiectasia (A-T) was first described over 80 years ago by Syllaba & Henner (1926). It falls into the category of autosomal recessive cerebellar ataxias and 50 years ago was recognized as a clinical entity (Boder & Sedgwick, 1957). Most ATM mutations are unique to single families and founder effects are mostly observed in populations of Russians, Poles, Norwegians, Turks, Moroccan Jews and Costa Ricans (Lavin, 2008). A-T patients first show symptoms at the age of 2 years. The disease manifests with ataxia of upper and lower limbs and by puberty most patients require a wheelchair for mobility. It is also characterised by eye mobility and speech impairment. Patients show increased sensitivity to ionizing irradiation and immunodeficiency. In A-T syndrome thymic hypoplastia is also recognized as well as telangiectasia of different body parts especially bulbar conjunctiva, growth retardation and high serum alfa-fetoprotein (AFP) concentrations. Around 15% of UK A-T patients die of leukemia or lymphoma in infancy (Taylor & Byrd, 2005).

Gatti et al. (1988) mapped the position of *ATM* (ataxia telangiectasia-mutated) gene to chromosome 11q22–23 and in 1995 the *ATM* gene was sequenced (Savitsky et al., 1995a & 1995b). It has been reported to stretch for 160kb, to contain 66 exons and to be transcribed to give a 13kb mRNA (Uziel et al., 1996). The ATM protein is 350K and consists of 3056 amino acids (Figure.1.3.). In humans over 400 mutations have been reported and most patients are heterozygotes, inheriting different mutations from each parent. Null alleles predominate with around 85% of all mutations affecting splicing or creating nonsense mutations that cause premature termination of translation. The mutations are distributed over the whole gene and none of them appears with more than 3% frequency (Figure.1.3., Chun & Gatti 2004).

ATM protein is predominantly nuclear but variable amounts of around 10-20% have been found in the cytoplasm (Lim et al., 1998; Watters et al., 1999). ATM's major role in the nucleus is in DNA damage sensing and repair (Canman et al., 1998). Cytoplasmic ATM is localized in the peroxisomes, cellular organelles that contain enzymes for oxidative reactions of very-long-chain fatty acids (β-oxidation) and enzymes that neutralize toxic peroxides (Watters et al., 1999).

ATM is also present in the endosomes which perform endocytosis and intracellular routing of receptors and other molecules (Lim, 1998; Watters, 1999). ATM also exists in a soluble state in the cytoplasm, where it is suggested to phosphorylate 4E-BP1 protein in a process that is insulin dependent (Yang & Kastan, 2000).

ATM is a protein serine/threonine kinase that is a member of the PIKK kinase family

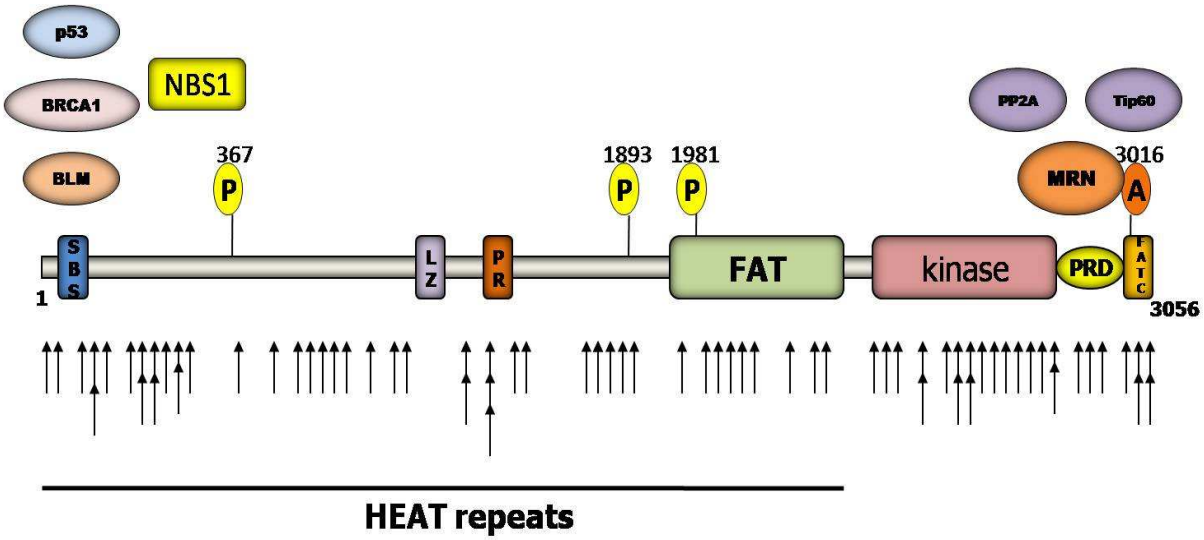

Figure.1.3. The ATM protein and the distribution of patients' mutations along the protein. Distribution of ATM domains, autophosphorylation sites (P) and adenylation site (A). SBS-substrate binding site; LZ-leucine zipper; PR-proline rich motif; FAT-FRAP, ATM, TRRAP; kinase-PI3K-related kinase domain; PRD-PIKK regulatory domain; FATC-FAT C-terminus. The arrows indicate some of the mutations described in A-T patients and their overall distribution along the whole of the protein. HEAT (**H**untingtin, **E**longation factor 3, **A** subunit of protein phosphatase 2A and **T**OR1)-repeats. Most important ATM interacting proteins are depicted at the sites where they bind to ATM.

(phosphoinositide 3-kinase (PI3K) – related kinase) and phosphorylates its substrates at a SQ/TQ consensus site. A greater degree of specificity has been suggested with ATM preferentially phosphorylating LS/TQE motifs (O'Neill et al., 2000). The presence of adjacent positively charged residues inhibits phosphorylation (Kim et al., 1999).

The members of the PIKK family include: ATR (ATM and Rad3-related), DNA-PKcs (DNA-dependent protein kinase catalytic subunit), SMG1 (suppressor with morfogenetic effect on genitalia 1, also referred to as ATX), mTOR (mammalian target of rapamycin) and TRRAP (transformation/transcription domain-associated protein) which does not possess kinase activity (Abraham, 2004). As shown in Figure.1.3. the N-terminal region of ATM contains an SBS (substrate binding site), between amino acids 82 and 89 which was identified as the binding site for the BLM protein (Beamish et al., 2002) and amino acid residues 91-97 which has been shown to be responsible for interactions with BRCA1 and p53 (Gatei et al., 2000; Khanna et al., 1998; Fernandes et al, 2005). Deletion of this region disables ATM's p53 activation in response to bleomycin (Turrene et al., 2001). The N-terminal region of Tel1/ATM has also been reported to be involved in the interaction with Xrs2/NBS1 in *S. pombe.* (You et al. 2005). The N-terminal and middle regions of ATM consist of HEAT (**H**untingtin, **E**longation factor 3, **A** subunit of protein phosphatase 2A and **T**OR1) repeats, which, as a single unit, are a pair of interacting anti-parallel α-helices linked by a flexible "intra-unit" loop. They account for 63% of the non-kinase-domain residues. The leucine zipper and the proline rich motifs are also located in the middle region of the protein. The kinase domain is located in the C-terminal region and is flanked by FAT (FRAP, ATM, TRRAP) and FATC (FAT C-terminus) domains which are conserved among the PIKK family members. The kinase domain accounts for only 5-10% of the protein sequence (Perry & Kleckner, 2003). The FATC domain is a small domain consisting of ~35 aa and is necessary for the kinase activity although the precise function of FAT

domain remains to be elucidated. However, as FAT and FATC domains flank the kinase domain, it has been suggested that they may be important as structural scaffolds or as protein-protein binding motifs (Bosotti et al, 2000; Lovejoy et al., 2009). The C-terminus of the ATM kinase also contains the PRD region (PIKK regulatory domain) which is responsible for interaction with activating proteins which in the case of ATM is the MRN complex (Mre11-Rad50-NBS1; Lee & Paull, 2005). ATM possesses an acetylation site, K3016, for Tip60 acetylase and mutations that prevent acetylation abrogate ATM's activation (Sun et al., 2007). After DSBs ATM, from an inactive dimer, dissociates into monomers and during activation it also undergoes autophosphorylation on S1981 (Bakkenist & Kastan, 2003) and S367 together with S1893 (Kozlov et al, 2006). ATM's activation is also orchestrated by its interacting proteins PP5 (protein serine–threonine phosphatase 5; Ali et al, 2004) and PP2A (protein phosphatase 2A; Goodarzi et al., 2004).

As ATM is a protein kinase its activation after DSB DNA damage leads to a phosphorylation casacade. Its downstream targets include p53 (Banin et al., 1998; Canman et al., 1998), BRCA1 (Cortez et al., 1999), NBS1 (Lim et al., 2000; Zhao et al., 2000), Chk2 (Blasina et al., 1999a & 1999b; Matsuoka et al., 2000), SMC1 (Yazdi et al., 2002; Kim et al., 2002), BLM (Beamish et al., 2002), FANCD2 (Taniguchi et al., 2002), Pin2/TRF1 (Kishi et al., 2001), CtIP (Li et al., 2000) and many more, as shown in Figure.1.4. The variety of ATM targets indicates that it is involved in initiating many cellular processes after DNA double strand breaks, most of which lead to the cell cycle check-point response and DNA repair. Over 700 possible ATM and ATR targets have been identified, which form an extensively developed network of response to the DNA damage (Matsuoka et al., 2007).

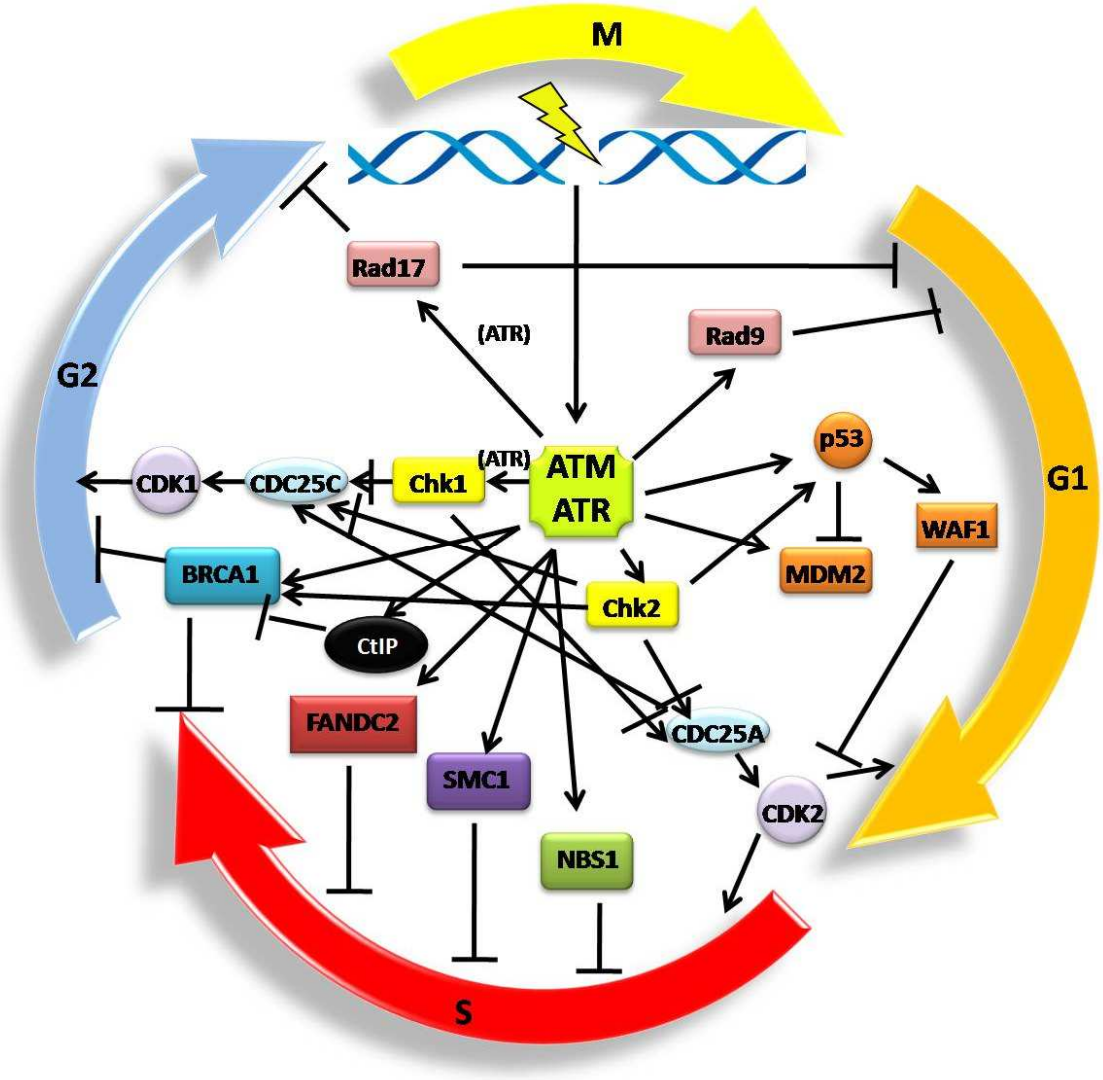

Figure.1.4. ATM/ATR mediated response to DSBs. This cartoon illustrates the variety of ATM/ATR phosphorylation targets during the cell cycle after DNA damage. It also illustrates the checkpoint responses initiated by ATM/ATR kinases. Arrows indicate stimulation, blunt T-ends indicate inhibition (adapted from Shiloh, 2003).

1.2.2. Nijmegen breakage syndrome (NBS).

Nijmegen breakage syndrome is a rare autosomal recessive genetic disease that is classified as a chromosome instability syndrome. It was first described in two young Dutch patients by Weemaes C. M. et al., 1981. However, the majority of patients are of Polish or Czech origin (Digweed & Sperling, 2004). NBS patients have prominent midface, receding foreheads and receding mandibles followed by long noses, large ears and freckles on the nose and cheeks. Not all patients are microcephalic at birth but the condition increases with age and by a few months all suffer from severe microcephaly. The facial features are described as 'bird-like', the body build is retarded and the patients show mild to moderate mental deficiency. The chromosome structural rearrangements preferentially involve chromosome 7 and 14. The patients have serious cellular and humoral immune system defects and most of them suffer from reccurring infections of the respiratory tract (Chrzanowska et al., 1995). Chromosome instability and immunodeficiency possibly predispose the patients to malignancies and there is a tendency to develop lymphomas at a young age and, in a few cases, other types of cancer. Radiotherapy is not suitable for NBS patients as they show increased sensitivity to γ-irradiation (van der Burgt et al., 1996). Initially NBS patients were treated as a subclass of A-T patients until 1998, when the gene mutated in this disease was recognized and cloned (Varon et al., 1998; Carney et al., 1998; Matsuura et al.,1998).

Over 90% of all NBS patients share a homozygous truncating mutation of 5bp, referred to as 657del5 in the 6th exon (Varon et al., 1998) and the remainder were found to have one of seven other mutations (Figure.1.5.). These are much rarer and occur between 657 and 1142 nucleotides and cause, as well as the 657del5 mutation, truncation of the protein after the first BRCT domain. The N-terminal 26K fragment of NBS1 is present in the patients with the 657del5 mutation, as well as the 70K protein, which is produced, by alternative initiation of translation, from a new start codon

located upstream from the deletion. However this polypeptide appears at much lower concentrations and only in EBV-transformed lymphoblastoid cells (Maser et al., 2001). The appearance of NBS1 mutated protein may be necessary to rescue otherwise lethal phenotype. It has been shown, that knock-out mice die early in embryonic development, and heterozygous knock-out mice develop a range of tumours, resembling the NBS phenotype. Thus it has been suggested that the presence of truncated NBS1 species partially rescues the phenotype, thus preserving the viability of the patient (Figure.1.5.; Dumon-Jones et al., 2003; Zhu et al., 2001).

NBS1, that encodes the Nibrin or p95 protein, is a 50kb gene containing 16 exons and was mapped to the chromosome 8q21–24 (Carney et al., 1998; Matsuura et al., 1998; Varon et al., 1998). The 95K protein consists of 754 residues. The N-terminal region contains an FHA (fork-head associated) domain stretching from 24–108 aa (Durocher & Jackson, 2002) followed by a tandem repeat of the BRCT (BRCA1 C-terminal) domains, 108–196 aa and 221-330 aa (Bork et al., 1997; Becker et al., 2006).

It has been shown that the FHA/BRCT domain is involved in binding to the phosphorylated form of H2AX (γ-H2AX) and is responsible for localizing the MRN complex in close proximity to the double stranded lesion (Kobayashi et al., 2002; Lee et al., 2003; Paull & Gellert, 1999). However the N-terminal region of NBS1 is dispensable in ATM signalling cascade but instead is needed in the ATR response to DNA damage (Stiff et al., 2008). The middle region contains three ATM phosphorylation sites: S278, S343 and S397 and serves in DNA damage signalling as a signal transducer in S phase cell cycle check point (Lim et al., 2000; Wu et al., 2000b; Zhao et al., 2000). The C-terminal region incorporates an Mre11 binding site (Desai-Mehta et al., 2001) and an ATM binding region, that is conserved throughout proteins

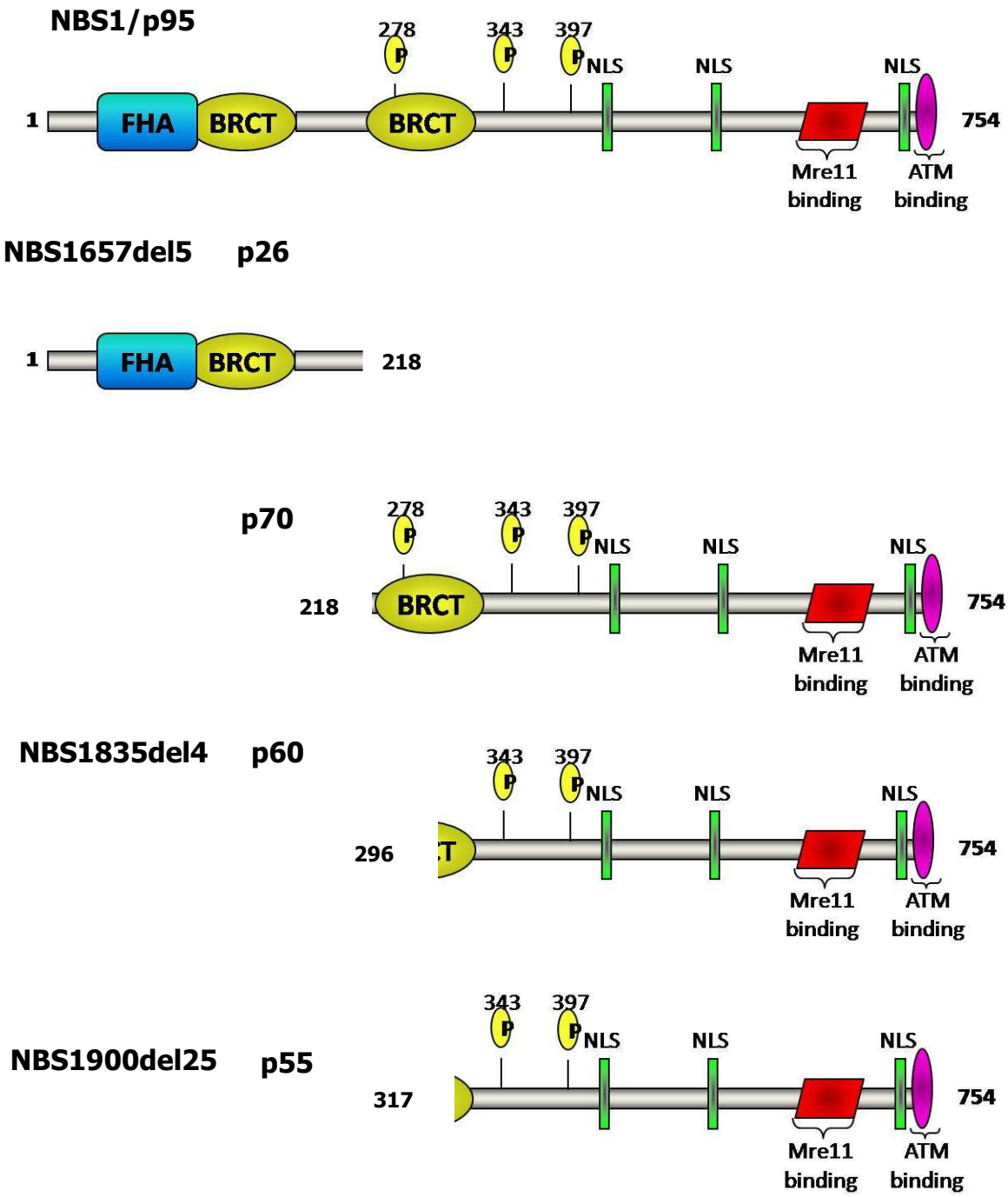

Figure.1.5. The NBS1 protein with known domains and ATM phosphorylation sites. In the lower part of the figure mutated NBS1 proteins are shown detected in NBS1 patients derived cell lines with the mutation depicted and possible domain structure.

that bind PIKK kinases, including NBS1, ATRIP and Ku70/80 (Falk et al., 2005).

NBS1 takes part in cell cycle checkpoint control (Ito et al., 1999; Shiloh, 1997) and control of telomere length (Ranganathan et al., 2001) such that patients suffering from Nijmegen breakage syndrome have decreased homologous recombination efficiency (Tauchi et al., 2002). These features indicate that NBS1 is an important guardian of genome stability. When associated with Mre11 and Rad50 in the MRN complex (Figure.1.6.) it regulates the nuclear localization, signal transduction ability and the catalytic activation of the complex (Mirzoeva & Petrini, 2001; Desai-Mehta, et al., 2001). In individuals with NBS disorder with the 657del5 mutation the p70 protein is localized to the nucleus and is associated with around 50% of the Mre11 protein pool present, which would suggest that the p70 protein facilitates the retention of Mre11 in the nucleus (Maser et al., 2001).

During DSB repair the NBS1 subunit of the MRN complex is responsible for direct interactions with other proteins that take part in DSB processing such as ATM, γ-H2AX, MDC1, BRCA1, SMC1, WRN, Chk2 and FANCD2 (Cheng et al., 2004;Falk et al., 2005; Girard et al., 2002; Lane, 2004; Lukas et al., 2004; Nakanishi et al., 2002; Yazdi et al., 2002).

The MRN complex is relocalized to sites of DNA damage within minutes of its occurrence and is recognized as the first sensor in the DNA damage response (Figure.1.13; Williams et al., 2007). Mre11 possesses a nuclease activity, Rad50 is an ATPase and NBS1 is responsible for protein-protein interactions. Mre11 gene is mutated in ATLD disorder and will be described later in this chapter. The subunit Rad50 is a large coiled-coil ATP-binding cassette (ABC) and possesses DNA binding activity. Originally, a hypomorphic mutation in Rad50 was recognized in yeast (Alani et al., 1990) but later it was found to cause cancer susceptibility and embryonic lethality in mice (Bender et al., 2002). Recently a patient with an NBS-like disorder has been

reported (Waltes et al., 2009). She was found to be a compound heterozygote for the mutations in the Rad50 gene. This mutation is characterized by low and unstable levels of Rad50 protein. The cells derived from the patient are radiosensitive, fail to form DNA-damage induced MRN foci, are defective in ATM signaling and show chromosomal instability. The facial features of the patient resemble of those of NBS syndrome, thus the disorder was described as NBSLD – NBS-like disorder (Waltes et al., 2009). Rad50 belongs to the family of proteins classed as the structural maintenance of chromosome (SMC) family. Those proteins act in sister-chromatid cohesion and chromosome condensation (Hopfner & Tainer, 2003). The N- and C-terminal regions of Rad50 contain a Walker motif (A and B respectively; Figure.1.6.a) which resembles motifs found in the ATP-binding cassette (ABC) of proteins classed in the transporter family. These motifs are required for Rad50 and Mre11 binding (Williams et al., 2007). The middle region of Rad50 contains a zinc hook motif (CXXC) which is connected with the Walker motifs by the coiled-coil regions (Hopfner & Tainer, 2003). The zinc hook motif serves in Rad50's inter- and intra-molecular interactions which gives the MRN complex its flexibility needed for its efficient functioning (Hopfner et al., 2002).

Mre11 and Rad50 are conserved proteins through evolution (Aravind et al., 1999; Blinov et al., 1989; Gorbalenya & Koonin, 1990) and form an ATP-stimulated 3'-5'-exonuclease which can process most types of DNA ends and hairpins. The conservation of the Mre11/Rad50 subunit suggests that they were the primary DNA damage sensing proteins and NBS1, as it is only found in eukaryotes, has joined the complex later during the evolution (D'Amours & Jackson, 2002). The MRN complex seems to have a bipolar structure consisting of a globular head and two tails (Figure.1.6b; Anderson et al., 2001; de Jager et al, 2001). The head is formed of one NBS1, two Rad50 ABC ATPase domains and two Mre11 molecules and has an ATP-stimulated nuclease

a)

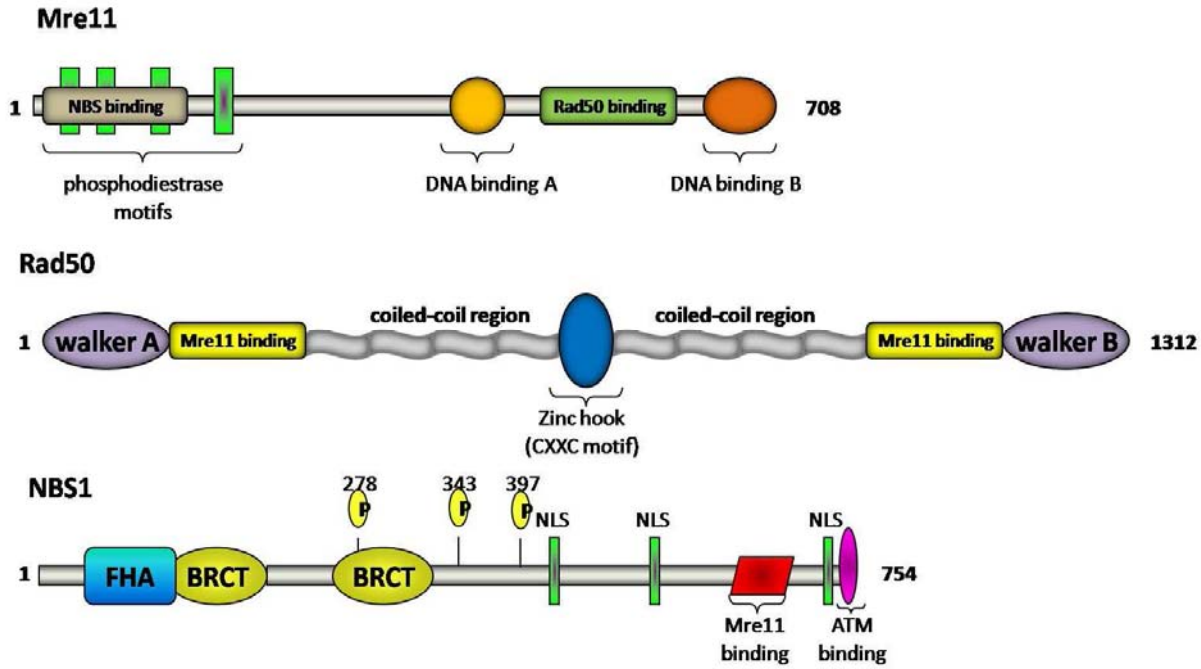

b)

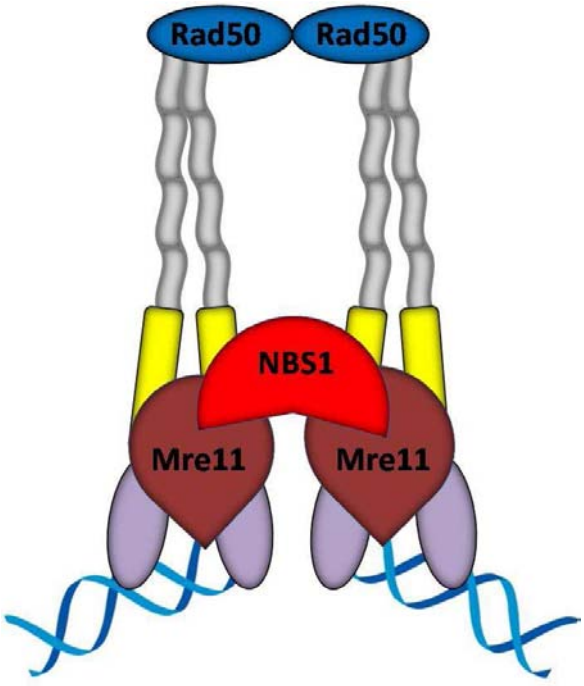

Figure.1.6. The MRN complex. a) The members of the MRN complex with positioning of known domains and phosphorylation sites. NLS-nuclear localizing signal. **b)** The MRN complex associated with broken DNA ends.

activity. The tails consist of 60 nm long antiparallel coiled-coils of the Rad50 ATPase and at their apex a zinc-hook is found that serves as a bridging device for Rad50-Rad50 interaction (Hopfner et al., 2002). Mre11 possesses binding sites for both NBS1 and Rad50 and all of the components have DNA binding ability (Arthur et al., 2004; de Jager et al., 2001; Trujillo et al., 2003). As a biochemical entity the MRN complex is a nuclease stimulated by ATP that acts exonucleolytically and endonucleolytically on hairpins and ssDNA and possesses exonuclear activity for a variety of dsDNA ends (Arthur et al., 2004; Connelly et al., 1997; Hopfner et al., 2000a&b; Paull & Gellert, 1998; Trujillo et al., 1998). The MRN complex, together with CtIP, plays a major role in homologous recombination by resectioning the DNA ends at DSBs prior to rejoining (see section 1.4.2.1; Sartori et al., 2007).

1.2.3. Ataxia telangiectasia-like disorder (ATLD).

ATLD is a genetic disorder involving mutation in the Mre11 gene. Up to now there have only been 16 cases reported, involving four patients from UK, two from Italy and ten from Saudi Arabia. Patients show normal eye movement that progresses over time into saccadic movement but no head thrusts were observed, unlike in A-T patients. One patient showed strabismus at distance. Patients also have their eye convergency affected but do not show any telangiectasia (Khan et al., 2008). They are, like A-T patients, hypersensitive to ionizing radiation and have chromosome 7/14 translocations. Their level of serum alfa-fetoprotein (AFP) is normal as are the total levels of IgG, IgA and IgM. Patients also show immunodeficiency but predisposition to cancer has not been reported (Taylor et al.,2004).

The *Mre11* gene consists of 20 exons and its total size has been determined to be ~75kb. Two of the British patients and both Italian patients were found to have a the same nonsense mutation in exon 15, whilst the other two British patients, who were sibs, had a nonsense mutation in exon 17. Both nonsense mutations would have been

expected to cause premature termination of translation and truncation of any Mre11 protein produced. However, truncated Mre11 protein was only evident in the individuals with the nonsense mutation in exon 17. The mutation in exon 15 causes the transcript to be degraded by NMD (nonsense mediated mRNA decay) thus the truncated protein is not detectable in those individuals. However those patients are heterozygous thus the other allele, which harbours a missense mutation (117N>S) still produces full length Mre11 mutated protein. Whereas the mutation in exon 17 causes the appearance of a truncated species detectable as a ~70k protein band on a Western blot (Pitts et al., 2001). Ten patients from Saudi Arabia all harbour the same mutation in exon 7. It leads to a change of a highly conserved tryptophan residue at position 210 to cysteine which possibly causes conformational changes within the protein - thus affecting its function and causing the ATLD disorder (Fernet et al., 2005). The level of expression of Mre11 in ATLD patients is lower than in healthy individuals and varies depending on genotype. However, more intriguing is the fact that the level of NBS1 and Rad50 protein expression is much lower in comparison to healthy individuals. The affinity of Mre11 for NBS1 and Rad50 in ATLD patients depends on the type of mutation. Proteins in individuals with mutation in exon 15 or 17 both interact with NBS1 to the same degree. However the interaction with Rad50 varies, being stronger in patients with mutation in exon 17 than in patients with mutation in exon 15 (Taylor et al., 2004).

The Mre11 protein is essential for cell survival and knock-out mice are not viable (Luo et al., 1999; Xiao & Weaver, 1997). It is of ~80K molecular weight and the N-terminal region contains four phosphodiestrase motifs and a binding site for the C-terminal region of NBS1. The N-terminal region is also necessary for nuclear localization of the Mre11 protein. The middle and C-terminal region contains a DNA binding motif, and a Rad50 binding site is located between them (Figure.1.6.a; Rupnik et al., 2008).

The phosphodiesterase motif possesses 3'-5' exonuclease activity which significantly increases when it forms the complex with NBS1 and Rad50 (D'Amours & Jackson, 2002; Trujillo et al., 1998). Mre11 also has endonuclease activity that processes ssDNA and dsDNA (Paull & Gellert, 1999).

The MRN complex (Figure.1.6.b) has been reported to rapidly relocalize to the sites of DSBs (Figure.1.13.b; Nelms et al., 1998). Three types of foci have been reported for the MRN complex. Type I is recognized in untreated cells and colocalizes with PML bodies (Lombard & Guarente, 2000; Mirzoeva & Petrini, 2001; Wu et al., 2000b). In cells treated with DNA damage inducing agents within 10 mins and up to 8h post induction numerous small foci are seen, which are classed as Type II. Type III foci last from 4h up to 24h post irradiation and are described as IRIF (irradiation induced foci, Bekker-Jensen et al., 2006) which are large, irregular concentrations of proteins. Cell lines derived from patients with NBS and ATLD disorders are unable to form Type III foci (Carney et al., 1998; Stewart et al., 1999). Recent reports describe the MRN complex as the first sensor of DNA damage. The MRN complex's first function is to tether the broken DNA ends and recruit ATM to initiate the ATM signalling cascade. The Mre11 subunit binds to the free DNA ends. Rad50, which is associated with it in the MRN complex, binds another Rad50 molecule, on the opposing end of the break, forming a clamp which holds the two strands in close proximity for DNA repair to proceed (Figure.1.6.b; Bhaskara et al., 2007). The MRN complex partially unwinds the DNA to make it accessible for the exo- and endonucleotityc activity of Mre11 which resects the 3' DNA ends. This process as mentioned before requires CtIP which promotes Mre11 nucleolytic activity (see section 1.4.2.1; Sartori et al., 2007).

1.2.4. Seckel syndrome (SS).

The Seckel syndrome is a recessive autosomal disorder whose main characteristics comprise developmental delay and apparent microcephaly. Features that are used for clinical diagnosis include severe pre-birth growth retardation with low birth weight, pronounced proportionate short stature, marked microcephaly, mental retardation and 'bird-like' facial features with receding forehead and prominent nose. Five patients from two separate consanguineous Pakistani families are all homozygous for the same allele which maps to chromosome 3q22.1-3q24 (SCKL1) in which region the *ATR (ATM and Rad3-related)* gene is located (Faivre et al., 2002; Goodship et al., 2000; O'Driscoll et al., 2003). In 2001 Borglum et al. reported four more patients with Seckel syndrome from a consanguineous Iraqi family but the mutation was mapped to chromosome 18p11.31-q11.2 (SCKL2). A third locus was mapped by Kilinç et al. to chromosome 14q23 in 13 Turkish families which were, apart from one, consanguineous. Few patients showed linkage to either the SCKL1 or SCKL2 locus (Kilinç et al., 2003). This and previous reports suggest that Seckel syndrome is very heterogenous in genetic and clinical backgrounds. From over 60 reported cases since 1960 only a third fulfil the characteristics set by Seckel (Borglum et al., 2001; Majewski & Goecke, 1982; Seckel, 1960). However Seckel and Seckel-like syndromes are linked to genes involved in DNA repair.

Genes for two Seckel-like disorders, NBS and LIG4 (mutation in DNA ligase IV gene; O'Driscoll et al., 2001) as well as the only gene linked to Seckel syndrome – ATR are involved in DNA damage repair (Kilinç et al., 2003; O'Driscoll et al., 2003). A cell line derived from a Seckel syndrome patient with SCKL1 locus is not radiosensitive. It also shows impairment in phosphorylation of ATR targets following exposure to UV irradiation and a standard response to ionizing irradiation carried out by ATM kinase. Sequence analysis revealed that a mutation in exon 9 of *ATR* gene, which is a

synonymous one, impairs the gene's splicing. At the protein level there is a large decrease of expression of the ATR kinase. Analysis of cell lines derived from other Seckel patients showed, in each case, an impairment of the ATR kinase pathway although the defective gene was not always ATR (O'Driscoll et al., 2004).

The *ATR* gene has 47 exons and is around 129kb long and located on chromosome 3q22-q24. Experiments with knock-out mice showed that ATR is necessary for their viability as they die in the pre-gastrulation stage of embryonic development and heterozygous mice are prone to benign tumours (de Klein et al., 2000). Thus ATR plays a major role in prevention of DNA damage in early embryonic stages of development (Brown & Baltimore, 2000).

The ATR protein belongs to the same family of protein kinases as ATM – PIKK kinases. The N-terminal region of ATR contains an ATRIP (ATR-interacting protein; Figure.1.7.) binding site, the middle region contains HEAT repeats and the C-terminal region contains FAT, kinase, PRD and FATC domains which were described previously. The FATC domain, in the case of ATR, is essential for even basal ATR kinase activity. Activation of ATR following the DNA damage response requires recruitment of ATRIP and 9-1-1 complex to the site of lesion. ATRIP brings associated ATR with it and Rad9 from the 9-1-1 complex brings TopBP1 (Melo et al., 2001; Zou et al., 2002). TopBP1 in turn binds to the PDR of ATR and to the middle region of ATRIP stimulating the kinase activity of the complex (Figure.1.7; Kumagai et al., 2006; Mordes et al., 2008). ATR as a protein kinase phosphorylates its targets at PIKK kinase consensus sites: SQ/TQ. Main targets of ATR in response to SSBs are Chk1 (Liu et al., 2000), p53 (Tibbetts et al., 1999) and RPA32 (Block et al., 2004; Liu et al., 2006).

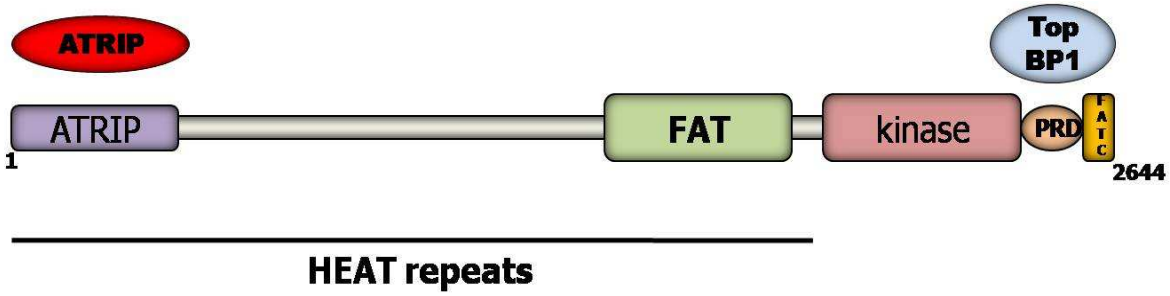

Figure1.7. The ATR protein. Distribution of ATR domains: ATRIP-ATRIP interacting motif; FAT-FRAP, ATM, TRRAP; kinase-PI3K-related kinase domain; PRD-PIKK regulatory domain; FATC-FAT C-terminus. HEAT (Huntingtin, Elongation factor 3, A subunit of protein phosphatase 2A and TOR1)-repeats. Sites of ATRIP and TopBP1 interaction are depicted.

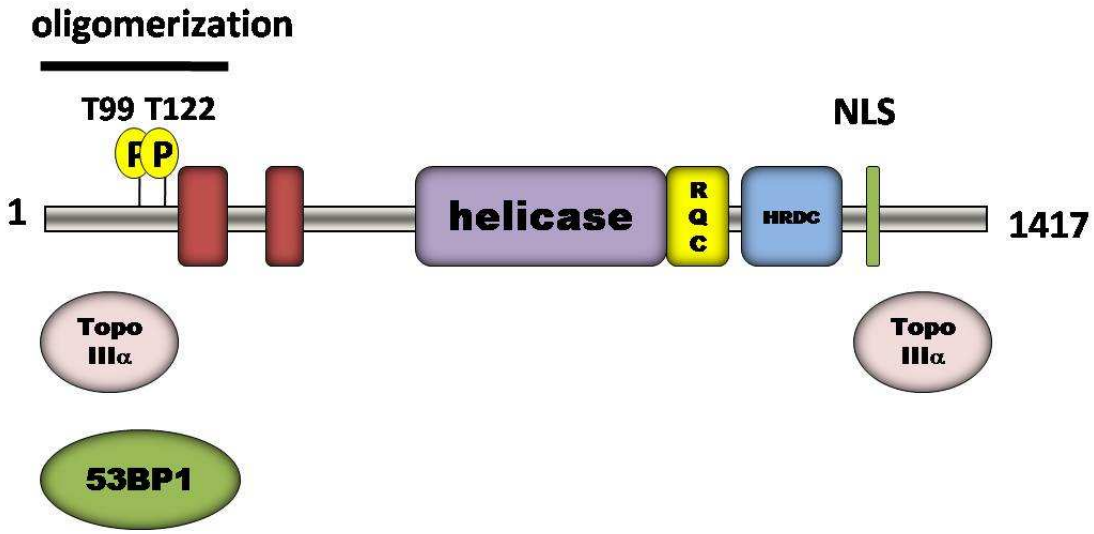

Figure.1.8. The BLM protein. Distribution of BLM domains and motifs: N-terminal oligomerization motif, two ATR phosphorylation sites (T99 and T122), in brown – conserved acidic patches, helicase domain, RQC – domain conserved in RecQ family members, HRDC – (helicase and RNase D C-terminal), NLS – nuclear localizing signal. Sites of interaction with TopoIIIα and 53BP1 are depicted.

1.2.5. Bloom's syndrome (BS).

Bloom's syndrome was first reported in 1954 (Bloom, 1954). It is a rare recessive autosomal genetic dysfunction. Patients with BS share several common clinical features such as short posture, immunodeficiency, male sterility, sun sensitivity and predisposition to cancer. BS individuals have greater risk of developing tumours compared to other disorders with enhanced risk of cancers. Cells derived from patients with defective BLM helicase show multiple types of chromosome rearrangements including exchanges between sister chromatids (SCE) and homologous chromosomes and chromosome breaks and gaps. The genetic instability is also present as mutations in a variety of different loci (German, 1993).

A candidate for BLM was identified by direct selection of a cDNA derived from a 250kb segment of the genome to which BLM had been assigned by somatic crossover point (SCP) mapping. cDNA analysis of the candidate gene identified a 4437bp cDNA that encoded a 1417 amino acid peptide with homology to the RecQ helicases, a subfamily of DExH box-containing DNA and RNA helicases (Ellis et al., 1995; German et al., 1994). Mutations identified in BS patients include frameshits, premature stop codons and missense mutations. It is predicted that mutations causing Bloom's syndrome involve loss of function mutations of the BLM helicase. However even homozygous patients with a mutated allele are viable, thus it was suggested that BLM is not essential for cell survival (Ellis et al., 1995).

BLM is a member of the RecQ family of helicases together with WRN (Werner's syndrome; Yu et al., 1996), RecQ1 (Seki et al., 1994), RecQ4 (RTS, Rothmnud-Thompson syndrome; Kitao et al., 1998 and 1999) and RecQ5 (Kitao et al., 1998). All members of RecQ family contain a highly conserved helicase region of around 450 aa comprising seven motifs including a 'Walker A-box' motif, ATP binding motif and a DExH box which is typical for this family of proteins (Figure.1.8.). RecQs are all 3'-5'

DNA helicases and WRN also possesses an exonuclease activity. BLM has been found to form oligomeric structures, mostly hexamers, of molecular weight of around 850K. BLM oligomeric rings can unwind a variety of DNA structures with the exception of fully duplexed and blunt-ended DNA molecules (Karow et al., 2000a). BLM's N- and C-terminal regions are not conserved in RecQ family members which may contribute to it playing a different role in cellular metabolism to other RecQ proteins (Karow et al., 2000b). Those regions possibly have a role in BLM's interactions with other proteins, such as RPA70 (Brosh Jr. et al., 2000), Topoisomerase III α (Wu et al., 2000a), 53BP1 (Tripathi et al., 2007) and p53 (Figure.1.8; Wang et al., 2001). BLM also interacts with 53BP1 and accumulates with it at stalled replication forks caused by HU arrest (Sengupta et al., 2004). It is a part of a multiprotein complex (BASC - BRCA1-associated genome surveillance complex) that is found at stalled replication foci together with BRCA1, MRN complex, MLH1, RPA, ATR, and ATM (Wang et al., 2000). Following DSBs BLM is phosphorylated by ATM although this phosphorylation is not crucial for BLM function in SCE suppression (Sister Chromatide Exchange; Beamish et al., 2002). It has also been reported that the phosphorylation of T99 and T122 on BLM by ATR is necessary to overcome S-phase arrest (Davies et al., 2004).

The expression of BLM is cell cycle regulated and reaches its maximum in late S phase and G2 (Dutertre et al., 2000) when it colocalizes with PML (Gharibyan & Youssoufian, 1999). After DNA damage BLM relocalizes to the sites of DSBs and colocalizes with γ-H2AX (Davalos & Campisi, 2003) RPA and Rad51 at IRIFs (Bischof et al., 2001). BLM also colocalizes with Rad51/DMC1 recombination foci mainly during the leptotene stage of meiosis (Moens et al., 2000).

1.2.6. The tumour suppressors BRCA1 and BRCA2 and Tamoxifen resistence in breast cancer.

In familial cancers mutations in BRCA1 and BRCA2 are found in 80% of the cases. Only one mutated BRCA gene in the germline is enough to predispose to breast cancer; however, in the tissues isolated from tumours from patients with recognized predisposition for breast cancer both of the genes are mutated. Thus BRCA1 and BRCA2 fit perfectly as tumour suppressor genes, although mutations in them rarely occur in sporadic cancers (Venkitaraman, 2002). BRCA1 mutations also contribute to ovarian cancer incidence unlike BRCA2 mutations which have not been linked to that disease (Miki et al., 1994).

In 1990 familial breast cancer was linked with alterations in chromosome 17q21. It has been observed that amongst the general population only a small number of the cases is connected with familial susceptibility. Thus families with inherited mutations usually rarely have sporadic breast cancer cases. On the other hand families with no genetic defect can have several cases of sporadic breast cancer. This observations suggest a highly heterogenic phenotype of the disease. However it is possible to recognize inherited susceptibility from sporadic cases by younger age of the patients, more frequent cases amongst men in the family and bilateral form of the disease (Hall et al., 1990). mRNA levels of BRCA1 are markedly reduced during the transition from carcinoma *in situ* to invasive cancer (Thompson et al., 1995).

The *BRCA1* gene was cloned in 1994 by Miki Y. et al. It was found to have 22 exons and span around 100kb of genomic DNA with the transcript length of 7.8kb. Mutations identified in that study are located in different exons thus again suggesting heterogeneity of the disease (Miki et al., 1994). About 85% of over two hundred identified BRCA1 mutations are nonsense or frameshift mutations leading to a truncated product and are spread throughout the whole protein. Another 15% are

concentrated in the RING domain. However the majority of tumour-associated mutations are concentrated in the RING domain and the BRCT domains (Huyton et al., 2000; Yang & Lippman, 1999).

BRCA1 has 1863 aa and a molecular weight of 220K. It is shown be a tumour suppressor gene as its over expression causes growth retardation of cancer cells in nude mice (Holt et al., 1996). As shown in Figure 1.9. at the N-terminus it contains a consensus zinc-finger motif (Cys3-His-Cys4) termed a RING-domain and a tandem repeat of BRCT domains (BRCA1 C-terminal) in the C-terminal region (Koonin et al., 1996). The RING-domain was reported to mediate interaction of BRCA1 with BARD1 (BRCA1 associated Ring Domain; Wu et al., 1996) and BAP1 (BRCA1-associated protein 1) which is an ubiquitin C-terminal hydrolase (Jensen & Rauscher 3rd, 1999). The middle region of BRCA1 interacts with p53 (Figure.1.9.; Zhang et al., 1998), MRN complex (Zhong et al., 1999) and further towards C-terminal region a Rad51 binding site was reported (Scully et al., 1997b). The BRCT domains have been reported to mediate interaction of BRCA1 and RNA polymerase II (Anderson et al., 1998; Scully et al., 1997a), CtIP (Wong et al., 1998; Yu et al., 1998), BACH1 (Cantor et al., 2001) and BRCA2 (Chen et al., 1998). BRCA1 also forms the BASC complex (Wang et al., 2000). ATR phosphorylates BRCA1 on S1423 after DNA damage (Chen, 2000). BRCA1 is also phosphorylated by ATM and Chk2 (S988) in response to ionizing irradiation (Cortez et al. 1999; Gatei et al., 2000; Lee et al., 2000) and in a cell cycle dependent manner by CDK2 and kinases associated with cyclins D and A. This indicates that BRCA1 is phosphorylated in mid G1 and stays in a hyperphosphorylated state during S phase (Chen et al., 1996). As mentioned before BRCA1 takes an active part in homologous recombination as well as being a part of the microhomology-mediated end-joining (MMEJ) pathway due to the interaction with the Rad50-Mre11-NBS1 complex

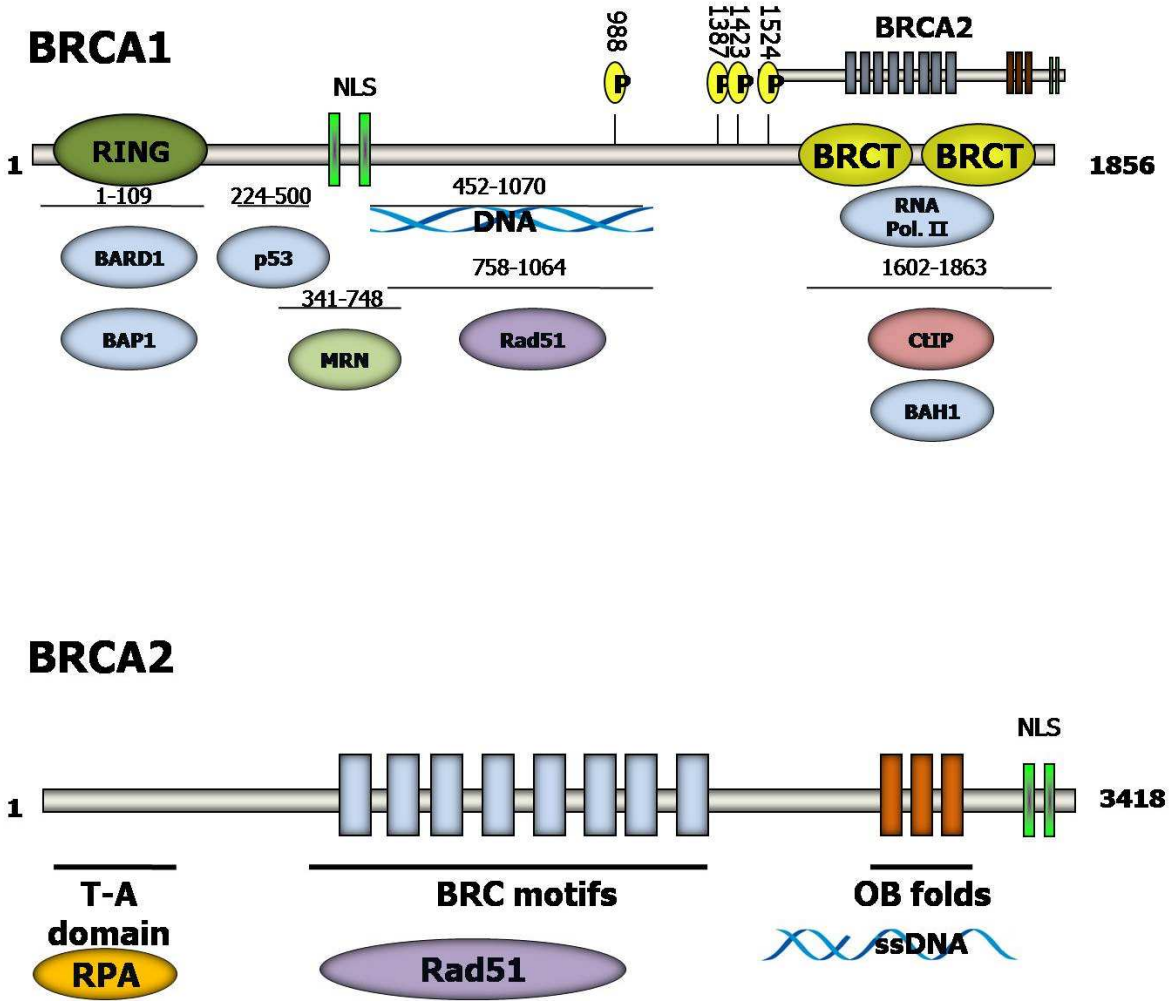

Figure.1.9. The BRCA1 and BRCA2 proteins. The localization of known domains and phosphorylation sites is shown and details of several of the interacting partners of BRCA1 are depicted. T-A domain – transcription-activation domain, NLS – nuclear localization signal. The eight BRC motifs on BRCA2 are shown with the three 'OB' (oligonucleotide-binding; binding site for ssDNA) folds. BRCA2 interacting proteins and the site where they bind to BRCA2 are depicted.

(Moynahan et al., 1999; Zhong et al., 2002).

BRAC2 was first linked to chromosome 13q12-13 in 1994 in patients with familial breast cancer (Wooster et al., 1994). Later it was reported to comprise 27 exons and span around 70kb of genomic DNA. In 1995 Wooster R. et al. reported the partial sequence of BRCA2 and highlighted six mutations that cause the truncation of the protein and subsequently predisposition to cancer (Wooster et al., 1995). The whole gene was eventually sequenced by Tavtigian et al., 1996. The mRNA transcript is approximately 10-12kb and the BRCA2 protein contains 3418 amino acids. The N-terminal region contains a transcription-activation domain that has been reported to bind RPA and a cancer predisposing mutation, Y42C, abolishes that interaction (Wong et al., 2003). The middle region has eight BRC motifs consisting of ~40 amino acid residues (Figure.1.9).

Through its BRC motifs BRCA2 binds directly to RAD51 and regulates its coating of ssDNA in preparation for strand exchange of paired DNA molecules in homologous recombination (Wong et al., 1997). Towards the C-terminal region three 'OB' (oligonucleotide-binding) folds were found that allow BRCA2 and ssDNA binding (Yang et al., 2002). The pattern of expression of BRCA2 is similar to that of BRCA1 and reaches its peak in late G1 and S phase (Yang & Lippman, 1999).

Estrogen is one of the key factors in initiation and progression of breast cancers and therefore the treatment has mainly focused on inhibiting its carcinogenic effects. One of the most widely used drugs that inhibits estrogen receptor activity is Tamoxifen. It is a nonsteroidal antiestrogen that was the first drug to be approved by the Food and Drug Administration in prevention and treatment of estrogen positive breast cancers. Nearly 70% of primary breast tumours show expression of estrogen receptor (Early Breast Cancer Trialists' Collaborative Group (EBCTCG); 2005). When the disease is in its early onset from about 10% of the patients treated with adjuvant systemic

tamoxifen therapy can be cured. However, in case of reccurring disease the majority of patients will gain tamoxifen resistance and will not respond to treatment (Clarke et al., 2003; Massarweh & Schiff; 2006). Thus it has been a major concern to uncover the pathways of acquired tamoxifen resistance. In one of the studies it has been observed that tamoxifen resistant estrogen positive breast cancer cells show a dramatic reduction in CtIP expression compared to the parental line. It has been also shown that estrogen receptor negative breast cancer cell lines have very low or no CtIP expression at all. Apart from that it has been reported that patients with progressive disease during the course of treatment show lower levels of CtIP expression. It has also been shown that reintroduction of CtIP into tamoxifen resistant cells makes the cells vulnerable to tamoxifen treatment again. Thus it has been concluded that CtIP expression could be a marker in assessing the treatment for breast cancer patients and their clinical management (Wu et al., 2007).

1.3. The structural and functional characterisation of CtIP.

CtIP was first reported as a CtBP interacting protein and was named **C**-**t**erminal Binding Protein **I**nteracting **P**rotein. Its cDNA was shown to contain 3247 bp and code for a protein of 897 aa with a predicted molecular weight of 125K. The gene is located on chromosome 18q11.2 and the amino acid sequence shows homology with yeast (Sae2), Xenopus and chicken genes. It is also found to be very conserved in mammals (Chinnadurai, 2006; Sartori et al., 2007). The amino acid sequence has a known CtBP-binding motif, PLDLS (Figure.1.10.; Schaeper et al., 1995). On the basis of this finding it was proposed and proven that CtIP binds to CtBP via this motif, that comprises amino acids 490 to 494 (Schaeper et al., 1998).

Following this report another group identified CtIP as an Rb (Retinoblastoma protein)

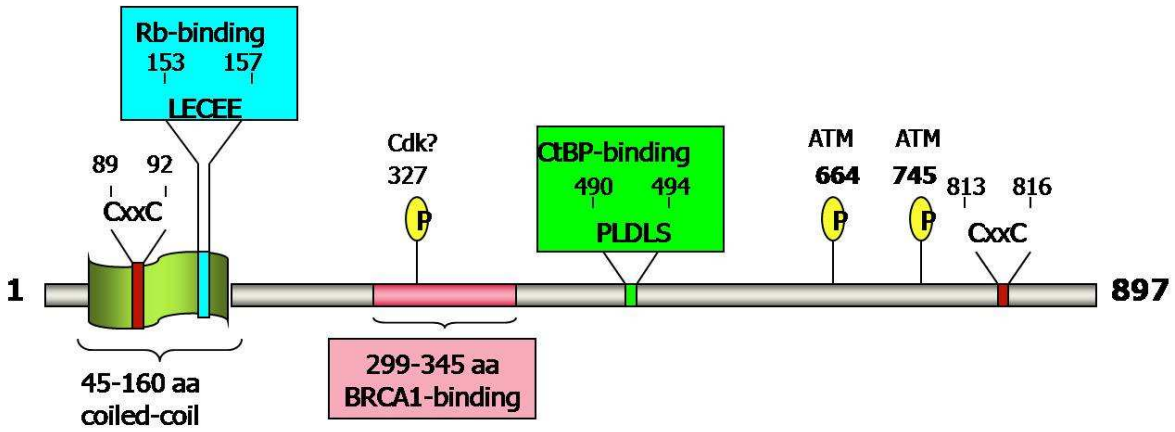

Figure.1.10. The CtIP protein. The sites of the interaction with Rb, BRCA1 and CtBP are depicted. Coiled-coil motif with zinc-hook like motif, a Cdk phosphorylation site, two ATM phosphorylation sites and a C-terminal zink-hook like motif are shown.

binding protein and named it Rim (Retinoblastoma interacting myosin-like) and, alternatively, RBBP8 (Retinoblastoma Binding Protein 8, HGMW-approved symbol; Fusco et al., 1998). There is an Rb-interacting motif (Taya, 1997) in the protein, LECEE, which is located between 153 and 157 aa and four nuclear localization signals (Fusco et al., 1998). However CtIP has been reported to interact with Rb even in the case of Rb mutation in CtIP's binding site, thus suggesting that there are two binding sites on Rb and CtIP (Dick et al., 2000). It is supported by the finding that not all CtIP homologues in animals contain that motif. CtIP modulates Rb-dependent G1/S transition. Mouse embryo fibroblasts depleted of CtIP would show hypophosphorylation of Rb and subsequent cell cycle arrest in G1/S (Chen et al., 2005).

CtIP has also been reported to contain two zinc-hook motifs (CXXC) at the N-terminal (89-92 aa) and C-terminal region (813-816 aa), similar to the ones found in Rad50. However, the metal binding ability has not been shown yet (Chinnadurai, 2006). The N-terminal fragment of the protein harbours a coiled-coil region which is known to be responsible for homodimerisation of CtIP (Dubin et al., 2004). The C-terminal region contains two reported ATM phosphorylation sites, S664 and S745 (Li et al., 2000) and CtIP has been reported to be hyperphosphorylated in response to ionizing irradiation which is dependent upon BRCA1 (Foray et al., 2003; Wu-Baer & Baer, 2001). CtIP has also been reported to be a BRCA1 binding protein and the interaction is modulated by phosphorylation of CtIP's S327 by CDK. This association is cell cycle dependent, occurring in G2, and is necessary for Chk1 activation after DNA damage. However the mechanism of activation is unclear (Yu & Chen, 2004). CtIP interacts with the BRCT domains of BRCA1 through a region spanning from 299 to 345 aa (Yu et al., 1998). Recently CtIP-BRCA1 interaction has been shown to be responsible for DNA repair pathway choice (Yun & Hiom, 2009). In G2/S phase CtIP is phosphorylated on S327 and subsequently interacts with BRCA1 directing the repair processes towards HR

(homologous recombination) and in G1, when S327 is not phosphorylated, the repair occurs through MMEJ (microhomology-mediated end-joining; Yun & Hiom, 2009). BRCA1 has also been reported to ubiquitynate CtIP which is necessary for its redistribution to IRIF in response to γ-irradiation (Yu et al., 2006).

A screen was performed to reveal *CtIP's* homozygous mutations in 89 different tumour human cell lines which did not show any homozygous deletions (Wong et al., 1998). On the other hand *CtIP* cDNA's analysis from those samples showed eleven silent and five missense mutations amongst which some were heterozygous and others were homozygous. In 11 of those cell lines a silent variation in codon 705 (G2115A) was found which may suggest that it is a common polymorphism in the *CtIP* gene in tumour-derived cell lines. More recently one mutation was found in a breast cancer cell line and an ovarian cell line which was caused by mutation in codon 589 of CtIP and resulted in substitution R=>H (Chinnadurai, 2006). Some colorectal cancers are reported to display microsatellite instability (MSI) which results in deletions or insertions in the coding region of the genes. This causes frameshift mutations. CtIP possesses A9 repeats in the middle of the coding region and has been found to be a target for MSI in colorectal cancers. Screen of 109 colorectal tumours revealed 1 bp deletion in that region with the frequency of ~22% (Vilkki et al., 2002). This mutation would cause the truncation of CtIP protein and expression of an N-terminal 357 aa fragment which would still possess the BRCA1 binding site intact but would lose the ATM phosphorylation sites and the CtBP binding motif. It is suggested that this mutation would contribute to colorectal oncogenesis and it has been reported that knock-out homozygous mice die in E4 of embryonic development and heterozygous individuals are prone to tumorigenesis. The most common are T and B lymphomas possibly because DNA repair is performed there at high rates (Chen et al., 2005; Chinnadurai, 2006).

CtIP has been shown to be involved in the DNA end resectioning after DSBs occurrence in G2/S phase (Sartori et al., 2007). It is the first step in HR which prepares the DNA strands for exchange. The C-terminal region of CtIP interacts with the MRN complex and enhances Mre11's endonucleolytic activity which generates ssDNA ends for efficient RPA-complex coating. The formation of RPA foci in damaged cells is greatly impaired in CtIP depleted cells. It has been reported that CtIP is necessary for recruitment of ATR to the sites of DNA damage by facilitating the generation of ssDNA ends which can be subsequently coated with RPA which in turn recruits ATR. Following ATR recruitment the phosphorylation cascade is released resulting in phosphorylation of RPA2 and phosphorylation and activation of Chk1 kinase (Sartori et al., 2007).

1.4. The DNA damage response – a rough guide to the sequence of events.

Genotoxic stress causes DNA lesions which can occur either in one strand or both at the same time. Double stranded breaks (DSBs; Bradley & Kohn, 1979) are the most deleterious and can lead to chromosomal rearrangements such as gene deletions or duplications, translocations or chromosome loss. They can be caused by γ-irradiation or anti-cancer drugs or can be intermediates of normal cellular processes such as meiotic recombination (Keeney & Neale, 2006), V(D)J recombination (Franco, Alt & Manis, 2006), class switch recombination (Chaudhuri et al., 2007) or replication fork collapse (Cox et al., 2000). Single stranded breaks (SSBs) on the other hand occur at a rate of thousands per day and can be caused by reactive oxygen species (ROS), alkylating agents or hydrolysis (Lindahl, 1993). They can also be caused by exogenous agents such as UV (Caldecott, 2006).

UV light that has the most effect on DNA is UVA (320-400nm) and UVB (290-320nm). UVA photons are known to penetrate the skin deeply and UVB photons are mostly absorbed by the epidermal layer of the skin. Both UVA and UVB generate damage in sugars and bases of the DNA molecule (Cadet et al., 2009).

UVB has a direct mutagenic effect on DNA causing direct damage to the bases whereas UVA causes an indirect damage inflicting oxidative stress towards the bases and sugars. UVA apart from mutational changes is also able to introduce strand breaks (Pfeifer, You & Besaratinia; 2005). IR (>10pm) introduces DNA strand breaks similarly to UVA causing oxidation of the sugar compounds of the DNA molecule (Breen & Murphy, 1995).

Drugs used to induce DNA damage are, amongst others, camptothecin (CPT), a cytotoxic quinoline alkaloid that inhibits DNA topoisomerase I (topo I) and causes the collapse of the replication fork (Pommier, 2006). Hydroxyurea (HU), an anti neoplastic drug and a DNA replication inhibitor that causes ribonucleotide depletion and results in DNA single and double strand breaks near the replication forks (Yarbro, 1992).

There are several different ways in which the cell carries out the DNA damage responses. Proteins taking part in them can be classified in two groups, those that function as gatekeepers promoting the cell cycle checkpoint arrest and/or apoptosis by signal transduction pathways and caretakers, functioning in repairing damaged DNA (Kinzler & Vogelstein, 1997). An example of a gatekeeper that is frequently mutated in the majority of sporadic tumours is Rb protein (Marshall, 1991; Weinberg, 1995; Sherr, 1996; Ortega et al., 2002). Rb regulates eukaryotic cell cycle progression at the G0/G1-S transition acting as a negative regulator of cellular proliferation and neoplasia (Sherr and McCormick, 2002). Caretakers are proteins that are involved in the DNA damage response. They recognize the breaks and perform repair, for example the MRN complex, RPA complex, ATM, ATR, BRCA1, BRCA2, 53BP1, MDC1, BLM and CtIP.

Following detection of DNA strand breaks a cell cycle checkpoint is activated. Different sets of proteins are utilized depending on the stage of the cell cycle during which the damage occurred. In general proteins taking part in the DNA damage response can be classed in five groups (Figure.1.11):

1. SENSORS which comprise of Mre11-Rad50-NBS1 (MRN) complex, Rad9-Hus1-Rad1 (9-1-1) PCNA-like sliding clamp and Rad17-RFC clamp loading complex (Abraham; 2001; Melo & Toczyski, 2002; Petrini & Stracker, 2003),
2. MEDIATORS: 53BP1, MDC1, BRCA1, TopBP1 and Claspin (Bartek & Lukas, 2003; Petrini & Stracker, 2003),
3. SIGNAL TRANSDUCING KINASES ATM, ATR and DNA-PK (Abraham, 2001; Shiloh, 2003),
4. EFFECTOR KINASES Chk1 and Chk2 (Bartek & Lukas, 2003),
5. EFFECTOR PROTEINS such as cell cycle regulators (Cdc25), transcription factors (p53 or E2F1), DNA repair proteins and several other types of protein (Bartek & Lukas, 2003; Donzelli & Draetta, 2003; Shiloh, 2003; Zhou & Elledge, 2000).

1.4.1. The cell cycle checkpoints.

The first step in the cellular response to DNA damage is carried out by an instant arrest of the progression of the cell cycle. The break in the cycle enables the cell to perform any necessary repair to the DNA, or in the case of the damage being too severe, undergo apoptosis. The mechanisms that the cell utilizes in order to prevent cell cycle progression in the case of acquiring DNA damage are termed 'the cell cycle checkpoints'. In a normal cell they act as a surveillance mechanism to track any disruptions to the integrity of the DNA thus they are not physical points at which the cell checks the state of its DNA as they are only activated upon DNA damage (van Vugt et al., 2005). Each of the checkpoints is termed after the cycle phase at which it can be activated upon the DNA damage.

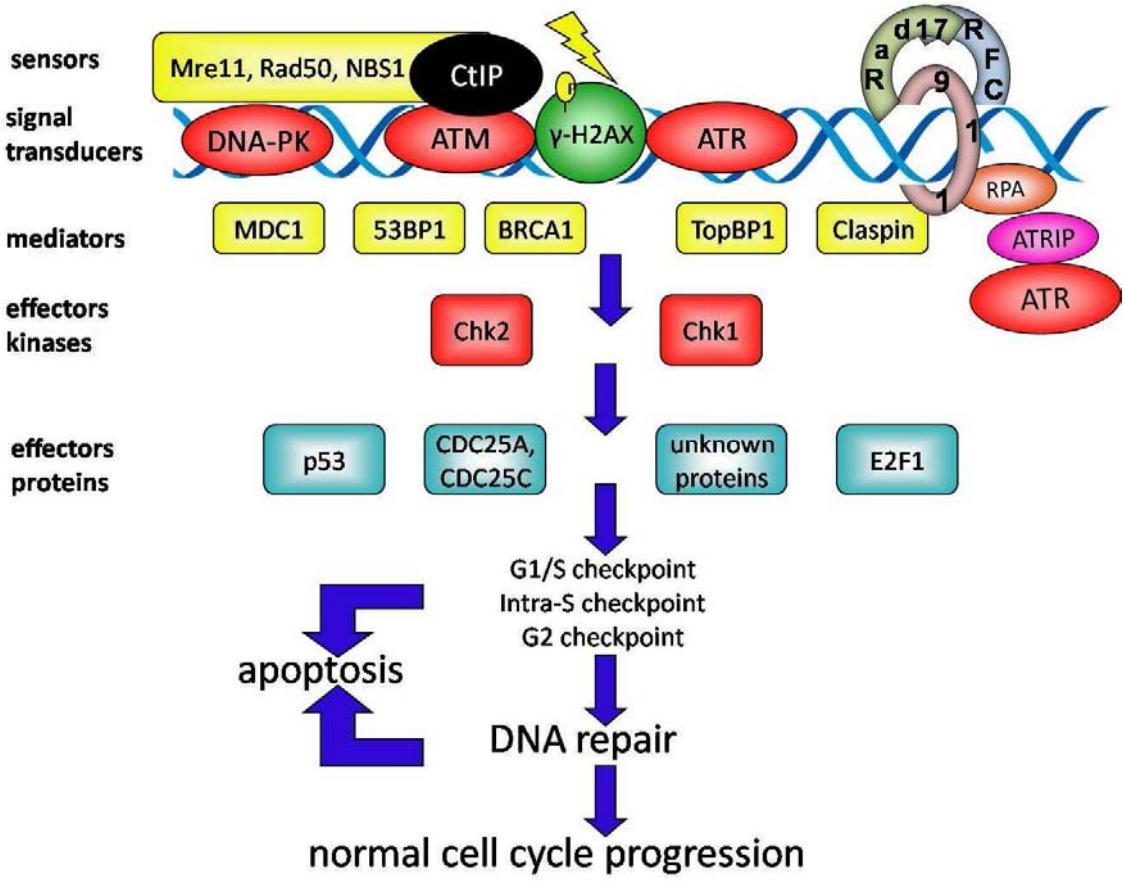

Figure.1.11. The classification of proteins taking part in the DNA damage response.

1.4.1.1. The G1 checkpoint.

The cell cycle checkpoint disabling entry into S-phase with damaged DNA is the G1 checkpoint, which inhibits DNA replication initiation. The main players involve ATM/ATR and Chk2/Chk1 kinases. They target Cdc25A phosphatase and p53 for phosphorylation. Phosphorylation of Cdc25A results in its inactivation. This in turn prevents the activation of Cdk2-cyclin E (Bartek & Lukas, 2001). The lack of activation of Cdk2 leads to lack of phosphorylation of Cdc45 and its inability to associate with the pre-RC complex which ultimately leads to inhibition of the initiation of DNA replication (Costanzo et al., 2000). Phosphorylation of p53 acts as a stabilizing modification. In this state p53 is able to activate the transcription of its target genes, such as p21 (Bartek & Lukas, 2001). p21 inhibits both Cdk2-cyclin E and Cdk4-cyclin D (Harper et al., 1993). The latter phosphorylates Rb which allows its release from E2F. This in turn is required for transcription of the genes needed for S phase progression. As Cdk4-cyclin D is inhibited by p21, the progression into S phase is also inhibited and the cell cycle arrests in G1 until the damage is resolved.

1.4.1.2. The intra-S checkpoint.

The intra-S checkpoint causes a slow-down of replication processes by inhibiting the assembly of new replicons. Thus it differs from other checkpoints by not being permanent and independent of p53 functions (Abraham, 2001; Bartek & Lukas, 2001; Shiloh, 2003). It is mainly executed by the Chk1/Chk2-Cdc25A pathway and by ATM phoshporylating NBS1 and SMC1. Mediator proteins such as BRCA1, 53BP1; FANCD2 play a role in it as well (Kim, Xu & Kastan, 2002; Nakanishi et al., 2002; Wang et al., 2002; Xu, Kim & Kastan, 2001; Yazdi et al., 2002). In general the phosphorylation of Cdc25A is performed by checkpoint kinases which prevents Cdc45 loading leading to the lack of replication origins firing (Falck et al., 2001). In this pathway, as mentioned

before, p53 is not required instead the independent branch of the DNA damage response is used utilizing the Chk1/Chk2 kinases as described above.

1.4.1.3. The G2/M checkpoint.

The G2/M checkpoint is the final checkpoint beyond which, if the DNA is not repaired, the mutations that have arisen will be passed on to progeny cells. The mechanism is similar to G1-checkpoint causing cell cycle delay or arrest via post-translational modifications of effector proteins and possible alterations in transcriptional mechanisms. It has been suggested that the accumulation of cells in G2/M is also caused by an additional S/M checkpoint, the so-called DNA replication checkpoint, which is very useful in cells with defective G1 or S checkpoints for example in the majority of tumours or A-T patient-derived cells (Kastan et al., 1992). The main event in the G2/M checkpoint is deactivation of cyclin B/Cdk1 by ATM/ATR and Chk2/Chk1 and/or inhibition of Cdc25C phosphatase, that would in normal circumstances activate Cdk1 before transition from G2 to M phase (Abraham, 2001; Nyberg et al, 2002). Additionally, all members of Cdc25 family, namely Cdc25A, Cdc25B and Cdc25C are positive regulators of cyclin B/Cdk1 in normal cells (Donzelli & Draetta, 2003; Mailand et al., 2002). Thus in response to DNA damage or inaccurately replicated DNA Cdc25A is degraded in G2 thus inhibiting activation of cyclin B/Cdk1. This mechanism is shared with the G1 and intra-S checkpoints as well (Bartek & Lukas, 2001 & 2003). Additionally 53BP1 and BRCA1 take part in the G2/M checkpoint (DiTullio Jr. et al., 2002; Fernandez-Capetillo et al., 2002; Wang et al., 2002; Xu et al., 2001). A third route has also been depicted involving Polo-like kinases Plk1 and Plk3 which seem to be upstream regulators of Cdc25C and/or cyclin B/Cdk1 (Nyberg et al., 2002).

1.4.2. Double-stranded break repair (DSBR).

The response to DSBs is initiated by the MRN complex that recognizes the break and rapidly relocalizes to the site of the lesion (Figure.1.12.; Petrini & Stracker, 2003). There are several lines of evidence suggesting that MRN is the initial DNA damage sensing agent. Firstly, Rad50 recognizes and binds to broken DNA ends (Moreno-Herrero et al., 2005), secondly, NBS1 has been found to be necessary for ATM recruitment to DSB (Falk et al., 2005; You et al., 2005) and assembly of IRIF containing MRN complex has not been reported to depend on any other DNA damage response protein (Figure.1.12.b; Bekker-Jensen et al., 2006). The initial association of MRN and the double-stranded lesion is only transient; however it is sufficient to recruit ATM via direct interaction of NBS1 C-terminal region and HEAT repeats in ATM. It is still debatable whether ATM is recruited in its activated state or its autophosphorylation is triggered by association with NBS1 (Bakkenist & Kastan, 2003; Cerosaletti et al., 2006; Falk et al., 2005; You et al., 2005). Nevertheless, autophosphorylation of ATM on serine residues 1981, 367 and 1893 activates the kinase which in turn phosphorylates histone H2AX, which is referred to as γ-H2AX (Figure.1.12.c; Bakkenist & Kastan, 2003; Kozlov et al., 2006; Rogakou et al., 1998). The C-terminal region of γ-H2AX with the phosphorylated S139 recruits the adaptor-mediator protein MDC1 through its tandem BRCT domains (Figure.1.12.d; Stucki et al., 2005). MDC1 also serves as a stabilizing protein for the MRN-DNA interaction, as it directly binds to NBS1 (Stucki & Jackson, 2006). This firm scaffold facilitates H2AX phosphorylation spread and recruitment of other DNA damage repair proteins (Lukas et al., 2004) which include 53BP1, BRCA1 and another set of MRN complexes and the ATM kinase (Figure.1.12.e; Bekker-Jensen et al., 2005; Bekker-Jensen et al., 2006). The fact that ATM is concentrated in IRIF enhances its phosphorylation potential thus increasing the

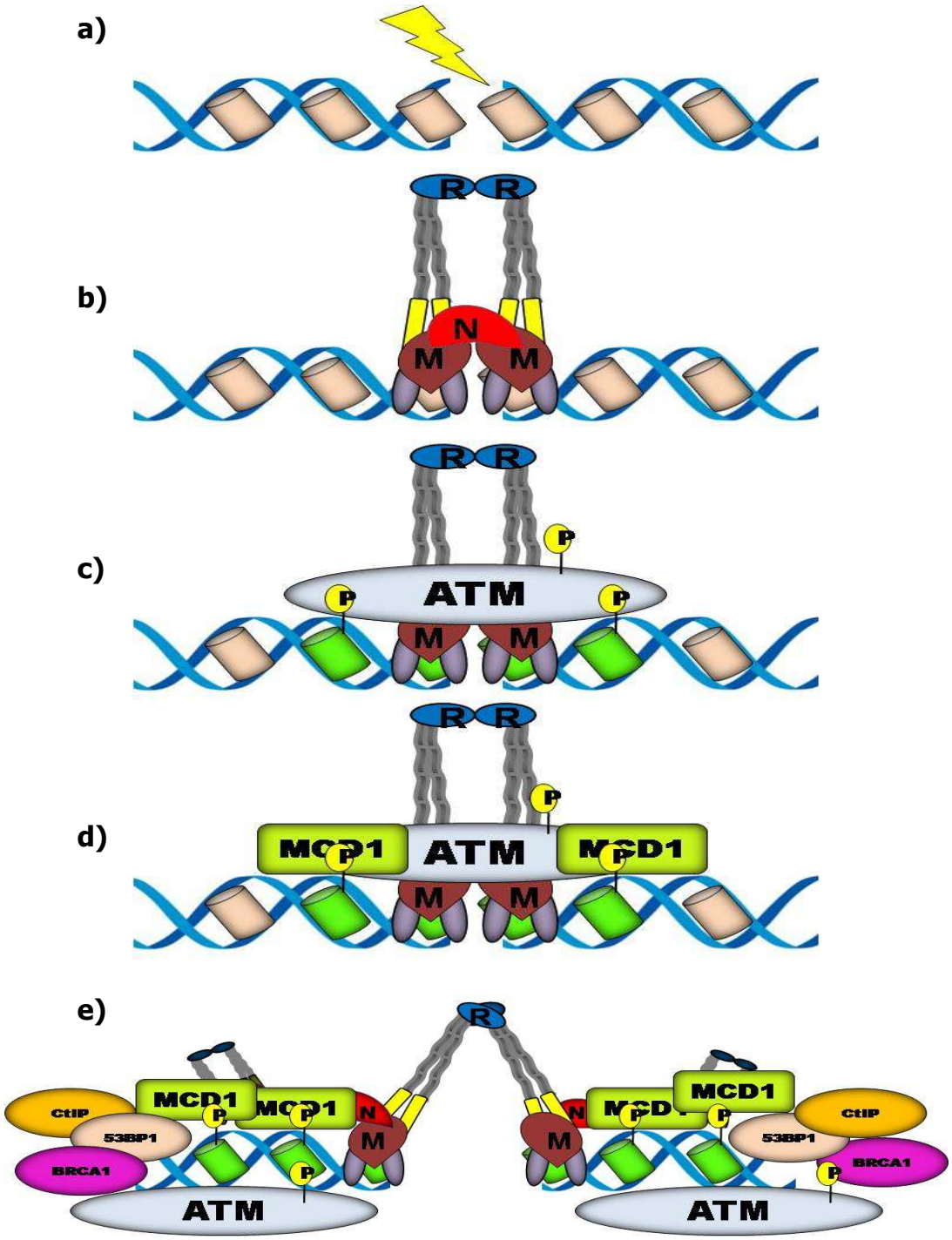

Figure.1.12. The DSB DNA damage response. The sequence of events during the DSB DNA damage response. **a)** occurrence of DSB, **b)** detection of the lesion by MRN complex (R-Rad50, N-NBS1, M-Mre11), **c)** recruitment of the transducer ATM kinase to the DBS and phosphorylation of the histone H2AX (H2AX-beige, γ-H2AX-green), **d)** MRN and ATM recruit MDC1 mediator, **e)** amplification of the signal due to recruitment of more DNA damage response proteins.

number of phosphorylation events performed by it in a short space of time. These events would include phosphorylation of Chk2 or Kap1 (KRAB-associated protein 1), which is involved in global chromatin condensation, thus changing the availability of the DNA for repair (Ziv et al., 2006).

1.4.2.1. The DNA end resectioning.

The MRN complex together with ATM is also essential for performing DNA end resectioning. This process is carried out mainly by Mre11 and creates ssDNA overhangs which are rapidly coated by RPA complex (Figure.1.13.). This event is necessary to involve ATR in DNA damage signalling and for initiation of homologous recombination (Adams et al., 2006; Cuadrado et al., 2006; Jazayeri et al., 2006; Kim et al., 2005; Myers & Cortez, 2006). DSB end resectioning, unlike chromatin response (chromatin decondensation), requires activation of CDKs and only occurs in S and G2 cell cycle phases (Bekker-Jensen et al., 2006; Jazayeri et al., 2006). As mentioned before, resected DNA ends are coated with the RPA complex and subsequently recruit ATR-ATRIP to the sites of damage (Figure.1.13; Zou & Elledge, 2003). ATR for its full activation requires binding of TopBP1, which is recruited to the site of repair by an independent pathway (Kumagai et al., 2006). Activated ATR phosphorylates its targets with the exception of Chk1, which requires recruitment of Claspin before it becomes phosphorylated. In turn Claspin assembly on ssDNA requires phosphorylation of Rad17 by ATR which is stimulated by replication stress (Wang et al., 2006b).

As mentioned before MDC1 binds to γ-H2AX and this interaction serves as a scaffold for further recruitment of other proteins taking part in DSBR. It has been reported that MDC1 knock-out mice fail to form foci containing 53BP1, BRCA1, NBS1 and pATM (Lou et al., 2006). However Celeste et al. (2003) showed that the initial relocation of 53BP1, BRCA1 and NBS1 is not dependent upon H2AX or MDC1. Apart from that it has been

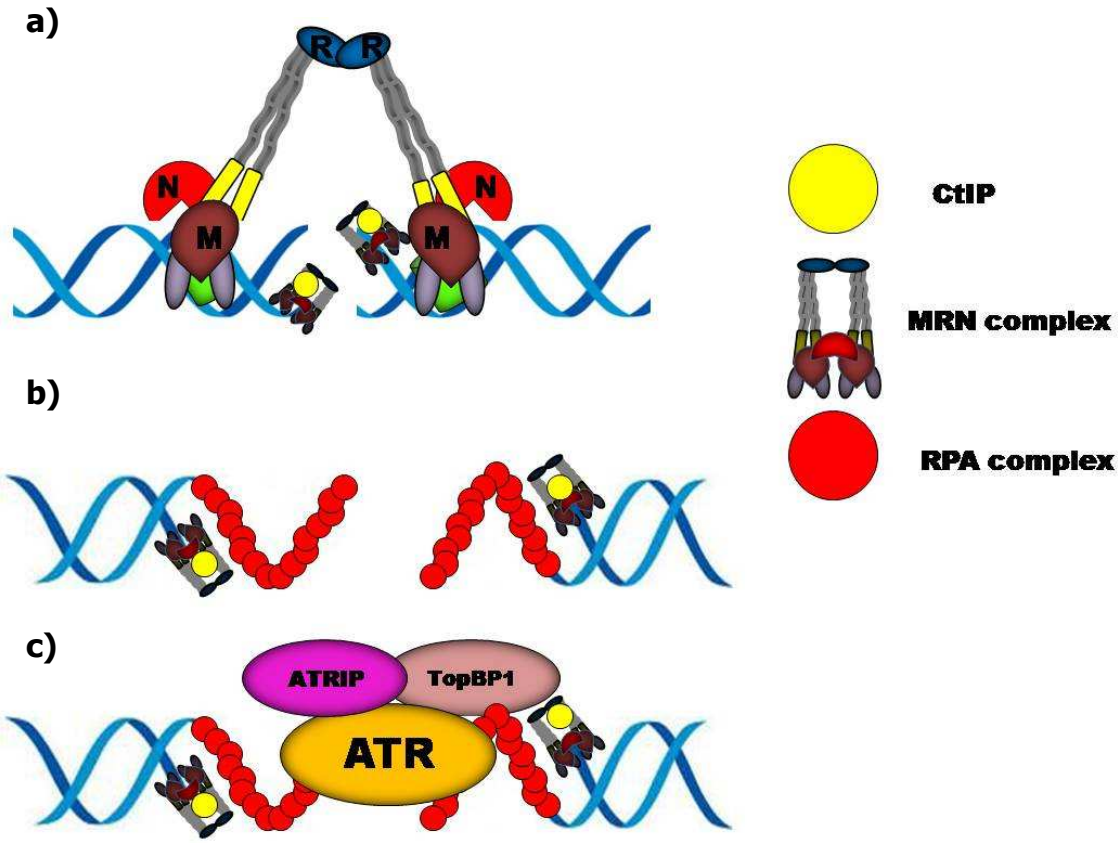

Figure.1.13. DNA end resectioning and ATR signalling initiation. a) The MRN complex (R-Rad50, N-NBS1, M-Mre11) together with CtIP (yellow circle) performs dsDNA ends resectioning, **b)** ssDNA ends are subsequently coated by the RPA complex (red circles), **c)** ATR/ATRIP/TopBP1 are recruited to ssDNA ends coated by the RPA complex.

reported that 53BP1 can be recruited to the sites of damage by its interaction with methylated H3. This association seems to be mediated by the tandem repeat of 53BP1's Tudor domains (Huyen et al., 2004). On the other hand, it has been noted that the retention of 53BP1, BRCA1 or NBS1 is dependent upon MDC1; thus it is suggested that the initial relocation may be due to a different mechanism but the stable foci formation is dependent upon MDC1 and its binding to γ-H2AX (Lou et al., 2006).

1.4.2.2. MDC1 (Mediator of DNA damage checkpoint protein 1).

MDC1 is also known as NFBD1 (nuclear factor with BRCT domains 1). It was first isolated in a random analysis of a cDNA library obtained from human myeloid cells (Nagase et al., 1996). Subsequently it was shown to be a nuclear protein with a tandem repeat of BRCT domains in the C-terminal region and to have an *in vitro* DNA binding capability (Ozaki et al., 2000). The N-terminal region possesses an FHA domain, which is another typical motif in DNA damage response proteins (Figure.1.14; Durocher & Jackson, 2002; Hofmann & Bucher, 1995). It has also been reported that MDC1 exists *in vivo* in at least three variants, which are most likely splice variants. It was found to be a member of a cellular protein multicomplex interacting with ATM, MRN complex, BRCA1, BARD1, FANCD2, Chk2 and 53BP1 and to regulate ionizing irradiation induced foci formation (Eliezer et al., 2009; Goldberg et al., 2003; Lou et al., 2003a&b; Peng & Chen, 2003; Wu et al., 2008; Xu & Stern, 2003). The middle region of MDC1 contains fourteen repeats which are not homologous to protein domains in the data base. However this region, the PST domain, has been shown to interact with Ku70/Ku80. MDC1 also plays a role in facilitating the autophosphorylation of DNA-PK by interaction with it via Ku70/Ku80, thus placing MDC1 in the DNA-PK/Ku70/Ku80 mediated error-free end-joining pathway (Lou et al., 2004).

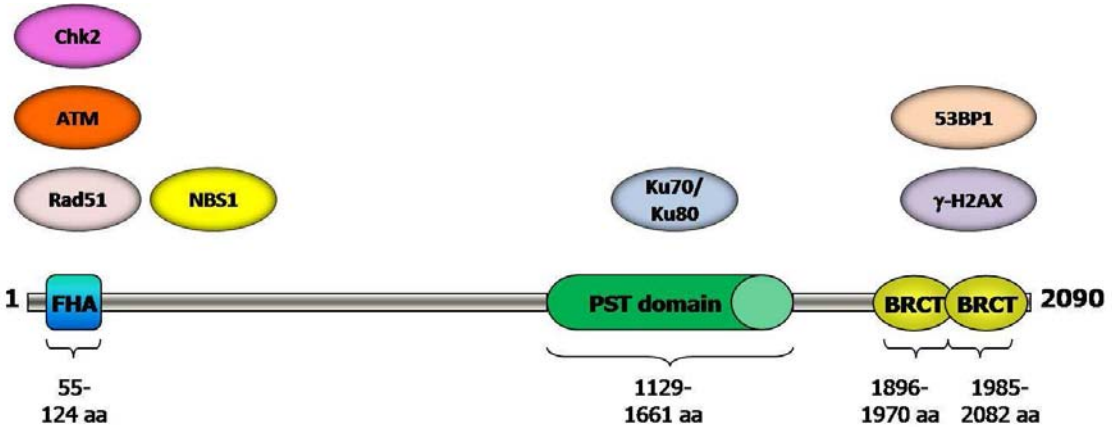

Figure.1.14. The MDC1 protein. The positioning of known domains and the binding sites of several interacting partners are shown.

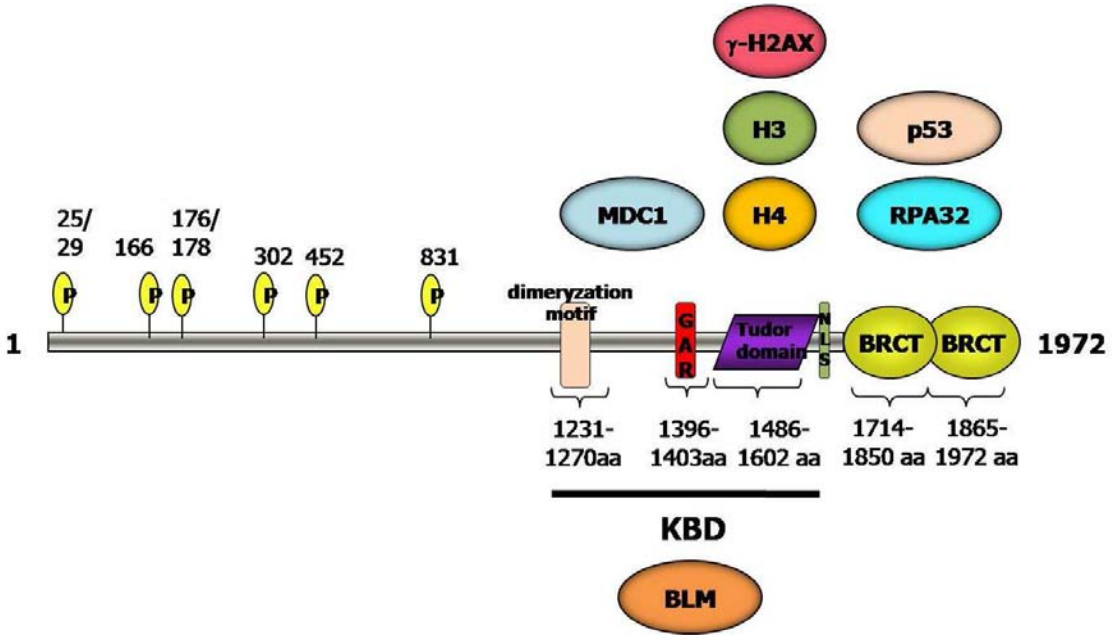

Figure.1.15. The 53BP1 protein. The positioning of known domains and the ATM/ATR phosphorylation sites are shown, as well as the binding sites of several interacting partners; GAR – glycine-arginine rich, KBD – kinetochore binding domain, NLS – nuclear localization signal.

MDC1 is phosphorylated in a cell cycle dependent manner and as a part of the DNA damage response pathway. In response to IR MDC1 phosphorylation is ATM-dependent and NBS1-independent. Approximately twenty potential ATM/ATR phosphorylation sites are scattered through the N-terminal region of the protein (Stewart et al., 2003).

Cells depleted of MDC1 are sensitive to IR and have S and G2/M checkpoint deficiency (Goldberg et al., 2003; Stewart et al., 2003). MDC1 has also been found to interact with Rad51 and prevent its degradation by locating it in the insoluble part of the chromatin associated with DNA. Thus MDC1 is thought to facilitate Rad51 binding to the chromatin as well as facilitating the formation of Rad51-containing filaments. It is suggested that MDC1 maintains a stable level of Rad51 protein in the chromatin and makes it readily available for filament formation in response to the DNA damage repair performed by HR machinery (Zhang et al., 2005).

1.4.2.3. 53BP1 (p53 Binding Protein 1).

53BP1 was first isolated in an yeast two-hybrid screen as an interacting protein of p53 (Iwabuchi et al., 1994 & 1998). The human protein consists of 1972aa and at the C-terminal region it contains a tandem repeat of BRCT domains, which have been found to directly bind to p53 (Figure.1.15.). As BRCT domains are found in a variety of DNA damage response proteins it was suggested that 53BP1 can be considered as one of them (Schultz et al., 2000). The N-terminal and middle region contains several ATM/ATR phosphorylation sites and the middle region comprises the dimerization domain and the glycine-arginine rich region (GAR; Jowsey et al., 2007; Ward et al., 2003). The C-terminal region contains the BRCT domains and two Tudor domains, which, as mentioned before, bind to methylated H3 and H4 in response to DNA damage (Huyen et al., 2004; Sanders et al., 2004). The binding to methylated H3 is only possible in case of chromatin structural rearrangements, as it is hidden by other

core histones. Thus 53BP1 is thought to sense chromatin remodelling after DNA damage (Huyen et al., 2004). The Tudor domains are also found to bind to γ-H2AX and are sufficient to relocalize 53BP1 to IRIF (Ward et al., 2003).

53BP1 has been reported to bind to RPA70 and RPA32 and the association with the latter is disrupted upon campthothecin (CPT) treatment. The interaction occurs through the C-terminal region containing the BRCT domains (Yoo et al., 2005). 53BP1 and BLM also form a complex that is phosphorylation dependent and the association is enhanced by 53BP1 phosphorylation by Chk1 in the KBD (kinetochore-binding domain; Tripathi et al., 2007).

53BP1 is also hyperphosphorylated in response to ionizing and UV irradiation by ATM and ATR, thus it takes part in DNA damage events stimulated by the PIKK kinases (Jowsey et al., 2007). However it has also been shown that it can play a role upstream of ATM as cells depleted of 53BP1 showed inefficient p53 accumulation, intra-S-checkpoint, G2/M checkpoint formation and retained phosphorylation of ATM targets such as SMC1, Chk2 or BRCA1 in response to IR (DiTullio Jr. et al., 2002; Fernandez-Capetillo et al., 2002).

The Tudor domains of 53BP1 have also been shown to be implicated in NHEJ (Non-homologous End-joining) by their interaction with DNA ligase IV/XRCC4 (Iwabuchi et al., 2003). It is suggested that 53BP1-mediated NHEJ occurs mainly in G1 and S and is distinct from the pathways governed by ATM/ARTEMIS and DNA-PK/Ku70-Ku80 (Iwabuchi et al., 2006).

Mice deficient of 53BP1 show intact V(D)J recombination but the class switch recombination is affected. This result suggests that as class switch recombination takes place in G1 it could be possible that 53BP1 takes part in the DNA damage response mainly by involvement in class switch recombination (Manis et al., 2004; Ward et al., 2004).

1.4.2.4. Sensing and signalling damage through ATR.

ATR is thought to be involved in checkpoint signalling in response to a variety of agents causing the stalling of the replication forks. It is also known to respond to DNA damage caused by other genotoxic insults such as UV or IR. This response enhances the G2 arrest (Cortez et al., 2001; Liu et al., 2000). As mentioned before the ATR gene is essential for cell viability and its deletion causes embryonic lethality in mice (Brown & Baltimore, 2000; de Klein et al., 2000).

As ATM and ATR are both members of the PIKK family, they share a number of structural and functional similarities. However, ATM-depleted cells are viable whereas ATR-depleted cells are not. ATM signalling seems to be mainly involved in resolving DSBs, that are a rather rare occurence in a normal cell's life cycle. On the other hand ATR is known to be involved in S phase in regulating the firing of replication forks, repairing damaged ones and preventing the premature onset of mitosis. This implies that ATR takes part in the normal cell cycle unlike ATM, which is activated upon DNA damage (Nyberg et al., 2002; Shechter et al., 2004).

ATR *in vivo* exists in a complex with ATRIP (ATR interacting protein). The loss of ATRIP expression causes loss of ATR expression as well as the disruption of ATR downstream signalling. This suggests that ATR and ATRIP are dependent upon each other and ATRIP stabilizes ATR (Cortez et al., 2001). ATRIP promotes ATR localization at sites of replication stress or DNA damage. Relocation of the ATR-ATRIP complex to the sites of DSBs depends upon Mre11's ability to resect damaged ends and subsequent RPA coating of ssDNA (Adams et al., 2006; Cuadrado et al., 2006; Jazayeri et al., 2006; Myers & Cortez, 2006). ATRIP binds directly to RPA70 (a large subunit of the RPA complex) via a conserved motif (Ball et al., 2007). However this interaction is not sufficient for ATR activation. The ATR-ATRIP complex must associate with the Rad9-Rad1-Hus1 (9-1-1) complex, which in turn recognizes and binds to ssDNA with the

adjacent RPA coating (Bermudez et al., 2003; Majka et al., 2006; Zou et al., 2003). Thus, in general, for ATR checkpoint activation a structure containing ssDNA coated with RPA complex and connected to dsDNA is needed and this conformation can be described as a "5' junction". This structure in normal circumstances occurs when for example DNA polymerase and MCM helicase uncouple during replication which causes replication fork stalling and in fact is needed to trigger checkpoint response. It can also form upon end resectioning during DSBR and NER (Figue.1.13; Byun et al., 2005; Costa et al., 2003; Nedelcheva et al., 2005; Williams et al., 2007).

The 9-1-1 complex activates ATR by coupling it to its activator protein TopBP1. Phosphorylated Rad9 binds to the BRCT domains I and II in TopBP1 and bridges ATR-TopBP1 binding. The ATR binding site on TopBP1 is located between its VIth and VIIth BRCT domains (Delacroix et al., 2007; Kumagai et al., 2006; Lee et al., 2007; St Onge et al., 2003). TopBP1 interacts with ATR-ATRIP complex through binding to ATR, in the PRD region (Figure 1.7.) and interaction with ATRIP. Mutations in the PRD domain of ATR have no effect on its basal activity but they do abolish ATR's interaction with TopBP1 and are found to cause checkpoint defects and mimic complete depletion of ATR in somatic cells (Mordes et al., 2008). It is also known that ATM phosphorylates TopBP1 on S1131 in response to DSBs and this modification induces interaction between TopBP1 and ATR-ATRIP complex. Thus this could be another mechanism for enhancing the activation of ATR during DSBR. However, it has been reported that TopBP1 S1131 can be phosphorylated by ATR in response to replication stress; thus phosphorylation of S1131 seems to be important for DNA repair both during ATM-initiated and ATR-initiated responses giving the same end result – enhancement of ATR activation (Cimprich & Cortez, 2008; Yoo et al., 2007).

One of the best known ATR targets in the DNA damage response is Chk1 kinase which is phosphorylated at S317 and S345. Chk1, as mentioned before, is a signal effector

kinase that transduces the signal to the effector proteins. Claspin has been found to be a mediator protein in ATR-dependent Chk1 phosphorylation that bridges their interaction. After ATR-dependent phosphorylation of Claspin it binds to Chk1 kinase. Subsequently Claspin binds to Rad17, which is a component of a clamp loader complex Rad17-RFC, that loads the 9-1-1 sliding clamp complex onto DNA lesion. This interaction is needed to maintain Chk1 phosphorylation (Kumagai & Dunphy, 2000; Wang et al., 2006b). After activation, Chk1 phosphorylates downstream targets such as Cdc25. This causes inhibition of Cdc25 phosphatase activity, thus preventing activation of CDK and subsequently arresting the cell before entry into mitosis (Furnari et al., 1997; Sanchez et al., 1997). The ATR-Chk1 signalling cascade is also crucial in regulating the firing of replication origins. This phosphorylation cascade slows down DNA replication by slowing down origin firings. This is crucial, when a cell encounters DNA damage, while replicating its DNA (Feijoo et al., 2001; Heffernan et al., 2002; Tercero & Diffley, 2001).

Other ATR targets include RPA32 which is phosphorylated after replication fork collapse. The RPA complex interacts with the MRN complex at the sites of DNA damage and the presence of NBS1 is required for RPA32 phosphorylation (Manthey et al., 2007; Olson et al., 2006 & 2007; Robison et al., 2004). ATR also phosphorylates proteins involved in DNA recombination such as BRCA1, BLM and WRN. They become ATR substrates in the vicinity of collapsed replication forks (Davies et al., 2004; Pichierri et al., 2003;Tibbetts et al., 2000).

1.4.2.4.1. RPA (Replication protein A) complex.

The RPA complex consists of three proteins, named according to their molecular weight: RPA70 (RPA1), RPA32 (RPA2) and RPA14 (RPA3, Figure.1.16.a). The RPA proteins do not have any enzymatic activity and their main role is to bind to ssDNA and orchestrate protein-protein interactions during replication stress and DNA damage

(Bochkareva et al., 2002; Mer et al., 2000; Wold, 1997). RPA70 is a 70K protein consisting of 616 aa residues. It has four OB (ologonucleotide-binding) folds stretching between amino acid residues 1–110 (RPA70N), 181–290 (RPA70A), 300–420 (RPA70B) and 436–616 (RPA70C). RPA70C is distinguished by the fact that it also contains a zinc-ribbon domain and a three-helix-bundle (3HB) motif, which makes it unique amongst the OB folds in RPA complex (Jacobs et al., 1999). RPA32 is a 32K protein possessing 270 aa residues. The N-terminal region is unstructured (1-41 aa) and contains all of the known RPA32 phosphorylation sites, the central region includes an OB fold (43-170 aa) and the C-terminal region is a Helix-turn-Helix (HtH) domain (RPA32C, 200-270 aa; Bochkarev et al, 1999). The RPA32 subunit is phosphorylated in a cell cycle dependent manner by CDKs on S23 and S29 (Dutta & Stillman, 1992; Fang & Newport, 1993). It is also phosphorylated upon DNA damage by the PIKK kinases on S4/8, T21, S33 and possibly on S11, S12 or S13 (Manthey et al., 2007; Zernik-Kobak M. et al., 1997). RPA14 is a 14K protein comprising of 121 aa residues and the whole of it structured into an OB fold. An α-helix is incorporated into the C-terminal region of RPA70B, RPA70C, RPA32D and RPA14 and the same α-helix from RPA70C, RPA32D and RPA14 is a contact surface in the formation of the RPA complex (Bochkareva et al., 2002). The RPA complex binds to ssDNA via RPA70A, RPA70B, RPA70C and RPA32D (Figure.1.16.b). RPA14 has not been reported to bind to ssDNA. The assembly of the RPA complex on ssDNA involves a sequence of events. The RPA70A domain binds first

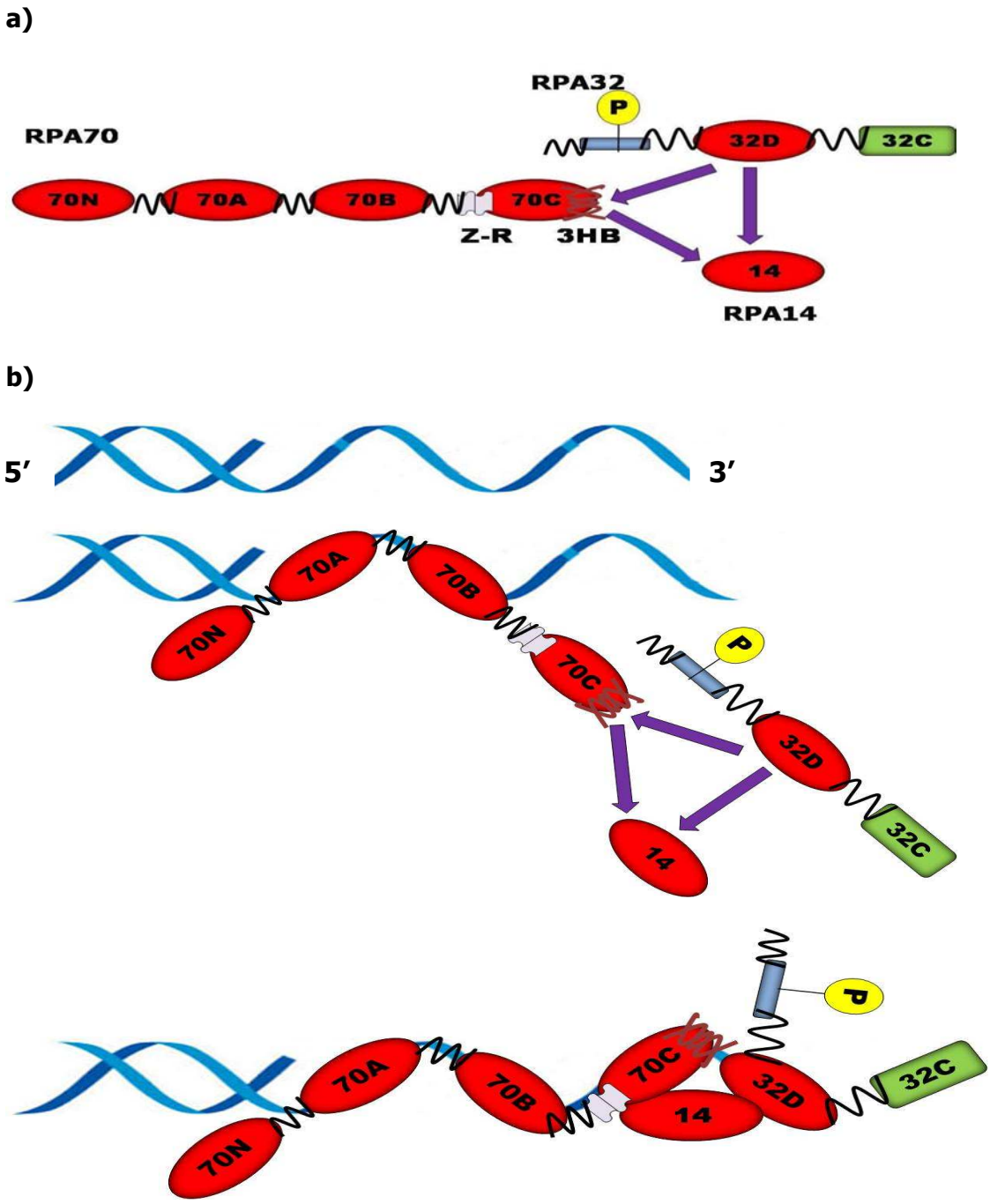

Figure.1.16. The RPA complex. a) the domain structure of the subunits of the RPA complex. RPA70 consists of four OB folds: 70N, 70A, 70B and 70C. OB 70C also contains a Z-R – zinc-ribbon motif and 3HB – three-helix-bundle motifs. RPA32 contains N-terminal phosphorylation sites (P), 32D OB fold and 32C Helix-turn-Helix motif. OB folds of RPA70 are connected with flexible linkers just like motifs in RPA32. RPA14 consists of a single OB fold. The interacting surfaces of each RPA subunit are indicated with purple arrows. **b)** sequential binding of RPA complex OB folds to ssDNA in 5'=>3' direction.

to the 5'-3' ssDNA end and subsequently RPA70B, RPA70C and RPA32D bind as well (Iftode & Borowiec, 2000).

The RPA complex has been reported to co-localize and interact with the MRN complex and the interaction is not dependent upon DNA damage (Robison et al., 2004). It has also been shown to interact with ATR/ATRIP, Rad51, Rad52, BRCA1, BRCA2 and 53BP1 (Ball et al., 2005; Choudhary & Li, 2002; Park et al., 1996; Wong, Ionescu & Ingles, 2003; van Komen et al., 2002; Yoo et al., 2005).

The RPA complex is also involved in base excision repair (BER), nucleotide excision repair (NER), mismatch repair (MMR), double-stranded break repair (DSBR) and single-stranded break repair (SSBR) thus is a crucial component of DNA surveillance mechanism (Zou et al., 2006).

1.4.2.4.2. TopBP1 (Topoisomerase IIβ Binding Protein 1).

TopBP1 is a 1435 aa nuclear protein. It contains eight BRCT domains and an ATR activating domain between the VIth and VIIth BRCT domain (Figure.1.17.). The first two BRCT domains are responsible for its interaction with phosphorylated Rad9 protein (Delacroix et al., 2007; Kumagai et al., 2006; Lee et al., 2007; St Onge et al., 2003). In response to IR it is phosphorylated by ATM on S1131. This modification enhances its ability to bind ATR/ATRIP (Cimprich & Cortez, 2008; Yoo et al., 2007).

TopBP1, together with BRCA1, participates in the G2/M cell cycle checkpoint although TopBP1 is thought to take part in it via the ATR route (Yamane et al., 2003). TopBP1 like BRCA1 forms IRIF and colocalizes with PCNA at the site of stalled replication forks. Its expression is shown to be strongly induced in S phase and it also interacts with DNA pol-ε which implicates its function in replication (Makiniemi et al., 2001).

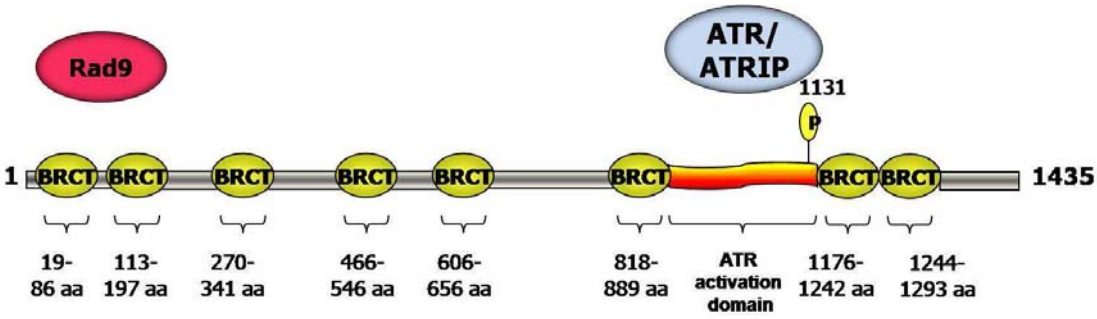

Figure.1.17. The TopBP1 protein. The domain structure and the distribution of the BRCT domains is shown. The ATM phosphorylation and the binding sites for Rad9 and ATR/ATRIP complex are depicted.

1.4.2.4.3. ATM and ATR – overlapping territories.

Initially ATM and ATR functions were studied separately. However, the emerging evidence suggests that they are components of an integrated circuit, that responds to a variety of DNA lesions and enables coordinated execution of checkpoint responses (Hurley & Bunz, 2007).

ATM is best known to respond to DSBs and subsequently initiates the checkpoint response and arrest of the cell cycle (Shiloh, 2003). ATR, on the other hand, is known to be activated most markedly by agents that cause inhibition of DNA replication such as hydroxyurea (HU) or ultraviolet light (UV), both of which block the synthesis of nucleotide precursors. In general ATR is activated by DNA replication intermediates which means that it monitors the progression of the replication fork (Kumagai & Dunphy, 2006; Osborn et al., 2002).

As mentioned previously ATM is not essential for cell viability which is not the case with ATR. This suggests that ATR is essential for a cell's normal physiology (Brown & Baltimore, 2000). The fact that ATM and ATR take part in two distinct DNA damage pathways, involving either DSBs or SSBs, respectively, was instinctively directing research towards distinguishing two separate cascades of response. However, several groups found that ATR is activated by ATM in response to IR (Adams et al., 2006; Cuadrado et al., 2006; Jazayeri et al., 2006; Myers & Cortez, 2006). This discovery led to the investigation of possible overlaps in ATM and ATR activities. Further findings showed that ATR activates ATM in response to DNA damage caused by UV and replication fork stalling, thus giving a firm foundation to the concept of ATM and ATR pathway cross-talk (Stiff et al., 2006).

It has also been reported that proteins that are thought to be involved in the ATM pathway are phosphorylated and utilized in an ATR-dependent manner. Stiff et al. (2008) showed that NBS1 is required for the replication independent G2/M cell cycle

checkpoint which is generated by ATR signalling and which also involves 53BP1 and MDC1 as mediators in the ATR-dependent phosphorylation cascade (Stiff et al., 2008). The same group had previously shown that NBS1 is required for RPA32 phoshorylation performed by ATR (Stiff et al., 2005).

ATM and ATR are known to take part in cell cycle checkpoints and play similar roles in triggering the G2/M cell cycle checkpoint and regulation of the progression of firing of the origins of replication in S-phase. However ATM at the G1/S stage of the cell cycle triggers a checkpoint whereas ATR prevents G1/S stasis and thus pushes the cell to continue to reach S phase. ATR is also reported to have some inhibitory effect on ATM signalling (Hurley & Bunz, 2007; Hurley et al., 2007).

1.4.3. Single-stranded break repair (SSBR).

Single-stranded DNA lesions are first recognized by PARP-1 and PARP-2 (Poly ADP-ribose polymerase 1 and 2) which are rapidly relocalized to the sites of lesions and activated by them (Ame et al., 1999; Benjamin & Gill, 1980). When PARP-1 is activated it modifies itself and other proteins by adding negatively charged poly ADP-ribose (PAR) chains (D'Amours et al., 1999). Once PARP-1 is modified it quickly dissociates from DNA as it has the same, negative charge. After dissociating from DNA, the PAR chain is degraded by poly ADP-ribose glycohydrolase and PARP-1 and other proteins that had the PAR chain added can be utilized elsewhere to repair another lesion (Zahradka & Ebisuzaki, 1982).

PARP-1 can be also activated by ssDNA that is formed during BER (Base Excision Repair; Durkacz et al., 1980). As the ends of DNA are damaged they require processing to restore 5'-phosphate and 3'-hydroxyl groups. This step is enzymatically very complicated and the nature of the modification requires specific enzymes to restore it. For example, to remove 5'-deoxyribose phosphate (dRP) the activity of DNA polymerase (Pol) β is needed. After restoring the 5'-phosphate group BER can proceed

(Sobol et al., 2000). In the case of modifications of the 3'-terminus, the most common modifications that arise from the damage caused by ROS, are 3'-phosphate and 3'-phosphoglycolate. The 3'-phosphate is a major substrate for polynucleotide kinase 3'-phosphatase (PNKP, Jilani et al., 1999) and the 3'-phosphoglycolate for apurinic–apyrimidinic (AP) endonuclease I (APE1; also referred to as APEX1, Winters et al., 1994).

Other types of damaged termini include DNA ends that are processed by cellular machinery when the processes do not go to completion. For example, when Topoisomerase 1 (TOP1) is bound to ssDNA it can collide with RNA polymerase (RNAP) or approach a lesion in DNA. These situations create TOP1-linked single-stranded breaks (TOP1-SSB) that are repaired by the activity of tyrosyl-DNA phosphodiesterase 1 (TDP1, Pouliot et al., 1999; Yang et al., 1996). Another example of ssDNA termini covalently bound are 5'-phosphate termini linked with AMP which are the result of abortive activity of DNA-ligase. These intermediates are fixed by aprataxin (APTX, Ahel et al., 2006). When the damaged DNA ends are undergoing repair, XRCC1 directly interacts with either PNKP, APTX and Pol β or indirectly with TPD1 via DNA ligase IIIα. In the case of PNKP, XRCC1 stimulates both kinase and phosphatase activity. When XRCC1 is associated with PNKP, APTX or Pol β it facilitates their accumulation at oxidative chromosomal breaks caused by H_2O_2 or UVA (Clements et al., 2004; Kubota et al., 1996; Loizou et al., 2004; Plo et al., 2003; Whitehouse et al., 2001).

After successful restoration of damaged DNA ends the process of gap filling occurs. This can involve filling in just one nucleotide (short-patch repair) or a few nucleotides. In this case FEN1 (Flap Endonuclease 1) removes the displaced 5'-residues either one at a time or several in one go (long-patch repair). *In vitro* studies show that Pol β is mainly involved in filling in the gaps arising in BER and after oxidative stress, although Pol δ and/or Pol ε (Pol δ/ε) can also take part in this process (Caldecott, 2006).

The next step involves the ligation of the recovered ends. Three human genes have been described: LIG1, LIG3 and LIG4. They encode five DNA ligases of which LIG3 encodes DNA ligase IIIα (LIG3α), DNA ligase IIIβ (LIG3β) and a mitochondrial isoform (mtLIG3). Of those ligases, LIG1, LIG3α and mtLIG3 are known to be involved in single-stranded break repair. LIG1 seems to be involved in long-patch repair and is recruited to the sites of damage by interaction with PCNA (Proliferating Cell Nuclear Antigen). LIG3α has been shown to play a role in the short-patch repair and interacts with XRCC1 via its C-terminal BRCT domains (Mortusewicz et al., 2006). mtLIG3 has been reported to interact with Pol γ and takes part is maintaining mitochondrial genome stability (De & Campbell, 2007).

There are a few genetic disorders that impact SSBR such as mutation in aprataxin gene (Ataxia-oculomotor apraxia 1, AOA1, Aicardi et al., 1988) or Spinocerebellar ataxia with axonal neuropathy 1 (SCAN1) which is connected with mutation in TDP1 gene (Takashima et al., 2002).

The single stranded DNA damage inflicted, for example by, UV and undergoing repair by the NER mechanism can stimulate ATR signaling. This occurs in non-cycling cells in the case of insufficient amounts of replication proteins such as Pol δ, Pol ε and/or PCNA, and would subsequently activate the ATR-dependent DNA repair. Insufficient amounts of replication proteins would cause inefficient filling of the gaps and lead to the accumulation of ssDNA intermediates. They are subsequently coated by the RPA complex and trigger the ATR-dependent DNA damage response (Matsumoto M. et al., 2007).

1.5. DNA damage repair mechanisms.

Depending on the nature of the damage, different, but partially overlapping mechanisms are employed to deal with it. If the lesion occurs in one of the strands and is a small gap (the double helix is not distorted) it can be repaired by base excision repair (BER). If the lesion is greater and the structure of the helix is distorted nucleotide excision repair (NER) occurs. There are around 30 proteins that take part in NER and the process, briefly, is based on damage recognition, opening the double helix around the break, excision of around 24-32 nucleotides surrounding the lesion and subsequent filling in the gap and ligation (de Boer & Hoeijmakers, 2000).

When the lesion occurs in both strands, depending on the stage of cell cycle two different mechanisms are employed: homologous recombination (HR) in the S and M phases, when sister chromatids are available, and non-homologous end-joining (NHEJ) in G1 and G2.

1.5.1. Homologous recombination (HR).

Homologous recombination is, in general, considered as an 'error free' method of repairing double-stranded lesions. It is initiated by extensive 5'=>3' DNA end processing performed and regulated by the MRN/MRX complex together with CtIP/Sae2, Exo1 and BLM/Sgs1 (Figure.1.13., Figure.1.18.; Mimitou & Symington, 2008; Sartori et al., 2007). As the result of this process 3' ssDNA ends are obtained which are rapidly coated with RPA. Subsequently, a portion of RPA is exchanged for Rad51 and this reaction is catalyzed by Rad52 and Rad51 paralogs (XRCC2, XRCC3, Rad51B, Rad51C, and Rad51D). Rad51-coated ssDNA scans for homologous regions and once they are found the duplex is aligned and DNA strand exchange begins (Sung et al., 2003). Rad52 and RPA together are thought to stimulate Rad51 filament formation by securing Rad51's binding to ssDNA ends. The collaboration of Rad52, RPA

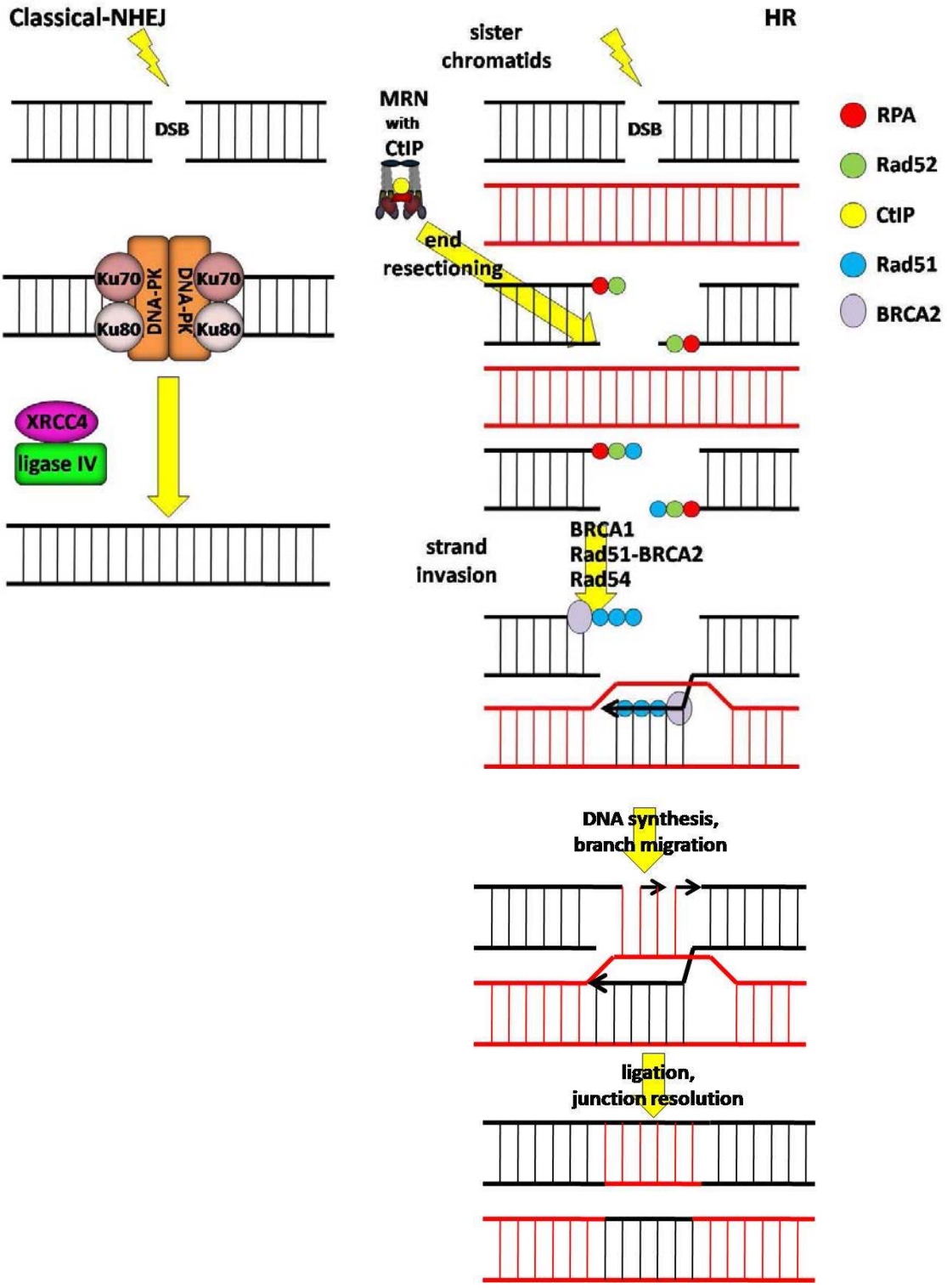

Figure.1.18. The two main DBS repair mechanisms: Classical-NHEJ and HR; see text for explanation.

and Rad51 results in Rad51 mediated DNA strand exchange enhancement (Shinohara & Ogawa, 1998). In turn, Rad52 catalyses the annealing of complementary ssDNA ends stimulated by RPA. The RPA2 subunit of the RPA complex has been found to bind directly to Rad52 and it is suggested that RPA either recruits Rad52 to the ssDNA or stabilizes Rad52-ssDNA binding (Mortensen et al., 1996; Park et al., 1996; Shinohara et al., 1998). The primary role of RPA binding to ssDNA is removal of its secondary structure, which, in turn, facilitates Rad51-ssDNA binding and Rad51 nucleofilament formation (Figure.1.18.; Baumann & West, 1997 & 1999).

It has been proposed that BRCA2 acts as a recombination repair mediator (Kowalczykowski, 2002). It binds to Rad51 via its BRC repeats and its C-terminal region which possesses three 'OB' (oligonucleo-binding, Figure.1.9.) folds. Thus it is proposed, that BRCA2 stabilizes Rad51-ssDNA binding (Kowalczykowski, 2002; Yang et al., 2002). The association of Rad51 and Rad54 leads to D-loop formation. The energy from ATP hydrolysis fuels Rad54/Rad51 movement along the DNA which forms positive supercoils at the front of the complex and negative supercoils behind. The remodelling of the DNA duplex enables pairing of the homologous regions and strand exchange (Figure.1.18.; Symington, 2002).

As mentioned before BRCA1 and BRCA2 are tumour suppressor genes that play a key role in maintaining genome integrity. Cell lines defective for BRCA1 or BRCA2 show defects in HR DNA repair systems mediated by Rad51 (Moynahan et al., 1999; Moynahan et al., 2001; Sharan et al., 1997). BRCA2 binds directly to RPA (Wong et al., 2003) and BRCA1 has been shown to colocalize with Rad51 foci together with BRCA2 (Kowalczykowski, 2002; Scully et al., 1997b; Tarsounas et al., 2003). BRCA2 possibly serves as a scaffold for Rad51 and keeps it in an inactive state until DNA damage occurs and Rad51 is needed for strand invasion (Figure.1.17; West, 2003).

DNA repair mediator proteins containing BRCT domains like MDC1 (Mediator of DNA damage checkpoint) or 53BP1 (p53 Binding Protein) are also known to be involved in homologous recombination events and in DNA damage sensing and signalling pathways, especially in S-phase (Lou et al., 2003; Sengupta et al., 2004). 53BP1 is reported to possess antirecombinogenic abilities in HR together with BLM. BLM in turn enhances 53BP1-Rad51 interaction. And in this feed-back loop 53BP1 facilitates BLM's accumulation at stalled replication forks (Sengupta et al., 2004; Tripathi et al., 2007). Overall 53BP1 suppresses HR and promotes NHEJ (Xie et al., 2007).

BLM helicase is suggested to act in replication, recombination and DNA damage repair events (Hickson, 2003). It may also regulate HR by modulating the functions of its interacting proteins, such as Rad51 (Bischof et al., 2001). Cells exposed to replication stress or IR show colocalization of BLM and Rad51 in nuclear foci. BLM together with p53 affects HR as inactivation of p53 in BS derived cells causes sister chromatid exchange (SCE) increase (Sengupta et al., 2003; Wu et al., 2001).

MDC1 also interacts with Rad51 and the partnership facilitates homologous recombination events in response to IR (Zhang et al., 2005). It promotes HR mainly through its interaction with γ-H2AX and this route is independent of 53BP1 and BRCA1. MDC1 dependent homologous recombination events are mediated via its FHA and PST domains (Xie et al., 2007). On the other hand the central region of MDC1 contains a DNA-PK binding region and is required for DNA-PK's phosphorylation after DNA damage and subsequent repair processes stimulated by DNA-PK (Stucki & Jackson, 2004).

1.5.2. Non-homologous End-joining (NHEJ).

Non-homologous End-joining accounts for around 50-70% of repair processes performed in mammalian cells in which the DSBs were caused by the I-SceI endonuclease. The rest of them are repaired by HR (Liang et al., 1998).

Non-homologous End-joining comprises two main routes: classical-NHEJ and alternative-NHEJ (alt-NHEJ) none of which rely on the template to reseal the DNA ends. Classical-NHEJ in mammalian cells involves mainly the DNA-PK kinase with its interacting partner the Ku70/Ku80 heterodimer, which binds to broken DNA ends and DNA ligase IV with its interacting partner, XRCC4 (Figure.1.18.). In budding yeast the MRX complex is also utilized to resolve DSBs (Chen & Kolodner, 1999; Haber, 2000). Classical-NHEJ is also regarded as requiring the minimal amount of end processing. In general it involves DNA end processing to reveal only short, complementary (1-4nt) sequences on either side of the break. They serve in the alignment of the DNA molecule and excess nucleotides are either trimmed or if a gap is produced, it is filled in. Those processes result either in deletions or insertions, thus classical-NHEJ is regarded as error-prone method of repairing the DSBs (Figure.1.18.; Burma et al., 2006; Guirouilh-Barbat et al., 2004). The alt-NHEJ is independent of DNA-PK and its mechanism is not clearly understood (DiBiase et al., 2000).

The first step of classical-NHEJ involves the heterodimer Ku70/Ku80 binding to the broken ends and recruiting the DNA-PK kinase. DNA-PK in turn recruits Artemis and this complex possesses an endonuclease activity that cleaves 5'- or 3'-overhangs. The ligation of DNA ends is performed by XRCC4/ligase IV complex (Grawunder et al., 1997). Recently another protein, XLF/Cernunnos, has been recognized as stimulating the XRCC4/ligase IV activity and promoting NHEJ (Ahnesorg et al., 2006). The gaps created during the classical-NHEJ are filled in by DNA polymerases Pol μ and Pol γ. Classical-NHEJ operates in G0/G1 and the majority of DSBs are repaired within minutes after they occur (Lee et al., 2004; Ma et al., 2004)

The alt-NHEJ recently described as MMEJ (Microhomology-mediated End-joining; Figure.1.19.) is a DNA-PK-independent pathway that operates even in cells with malfunctioning DNA-PK, mainly in G1 but also in the S and G2 phases of the cell cycle.

Its kinetics are 20- 30-fold slower than those of classical NHEJ and it requires four or more nucleotides for microhomology. It is recognized as error-prone as fairly large deletions may occur during its course (McVey & Lee, 2008; Yun & Hiom, 2009). MMEJ requires other proteins which are normally involved in different pathways, such as the MRN complex, CtIP, BRCA1, DNA ligase I and III, ERCC1/XPF (excision repair cross complementation group 1/xeroderma pigmentosum complementation group F) endonuclease and PARP-1 (poly(ADP-ribose) polymerase 1) and recently a possible role for NBS1 was revealed in this process (Ahmad et al., 2008; Audebert et al., 2004; Bennardo et al., 2008; Deriano et al., 2009; Liang et al., 2005; Yun & Hiom, 2009). There are reports that suggest that MMEJ is inhibited by Rad51, Ku70/Ku80 dimer and DNA-PK (Decottignies, 2007; McVey & Lee, 2008; Perrault et al., 2004). Additionally, PARP-1 competes with Ku70/Ku80 for binding to the DNA ends thus directing the repair towards MMEJ (Wang et al., 2006a).

MMEJ is thought to be initiated by the DNA end resectioning by the MRN complex, supported by CtIP and Exo1 nuclease. The microhomologies exposed during the resectioning are annealed in a way that provides stability. After the annealing the remaining non-complementary 3'-flaps are removed by ERCC1/XPF endonuclease complex (Ahmad et al., 2008). The insertion of additional nucleotides at many MMEJ sites suggests that the polymerases that fill the gaps are error-prone. The ligation step is performed by either DNA ligase I or IIIα/XRCC1 and PARP-1 (Audebert et al., 2004; Liang et al., 2008).

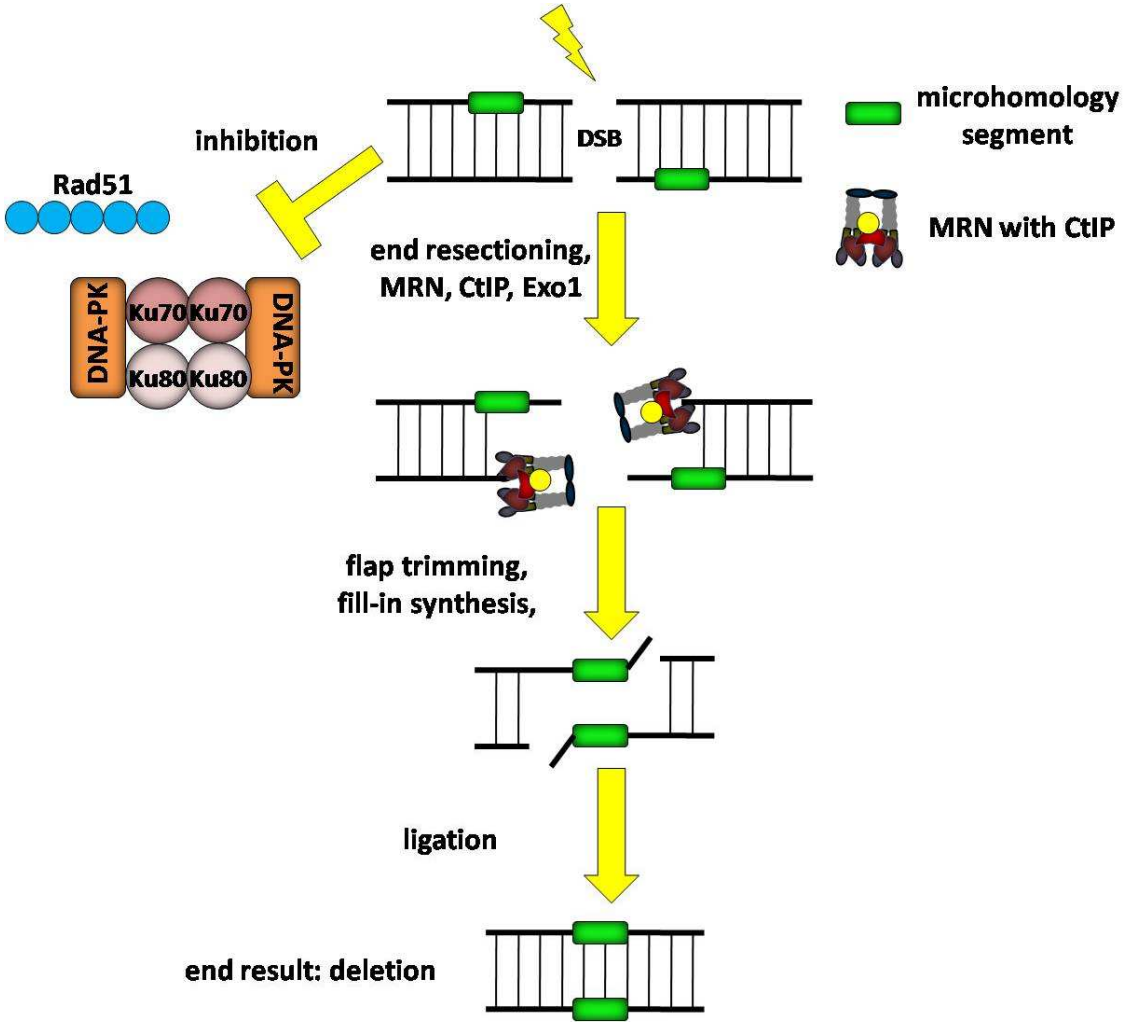

Figure.1.19. The microhomology-mediated end-joining (MMEJ); see text for explanation.

1.6. Ubiquitylation in DNA damage signaling.

As discussed previously and in section 5.1. phosphorylation plays a key role in the regulation of DNA damage responses as well as in a variety of other cellular signalling processes (Stryer, 1995). The FHA domain and the BRCT domains are only two examples of phosphopeptide binding domains (Durocher & Jackson, 2002; Manke et al., 2003) that are present in proteins taking part in DNA damage responses. Recently ubiquitination and deubiquitination have been recognized as additional ways of regulating DNA damage signalling. It has also emerged that the PIKK kinases phosphorylation cascade mediates the assembly of E3 ligase complexes at the sites of DSBs (Messick & Greenberg, 2009).

Ubiquitination regulates several cellular processes such as protein degradation, transcription, endocytosis, cell cycle and DNA damage response (Di Fiore et al., 2003). It is performed by the cooperative action of three groups of enzymes: E1, E2 and E3 and results in covalently linked mono- or polyubiquitin in several different conformations. E1 is an ubiquitin-activating enzyme which activates the ubiquitin polypeptide and transfers it to E2 – the ubiquitin-conjugating enzyme. E2 together with E3 (ubiquitin ligase) links the ubiquitin chain to the target protein (Hershko et al., 2000; Pickart, 2001). Typically, ubiquitin molecules are linked together via K48 and this modification directs the target protein for degradation (Pickart and Cohen, 2004). If ubiquitin particles are linked via K63 this serves for localizing or signalling events (Chen & Sun, 2009). Ubiquitins can also be linked via K6 as in the case of autoubiquitination of BRCA1/BARD heterodimer (Wu-Baer et al., 2003). On the other hand, ubiquitin chains can be linked together via one residue forming homogenous chains, as described above or via multiple residues forming branched chains, which broadens the spectrum of posttranslational modifications (Kim et al., 2007b).

As mentioned above phosphorylation and ubiquitination in response to DNA damage is coordinated. It has been shown that FANCD2 is phosphorylated by ATR in S phase which is subsequently followed by its monoubiquitination that is required for FANCD2 localization at the DSB and its chromatin association (Andreassen et al., 2004; Wang et al., 2004). Another example includes ATM/ATR dependent phosphorylation of BRCA1/BARD complex, an E3 ubiquitin ligase. After its activation by ATM/ATR it performs autoubiquitination together with the E2 (ubiquitin-conjugating enzyme) Ubch5c linking a K6 ubiquitin chain (Wu-Baer et al., 2003; Nishikawa et al., 2004). Furthermore the BRCA1/BARD complex links K6 ubiquitin chain to CtIP, this has been reported to be required for CtIP localization at DSB sites although the mechanism of CtIP-Ub foci formation awaits further understanding (Figure.1.19; Yu et al., 2006).

BRCA1 is targeted to the DSBs via interaction with a multicomplex encompassing RAP80, BRCC36, BRCC45, Abraxas, and MERIT40/NBA1 (Feng et al., 2009; Shao et al., 2009b; Wang et al., 2009). RAP80 is known to specifically recognize K6 and K63 polyubiquitin chains and bind them via its Ub-interacting motifs (UIMs; Sobhian et al., 2007). It has also been shown to interact with ubiquitylated γ-H2AX. BRCC36 is a member of the JAMM family of metalloprotease DUB (deubiquitynase) enzymes which deubiquitynates specifically K63-linked chains (Cooper et al., 2009; Shao et al., 2009a). BRCA1 has been reported to interact with the coiled-coil domain-containing 98 (CCDC98)/Abraxas mediator protein that is a part of the multicomplex formed by RAP80 (Kim et al., 2007a). It is also suggested that ubiquitynated γ-H2AX binds to RAP80 UMIs and this relocalizes the whole complex together with BRCA1 to DSBs (Mailand et al., 2007). Thus the initial sequence of events after DSB occurrence involves recognition of the break by MRN/CtIP complex, activation of ATM and subsequent phosphorylation of H2AX (Yuan & Chen, 2009). Secondly MDC1 is recruited to associate with γ-H2AX (Stucki et al., 2005). MDC1 is also known to recruit other DNA

damage response proteins such as 53BP1, BRCA1 and another set of MRN complexes and the ATM kinase (Figure.1.12.e; Bekker-Jensen et al., 2005; Bekker-Jensen et al., 2006). Apart from that it binds to RNF8, which is an E3 Ub-protein ligase, which ubiquitynates H2A, H2AX and γ-H2AX, together with E2 Ub-conjugating enzyme UBC13, in response to IR. Subsequently, ubiquitynated γ-H2AX recruits the RAP80 complex together with BRCA1 to IRIF (Figure.1.20.; Huen et al., 2007; Kolas et al., 2007; Mailand et al., 2007). Another protein that recognizes the Ub-chains synthesized by RNF8 is E3 Ub-protein ligase RNF168, mutated in the RIDDLE syndrome. RNF168, similarly to RNF8, associates with UBC13 to orchestrate ubiquitynation of H2A histone variants and synthesis of K63 Ub-chains at DSBs (Doil et al., 2009; Stewart et al., 2009).

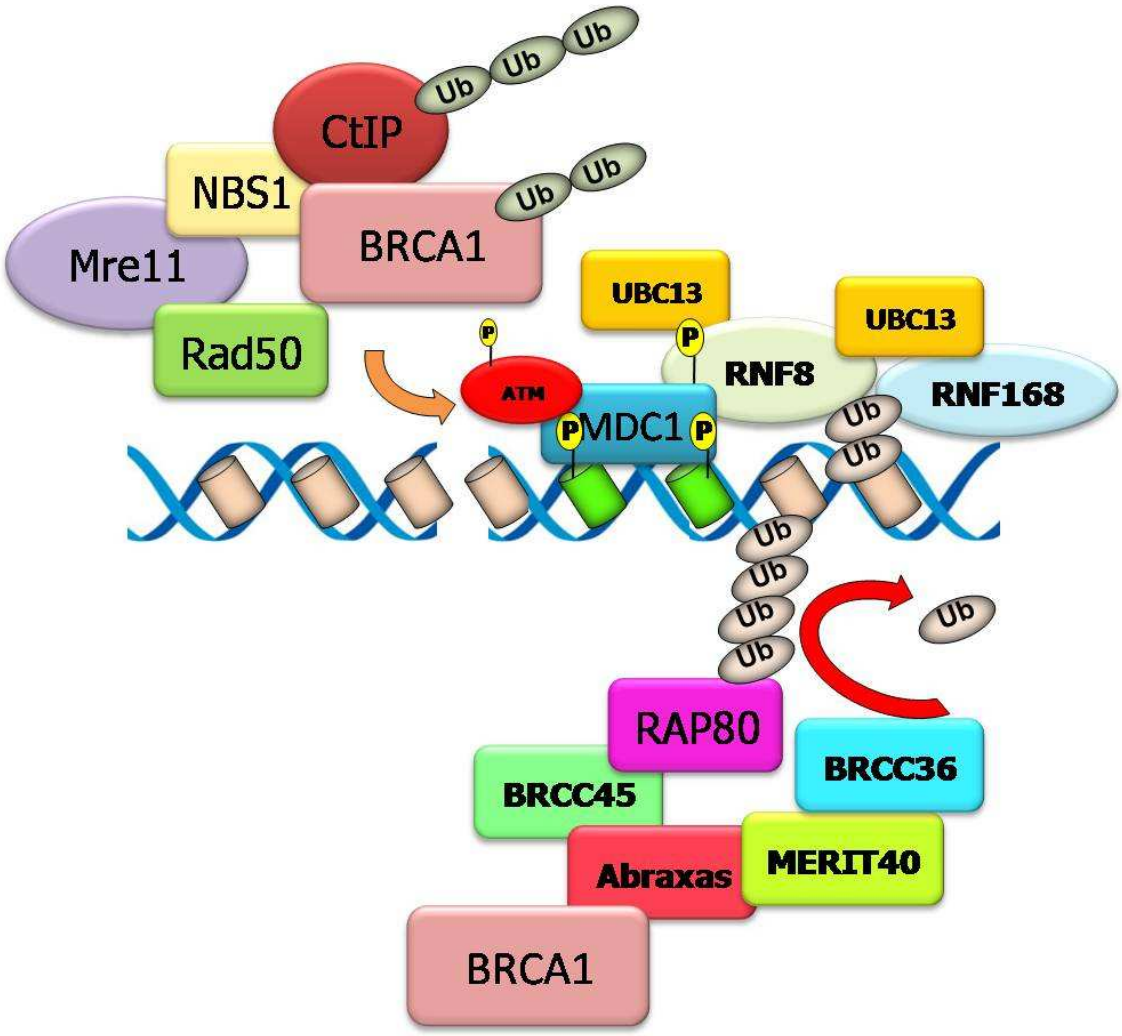

Figure.1.20. Ubiquitylation in early DNA damage response. For Figure description refer to the text. Orange arrow – detection of DSB by MRN/CtIP and BRCA1; red arrow – BRCC36 performing deubiquitylation, pink cylinder – H2AX, green cylinder - γ-H2AX (adapted form Messick & Greenberg, 2009).

1.7. Aims.

When this studentship began the major interest in CtIP was its proposed ability to modulate the activity of the transcriptional co-repressors Rb and CtBP. However, in view of CtIP's interaction with BRCA1 a study of its role in the DNA damage response was undertaken.

Specifically, the aims of this project were:

1. Determine CtIP's direct interaction with proteins containing BRCT domains such as 53BP1, MDC1, TopBP1 and NBS1.
2. Establish CtIP's nuclear localization before and after DNA damage and its co-localization wth damage response proteins.
3. Investigate CtIP's involvement in phosphorylation cascades that follow DNA damage caused by IR, UV and CPT.
4. Study CtIP's *in vivo* complex formation.
5. Determine novel phosphorylation sites on CtIP.

It should be noted that whilst my study was underway results similar to my own were published by Sartori et al., (2007).

CHAPTER II

MATERIALS AND METHODS

2.1. Cell biology techniques.

2.1.1. Cell lines.

Cells used during the course of this study were all of human origin, and individual lines are listed in Table 2.1.

Table.2.1. Cell lines used in this study.

Cell Line	Cell Type	Source	Culture Media
Normal LCL	B cell	Lymphoid tissue	RPMI
ATLD LCL	B cell	Lymphoid tissue	RPMI
A-T LCL	B cell	Lymphoid tissue	RPMI
HeLa	Epithelial	Cervical carcinoma	RPMI
HeLa shATM	Epithelial	Cervical carcinoma	RPMI
NBS LCL	B cell	Lymphoid tissue	RPMI

2.1.2. Cell culture media.

Cell lines were maintained in Roswell Park Memorial Institute (RPMI) 1640 medium (Invitrogen) which was supplemented with 8% foetal calf serum (FCS; Invitrogen). Antibiotics were not used. Media were stored at 4˚C for up to three months.

2.1.3. Maintenance and passage of cell lines.

All cells were cultured at 37˚C in humidified incubators supplied with 5% CO_2. The HeLa cell line was grown in monolayer and LCL cell lines were grown in suspension. HeLa cells during passage, after removal of medium, were washed twice with PBS, pre-warmed to 37˚C. Trypsin (Invitrogen) was added (1 ml/10cm dish) and incubated at 37˚C until cells had detached. Fresh medium was added to quench the trypsin, and

cells were pelleted by centrifugation at 1500 rpm for 5 min. Pellets were resuspended in medium, and re-plated at appropriate dilution. While passaging LCLs medium was removed, cells were resuspended in fresh medium and divided into fresh flasks at appropriate dilution.

2.1.4. Cryopreservation of cell lines.

HeLa cells were trypsinized and pelleted as above, but resuspended in 10% DMSO in FCS. LCL cells were pelleted and resuspended in 10% DMSO in FCS. Aliquots of 1ml were cooled to -80˚C at a controlled rate of 1˚C/min in isopropanol. Frozen samples were then transferred to liquid nitrogen storage tanks, to be kept long term at -180˚C. When required, cells were rapidly thawed in medium at 37˚C, pelleted by centrifugation, and resuspended in fresh medium before plating.

2.1.5. Drug treatments.

2.1.5.1. HeLa cells drug treatments.

Cells were treated with camptothecin (CPT), a cytotoxic quinoline alkaloid, at a final concentration of 1μM to inhibit DNA topoisomerase I (topo I). The drug was left in medium for 1h. After that time medium was removed, cells were washed twice with PBS, fresh medium was added and cells were harvested at the appropriate time points.

Cells were treated for 16h with 1mM hydroxyurea (HU), an anti neoplastic drug and DNA replication inhibitor that causes ribonucleotide depletion and results in DNA double strand breaks near replication forks. After treatment cells were harvested to perform the appropriate experiments.

2.1.5.2. LCL cells drug treatment.

Cells were treated for 1h with caffeine, a xanthine alkaloid compound, at a final concentration of 5mM to inhibit caffeine-sensitive kinases. After treatment cells were harvested and used to perform kinase assays.

2.1.6. IR and UV irradiation.

2.1.6.1. HeLa cells.

Subconfluent cells were mock-treated or treated with ionizing γ-rays from a ^{137}Cs source at an appropriate dose. Prior to UV irradiation, medium was removed from exponentially growing cells and stored at 37˚C. Cells were washed with PBS and mock-irradiated or irradiated with the appropriate dose of UV light, after which the cells' original medium was replaced. UV radiation with a wavelength of 254nm was delivered in a single pulse using a Stratalinker UV crosslinker 1800 (Stratagene).

2.1.6.2. LCL cells.

Confluent cells were treated with ionizing γ-rays from a ^{137}Cs source at a dose rate of 5 Gy and left for 30 min at 37˚C for full activation of ATM kinase, then harvested to perform kinase assays.

2.1.7. RNA interference (RNAi).

Control small interfering RNAs (siRNA) and siRNAs targeting CtIP or Mre11 are shown in Table 2.2.

Table 2.2. siRNA sequences used in this study.

Target	siRNA	Sense sequence	Company
None	AllStars	Proprietary	Qiagen
CtIP	CtIP4	5′-CUG CUU GGG CAC ACG UGU A-3′	Qiagen
Mre11	Mre11	5′-GCU AAU GAC UCU GAU GAU A -3′	Ambion

RNAi was carried out using different protocols, depending on the target protein. In each case HeLa cells were plated into 6 cm dishes 24h prior to transfection, so as to be 50-70% confluent the following day. Oligofectamine (OF) reagent (Invitrogen) was used to deliver siRNA duplexes into cells. To target CtIP 10 µl of OF was diluted to 500 µl with RPMI, and left for 5 min. 20 µl of CtIP siRNA (20 mM) was then diluted to 500 µl with RPMI, and added to the OF mix. OF-siRNA complexes were left to form for 20 min. After that time the mix was added to the appropriate dishes and left for 3 days before utilising them in an experiment. To target Mre11 a similar protocol was used except that 20 µl of OF was used for each knock-down and the transfection was repeated 24h after the initial treatment. Cells were harvested and used for experiments 96h after the first transfection.

2.2. Molecular biology techniques.

2.2.1. Preparation of media and plates.

Luria broth (LB) was made with 10 g/l NaCl (Sigma), 10 g/l bacto-tryptone (BD) and 5 g/l yeast extract (BD) in water, and sterilized by autoclaving at 120˚C and 100 kPa for 30 min. LB-agar was made by adding 15 g/l agar (BD) to LB, and sterilizing the solution by autoclaving as above. After cooling, ampicillin was added to a final concentration of 100 µg/ml. Before solidifying, aliquots of LB-agar were poured into

plates and left to cool. LB-agar plates were stored at 4°C until used for bacterial transformations.

2.2.2. Bacterial transformations.

Bacterial transformations were carried out in competent *Escherichia coli* cells. The NEB 1-beta DH5α strain (New England BioLabs) was used for recombinant plasmid production and propagation, XL10-Gold Ultracompetent cells (Stratagene) were used for directed site mutagenesis and BL21-CodonPlus (DE3)-RIL bacteria were used to generate recombinant proteins. For each transformation, a 25 μl aliquot of competent cells was thawed on ice before addition of up to 100 ng of DNA or ligation mixture; in the case of XL-10-Gold, cells were incubated with 1 μl of β-mercaptoethanol for 10 min before addition of plasmid DNA. Bacteria were incubated on ice for 30 min, before being heat-shocked at 42°C for 30 sec. They were placed back on ice for 5 min, before addition of 300 μl of LB medium described above, pre-warmed to 37°C. Cultures were placed in an incubator at 37°C with shaking at 200 rpm for 1h. Bacteria were then spread onto LB-agar plates containing ampicillin, and incubated at 37°C overnight.

2.2.3. Preparation of plasmid DNA.

Plasmids used in this study and the proteins they encode are detailed in Table 2.3.

Table 2.3. Plasmids used in this study.

Vector	Product	Tag	Amino acids	Origin
pGEX-4T-1	53BP1	GST	1-356	G. Stewart
pGEX-4T-1	53BP1	GST	333-759	G. Stewart
pGEX-4T-1	53BP1	GST	722-1039	G. Stewart
pGEX-4T-1	53BP1	GST	992-1331	G. Stewart
pGEX-4T-1	53BP1	GST	1309-1620	G. Stewart
pGEX-4T-1	53BP1	GST	1584-1972	G. Stewart

pcDNA4/His	53BP1	His	1584-1972	In-house
pcDNA3	CtIP	none	Full length - 1-897	In-house
pGEX-4T-1	CtIP	GST	Full length – 1-897	J. Last
pGEX-4T-1	CtIP	GST	324-897	J. Last
pGEX-4T-1	CtIP	GST	42-132	R. Baer
pGEX-4T-1	CtIP	GST	45-620	R. Baer
pGEX-4T-1	CtIP	GST	133-462	R. Baer
pGEX-4T-1	CtIP	GST	371-620	R. Baer
pGEX-4T-1	CtIP	GST	620-897	R. Baer
pGEX-4T-1	CtIP	GST	775-897	R. Baer
pGEX-4T-1	MDC1	GST	1-380	G. Stewart
pGEX-4T-1	MDC1	GST	341-724	G. Stewart
pGEX-4T-1	MDC1	GST	791-1118	G. Stewart
pGEX-4T-1	MDC1	GST	1052-1720	G. Stewart
pGEX-4T-1	MDC1	GST	1686-2090	G. Stewart
pcDNA4/His	MDC1	His	1686-2090	In-house
pRS314	Mre11	none	Full length – 1-708	J. Petrini
pcDNA3β	NBS1	myc	Full length – 1-754	X. Wu
pcDNA3β	NBS1	myc	1-116	X. Wu
pcDNA3β	NBS1	myc	92-246	X. Wu
pcDNA3β	NBS1	myc	209-363	X. Wu
pcDNA3β	NBS1	myc	343-501	X. Wu
pcDNA3β	NBS1	myc	475-634	X. Wu
pcDNA3β	NBS1	myc	613-754	X. Wu
pGEX-4T-1	p53	GST	1-72aa	J. Last
pRS314	Rad50	none	Full length - 1-1312	J. Petrini
pGEX-4T-1	RPA32	GST	Full length – 1-270	J. Last
p-BIND	TopBP1	GAL4	Full length – 1-1435	M. Morgan
p-BIND	TopBP1	GAL4	2-591	M. Morgan
p-BIND	TopBP1	GAL4	253-914	M. Morgan
p-BIND	TopBP1	GAL4	789-1435	M. Morgan

2.2.3.1 Large scale preparation.

Single colonies from plates containing successful transformants were picked and used to inoculate 5 ml cultures of LB containing 100 μg/ml ampicillin. Minicultures were incubated at 37°C with shaking at 200 rpm. After 6-8h the 5 ml cultures were added to flasks containing 500ml LB supplemented with 100 μg/ml ampicillin, and left to grow overnight at 37°C with shaking at 200 rpm. The following day, cells were pelleted by centrifugation at 6000 rpm for 15 min at 4°C. Plasmid DNA was extracted from bacterial pellets using a PureLink HiPure Plasmid Maxiprep Kit (Invitrogen), according to the manufacturer's instructions. DNA was concentrated with 2 volumes of isopropanol and pelleted by centrifugation at 6000 rpm for 1h at 4°C. Pellets were washed with 1.5 ml of ethanol, centrifuged as before and air dried under sterile conditions. DNA was resuspended in 400 μl of nuclease-free water (Ambion) and the concentration was measured using a NanoDrop spectrophotometer (Thermo Scientific).

2.2.3.2. Small scale preparation.

Single colonies from plates containing successful transformants were picked and used to inoculate 15 ml cultures of LB containing 100 μg/ml ampicillin. Minicultures were incubated at 37°C with shaking at 200 rpm overnight. The following day cultures were pelleted at 3000 rpm for 15 min at 4°C. Plasmid DNA was extracted from bacterial pellets using a QIAprep Spin Miniprep Kit (QIAGEN) according to the manufacturer's instructions and eluted in 30 μl of nuclease-free water (Ambion) and the concentration was measured using a NanoDrop spectrophotometer (Thermo Scientific).

2.2.4. Agarose gel electrophoresis.

Agarose gels were prepared by dissolving agarose (Invitrogen) in TBE (100 mM Tris-HCl, 100 mM boric acid, 2 mM EDTA, pH 8.0) buffer to a final concentration of 0.8%.

The resultant slurry was boiled in order to dissolve the agarose and allowed to cool before the addition of SybrSafe stain in DMSO solution (Invitrogen) at a 1:10 000 dilution and poured into the casting tray. Gels were allowed to set at room temperature. Samples were diluted with 6x loading buffer (0.25% bromophenol blue, 50% glycerol in a 10 mM Tris-HCl, 1 mM EDTA, pH 8.0 solution). Electrophoresis was carried out at 50V in TBE buffer for 30 min. DNA was visualized with a Safe Imager (Invitrogen).

2.2.5. Restriction enzyme digestion and insert purification by gel extraction.

Restriction enzymes: BamHI and Not1 were obtained from Roche and stored at -20˚C. Restriction enzyme digestion of GST-53BP1 1584-1972 aa, GST-MDC1 1686-2090 aa or pcDNA4/His C (Invitrogen) was carried out in a total volume of 50 μl at 37˚C for 3h in buffer 3 (NEB) with addition of Bovine Serum Albumin (BSA, NEB). Digestion products were separated by agarose gel electrophoresis and appropriate bands cut out from the gel. The gel extraction procedures were performed using QIAquick Spin Columns in accordance with manufacturer's instructions (QIAGEN). Briefly, bands of the expected size were excised from the gel and placed in a microfuge tube which was weighed. Three times the volume of the slice of QG buffer was added and mixtures were incubated at 50˚C until the slices dissolved. Mixtures were applied onto the column and centrifugated at 13000 rpm for 1 min. Columns were washed with PE buffer and bound DNA eluted in 30 μl of sterile distilled water by centrifugation at 13000 rpm for 1 min.

2.2.6. Ligations.

A vector:insert ratio of 1:5 was prepared in a total volume of 12μl that also contained 1μl (400 cohesive end units) of T4 DNA ligase and 1.2μl of ligase buffer as supplied by the manufacturer (NEB). The reaction was incubated at 16˚C overnight.

2.2.7. GST fusion protein expression and purification.

Plasmids encoding glutathione *S*-transferase (GST)–tagged proteins were used to transform BL21 bacteria as described above. Colonies from successful transformations were picked and used to inoculate 20ml LB media containing 100 μg/ml ampicillin. Cultures were incubated overnight at 37˚C with shaking at 200 rpm. The following day, 15ml of the overnight cultures were added to flasks containing 500ml LB with 100μg/ml ampicillin (the remainder of the overnight cultures was aliquoted, prepared for long-term storage by addition of sterile glycerol to final concentration of 50%, and kept at -80˚C). The flasks of bacterial cultures were incubated at 37˚C with shaking at 200 rpm. Once the cultures had reached an optical density of $A_{600} \cong$ 0.6-0.7, protein production was induced by addition of isopropyl-β-thiogalactopyranoside (IPTG) to a final concentration of 1 mM. The cultures were then transferred to an orbital incubator set at 30˚C and shaken at 200rpm for 4h, before centrifuging bacteria at 6000rpm for 10 min at 4˚C. Pellets were stored at -80˚C until used for protein purification.

To purify tagged proteins bacterial pellets were thawed and resuspended in ice-cold bufferA (1% Triton X-100, 2mM EDTA in PBS). Lysates were sonicated (3 x 30s) and centrifuged at 18,000 rpm for 20min at 4˚C to remove insoluble material. Supernatants were incubated twice with glutathione-agarose beads (Sigma-Aldrich) for 90 min with rotation at 4˚C. Beads were collected by centrifugation at 3000 rpm for 5 mins at 4˚C. Complexes were washed three times in buffer A and twice in buffer B (2mM EDTA in PBS). GST-fusion proteins were released by addition of GST elution buffer (25 mM glutathione, 50 mM Tris-HCl, pH 8.0). Beads were removed by centrifugation at 3000 rpm for 5 min at 4˚C, and supernatants were dialysed overnight at 4˚C against a solution of 10% glycerol, 150 mM NaCl, 1mM DTT, 50 mM Tris-HCl, pH 7.2. The

following day dialysis was repeated for 3 h in fresh buffer and GST-fusion proteins were collected, aliquoted and stored at -80˚C until further use.

Table 2.4. GST-tagged proteins used in this study.

Vector	Product	Tag	Amino acids	Origin
pGEX-4T-1	53BP1	GST	1-356	G. Stewart
pGEX-4T-1	53BP1	GST	333-759	G. Stewart
pGEX-4T-1	53BP1	GST	722-1039	G. Stewart
pGEX-4T-1	53BP1	GST	992-1331	G. Stewart
pGEX-4T-1	53BP1	GST	1309-1620	G. Stewart
pGEX-4T-1	53BP1	GST	1584-1972	G. Stewart
pGEX-4T-1	CtIP	GST	Full length – 1-897	J. Last
pGEX-4T-1	CtIP	GST	324-897	J. Last
pGEX-4T-1	CtIP	GST	42-132	R. Baer
pGEX-4T-1	CtIP	GST	45-620	R. Baer
pGEX-4T-1	CtIP	GST	133-462	R. Baer
pGEX-4T-1	CtIP	GST	371-620	R. Baer
pGEX-4T-1	CtIP	GST	620-897	R. Baer
pGEX-4T-1	CtIP	GST	775-897	R. Baer
pGEX-4T-1	MDC1	GST	1-380	G. Stewart
pGEX-4T-1	MDC1	GST	341-724	G. Stewart
pGEX-4T-1	MDC1	GST	791-1118	G. Stewart
pGEX-4T-1	MDC1	GST	1052-1720	G. Stewart
pGEX-4T-1	MDC1	GST	1686-2090	G. Stewart
pGEX-4T-1	p53	GST	1-72	J. Last
pGEX-4T-1	RPA32	GST	1-270	J. Last

2.2.8. In vitro transcription/translation.

Eukaryotic *in vitro* transcription and translation was carried out using the TNT T7/T3 Coupled Rabbit Reticulocyte Lysate System, according to the manufacturer's instructions (Promega). Briefly, a reaction was assembled using 25μl rabbit reticulocyte

lysate, 2 μl TNT reaction buffer, 1 μl T7 polymerase or SP6 polymerase in case of pcDNA3-CtIP construct, 1 μl 1mM amino acid mixture minus methionine, 2 μl [^{35}S]-methionine (1000 Ci/mmol at 10 mCi/ml), 1 μl Protector RNase Inhibitor (Roche), 2 μg DNA template and nuclease-free water (Ambion) to a final volume of 50 μl. Reactions were incubated at 30˚C for 90 min. The resultant protein was stored at -80˚C until required. All plasmids use to produce labelled proteins and polypeptides are listed in Table 2.5.

Table 2.5. Plasmids use to produce labelled proteins and polypeptides.

Vector	Product	Tag	Amino acids	Origin
pcDNA4/His	53BP1	His	1584-1972	In-house
pcDNA3	CtIP	none	Full length - 1-897	In-house
pcDNA4/His	MDC1	His	1686-2090	In-house
pRS314	Mre11	none	Full length – 1-708	J. Petrini
pcDNA3β	NBS1	myc	Full length – 1-754	X. Wu
pcDNA3β	NBS1	myc	1-116	X. Wu
pcDNA3β	NBS1	myc	92-246	X. Wu
pcDNA3β	NBS1	myc	209-363	X. Wu
pcDNA3β	NBS1	myc	343-501	X. Wu
pcDNA3β	NBS1	myc	475-634	X. Wu
pcDNA3β	NBS1	myc	613-754	X. Wu
pRS314	Rad50	none	Full length	J. Petrini
p-BIND	TopBP1	GAL4	Full length – 1-1435	M. Morgan
p-BIND	TopBP1	GAL4	2-591	M. Morgan
p-BIND	TopBP1	GAL4	253-914	M. Morgan
p-BIND	TopBP1	GAL4	789-1435	M. Morgan

2.2.9 Polymerase Chain Reaction (PCR) based techniques.

2.2.9.1 Site directed mutagenesis.

Primers used to generate mutated forms of GST-CtIP fragments are detailed in Table 2.6.

Table 2.6. Primer sequences used to generate mutated forms of GST-CtIP fragments.

GST-CtIP target fragment and mutated residues	Primer sequence	Company
371-620 aa, 506 S > A	**FWD:** 5′ CGT CAA GAG AAA GCC CAA GGA AGT GAG ACT 3′ **REV:** 5′ AGT CTC ACT TCC TTG GGC TTT CTC TTG ACG 3′	AltaBiosciences
371-620 aa, 555 S > A	**FWD:** 5′ GGG GAG CCC TGT GCA CAG GAA TGC ATC ATC 3′ **REV:** 5′ GAT GAT GCA TTC CTG TGC ACA GGG CTC CCC 3′	AltaBiosciences
324-897 aa, 506 S > A	**FWD:** 5′ CGT CAA GAG AAA GCC CAA GGA AGT GAG ACT 3′ **REV:** 5′ AGT CTC ACT TCC TTG GGC TTT CTC TTG ACG 3′	AltaBiosciences
324-897 aa, 555 S > A	**FWD:** 5′ GGG GAG CCC TGT GCA CAG GAA TGC ATC ATC 3′ **REV:** 5′ GAT GAT GCA TTC CTG TGC ACA GGG CTC CCC 3′	AltaBiosciences

324-897 aa, 664 S > A	**FWD:** 5′ GGA GCA GAC CTT GCT CAG TAT AAA ATG GAT 3′ **REV:** 5′ ATC CAT TTT ATA CTG AGC AAG GTC TGC TCC 3′	AltaBiosciences
324-897 aa, 679 S > A	**FWD:** 5′ ACA AAG GAT GGC GCT CAG TCA AAA TTA GGA 3′ **REV:** 5′ TCC TAA TTT TGA CTG AGC GCC ATC CTT TGT 3′	AltaBiosciences
324-897 aa, 745 S > A	**FWD:** 5′ GCA GAC AGT TTC GCC CAA GCA GCA GAT GAA 3′ **REV:** 5′ TTC ATC TGC TGC TTG GGC GAA ACT GTC 3′	AltaBiosciences
324-897 aa, 859 T > A	**FWD:** 5′ GGT TTT CCT TCC GCT CAG ACT TGT ATG GAA 3′ **REV:** 5′ TTC CAT ACA AGT CTG AGC GGA AGG AAA ACC 3′	AltaBiosciences

Site directed mutagenesis was carried out using reagents from Promega unless otherwise stated. Briefly, the reaction mix was assembled as follows: 5 μl of 10x Buffer containing 20mM $MgSO_4$, 50 ng of plasmid DNA template, 1 μl of appropriate primer set, 1 μl deoxynucleotide triphosphate (dNTP) mix (10 mM), 1 μl *Pfu* DNA Polymerase all made up to 50 μl with nuclease-free water (Ambion). The reaction was performed in a thermocycler (Applied Biosystems) according to the below protocol:

95˚C => 30 s

16 cycles

95˚C => 30 s

55˚C => 1 min

68˚C => 13 min for GST-CtIP 324-897aa or 11 min for GST-CtIP 371-620

4˚C => ∞

To remove the parental unmutated plasmid DNA after PCR, 1 μl of DpnI enzyme was added and the mix was incubated for 3h at 37°C. Following the digestion, mutated plasmid DNA was transformed into XL10 Gold bacteria as described above. Successful transformants were picked for small scale plasmid DNA purification. Purified DNA was used to transform BL21 bacteria to produce mutated GST-CtIP proteins.

2.2.9.2. DNA sequencing.

Site-directed mutagenesis products and pcDNA4/His-53BP1 and pcDNA4/His-MDC1 constructs were purified and sequenced in 20 μl reactions containing 1 μl ABI Prism Big Dye Terminator (Applied Biosystems), 4 μl 5x buffer (Applied Biosystems), 250 ng plasmid DNA, 5 pmol sequencing primer. PCR conditions were as follows:

29 cycles

96°C => 10 s
50°C => 5 s
60°C => 4 min

4°C => ∞

Sequencing reactions were subsequently isopropanol precipitated and resuspended in 10 μl Hi-Di Formamide for use with the ABI Prism 3130xl Genetic Analyser DNA Sequencer (Applied Biosystems).

2.3. Protein biochemistry techniques.

2.3.1. Preparation of total cell lysates.

Cell culture medium was removed and cells were washed twice in PBS. Samples were lysed and harvested by addition of denaturing buffer (9 M urea, 150 mM β-

mercaptoethanol, 50 mM Tris-HCl, pH 7.3). Cells were sonicated for 15 s on ice and samples were used immiediately or stored at -80˚C.

2.3.2. Determination of protein concentration.

Protein concentrations were determined by Bradford assay. A small volume (1 – 2 μl) of lysate was mixed with 1 ml of Bradford reagent (BioRad) diluted 1:4 with deionised water. The same procedure was applied to BSA to obtain concentrations ranging from 0 – 10 μg/ml to generate a standard curve for comparison purposes on a spectrophotometer (Cecil, CE9200) at a wavelength of 595 nm against a blank of deionised water.

2.3.3. SDS-polyacrylamide gel electrophoresis (SDS-PAGE).

Protein samples were separated by SDS-PAGE. Polyacrylamide gels were made using 30% Acrylamide/Bis Solution (Severn Biotech) diluted with deionised water to give the appropriate percentage. Generally, gels used to separate molecules of around 200 – 350 kDa contained 8% acrylamide and 11% for separation of lower molecular weight proteins. Gel solutions also contained 100 mM Tris, 100mM Bicine, 0.1% SDS and 0.25% TEMED. Acrylamide polymerisation was initiated by addition of ammonium persulfate (APS) to a final concentration of 0.05%. Gels were assembled using Hoeffer Scientific apparatus according to the supplied instructions and electrophoresis was carried out in buffer containing 100 mM Tris, 100mM Bicine and 0.1% SDS. Protein samples were prepared for SDS-PAGE by addition of Laemmli Sample Buffer (BioRad), before being heated at 90˚C for 5 min. Pre-stained protein molecular weight markers were used to identify analysed proteins. After loading samples onto the gel the electrophoresis was generally run overnight at constant current depending on the size of the proteins of interest.

2.3.4. Protein visualization in polyacrylamide gels.

After electrophoresis, gels were stained with 0.1% Coommassie Brilliant Blue R-250 (Sigma-Aldrich), 10% glacial acetic acid, 20% methanol in deionised water and left at room temperature for 30 min with agitation. To visualise protein bands gels were destained in 10% glacial acetic acid, 20% methanol in deionised water until the bands were clearly visible.

2.3.5. GST-pull down assays with radioactive proteins.

GST-fusion proteins and [^{35}S]-labelled proteins were produced as described above. Typically, 30 μg of GST-fusion protein diluted in 150 μl of buffer A, described above, supplemented with 1% BSA was mixed with 10 μl of [^{35}S]-labelled protein reaction mixture and incubated on ice for 1.5 h. Protein complexes were isolated by incubation with glutathione-agarose beads for 1h with rotation. Beads were washed three times in buffer A and twice in buffer B described above. Samples were analyzed by SDS-PAGE, followed by fluorography and autoradiography.

2.3.6. Detection of radioactive proteins by fluorography and autoradiography.

Gels were incubated twice in DMSO for 30 min each time and subsequently in 23% 2,5-Diphenyloxazole solution in DMSO for 3 h. Gels were rehydrated for 1h in deionised water and dried for 2h under vacuum at 80˚C. Dried gels were exposed for autoradiography at -20˚C using KODAK Medical X-ray film. Alternatively gels were agitated in Amplify (GE Healthcare) for 30 min and then dried.

2.4. Immunocytochemistry techniques.

2.4.1. Antibodies.

All antibodies used in this study and their origins are shown in Table 2.7.

Table 2.7. Primary antibodies used in this study.

Antigen	Antibody	Source	Use	Dilution	Origin
53BP1	3661	Rabbit	IF, WB	1/500	G. Stewart
53BP1	3662	Rabbit	IP	1/100	G. Stewart
53BP1-pS1778	2675	Rabbit	WB	1/1000	Cell signalling
β-actin	AC-74	Mouse	WB	1/50000	Sigma-Aldrich
ATR	2B5	Mouse	IP, WB	1/200;1/1000	Abcam
ATM	11G12	Mouse	IP, WB	1/100; 1/500	J. Last
ATM-pS1981	1655	Rabbit	WB	1/500	R&D Systems
BLM	C-18	Goat	IP, WB	1/50; 1/500	Santa Cruz
BRCA1	D-9	Mouse	IF	1/10	Santa Cruz
CtIP	14-1	Mouse	IF, WB	1/20; 1/250	R. Baer
CtIP	222	Rabbit	IP	1/100	In-house
H2AX	07-627	Rabbit	WB	1/1000	Upstate
γ-H2AX	JBW301	Mouse	IF, WB	1/1000	Upstate
MDC1	12/13	Rabbit	IF, WB	1/100; 1/500	G. Stewart
MDC1	40/41	Rabbit	IP	1/100	G. Stewart
MDC1	M2444	Mouse	WB	1/1000	Sigma-Aldrich
Mre11	12D7	Mouse	WB	1/1000	Gene Tex
NBS1	1C3	Mouse	WB	1/1000	Gene Tex
NBS1-S343	12297	Rabbit	WB	1/500	Abcam
Rad50	13B3/2C6	Mouse	WB	1/1000	Ambion
RPA70	Ab-1	Mouse	WB	1/1000	Calbiochem

SMC1	A300-055A	Rabbit	WB	1/500	Bethyl Laboratories
SMC1-pS966	A300-050A	Rabbit	WB	1/500	Bethyl Laboratories
SMG1	A300-393A	Rabbit	WB	1/500	Bethyl Laboratories
SMG1	A300-394A	Rabbit	IP	1/100	Bethyl Laboratories

Table 2.8. Secondary antibodies used in this study.

Antigen	Antibody	Source	Use	Dilution	Origin
Goat IgG	P0449	Rabbit	WB	1/2000	DAKO
Goat IgG	AlexaFluor488	Donkey	IF	1/1000	Molecular Probes
Goat IgG	AlexaFluor594	Donkey	IF	1/1000	Molecular Probes
Mouse IgG	P0447	Goat	WB	1/2000	DAKO
Mouse IgG	AlexaFluor488	Donkey	IF	1/1000	Molecular Probes
Mouse IgG	AlexaFluor594	Donkey	IF	1/1000	Molecular Probes
Rabbit IgG	P0399	Swine	WB	1/3000	DAKO
Rabbit IgG	AlexaFluor488	Donkey	IF	1/1000	Molecular Probes
Rabbit IgG	AlexaFluor594	Donkey	IF	1/1000	Molecular Probes

2.4.2. Immunoprecipitations.

Cell lysates were prepared by washing dividing cells twice in PBS followed by addition ice-cold immunoprecipitation (IP) buffer containing 1% Nonidet P-40, 150 mM NaCl, 1 mM EDTA, 50 mM Tris-HCl (pH 7.3). Cell lysates were homogenized using a Wheaton-Dounce glass homogeniser and centrifuged at 40,000 rpm for 30 min at 4°C to remove insoluble material. Antibodies were added to cleared lysates and antibody-antigen

complexes were left to form overnight at 4°C. The following day Protein G-Sepharose beads (Sigma-Aldrich) were added to the samples for 1 h at 4°C with rotation. The sepharose beads were centrifuged and washed four times in ice-cold IP buffer, before addition of 30 μl Laemmli Sample Buffer (BioRad) to elute proteins. Samples were boiled and centrifuged in preparation for SDS-PAGE and Western blotting.

2.4.3. Western blotting.

After SDS-PAGE, separated proteins were transferred onto a nitrocellulose membrane using a Hoeffer Scientific transfer system. Briefly, gels and nitrocellulose membranes were soaked for 5 min in blotting buffer (50 mM Tris, 190 mM glycine, 20% methanol). Individual gels were laid onto a nitrocellulose membrane of similar size, sandwiched between two pieces of pre-soaked Whatman 3 MM blotting filter paper and two blotting pads, and placed in plastic cassettes. These were then put into the blotting tank and electro-transfer was carried out for 6–8 h at 300 mA. After the transfer membranes were stained with a solution containing 0.1% Ponceau S (Sigma-Aldrich), 3% trichloroacetic acid for 3 min. To visualize the proteins membranes were washed in water and in 0.1% Tween 20, 150 mM NaCl, 20 mM Tris-HCl, pH 7.3 (TBST) to remove protein staining.

Nitrocellulose membranes were blocked in 5% skimmed dried milk powder in PBS for 1h at room temperature with agitation, followed by washing in TBST. Blots were shaken overnight at 4°C with antibodies at the appropriate dilution in TBST containing 5% milk. The following day, blots were washed six times in TBST, before incubation at room temperature with the appropriate horseradish peroxidise-conjugated (HRP) secondary antibodies in TBST containing 5% milk with agitation. After 2 h blots were again washed six times in TBST. Specific antigens were detected using ECL reagent

(GE Healthcare) or Immobilon Western HRP Substrate (Millipore) and KODAK Medical X-ray film.

2.4.4. Kinase assay.

Cell lysates were prepared in several ways. For the ATM kinase assay dividing LCLs were irradiated with 5Gy and harvested 30 min post-irradiation. For the ATR kinase assay dividing LCLs were harvested without previous irradiation . For the SMG1 kinase assay dividing LCLs were mock-treated or treated with 5mM caffeine and harvested 1 h post-treatment. For the CtIP kinase assay HeLa cells depleted of ATM we irradiated with 5Gy and harvested 30 min post treatment or LCLs were mock-treated or treated with 5mM caffeine for 30 min and subsequently irradiated with 5Gy and harvested 30 min post-irradiation. After harvesting, the cells were washed twice in PBS and subsequently lysed in ice-cold immunoprecipitation buffer (TGN) containing 50mM Tris pH7.5, 150mM NaCl, 10% Glycerol, 50mM β-Glycerophosphate, 1% Tween-20, 0.2% Nonidet P40 supplemented before use with 10mM NaF. Cell lysates were homogenized using a Wheaton-Dounce glass homogeniser and centrifuged at 40,000 rpm for 30 min at 4°C to remove insoluble material. Antibodies were added to cleared lysates and antibody-antigen complexes were left to form for 3 h on ice. Following the incubation Protein G-Sepharose beads (Sigma-Aldrich) were added to the samples for 1 h at 4°C with rotation. Sepharose beads were centrifuged and washed three times in ice-cold TGN buffer, once in TGN buffer supplemented with 0.5M LiCl and twice in kinase buffer containing 20mM HEPES pH 7.5, 50mM $MgCl_2$, 10mM $MnCl_2$ and supplemented before use with 1mM NaF and 0.5mM DTT. After the last wash 30μl of kinase buffer, 10μg of GST-CtIP protein or 10μg of GST alone or 20μg GST-53BP1 protein or 20μg of GST alone and 1μl of [^{32}P]γ-ATP (PerkinElmer) were added to each sample. Kinase assays were performed at 37°C for 5 min for the phosphorylation of GST-CtIP fragments and

for 10 min for the phosphorylation of the GST-53BP1 fragment. To stop the reaction Laemmli Sample Buffer was added and samples were heated to 95°C for 5 mins and separated over night in 11% SDS-PAGE gels. The following day gels were Coommassie-stained, dried and radioactive signals detected by autoradiography.

2.4.5. Immunofluorescence.

Hela cells were seeded on 12-well glass slides to densities of around 1-2 x 10^4cell/well. The following day the slides were mock irradiated or irradiated with 9Gy and incubated for 1 h. Cells were then washed twice in PBS, fixed in 4% w/v paraformaldehyde in PBS for 10 min and washed again in PBS. Methanol extraction was carried out for 15 min at -20°C. Cells were rehydrated in PBS and blocked in PBS for 1 h. Primary antibodies were diluted to appropriate concentration in 0.1% FCS in PBS, and were incubated with the cells for 1 h in light-proof container. After the incubation cells were washed five times in PBS and incubated with secondary antibodies diluted in 0.1% FCS in PBS for 1 h in the same container. Slides then were washed five times in PBS, air-dried and mounted in Vectashield Mounting Medium (Vector Laboratories) containing 4',6-diamidino-2-phenylindole (DAPI), and protected with glass coverslips. Cells were viewed on a Zeiss Axioskop microscope, and z-Layer images (0.1 μm horizontal sections) were recorded with Openlab v3.0.9 Biovision software package (Improvision). Single, deconvoluted z-Layers were merged to show colocalizations.

CHAPTER III

RESULTS

CtIP interacts with the DNA damage response proteins containing BRCT domains.

3.1. CtIP associates with proteins containing BRCT domains.

3.1.1. Introduction.

BRCT domains are found in a large number of proteins and as an evolutionarily conserved module they exist in a wide range of organisms from prokaryotes to eukaryotes. It was first identified as a 90-100 amino acid tandem repeat at the C-terminus of the BRCA1 gene product. It can appear as a single or multiple motif comprising several characteristic clusters of conserved hydrophobic residues that form the core of the BRCT fold. It is found in many proteins that are involved in DNA-damage check point control and DNA repair (Bork et al., 1997; Callebaut & Mornon, 1997). It has been shown that the tandem BRCT repeats of BRCA1 function as a phosphopeptide binding module, although, the isolated individual repeat does not (Manke et al., 2003; Rodriguez et al., 2003; Yu et al., 2003). The binding of BRCT domains to phosphorylated peptide targets has been reported for other proteins involved in the DNA damage response, thus it could be concluded that it may be a common property of the BRCT-containing proteins. The BRCT domain of BRCA1 binds with higher affinity to serine-phosphorylated peptides that contain phenylalanine three residues downstream of phosphoserine (pSer-X-X-Phe), than to unphosphorylated peptides (Manke et al., 2003; Yu et al., 2003). This may represent a general rule of how BRCT domains of BRCA1, as well as BRCT domains in other proteins, interact with their binding partners in response to the DNA damage-induced cellular signalling cascade.

In previous studies BRCA1 was shown to interact with CtIP via its BRCT domains; tumour-associated mutations in the BRCT domains abolished that interaction. (Li et al., 1999; Wong et al., 1998; Yu et al., 1998). This indicates the importance of this association and places CtIP as a possible tumour suppressor protein (Chinnadurai,

2006; Wu & Lee, 2006). Recently it has also been shown that the choice of DNA repair pathway depends on the phosphorylation status of CtIP's Ser327 and its subsequent interaction with the BRCT domains of BRCA1. Thus CtIP is not only required for repair of DSBs by homologous recombination together with BRCA1 in S/G2 phase but also for MMEJ (microhomology-mediated end-joining) in G1 (Yun & Hiom, 2009). These findings suggest that CtIP's interaction with the BRCT domains of BRCA1 is crucial for the cell's survival. Thus, one can hypothesise that CtIP would interact with the BRCT domains present in other proteins. As most BRCT domain-containing proteins are involved in crucial stages of cell survival and cell cycle, CtIP could be found as an adaptor protein that modulates the transitions into different repair pathways, depending on the stage of the cell cycle. Thus it was interesting to see which of the BRCT domain-containing proteins interact with CtIP and via which region that interaction occurred. It was decided to investigate possible interactions with four of those proteins namely 53BP1, MDC1, TopBP1 and NBS1. 53BP1 has been shown to be mainly involved in an XRCC4-dependent NHEJ as it interacts with dimethylated K20 of H4 and this DNA repair process is γ-H2AX independent. MDC1 has been reported to function primarily in HR in a γ-H2AX-dependent manner (Kotnis et al., 2009; Xie at el., 2007). NBS1, like MDC1, is involved in HR and recently has been shown to take part in MMEJ (Deriano et al., 2009; Tauchi et al., 2002). TopBP1 is involved in the DNA damage response via its interaction with ATR and ATRIP and subsequent activation of ATR (Kumagai et al., 2006).

3.1.2. Results.

3.1.2.1. The interaction of CtIP with 53BP1.

53BP1 is a DNA damage mediator protein containing several ATM/ATR phosphorylation sites, a dimerization motif followed by G-A (glycine-alanine) rich region, the tandem

Tudor domain (methylated protein binding domain), NLS (nuclear localization signal) and the tandem repeat of BRCT domain at the C-terminus. The dimerization motif, GAR and Tudor domain form a kinetochore-binding domain (KBD; Jullien et al., 2002; Figure.3.1.). Human 53BP1 protein was arbitrarily divided into six fragments and the corresponding cDNA was cloned into a pGEX vector. The GST-tagged proteins were expressed and purified as described in section 2.2.7. Figure.3.1. shows the domain localization and the distribution of amino acids in the GST-53BP1 fragments.

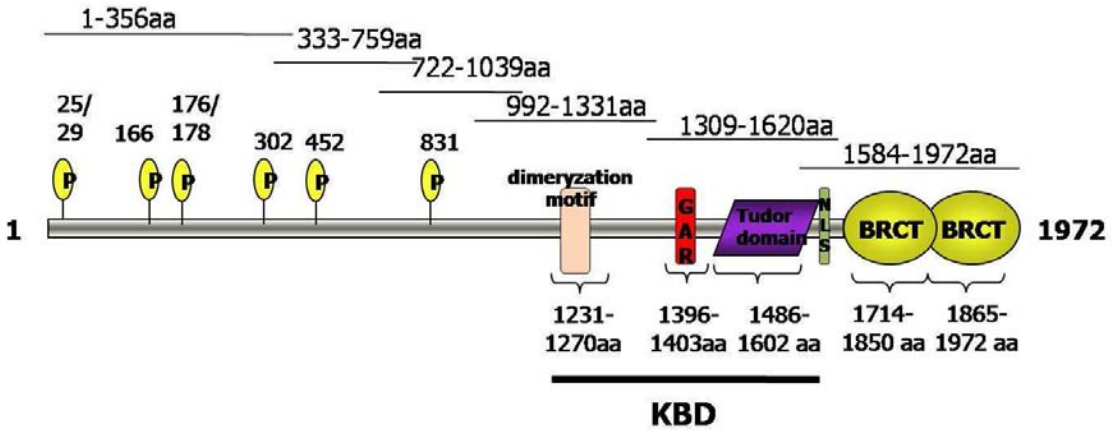

Figure.3.1. The amino acid distribution in the GST-53BP1 fragments, the domain structure and ATM/ATR phosphorylation sites of human 53BP1 protein. GAR – glycine-arginine rich, KBD – kinetochore binding domain, NLS – nuclear localization signal

To establish whether CtIP associates with 53BP1 a co-immunoprecipitation assay was performed. A rabbit antibody against 53BP1 was used and immunoprecipitated complexes were isolated with protein G-Sepharose beads as described in the section 2.4.2. Interacting CtIP was visualised by Western blotting as shown in Figure.3.2.a.

To determine direct interaction and the binding sites for CtIP on 53BP1 a GST-pull down assay was performed as described in the section 2.3.5. The equivalent of 10 μg of non-degraded GST-tagged 53BP1 fragments, assessed on the basis of previously

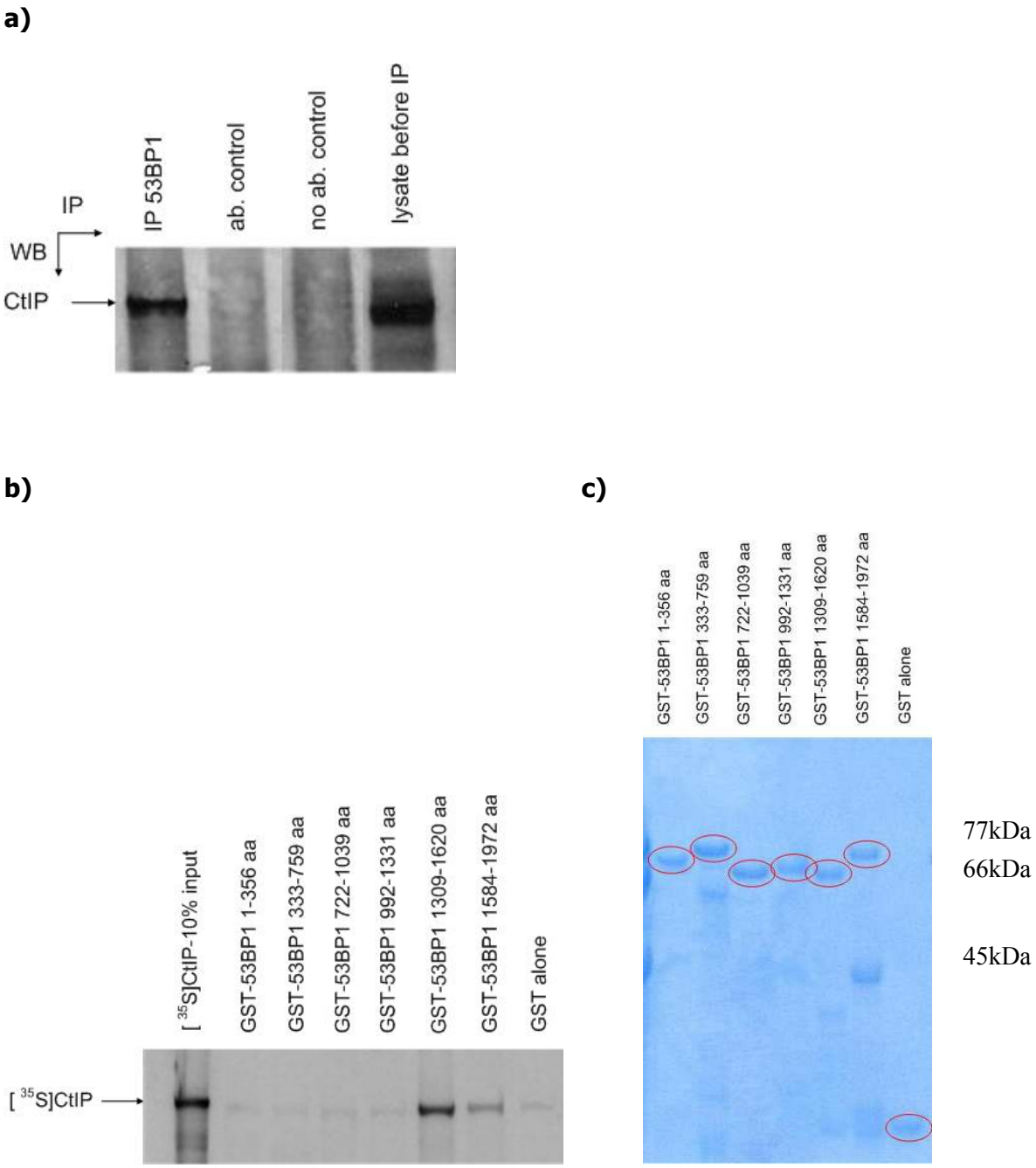

Figure.3.2. CtIP associates with 53BP1 *in vivo* and directly binds to 53BP1. **a)**, HeLa cell lysates were immunoprecipitated with an antibody against 53BP1 and coimmunoprecipitating CtIP was identified by Western blotting. **b)**, GST-53BP1 polypeptides were incubated with [^{35}S]CtIP, and complexes isolated with glutathione-agarose beads. Bound proteins were visualised by SDS-PAGE and audioradiography, **c)** Coomassie Brilliant Blue stained gel representing the GST-53BP1 fragments used in the experiment. This figure is representative of three independent experiments.

a)

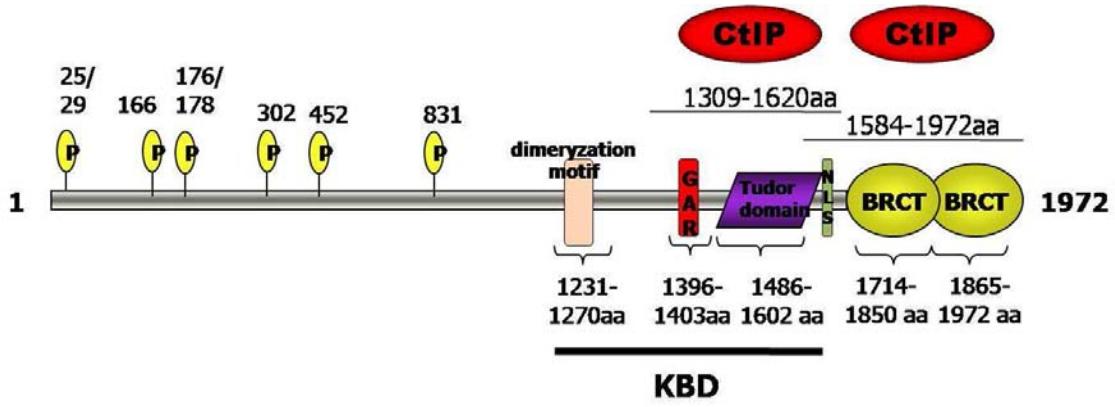

b)

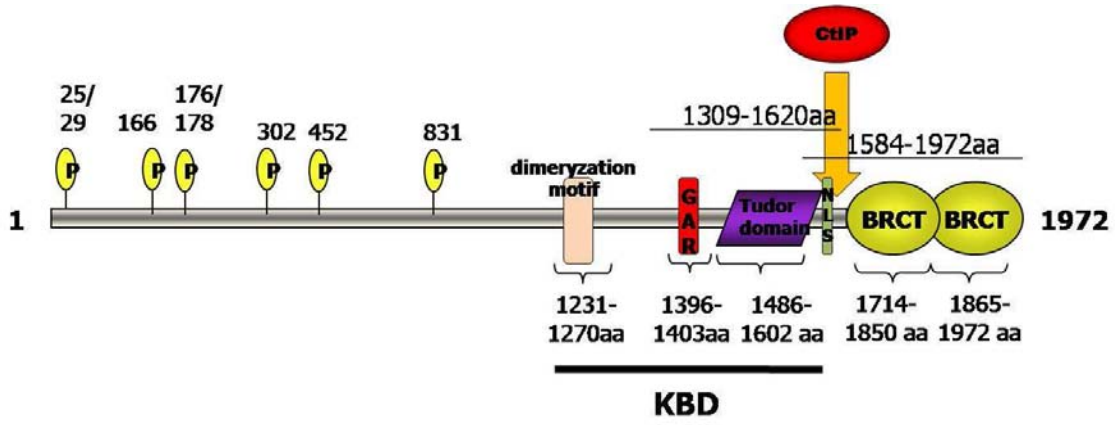

Figure.3.3. The possible interaction sites of CtIP with 53BP1. a) CtIP interacts with 53BP1 via its Tudor domain and the tandem repeat of the BRCT domains, **b)** CtIP interacts with 53BP1 via a polypeptide fragment that is located in the region where the two GST-53BP1 fragments, that bind to CtIP, overlap.

stained Coomassie Brilliant Blue stained gel was used in each reaction. Six different GST-53BP1 fragments, covering the whole of 53BP1 (Figure.3.1.) were incubated with full length [^{35}S]CtIP. Radioactively labelled CtIP was synthesized using full length CtIP cDNA cloned into a pcDNA3 vector, which has a SP6 promoter site for an *in vitro* transcription/translation reaction as described in section 2.2.8. Complexes were isolated with glutathione-agarose beads and fractionated by SDS-PAGE. The autoradiograph shows CtIP binding to two GST-53BP1 fragments stretching from 1309-1620aa and including the Tudor domain and 1584-1972aa including tandem repeats of the BRCT domain (Figure.3.2.b). This result suggests that there could be a binding site in each of the fragments or one binding site in the region where the two fragments overlap (amino acids 1584-1620, Figure.3.3.).

3.1.2.2. The interaction of CtIP with MDC1.

Following the demonstration that CtIP binds to 53BP1 a second novel associated protein was identified as MDC1. MDC1 is a DNA damage response mediator protein found to contain an FHA domain (phosphothreonine recognition domain, Durocher D. & Jackson S. P., 2002) at the N-terminus, a PST domain localized in the centre of the protein and tandem repeats of the BRCT domains at the C-terminus (Figure.3.4). Human MDC1 cDNA was arbitrarily divided into five fragments and the corresponding fragments were cloned into a pGEX vector. The equivalent of 10 μg of non-degraded GST-tagged MDC1 fragments, assessed on the basis of previously stained Coomassie Brilliant Blue stained gel was used in each reaction. The GST-tagged proteins were expressed and purified as described in section 2.2.7. Figure.3.4. shows the domain localization and the distribution of amino acids in GST-MDC1 fragments.

An immunoprecipitation experiment, as described in section 2.4.2, was performed to investigate the *in vivo* association of CtIP and MDC1. An MDC1 rabbit antibody was

used to immunopreciptate MDC1 and associated proteins from HeLa cell lysates. Complexes were isolated with protein G-Sepharose beads and associated CtIP was visualized by Western Blotting as shown in Figure.3.5.a.

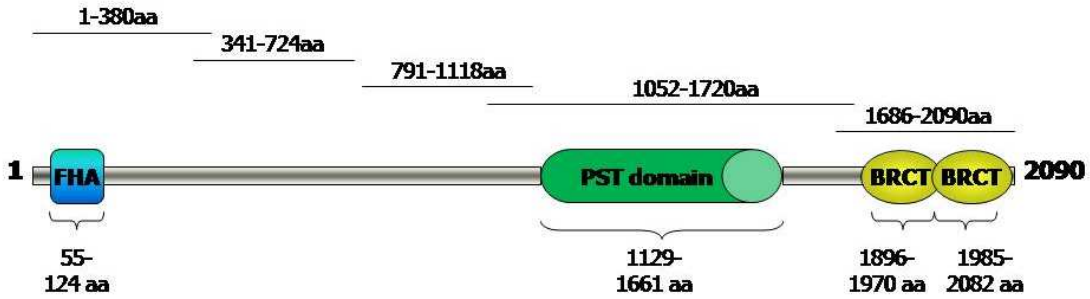

Figure.3.4. Cartoon of the amino acid distribution in the GST-MDC1 fragments and the domain structure of human MDC1.

To establish binding sites for CtIP on MDC1 a GST-pull down assay was performed (see section 2.3.5). Full length [^{35}S]CtIP, generated using full length CtIP cDNA cloned into a pcDNA3 vector and translated *in vitro* (see section 2.2.8.), was incubated with five GST-MDC1 fragments covering the whole of MDC1 (Figure.3.4.). Complexes were isolated with glutathione-agarose beads, fractionated by SDS-PAGE and visualised by autoradiography. A GST-MDC1 fragment which is composed of amino acid residues 1052-1720 and includes the PST domain and a fragment comprising 1686-2090aa including tandem repeat of the BRCT domain bind to full length [^{35}S]CtIP, Figure.3.5.b. This result suggests two CtIP binding sites on MDC1 or one binding site in the region where the two GST-MDC1 fragments overlap (amino acid residues 1686-1720, Figure.3.6.).

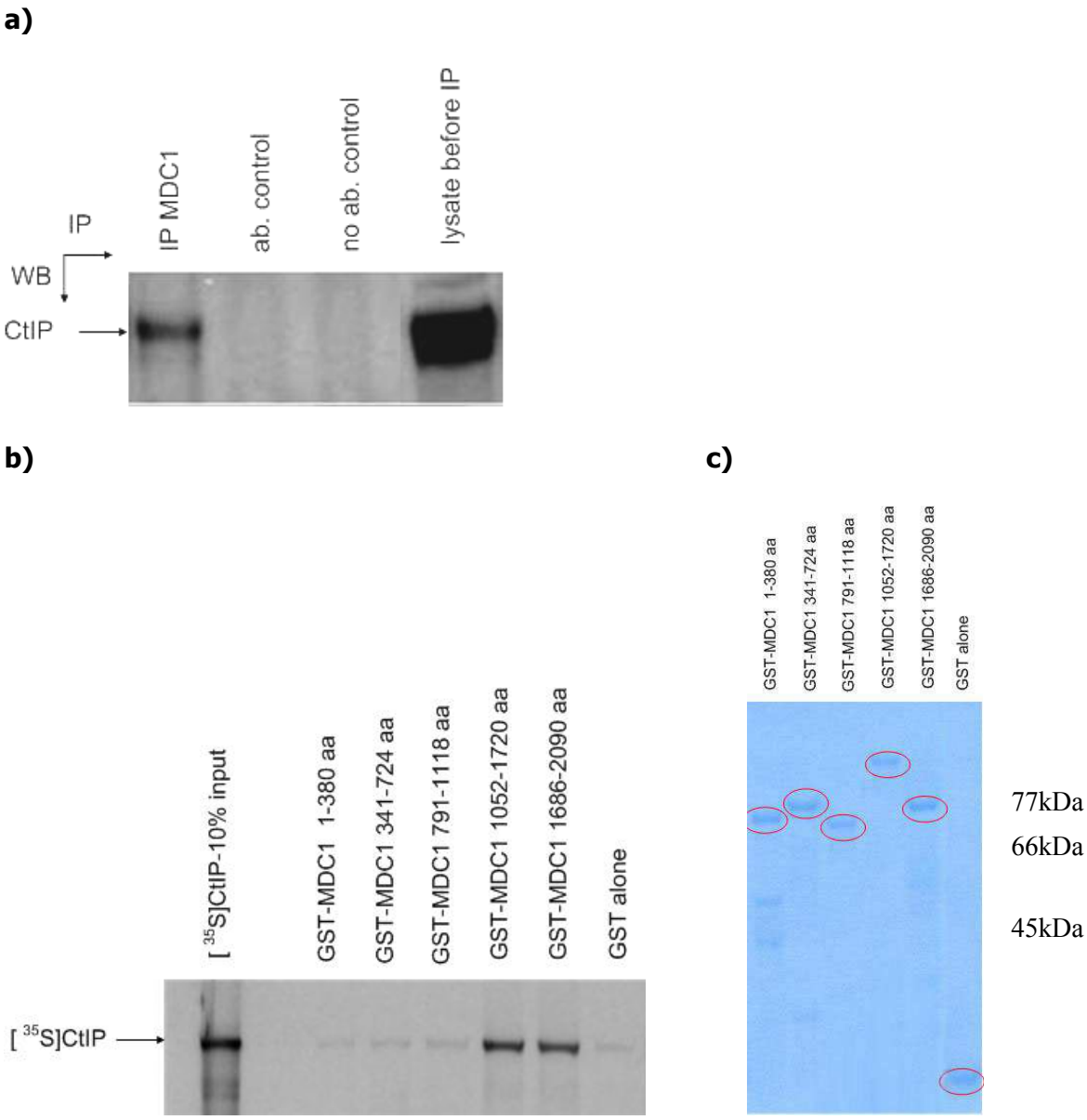

Figure.3.5. CtIP associates with MDC1 *in vivo* and directly binds to MDC1. a), Hela cell lysates were immunoprecipitated with an antibody against MDC1. Coimmunoprecipitating CtIP was identified by Western blotting. **b)**, GST-MDC1 polypeptide fragments were incubated with [^{35}S]CtIP, and complexes isolated with glutathione-agarose beads. Bound proteins were visualised by SDS-PAGE and audioradiography, **c)** Coomassie Brilliant Blue stained gel representing the GST-MDC1 fragments used in the experiment. This figure is representative of three independent experiments.

a)

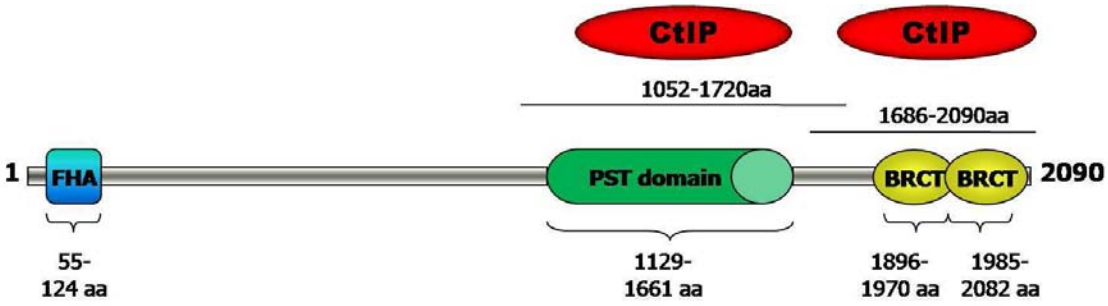

b)

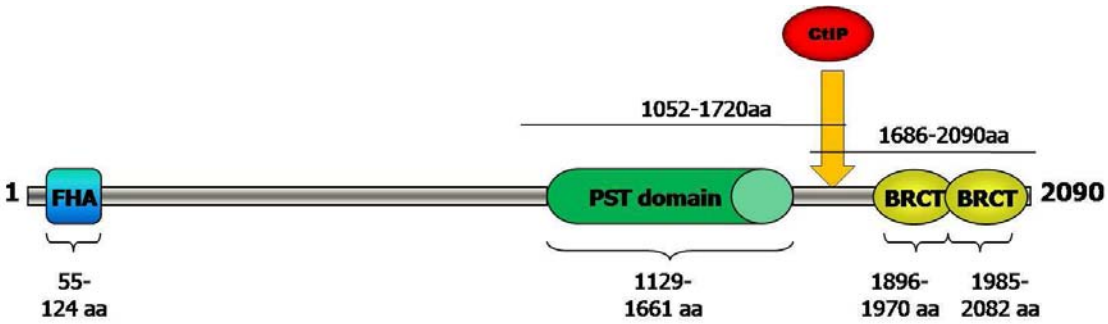

Figure.3.6. The possible interaction sites of CtIP with MDC1. a) CtIP interacts with MDC1 via its PST domain and the tandem repeat of the BRCT domains, **b)** CtIP interacts with MDC1 via a polypeptide fragment that is located in the region where the two GST-MDC1, that bind to CtIP, overlap.

3.1.2.3. The interaction of CtIP with TopBP1.

TopBP1, like 53BP1 and MDC1, falls into the DNA damage response mediator protein category. It contains eight BRCT domains which are spread throughout the whole of the protein. Human TopBP1 protein was arbitrarily divided into three fragments and the corresponding cDNAs, as well as the full length cDNA, were cloned into a pBIND vector (Wright et al., 2006), which has a T7 promoter site for *in vitro* transcription/translation as described in the section 2.2.8. Figure.3.7. shows the ATR activation domain and the BRCT domain localization and the distribution of amino acids in the pBIND-TopBP1 fragments.

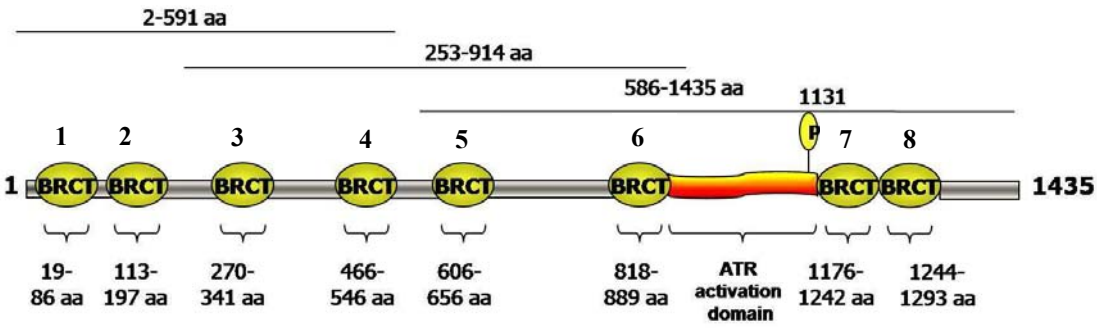

Figure.3.7. The amino acid distribution in the pBIND-TopBP1 fragments and the domain structure of human TopBP1 with the ATM phosphorylation site.

To assess CtIP and TopBP1 interaction *in vivo*, a co-immunoprecipitation experiment was performed. HeLa cell lysate was incubated with a rabbit TopBP1 antibody and bound protein complexes were isolated using protein G-Sepharose beads. To detect associated CtIP a Western blot was carried out. As shown in Figure.3.8.a. CtIP associates with TopBP1 *in vivo*.

In order to establish direct interaction and binding sites for CtIP on TopBP1 a GST-pull down assay was performed (see section 2.3.5). Full length [^{35}S]TopBP1 and three

[^{35}S]TopBP1 fragments covering the whole of the protein were incubated with three GST-CtIP fragments. The equivalent of 10 μg of non-degraded GST-tagged CtIP fragments, assessed on the basis of previously stained Coomassie Brilliant Blue stained gel was used in each reaction. Complexes were isolated with glutathione-agarose beads, fractionated by SDS-PAGE and detected by autoradiography. As shown in Figure.3.8.b.&c. full length [^{35}S]TopBP1 and a fragment composed of amino acid residues 2-591 bind to all three GST-CtIP fragments. As the fragment composed of residues 253-914 does not bind to CtIP we hypothesise that CtIP binds directly to TopBP1 via its first two BRCT domains (Figure.3.10.a).

Additional bands on the Coomassie Brilliant Blue stained gel, not marked by the red circles, are most likely a product of degradation of the originally GST-tagged protein or bacterial-protein contamination, Figure.3.8.c.

To investigate further the direct interaction of these two proteins and establish CtIP binding sites for TopBP1, another GST-pull down assay was performed. In this experiment full length TopBP1 and the 2-591aa fragment were incubated with five different overlapping GST-CtIP fragments covering different regions of CtIP. The equivalent of 10 μg of non-degraded GST-tagged CtIP fragments, assessed on the basis of previously stained Coomassie Brilliant Blue stained gel was used in each reaction. Complexes were isolated with glutathione-agarose beads, fractionated by SDS-PAGE and bound full length and 2-591aa fragment of [^{35}S]TopBP1 were visualized by autoradiography. As shown in Figure.3.9. full length [^{35}S]TopBP1 (Figure.3.9.a.) and the 2-591aa fragment (Figure.3.9.b.) each bind to four GST-CtIP fragments. On the basis of the GST-CtIP fragments composition it was concluded that TopBP1 has probably two binding sites on CtIP, within peptides encompassing residues 133-371aa and 620-775aa (Figure.3.10.b). The first of the CtIP regions contains

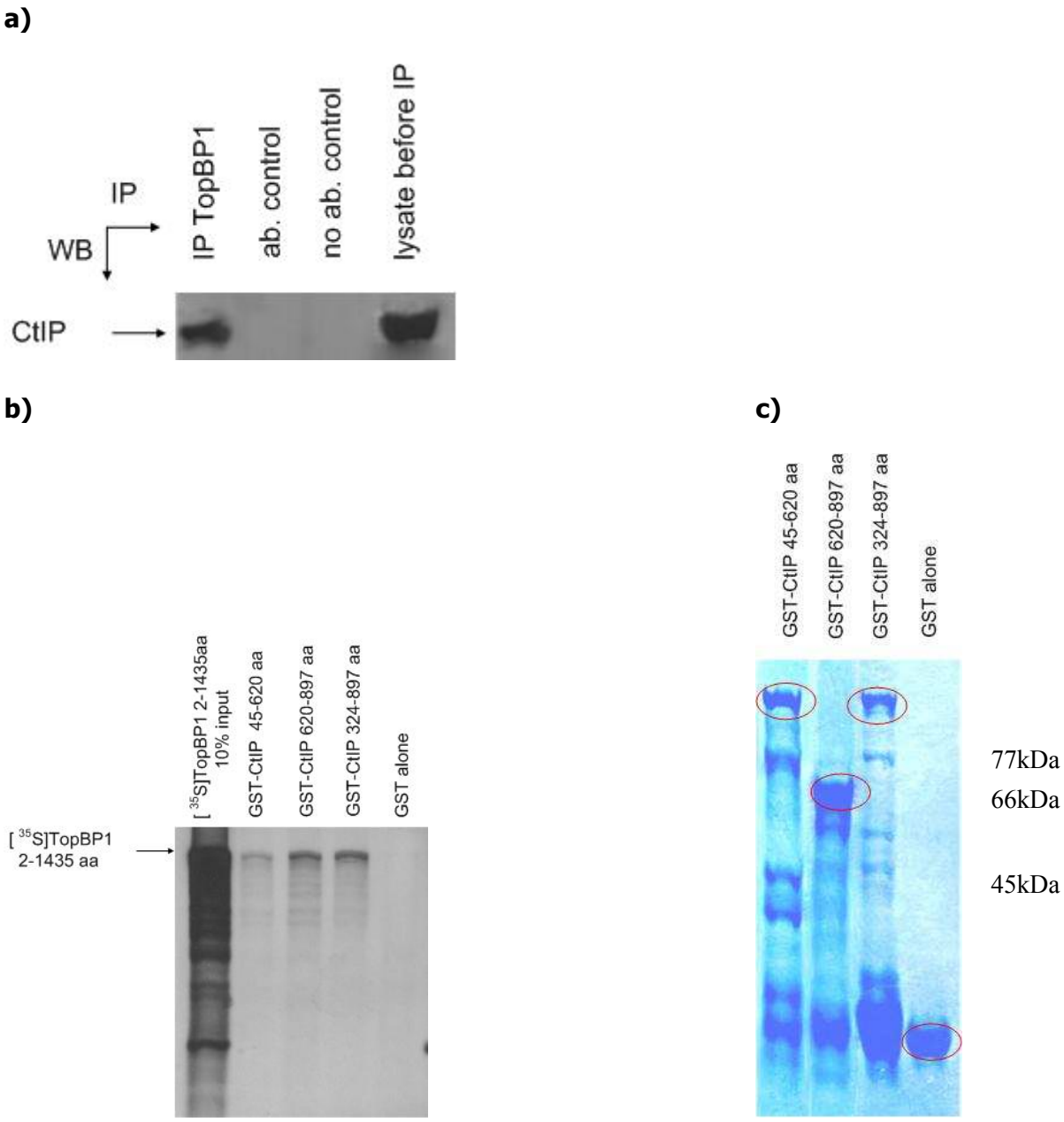

Figure.3.8. CtIP associates with TopBP1 *in vivo* and directly binds to TopBP1. a), Hela cell lysates were immunoprecipitated with an antibody against TopBP1. Coimmunoprecipitating CtIP was identified by Western blotting. **b)**, [^{35}S]TopBP1 full length fragment was incubated with various GST-CtIP polypeptide fragments, and complexes isolated with glutathione-agarose beads. Bound proteins were visualised by SDS-PAGE and audioradiography; **c)**, Coomassie Brilliant Blue stained gel representing GST-CtIP fragments used in the experiment,

d)

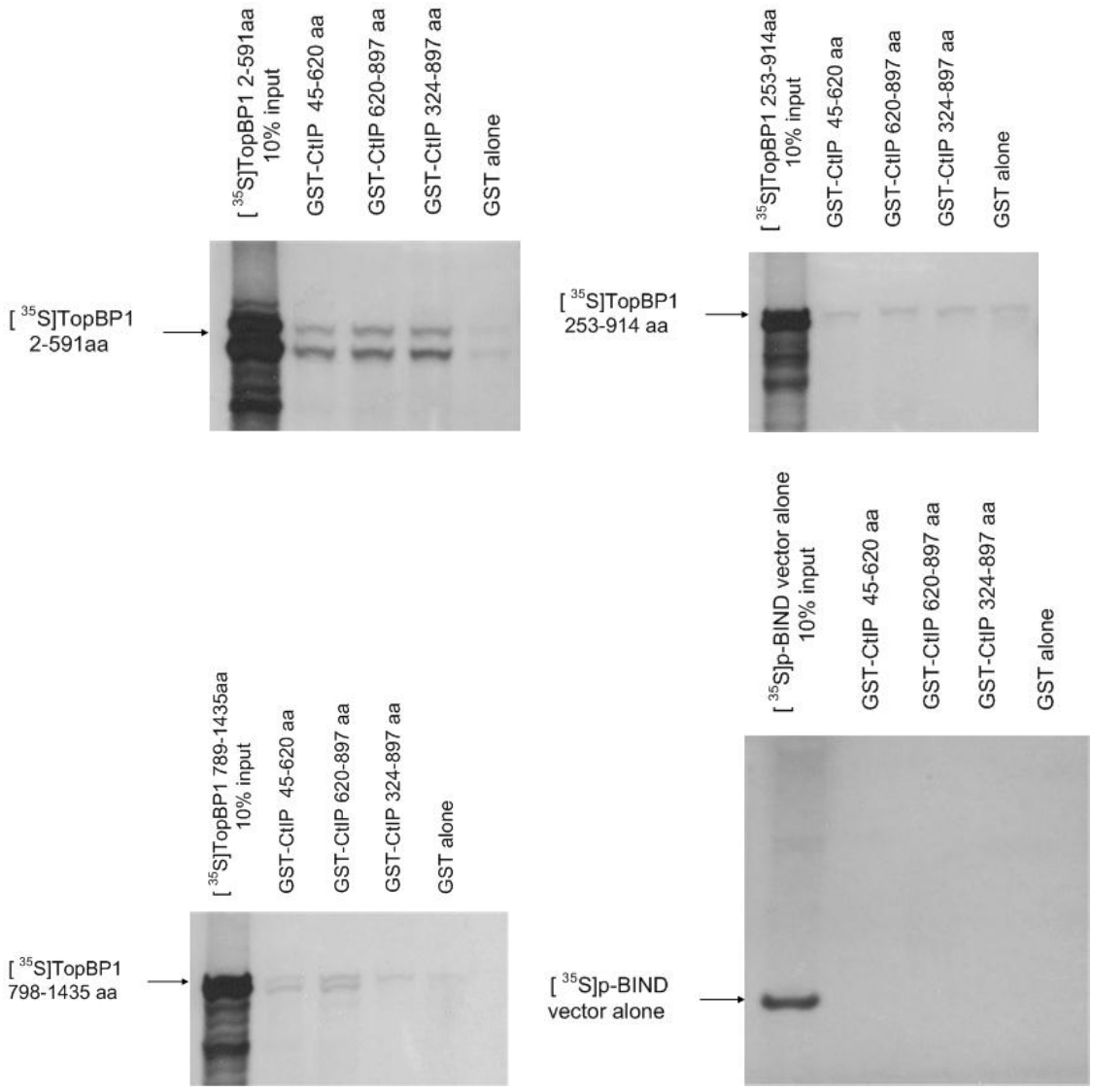

Figure.3.8. CtIP associates with TopBP1 *in vivo* and directly binds to TopBP1. d) three [^{35}S]TopBP1 polypeptide fragments and [^{35}S]p-BIND vector were incubated with various GST-CtIP polypeptide fragments, and complexes isolated with glutathione-agarose beads. Bound proteins were visualised by SDS-PAGE and audioradiography. This figure is representative of three independent experiments.

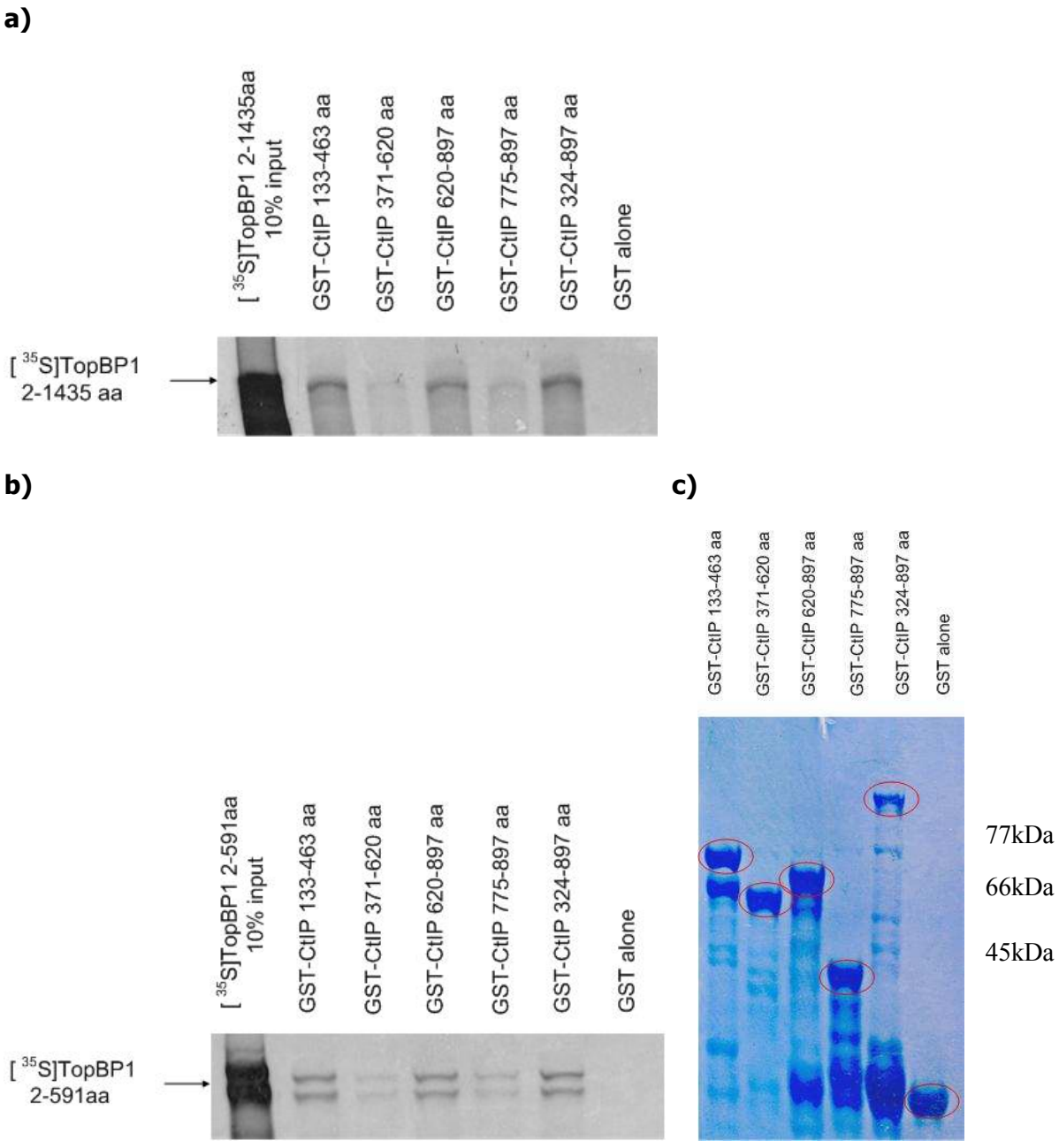

Figure.3.9. Establishing the CtIP binding sites for TopBP1. a), [^{35}S]TopBP1 full length or **b)**, [^{35}S]TopBP1 2-591aa was incubated with various GST-CtIP polypeptide fragments, and complexes isolated with glutathione-agarose beads. Bound proteins were visualised by SDS-PAGE and audioradiography, **c)** Coomassie Brilliant Blue stained gel representing the GST-CtIP fragments used in the experiment. This figure is representative of three independent experiments.

a)

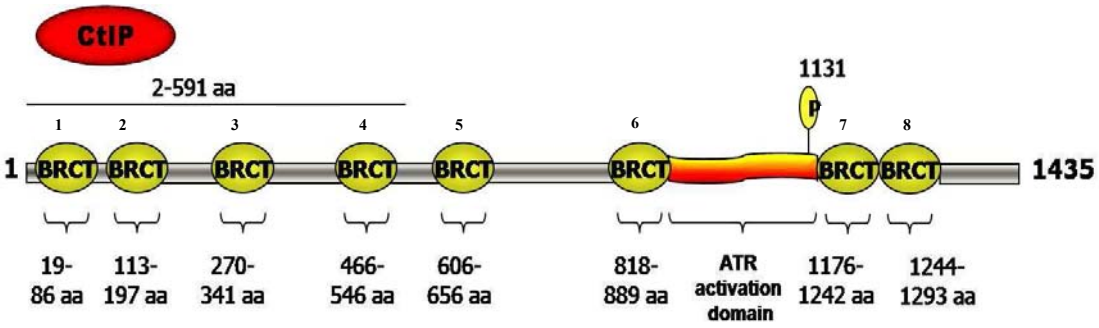

b)

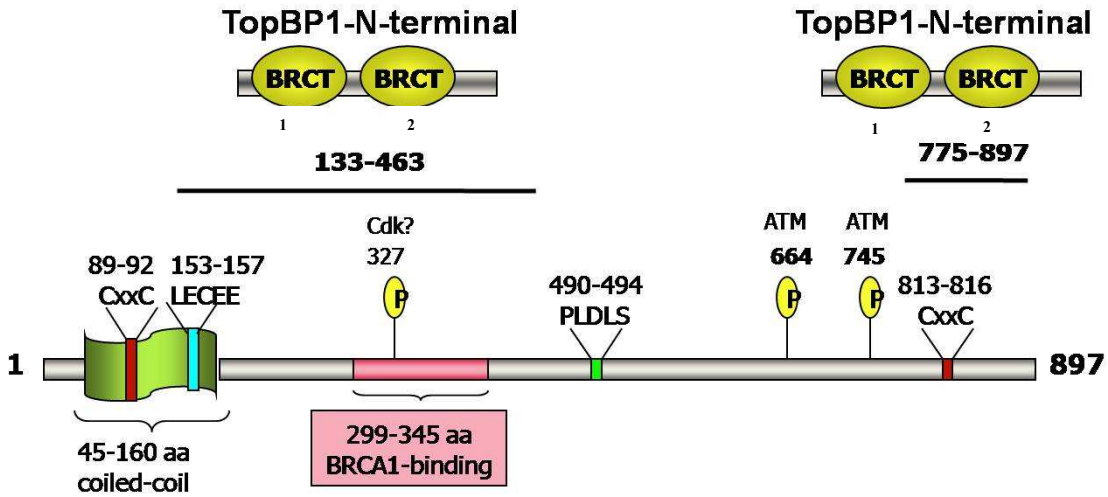

Figure.3.10. The possible interaction sites of CtIP with TopBP1. a) TopBP1 interacts with CtIP via its first two BRCT domains, **b)** TopBP1 (aa 2-591) interacts with CtIP via regions within residues 133-463aa and 775-897aa.

the BRCA1-binding domain and the second one includes two major phosphorylation sites reported to be phosphorylated upon DNA damage by ATM (Li S. et al., 2000).

Additional bands on the Coomassie Brilliant Blue stained gel, not marked by the red circles, are most likely a product of degradation of the originally GST-tagged protein or bacterial-protein contamination, Figure.3.9.c.

3.1.2.4. The interaction of CtIP with NBS1.

The final protein containing the BRCT domains to be examined in this study was NBS1, a modulator of DNA damage sensing and signalling, a cell cycle checkpoint controller and a telomere stabiliser (Zhang et al., 2006). The N-terminus of the protein contains an FHA domain (Durocher & Jackson, 2002) followed by a tandem repeat of BRCT domains (Becker E. et al., 2006), the middle region contains two ATM phosphorylation sites (Kurz & Lees-Miller, 2004) and two nuclear localisation signals (NLS) and the C-terminal region contains the Mre11-binding domain (Desai-Mehta et al., 2001), an NLS and an ATM-binding domain (Falk et al., 2005). Human NBS1 protein was arbitrarily divided into six fragments and the corresponding cDNAs, as well as the full length cDNA, were cloned into a pcDNA3□ vector, which has a T7 promoter site for *in vitro* transcription/translation as described in the section 2.2.8. Figure.3.11. shows the domain localization and distribution of amino acids in pcDNA3□-NBS1 fragments.

To investigate the CtIP and NBS1 interaction *in vivo* a co-immunoprecipitation assay was performed. HeLa cell lysate was incubated with a rabbit CtIP antibody and protein complexes were isolated with protein G-Sepharose beads. As seen in Figure.3.12. associated NBS1 was visualised by Western blotting. Co-immunoprecipitation of the proteins is consistent with data presented by Sartori et al. (Sartori et al., 2007).

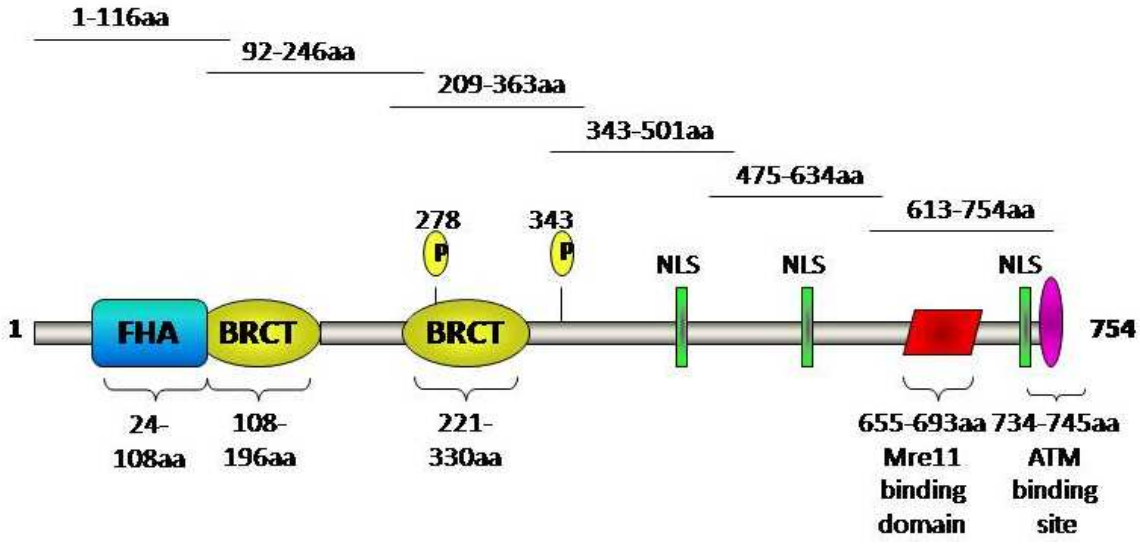

Figure.3.11. The amino acid distribution in NBS1 fragments and the domain structure of human NBS1.

In order to establish CtIP binding sites on NBS1 a GST-pull down assay was performed (see section 2.3.5). The equivalent of 10 μg of non-degraded GST-tagged CtIP fragments, assessed on the basis of previously stained Coomassie Brilliant Blue stained gel was used in each reaction. Radioactively labelled full length NBS1 and six overlapping NBS1 fragments were incubated with a GST-CtIP fragment and a full length protein. Complexes were separated using glutathione-Sepharose beads, fractionated by SDS-PAGE and visualized by autoradiography. Figure.3.13.a. shows direct interaction of the GST-CtIP fragments with full length [^{35}S]NBS1 and two [^{35}S]NBS1 fragments: 1-116aa, containing the FHA domain and 613-754aa, containing the Mre11-binding domain and the ATM binding site (Figure.3.15.).

Additional bands on both of the Coomassie Brilliant Blue stained gel, not marked by the red circles, are most likely a product of degradation of the originally GST-tagged protein or bacterial-protein contamination (Figure.3.13.c).

To confirm these results another GST-pull down assay was performed utilizing [^{35}S]CtIP and three overlapping GST-NBS1 fragments covering the whole protein. The

equivalent of 10 μg of non-degraded GST-tagged NBS1 fragments, assessed on the basis of previously stained Coomassie Brilliant Blue stained gel was used in each reaction. Complexes were isolated with glutathione-agarose beads, fractionated by SDS-PAGE and bound radioactive protein was detected by autoradiography. As seen in Figure.3.13.b. the C-terminal region of NBS1 binds to radioactively labelled CtIP. The N-terminal region, however, in this experiment does not interact; this may be caused either by degradation of the GST-NBS1 fragment or improper folding of the protein which could inhibit the binding. There was a problem with this GST-polypeptide fragment during the purification procedure (section 2.2.7) as it could only be isolated in very small amounts suggesting an inherent instability. It is also shown in Figure.3.13.c., right panel, that this fragment contains a lot of degradation products which is seen as a large low molecular weight band that is smeared at the bottom of that track. Other bands, not marked by red circles, are most likely degradation products of the GST-tagged protein or bacterial-protein contamination (Figure.3.13.c.).

A GST-pull down assay (section 2.3.5) was also performed to determine NBS1 binding sites on CtIP. Radioactively labelled NBS1 fragments containing amino acids 1-116 and 613-754 and the full length protein, previously found to bind GST-CtIP fragments, were incubated with five different, overlapping GST-CtIP fragments. The equivalent of 10 μg of non-degraded GST-tagged CtIP fragments, assessed on the basis of previously stained Coomassie Brilliant Blue stained gel was used in each reaction. Complexes were isolated with glutathione-agarose beads, fractionated by SDS-PAGE and visualized by autoradiography. As shown in Figure.3.14.a. the N-terminal NBS1 fragment binds most GST-CtIP fragments although with different avidity. The fragment composed of amino acid residues 371-620 does not show any interaction. On the basis of the binding to N-terminal region of CtIP we propose a binding region stretching from amino acid residues 133-371 and another one comprising amino acid residues 775-897

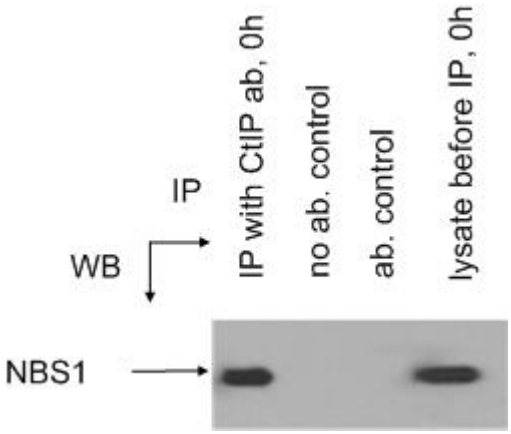

Figure.3.12. CtIP associates with NBS1 *in vivo*. Hela cell lysates were immunoprecipitated with an antibody against CtIP. Coimmunoprecipitating NBS1 was identified by Western blotting. This figure is representative of three independent experiments.

a)

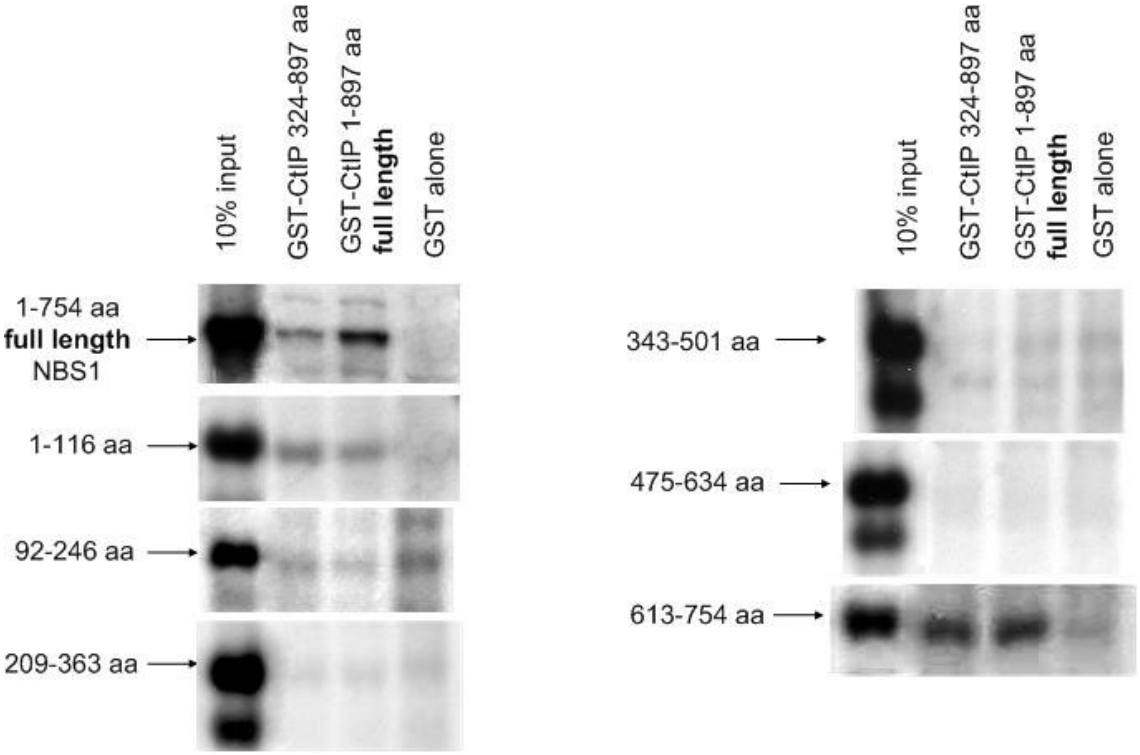

Figure.3.13. CtIP binds directly to NBS1. a) [^{35}S] labelled full length NBS1 as well as six NBS1 polypeptide fragments were incubated with GST-CtIP (full length, aa45-371 and aa324-897). Complexes were isolated with glutathione beads and bound proteins visualized by SDS-PAGE and autoradiography;

b)

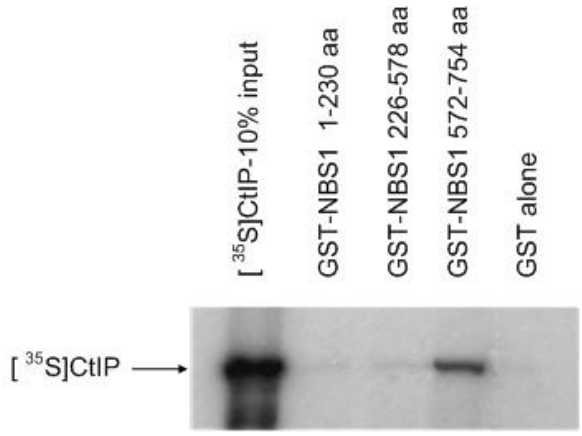

c)

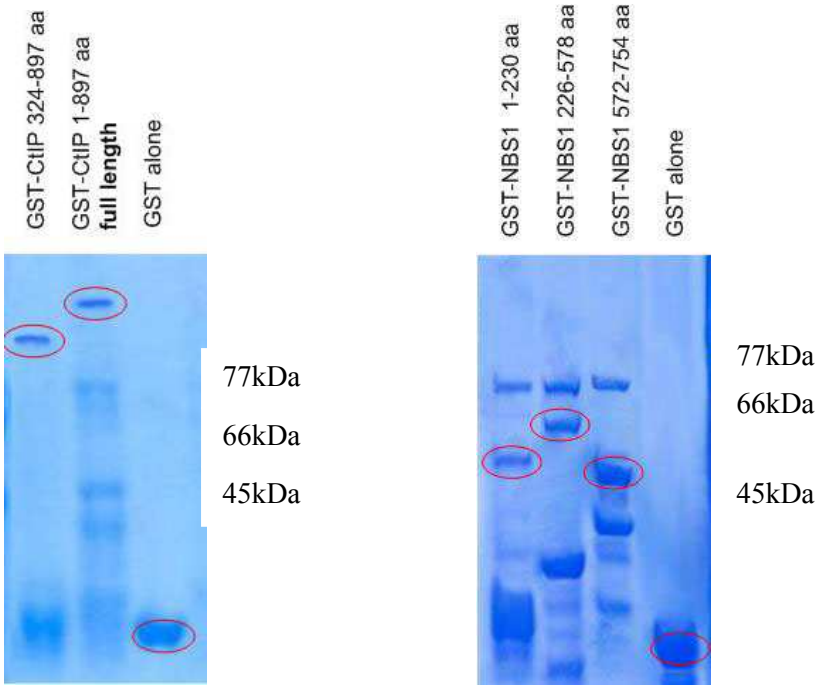

Figure.3.13. CtIP binds directly to NBS1. b) [^{35}S] labelled full length CtIP was incubated with three GST-NBS1 fragments (1-230 aa, 226-578 aa and 572-754 aa). Complexes were isolated and visualized as described above, **c)** Coomassie Brilliant Blue stained gels representing GST-CtIP fragments used in the experiments shown in **a)** and **b).** This figure is representative of three independent experiments.

as one could argue that weaker binding to the fragment comprising 620-897aa is due to an overlap of residues 775-897aa; thus we could conclude that it is the 775-897aa region of CtIP that shows interaction with N-terminal region of NBS1. As seen in Figure.3.14.b. the C-terminal fragment of NBS1 shows strong binding to the CtIP fragments containing amino acids 133-463, 620-897 and 324-897 and weaker binding to a fragment composed of residues 371-620.

On the basis of this result we can conclude that one of the two binding sites for NBS1 is located within the 133-463aa region of CtIP as we can argue that the weak binding to the fragment containing amino acid residues 371-620 is due to the fact that it overlaps the fragment composed of 133-463aa, and therefore contains the C-terminal region of that fragment, which is a part of the binding site. The C-terminal fragment of NBS1 also interacts with a GST-CtIP fragment containing residues 620-897 but as it does not bind to fragment 775-897aa we can conclude that the second binding site is located between amino acids 620- 775. The binding of full length NBS1 mainly to the three GST-CtIP fragments comprising amino acid residues 133-463, 620-897 and 324-897 confirms the previous result obtained with the N-terminal and C-terminal region of NBS1 and establishes the previously recognized binding sites for both of the fragments (Figure.3.16.). Taking into consideration the result shown in Figure.3.13.a. with the full length NBS1 binding to the full length CtIP it strongly enhances the importance of both of the binding sites on CtIP, as the full length protein associates with the full length NBS1 to a greater extent than the N-terminally truncated version.

Additional bands on the Coomassie Brilliant Blue stained gel, not marked by the red circles, are most likely a product of degradation of the originally GST-tagged protein or bacterial-protein contamination (Figure.3.14.d.).

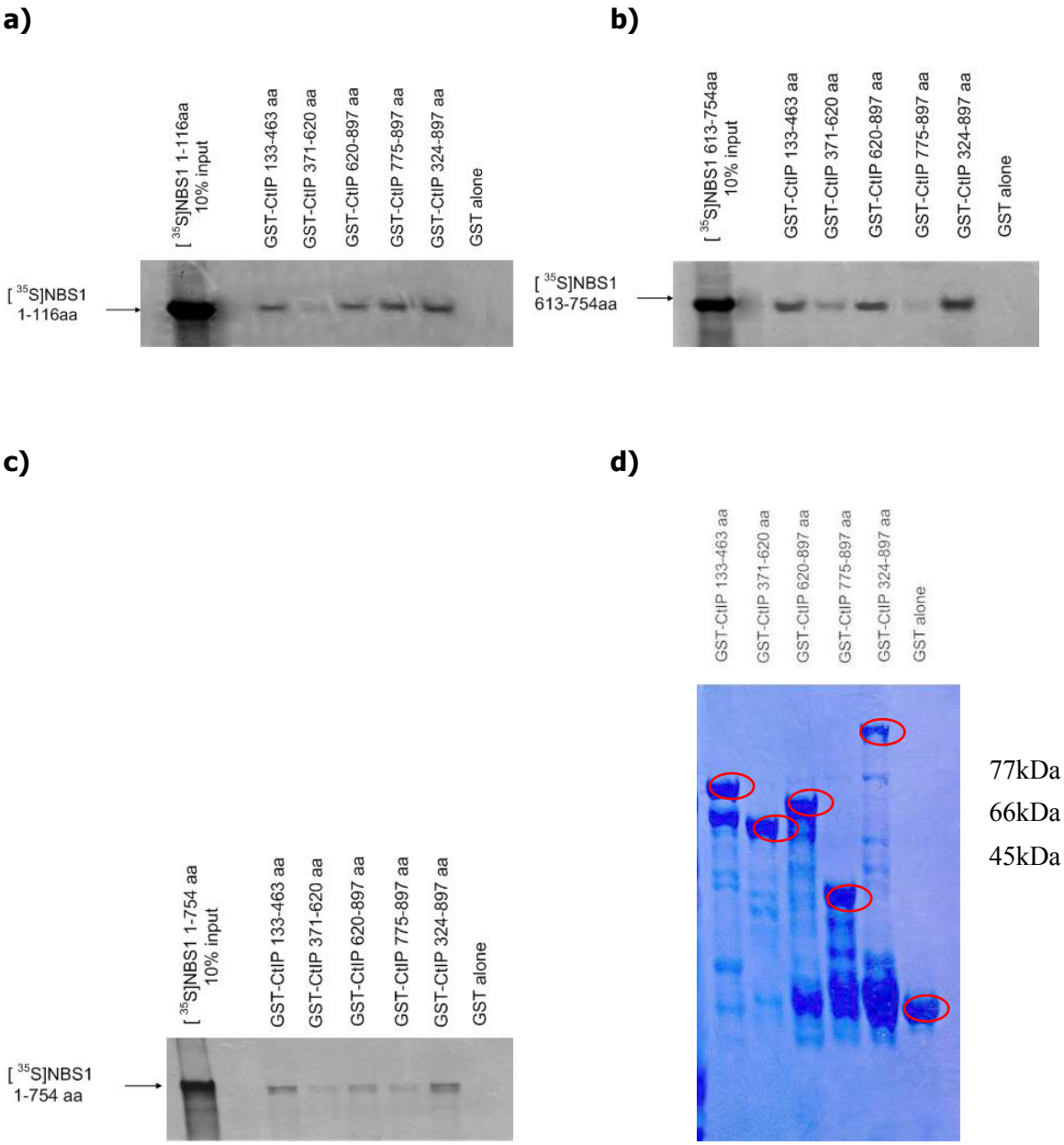

Figure.3.14. CtIP binding sites for NBS1. a), [^{35}S]NBS1 1-116aa or **b)**, [^{35}S]NBS1 613-754aa polypeptide fragments or **c)** [^{35}S]NBS1 full length were incubated with five GST-CtIP polypeptide fragments, and complexes isolated with glutathione beads. Bound proteins were visualised by SDS-PAGE and audioradiography; **d)** Coomassie Brilliant Blue stained gel representing the GST-CtIP fragments used in the experiment. This figure is representative of three independent experiments.

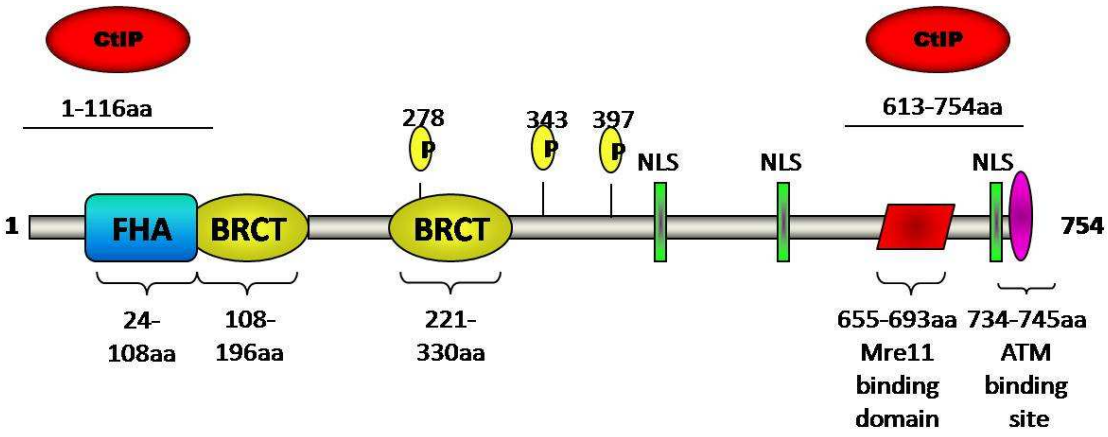

Figure.3.15. The possible interaction sites of CtIP on NBS1. NBS1 interacts with CtIP via its FHA domain and the region comprising Mre11 and ATM binding sites.

a)

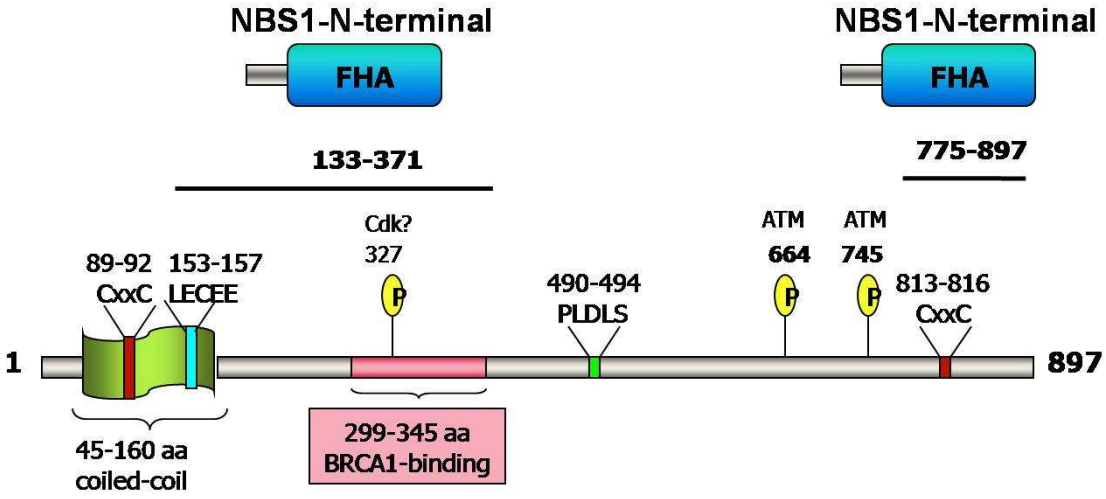

b)

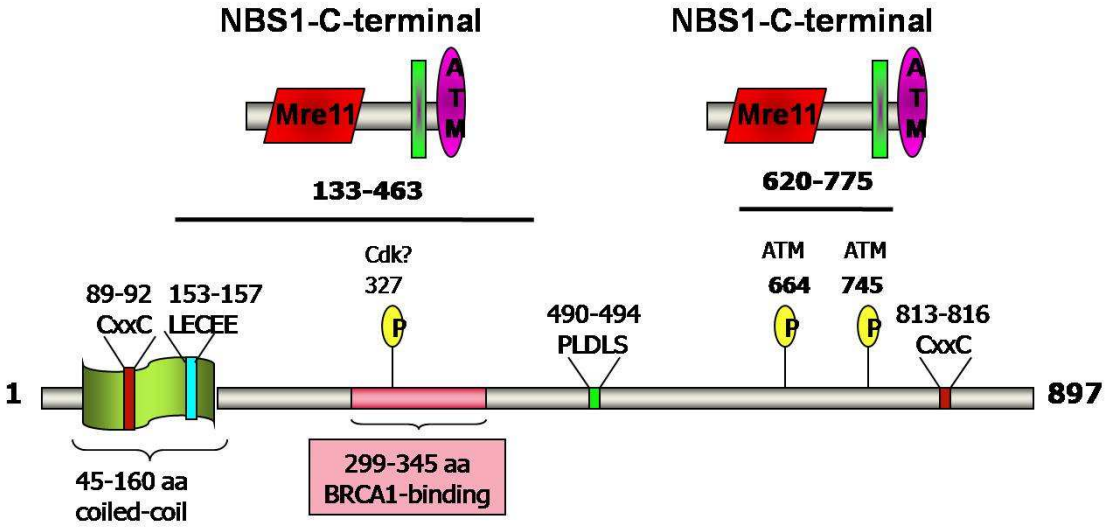

Figure.3.16. The interaction sites on CtIP for NBS1. a) NBS1 FHA domain interacts with CtIP via a region that is located in between the residues 133-371aa and 620-775aa, **b)** NBS1 C-terminal region interacts with CtIP via regions located in the residues 133-463aa and 775-897aa.

Some of those results have been confirmed by Chen et al. In that publication they reported binding of full length NBS1 mainly to the N-terminal (1-220aa) and C-terminal region of CtIP (631-897aa) and to a smaller extent to a GST-CtIP fragment comprising 439-649aa. It has also been shown that the C-terminal fragment of NBS1 does not bind to CtIP in the case of absence of the Mre11-binding domain (Chen et al., 2008).
A lot of work on CtIP's interaction with the MRN complex was started at the same time as this work and has been published already. Thus some of the results overlap published data however confirming it.

3.2. Nuclear localization of CtIP and the BRCT-domain containing proteins before and after DNA damage.

3.2.1. Introduction.

Eukaryotic cells, upon DNA damage, activate a signalling network that coordinates a rapid detection of the DNA lesions and activation of the repair machinery with a temporary delay in cell cycle progression (Zhou & Elledge, 2000). The effectiveness of genome surveillance pathways is dependent on carefully organized redistribution of their components to nuclear regions that contain and surround the damaged DNA (Lucas et al., 2004). Those rearrangements, in response to ionizing radiation (IR), on the cellular level are manifested by the appearance of nuclear foci, so-called IR-induced foci (IRIF; Shiloh, 2003).

IRIF are microscopically visible, dynamic structures containing vast numbers of proteins that are involved in various aspects of double-strand break (DSB) repair. Thus IRIF are widely used as a convenient marker of DSB location.

γ-H2AX is a phosphorylated form of the histone H2AX. H2AX in turn makes up 2-25% of the whole pool of the histone H2A variant, depending on the cell line and tissue

examined (Kinner et al., 2008). H2AX phosphorylation at Ser139 occurs just minutes after DNA damage and reaches its peak around 30 minutes later. It spreads approximately 2Mbp around the DNA lesion and the modification consists of ~2000 γ-H2AX molecules (Rogakou et al., 1999). Thus γ-H2AX staining is a very useful tool in DSBs recognition.

IRIF, apart from comprising various DNA repair-associated proteins, participate in restructuring large segments of chromatin in the vicinity of the DNA lesion (van Attikum & Gasser, 2005). This increases the accessibility of the damaged DNA for proteins that are engaged in DNA repair (Murr et al., 2006). IRIF formation is an important step in cellular protection against DNA lesions but not all proteins are readily located there. One of the key components of DNA damage surveillance machinery, Chk2, interacts with DSBs only transiently, without forming cytologically visible foci (Bekker-Jensen et al., 2006). Thus it has been concluded that it is not necessary for all proteins participating in the DNA damage repair to concentrate at the very site of the lesion as they may play a role in micro-compartments associated with the lesion. Also it has been suggested that not all damage induced foci are structurally similar which would reflect different roles of different proteins in the repair process (Bekker-Jensen et al., 2006).

3.2.2. Results.

The BRCT domain containing proteins, as part of the DNA damage surveillance mechanism, are known to form foci. Temporal studies of foci formation has revealed the sequence of events involving the recruitment of the MRN complex to the site of lesion and acetylation of ATM followed by its autophosphorylation at S1981 (Bakkenist & Kastan, 2003; Sun et al., 2007; Williams et al., 2007) Activated ATM phosphorylates histone H2AX forming so called γ-H2AX (Rogakou et al., 1999). γ-H2AX recruits MDC1

which in turn recruits another pool of the MRN complex and RNF8 (Ring Finger Protein 8), which is a E3 ubiquitin ligase (Goldberg et al., 2003; Mailand et al., 2007; Stewart et al., 2003). Further events are either NBS1- or RNF8-dependent (Mohammad & Yaffe, 2009).

Here, using immunofluorescence microscopy, we examined the localization of 53BP1, MDC1, TopBP1 and NBS1 IRIF in comparison with CtIP's nuclear localization before and after DNA damage caused by 9Gy of irradiation. The influence of CtIP's depletion on formation of 53BP1 and MDC1 IRIF occurring after irradiation with □-rays was also tested.

3.2.2.1. The nuclear localization of CtIP and 53BP1.

HeLa cells were seeded on 12 well slides at 1-2 x 10^4cells/well. The following day the slides were mock-irradiated or irradiated with 9Gy and incubated for 1 h. Cells were fixed and co-stained with a rabbit 53BP1 antibody and a mouse γ-H2AX antibody as described in section 2.4.5. The secondary antibodies used in this experiment are listed in Table 2.8 and were a green anti-rabbit for 53BP1 and a red anti-mouse for γ-H2AX. The nucleus is stained in blue using 4',6-diamidino-2-phenylindole (DAPI). Figure.3.17. shows the γ-H2AX and the 53BP1 staining in mock-irradiated cells and in cells irradiated with 9Gy. In cells treated with IR focal staining of 53BP1 and γ-H2AX is seen indicating localization of 53BP1 and phosphorylation of the histone H2AX at the sites of DNA DSBs. In the merged picture in the lower panel the yellow staining shows sites in the nucleus where both of the proteins co-localize.

In Figure.3.18. co-staining with a rabbit antibody against 53BP1 and a mouse antibody against CtIP is shown. In the first panel HeLa cells were mock-irradiated with CtIP staining, in red, being slightly granular and 53BP1 staining, in green, is evenly spread throughout the whole nucleus apart from the nucleoli. After irradiation, as seen in the

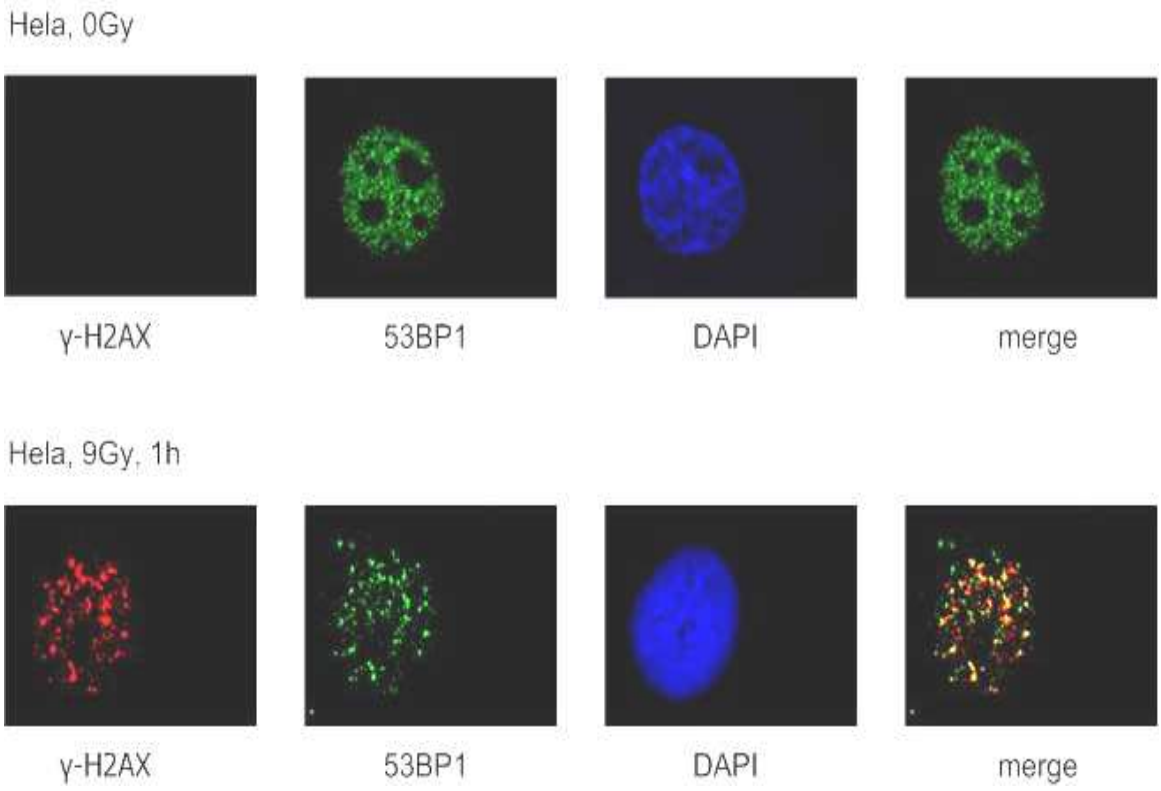

Figure.3.17. The localization of γ-H2AX and 53BP1 in the cell nucleus before and after DNA damage. HeLa cells were grown on slides and subsequently mock-irradiated or irradiated with 9Gy. Cells were fixed and stained with antibodies against γ-H2AX (red) and 53BP1 (green) and the nucleus was visualised using DAPI staining (blue). Merge picture shows the positioning of the γ-H2AX staining versus the 53BP1 staining and yellow indicates the sites where they co-localize. This figure is representative of three independent experiments.

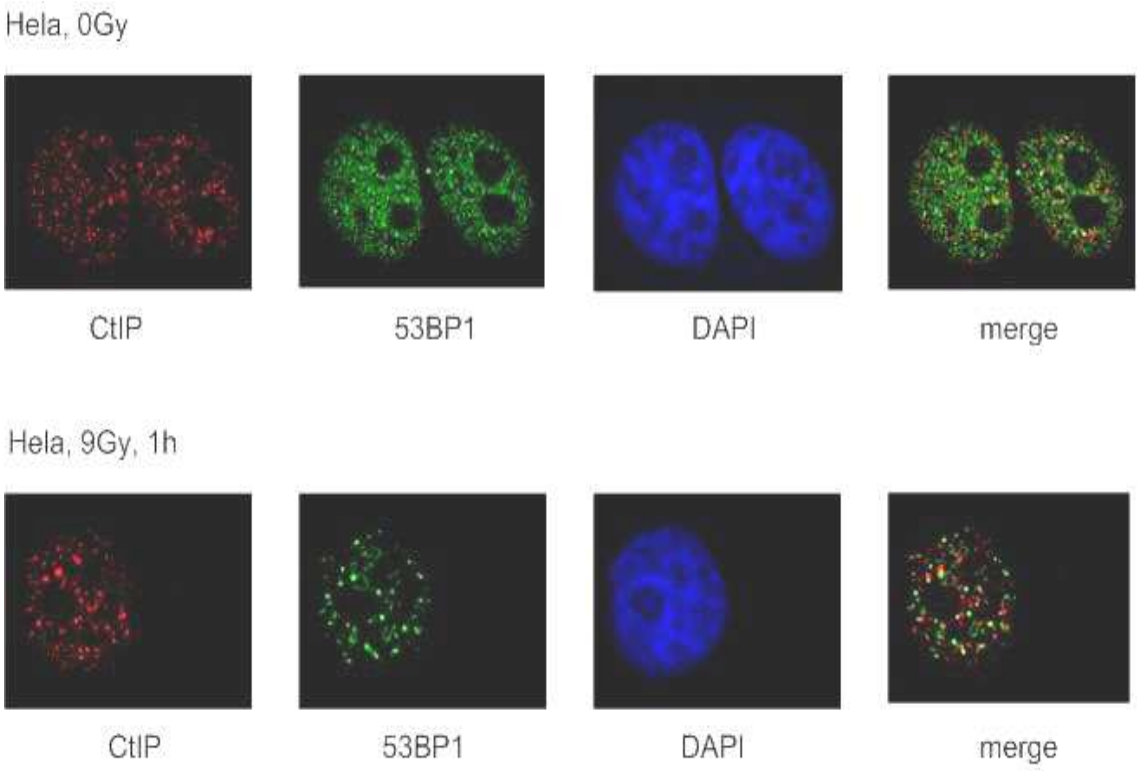

Figure.3.18. The localization of CtIP and 53BP1 in the cell nucleus before and after DNA damage. HeLa cells were grown on slides and subsequently mock-irradiated or irradiated with 9Gy. Cells were fixed and stained with antibodies against CtIP (red) and 53BP1 (green) and the nucleus was visualised using DAPI staining (blue). Merge picture shows the positioning of the CtIP staining versus the 53BP1 staining and yellow indicates the sites where they co-localize. This figure is representative of three independent experiments.

lower panel, CtIP's staining becomes more defined and granular and 53BP1 forms discrete foci – IRIF. In the right-hand the yellow staining indicates that the two proteins co-localize at the site of DSB.

3.2.2.2. The nuclear localization of CtIP and MDC1.

HeLa cells were seeded on 12 well slides at 1-2 x 10^4cells/well. The following day the slides were mock-irradiated or irradiated with 9Gy and incubated for 1 h. Cells were fixed and co-stained with a rabbit MDC1 antibody and a mouse γ-H2AX antibody (section 2.4.5.). The secondary antibodies used in this experiment are listed in the Table 2.8 and were a green anti-rabbit for MDC1 and a red anti-mouse for γ-H2AX. The nucleus is stained in blue using 4',6-diamidino-2-phenylindole (DAPI). In Figure.3.19. in the top panel staining of both of these proteins is shown in mock-irradiated cells. In the absence of DNA damage histone H2AX is not phosphorylated thus there is no staining with the γ-H2AX antibody. MDC1's green staining is present in the nucleus at all times. The lower panel shows formation of IRIF in the HeLa cells treated with 9Gy. Both of the proteins localize to the sites of DSBs and as seen in yellow in the merged picture at several sites of damaged DNA γ-H2AX and MDC1 co-localize.

Figure.3.20. shows localization of CtIP and MDC1 staining before and after DNA damage caused by 9Gy of irradiation. In the top panel the mock-irradiated cells are shown. The CtIP staining is again not well-defined and with granular proprieties and the MDC1 staining is evenly distributed throughout the nucleus with the exception of nucleoli regions. In the lower panel, after DNA damage, both of the proteins seem to aggregate and CtIP's staining becomes distinctively granular and MDC1 forms IRIF. In the last picture the yellow staining indicates sites at which both of the proteins localize together.

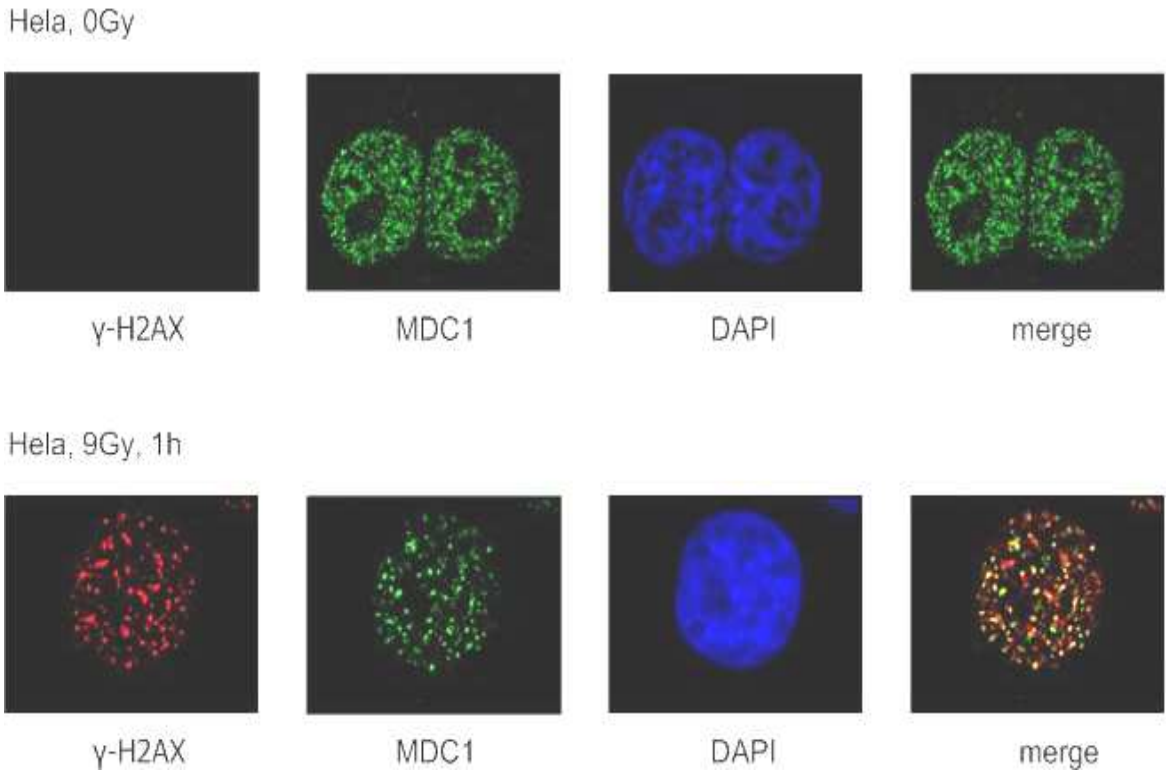

Figure.3.19. The localization of γ-H2AX and MDC1 in the cell nucleus before and after DNA damage. HeLa cells were grown on slides and subsequently mock-irradiated or irradiated with 9Gy. Cells were fixed and stained with antibodies against γ-H2AX (red) and MDC1 (green) and the nucleus was visualised using DAPI staining (blue). Merge picture shows the positioning of the γ-H2AX staining versus the MDC1 staining and yellow indicates the sites where they co-localize. This figure is representative of three independent experiments.

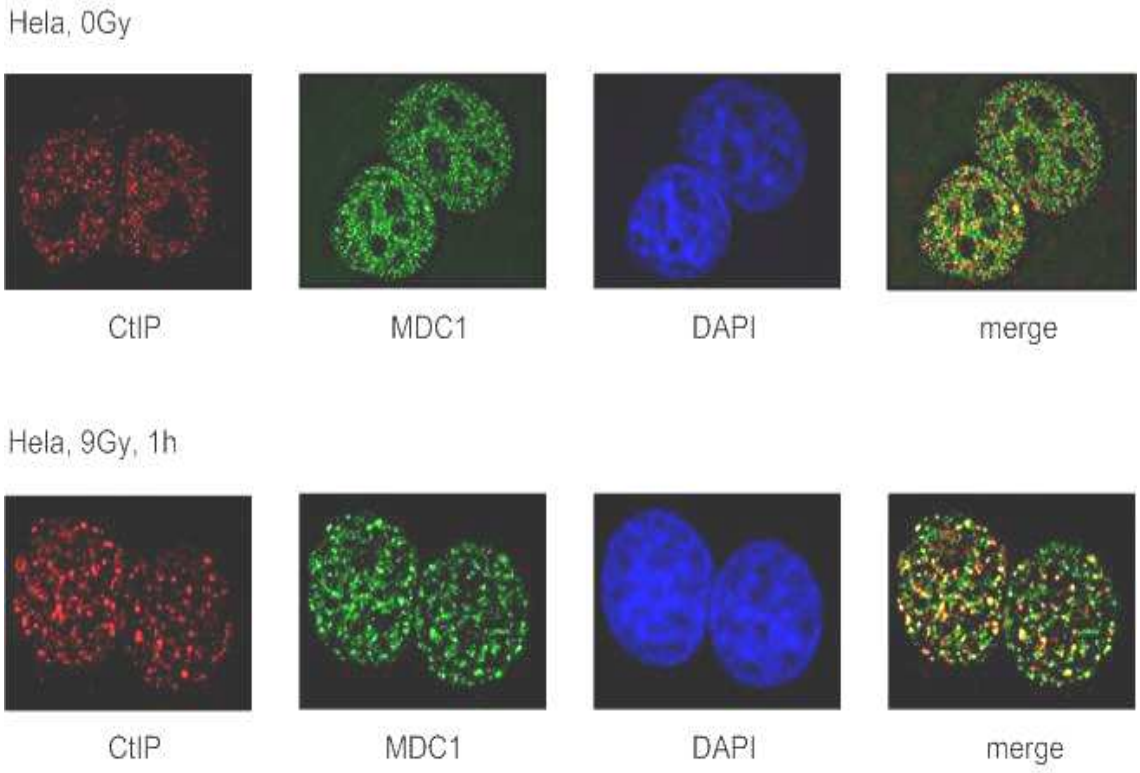

Figure.3.20. The localization of CtIP and MDC1 in the cell nucleus before and after DNA damage. HeLa cells were grown on slides and subsequently mock-irradiated or irradiated with 9Gy. Cells were fixed and stained with antibodies against CtIP (red) and MDC1 (green) and the nucleus was visualised using DAPI staining (blue). Merge picture shows the positioning of the CtIP staining versus the MDC1 staining and yellow indicates the sites where they co-localize. This figure represents is representative of three independent experiments.

3.2.2.3. The nuclear localization of CtIP and NBS1.

HeLa cells were seeded at a density of 1-2 x 10^4cells/well on 12 well microscope slides. The following day the slides were mock-irradiated or irradiated with 9Gy and incubated for 1 h. Cells were fixed and co-stained with a rabbit NBS1 antibody and a mouse γ-H2AX antibody as described in section 2.4.5. The secondary antibodies used in this experiment are listed in Table 2.8 and were a green anti-rabbit for NBS1 and a red anti-mouse for γ-H2AX. The nucleus is stained in blue using 4',6-diamidino-2-phenylindole (DAPI). As shown in Figure.3.21. γ-H2AX staining is not present in the mock-irradiated cells (in the top panel) and NBS1 staining is ill-defined and the two bright dots are possibly stained centrosomes. In the lower panel IRIF staining is observed indicating that γ-H2AX and NBS1 localized at the sites of DSBs. In the right-hand panel the yellow staining indicates that these two proteins localize at the same sites of DNA lesions.

Figure.3.22. shows CtIP and NBS1 localization in the cell's nucleus before and after DNA damage. In the top panel the distribution of the two proteins is demonstrated as an ill-defined nuclear staining. In the bottom panel CtIP shows more defined granular staining indicating the involvement in DNA lesion repair and the NBS1 staining is typical for a DNA damage repair protein. In the right-hand panel in yellow the overlap of the two staining patterns can be observed illustrating sites where CtIP and NBS1 co-localize.

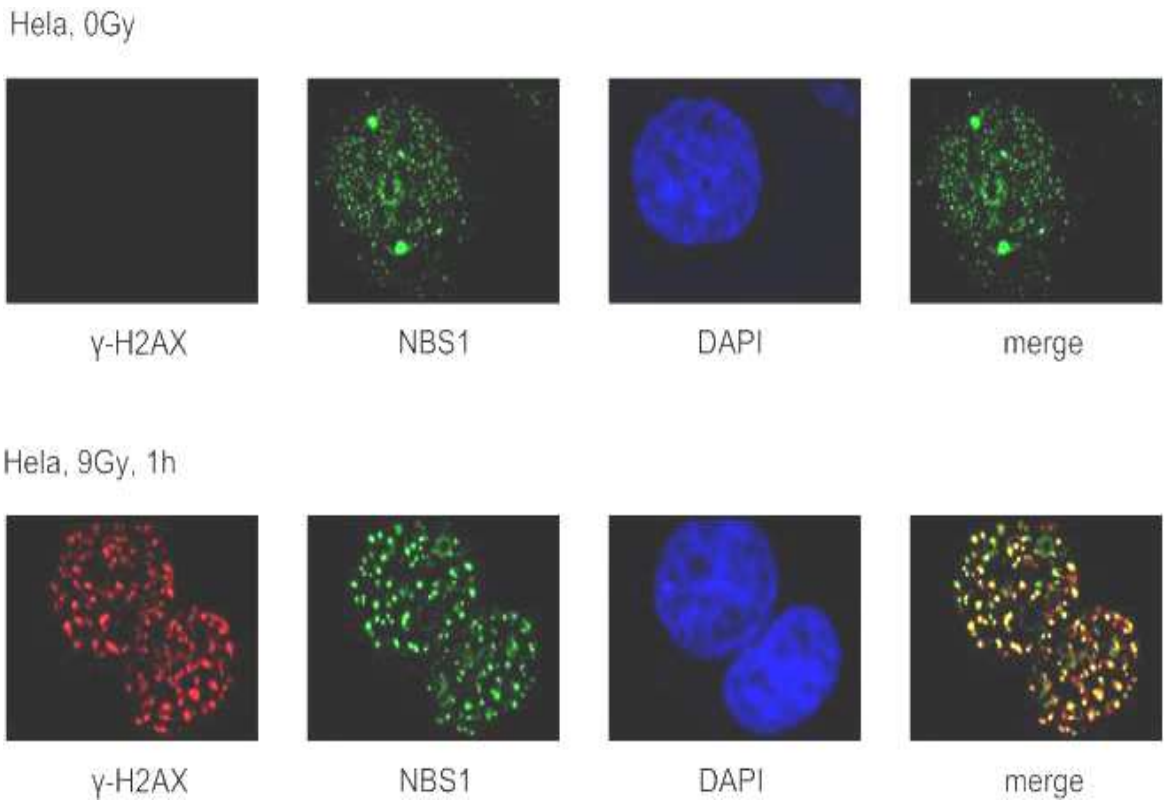

Figure3.21. The localization of γ-H2AX and NBS1 in the cell nucleus before and after DNA damage. HeLa cells were grown on slides and subsequently mock-irradiated or irradiated with 9Gy. Cells were fixed and stained with antibodies against γ-H2AX (red) and NBS1 (green) and the nucleus was visualised using DAPI staining (blue). Merge picture shows the positioning of the γ-H2AX staining versus the NBS1 staining and yellow indicates the sites where they co-localize. This figure is representative of three independent experiments.

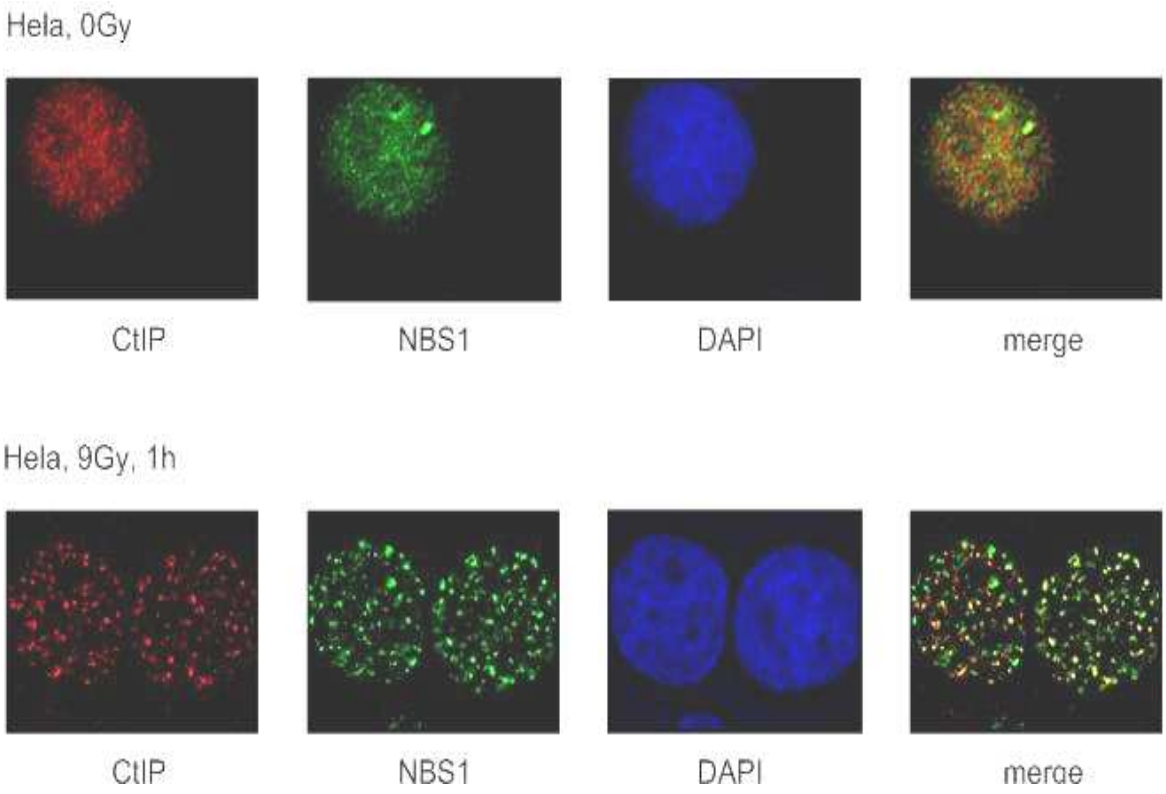

Figure.3.22. The localization of CtIP and NBS1 in the cell nucleus before and after DNA damage. HeLa cells were grown on slides and subsequently mock-irradiated or irradiated with 9Gy. Cells were fixed and stained with antibodies against CtIP (red) and NBS1 (green) and the nucleus was visualised using DAPI staining (blue). Merge picture shows the positioning of CtIP staining versus the NBS1 staining and yellow indicates the sites where they co-localize. This figure is representative of three independent experiments.

3.2.2.4. The lack of disruption of 53BP1 and MDC1 IRIF formation upon CtIP depletion.

In order to establish whether CtIP depletion influences 53BP1 and MDC1 IRIF formation a CtIP knock-down was performed (section 2.1.7.) followed by immunofluorescence staining (section 2.4.5.). HeLa cells were mock-treated or treated with the CtIP siRNA and after 48h they were seeded at a density of 1-2 x 10^4cells/well on 12 well microscopic slides. The following day the slides were irradiated with 3Gy and incubated for 1h (see section 2.1.6.2.). Cells were fixed and stained with a rabbit 53BP1 antibody or a rabbit MDC1 antibody as described in section 2.4.5. The secondary antibody used in this experiment is listed in the Table 2.8 and was a green anti-rabbit for both 53BP1 and MDC1. The nucleus is stained in blue using 4',6-diamidino-2-phenylindole (DAPI).

As shown in the Figure.3.23. the top panel represents 53BP1 IRIF formation in the presence of CtIP and the bottom panel represents 53BP1 IRIF formation in the absence of CtIP. The focal distribution of 53BP1 in both cases is similar; thus we can conclude that CtIP does not influence 53BP1 foci formation. This is consistent with other findings presented in this thesis and suggests that CtIP is a bridging protein in cellular protein-protein interactions.

Figure.3.24. shows the MDC1 IRIF formation in the presence and absence of CtIP expression, again showing that CtIP does not influence MDC1 focal redistribution.

Given the fact that CtIP does not influence the formation of 53BP1 and MDC1 IRIF in the presence of γ-H2AX we could conclude that CtIP might orchestrate the DNA repair processes that those proteins are involved in, such as HR in the case of MDC1, rather than their retention at the DSBs sites.

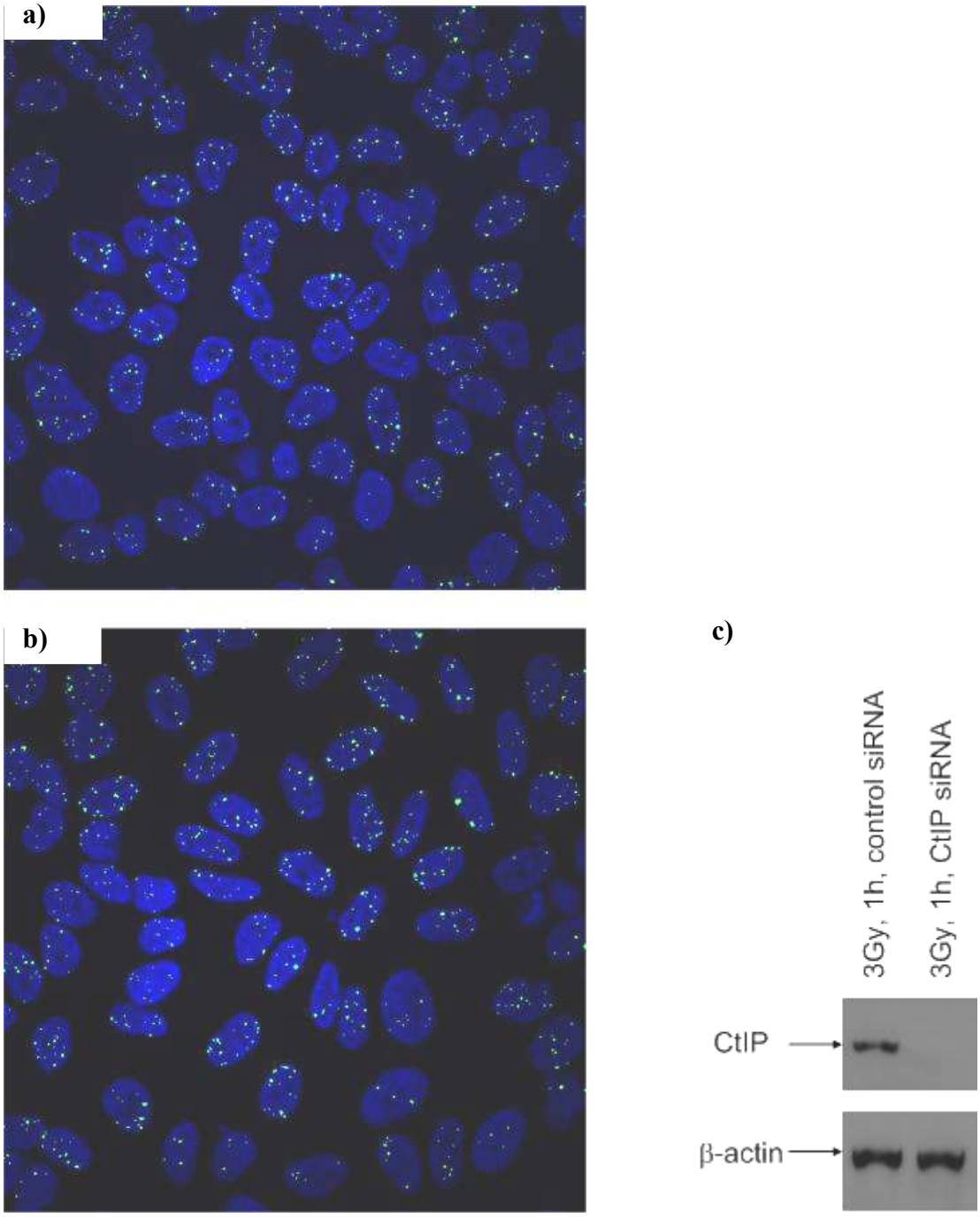

Figure.3.23. The formation of 53BP1 IRIF is not disrupted upon CtIP depletion. HeLa cells were mock-treated **(a)** or treated with CtIP siRNA **(b)** and subsequently irradiated with 3Gy and fixed an hour post IR. The green focal staining represents 53BP1 IRIF and the blue staining depicts the nucleus (DAPI staining), **c)** Western blot showing CtIP knock-down in the HeLa cells used in the experiment; β-actin indicates equal loading. This figure is representative of three independent experiments.

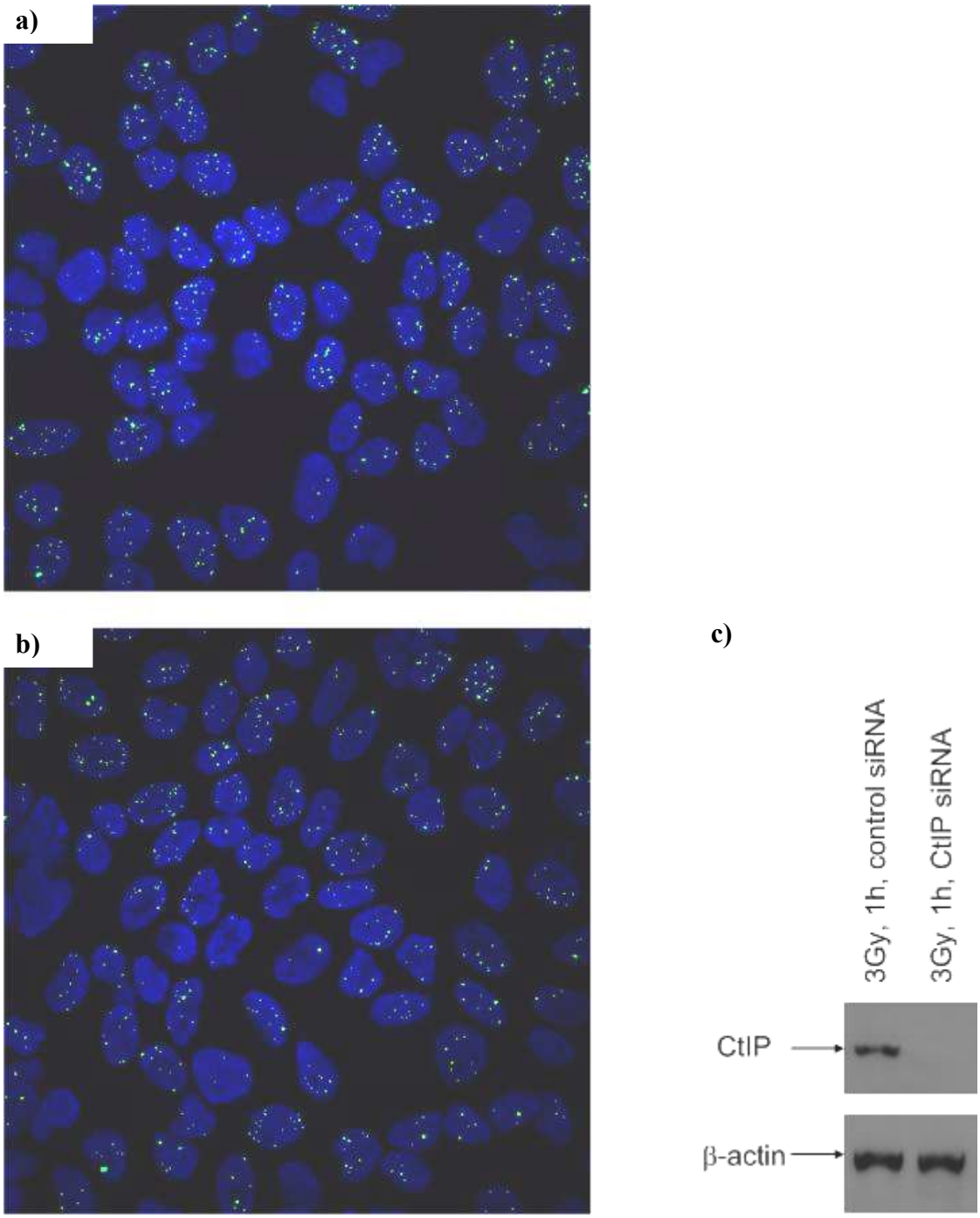

Figure.3.24. The formation of MDC1 IRIF is not disrupted upon CtIP depletion. HeLa cells were mock-treated **(a)** or treated with CtIP siRNA **(b)** and subsequently irradiated with 3Gy and fixed an hour post IR. The green focal staining represents MDC1 IRIF and the blue staining depicts the nucleus (DAPI staining). **c)** Western blot showing CtIP knock-down in the HeLa cells used in the experiment; β-actin indicates equal loading. This figure is representative of three independent experiments.

3.3. Discussion.

In previous studies CtIP has been shown to interact with the BRCT domains of BRCA1 and this interaction has been shown to be phosphorylation-dependent *in vivo* (Table.3.1; Yu et al., 1998; Yu & Chen, 2004). We have now shown that CtIP interacts *in vivo* and *in vitro* with the BRCT domains of other DNA damage proteins such as 53BP1, MDC1 and TopBP1. However, the direct interaction shown occurs with unphosphorylated CtIP protein. On the other hand we cannot rule out the fact that the *in vitro* translated protein could be post-translationally modified by the components of the *in vitro* transcription/translation reaction mixture as it consists of total rabbit reticulocyte lysate.

Table.3.1. Proteins containing BRCT domains interacting with CtIP.

protein binding CtIP	**domains involved in interaction with CtIP**
BRCA1	BRCT domains (aa 1602-1863); Yu et al., 1998; Yu & Chen, 2004
53BP1	Tudor/BRCT domains (aa 1309-1972)
MDC1	PST/BRCT domains (aa 1052-1720)
TopBP1	BRCT domains (aa 2-253)
NBS1	FHA/C-terminus (aa 1-116/aa 613-754)

To confirm 53BP1 and CtIP's association *in vivo* a co-immunoprecipitation assay was performed. As shown in Figure.3.2.a. 53BP1 and CtIP exist in a complex in HeLa cell lysates. In order to investigate whether it is a direct or an indirect interaction a GST-pull down assay was carried out. As seen in Figure.3.2.b. two GST-53BP1 fragments interact with the radioactively labelled full length CtIP and it seems likely there are two binding sites on 53BP1 for CtIP as shown in Figure.3.3.a., Table.3.1. The binding of [^{35}S]CtIP to the GST-53BP1 fragment that contains the BRCT domains is not very

strong; this could be caused by its dephosphorylated nature as the BRCT domains are known to be phospho-binding sites (Yu et al., 2003). However, 53BP1's BRCT domains have not been proven to bind specifically to phosphopeptides (Mohammad & Yaffe, 2009). Thus it is very likely that the GST-53BP1 fragment containing the G-A rich stretch and the Tudor domain is the main binding site for CtIP. The Tudor domain is known to bind to methylated proteins such as when 53BP1 interacts with methylated H3 and H4 (Huyen et al., 2004; Sanders et al., 2004). However, CtIP up to now has not been reported to be methylated, thus it is possible that the CtIP binding site is located in the C-terminal region of the fragment containing the Tudor domain and ends before the BRCT domains (Figure.3.3.b.).

53BP1 is most likely involved in the NHEJ pathway of DSB repair; however, total NHEJ is reported to be not influenced by the depletion of CtIP (Bennardo et al., 2008). Thus the process in which those two proteins take part together remains to be elucidated. However, as 53BP1 together with NBS1 and MDC1 is known to be involved in the G2/M replication independent cell cycle arrest orchestrated by ATR, we could hypothesise that CtIP could take part in that process (Stiff et al., 2008).

To establish the MDC1 and CtIP association *in vivo* a co-immunoprecipitation assay was carried out. As seen in Figure.3.5.a. they associate *in vivo* which may implicate either a direct interaction or involvement of a third, intermediary protein. To address that question a GST-pull down assay was performed. As shown in Figure.3.5.b. MDC1 and CtIP interact directly. The MDC1-CtIP binding is well defined with two of the GST-MDC1 fragments interacting with [^{35}S]CtIP (Figure.3.5.b, Table.3.1.). The interaction of [^{35}S]CtIP with the GST-MDC1 fragment containing the PST domain may implicate the PST domain as a stabilizing binding site for the CtIP-MDC1 complex *in vivo*, whereas [^{35}S]CtIP's binding to the GST-MDC1 fragment comprising the BRCT domains could be

phosphorylation dependent and have a higher affinity with a phosphorylated CtIP protein. The MDC1 BRCT domains have been reported to specifically bind to phopho-proteins phosphorylated in the C-terminal region (Mohammad & Yaffe, 2009). Thus we could hypothesise that CtIP binds to MDC1 constitutively through the PST domain and the binding through the BRCT domains may occur after the DNA damage when CtIP is phosphorylated on either the S664 or S745 (Figure.3.6.a).

An attempt to reveal which region of CtIP binds to either 53BP1 and MDC1 was made. *In vitro* translatable C-terminal regions of 53BP1 and MDC1 were cloned into pcDNA4/His vector, however the efficiency of radioactive labelling was not high enough to perform an informative GST-pull down with the available GST-CtIP fragments.

MDC1 is known to be involved in the homologous recombination pathway by which the broken DNA ends are repaired during S and G2 phases of the cell cycle (Zhang et al., 2005). This pathway is independent of and parallel to, the BRCA1-dependent HR pathway (Xie et al., 2007). CtIP has been shown to be involved in DSB repair and in the choice of the repair pathway depending on its phosphorylation status on S327 and subsequent interaction with BRCA1. Thus we can speculate that CtIP could engage MDC1 via a similar mechanism. We could hypothesise that CtIP could stimulate MDC1's involvement in the HR during S/G2 cell cycle phase after DNA damage (Yun & Hiom, 2009).

In order to investigate the *in vivo* association of TopBP1 and CtIP a co-immunoprecipitation assay was performed. As shown in Figure.3.8.a. the proteins form a complex in HeLa cell lysates. To assess the direct interaction a GST-pull down assay was carried out. The results in Figure3.8.b. indicate that [^{35}S]TopBP1 binds to GST-CtIP. The binding site on TopBP1 can be mapped to the N-terminal 19 amino acid

fragment followed by first two BRCT domains and a 56 amino acid fragment at the C-terminal region (Figure.3.10.a., Table.3.1.). To investigate further the direct binding of TopBP1 and CtIP a GST-pull down assay was performed, to establish which regions of the CtIP bind directly to the TopBP1. As Figure.3.9. shows several GST-CtIP fragments bind to the radioactively labelled TopBP1. On the basis of their amino acid composition it could be established that the CtIP regions that bind to TopBP1 encompass the previously determined BRCA1 binding site and the region that includes CtIP's two main phosphorylation sites, Ser664 and Ser745 (Figure.3.10.b.). We conclude further, that it is possible it is the BRCA1 binding site on CtIP that binds to the BRCT domains of TopBP1. We also hypothesise that as CtIP associates with TopBP1 in normal cells it constitutively binds to CtIP through one of the binding sites and the other binding site is utilized after DNA damage when both of the proteins are involved in DNA repair. We also conclude, that this would implicate two mechanisms of TopBP1 and CtIP interaction that rely on the cell cycle stage and absence or presence of DNA damage.

As TopBP1 is an ATR activator in response to DNA damage we suggest that CtIP's interaction with TopBP1 enhances ATR kinase activity. And indeed the depletion of CtIP decreases phosphorylation of the two best known ATR substrates, RPA32 and Chk1, in response to SSBs (Sartori et al., 2007). TopBP1 is also known to be involved in HR together with NBS1, thus it is possible that CtIP engages TopBP1 in HR in a similar manner to BRCA1 and MDC1. On the other hand the N-terminal region of NBS1 has been shown to bind to TopBP1 and enable it to form foci (Morishima et al., 2007).

As NBS1 and TopBP1 have two binding sites on CtIP we could hypothesise that each of these proteins binds to CtIP at a different site depending on the process that CtIP and NBS1 or CtIP andTopBP1 are taking part together in. Whether it is HR, MMEJ, ATR activation or end resectioning.

The association of NBS1 and CtIP was established by a co-immunoprecipitation assay as seen in Figure.3.12. To confirm their direct interaction a GST-pull down assay was performed. Figure.3.13.a. shows the direct interaction of radioactively labelled NBS1 and GST-CtIP fragments (Table.3.1.). The fragment containing the FHA domain and the fragment containing Mre11-binding domain and ATM-binding site interact with CtIP (Figure.3.15). To confirm this result another GST-pull down assay was performed using three GST-NBS1 fragments and [^{35}S]CtIP. As seen in Figure.3.13.b. [^{35}S]CtIP interacts with the C-terminal region of NBS1. However, the interaction with the N-terminal region was not seen in this experiment, which is possibly due to the degradation of the GST-NBS1 fragment and its low starting concentration or the conformation of that fragment that would inhibit the binding to the [^{35}S]CtIP. To assay which regions of CtIP bind to NBS1 a GST-pull down was performed. As shown in Figure.3.14.a&b. the N-terminal and the C-terminal regions of NBS1 were radioactively labelled and incubated with various, overlapping GST-CtIP fragments. On the basis of this experiment we can conclude that the N-terminal region of NBS1 containing the FHA domain binds to two regions on CtIP comprising amino acid residues 133-371 containing the C-terminal region of the coiled-coiled region with the Rb-binding motif and the BRCA1-binding site and 775-897aa comprising the second zinc-binding motif. The C-terminal region of NBS1 shows strong binding to the CtIP amino acid residues 133-463 which include the BRCA1 binding domain and 620-775aa region comprising the two major phosphorylation sites, Ser664 and Ser745.

NBS1 has been reported to take part in DSB sensing as a component of the MRN complex. It has also been shown to be involved in the MMEJ repair pathway, like CtIP (Deriano et al., 2009). Thus we could hypothesise that NBS1 could be CtIP's partner while redirecting the DNA damage repair from homologous recombination in S/G2 into microhomology-mediated end-joining in G1/G0 (Yun & Hiom, 2009). This observation

is supported by the observation that CtIP binds to NBS1 via the FHA domain and the C-terminal region thus the binding is not mediated by CtIP's phosphorylation on S327 by CDK during the cell cycle. On the other hand the C-terminal region of NBS1 binds to CtIP through the C-terminal region of CtIP that comprises the two phosphorylation sites known to be phosphorylated by ATM in response to DNA damage (Figure.3.16.b.), thus this interaction could be induced in damaged cells. However it is worth noting that CtIP interacts *in vivo* with NBS1 in normal cells as well and the overall interaction is not induced by DNA damage (Figure.4.1.). However as CtIP binds to NBS1 through two sites it is possible that in normal cells it binds through one motif and in damaged cell by the other and thus the overall level of interaction remains the same.

Taking into consideration all previously described results one can conclude that the BRCA1-binding region of CtIP must be highly active in protein-protein interactions. This region has been shown to be phosphorylated by CDKs in the S/G2 cell cycle stage thus this event may modulate CtIP's binding affinity for different protein partners (Chinnadurai, 2006). However in the course of the work described here we did not look at the influence of CtIP's phosphorylation at S327.

It has also been shown that the phosphorylation status of Ser327 in this region impacts the choice between the homologous recombination (HR) and the microhomology-mediated end-joining (MMEJ), favouring the HR in S/G2 and the MMEJ in G1/G0 (Yun & Hiom, 2009). This would suggest that as 53BP1, MDC1, TopBP1 and NBS1 take part in DNA damage repair through different pathways, CtIP could be orchestrating them for an efficient DNA repair process.

The modulation of CtIP's interaction with the different binding partners may also depend upon its phosphorylation by ATM in response to DNA damage. The fact that

one of CtIP's binding sites for TopBP1 and NBS1 encompasses the two serine residues known to be phosphorylated in response to the DSBs, S664 and S745, suggests that the interaction might have higher affinity in the presence of the DNA lesions. This implies that these sites are involved in the DNA damage response possibly transducing the signal together with TopBP1 and NBS1 to the ATR signalling cascade (Morishima et al., 2007).

To assess CtIP's localization in the cell before and after DNA damage a series of immunofluorescence microscopy experiments were carried out. HeLa cells were mock-irradiated or irradiated with 9Gy of γ-irradiation. Fixed cells were stained using different sets of antibodies and the results show that CtIP localizes in the nucleus of the cell and in unirradiated cells the staining pattern is diffuse with signs of granularity. In irradiated cells CtIP's staining becomes more granular, showing that it concentrates in the microcompartments that partially overlap with the irradiation induced foci (IRIF) of proteins that were previously reported to form IRIF, such as 53BP1, MDC1 and NBS1. This supports the idea that CtIP forms complexes with these proteins and that they aggregate in the vicinity of the DNA lesions. However, it was impossible to asses directly CtIP's localization at the DSBs using γ-H2AX as a marker of the DNA double lesions as both available antibodies against those proteins were of the same serotype. Nevertheless, we could deduce, that as 53BP1, MDC1 and NBS1 are known to co-localize with the γ-H2AX at DSBs and CtIP's staining partially overlaps the foci attributable to those proteins, that CtIP is likely to relocalize in the proximity of DNA lesions and therefore participates in the repair process.

CtIP remains at the DSBs for over 24h (data not shown) thus we could speculate that it dissociates from them only after they are repaired, and during the time it is

concentrated in the IRIF it orchestrates the repair processes carried out by a variety of nuclear factors.

As shown in Figure.3.23&24 the association of DNA damage proteins such as 53BP1 or MDC1 does not depend upon CtIP's presence. However those proteins have already been shown to be the 'recruiting factors' for proteins to concentrate in IRIF (Bekker-Jensen et al., 2006). Thus, as mentioned before CtIP could stimulate the change of active repair pathway depending on the stage of repair of a particular lesion as well as direct the repair towards a particular pathway depending on the cell cycle (Yun & Hiom, 2009). Thus it would behave as a 'repair manager' in the repair pathways.

CHAPTER IV

RESULTS

The in vivo association of CtIP with the DNA damage response proteins and the influence of CtIP siRNA depletion on phosphorylation events in response to DNA damage.

4. The in vivo association of CtIP with the DNA damage response proteins and the influence of CtIP siRNA depletion on phosphorylation events in response to DNA damage.

4.1. Introduction

As shown in section 3.1.2. CtIP interacts *in vivo* and *in vitro* with proteins involved in the DNA damage response such as 53BP1, MDC1, TopBP1 and NBS1. In this chapter CtIP's association with DNA damage response proteins was studied, focusing on the changes that occur after DNA damage. I have also examined how CtIP's siRNA depletion affects phosphorylation events after inflicting DSBs, SSBs and collapse of the replication fork.

Proteins associate into multicomplexes *in vivo*; thus it was of interest to examine how these complexes behave in response to DNA lesions. Following damage the first proteins to be engaged are sensor proteins. They have to recognize the problem and recruit transducer proteins which in turn spread the signal to mediator proteins and effector proteins. In the DNA damage response, proteins that are classified as sensor proteins are mainly the MRN complex consisting of Mre11, Rad50 and NBS1 for recognizing double stranded breaks (DSBs) and RPA70/32/14 complex involved in sensing single stranded breaks (SSBs). They activate transducer proteins such as the members of the PIKK family, namely ATM and ATR respectively. The kinases initiate a phosphorylation cascade which activates the downstream targets which take part in repairing the lesions. One of the classes of proteins to be activated by ATM and ATR are mediator proteins which orchestrate their downstream targets towards resolving the lesions and activating the cell cycle progression, 53BP1 and MDC1 are examples and have been examined in this chapter.

As CtIP was shown to interact with NBS1 and as NBS1 is a member of the MRN complex it was interesting to investigate this association in genetically impaired

backgrounds, such as the ataxia-telangiectasia-like disease (ATLD; Stewart et al., 1999) and Nijmegen breakage syndrome (NBS; Carney et al., 1998; Weemaes et al., 1981).

ATLD is caused by mutation in the Mre11 gene which produces either a truncated protein (homozygote) or full length and mutated protein (heterozygote). At the clinical level ATLD is characterized by progressive cerebellar ataxia and an onset of neurological features (Taylor et al., 2004). In the course of this study LCLs derived from a homozygote patient with a truncating mutation were used.

NBS is caused by a gene mutation, most commonly 657del5 (Varon et al, 1998), causing a premature truncation of the protein and expression of two smaller proteins (Maser et al., 2001). It is characterized by microcephaly, growth retardation, immunodeficiency and predisposition to tumourogenesis. Both disorders display an increased level of chromosome translocations and hypersensitivity to γ-irradiation. They fail to induce DNA damage-activated protein kinases (Taylor et al., 2004). Using cells derived from patients with ATLD and NBS has facilitated the study of CtIP's association with the MRN complex components in physiological backgrounds.

In this study, considerable use was made of CtIP-depleted cells following siRNA treatment. CtIP has been reported to be involved in facilitating the phosphorylation of Chk1 kinase and RPA32 in response to stalled replication forks (Sartori et al., 2007). Thus we examined the influence of CtIP's depletion on phosphorylation events in response to ionizing irradiation, UV irradiation and replication fork stalling.

As ATM is the main kinase involved in the DNA double stranded break response we examined its substrates such as NBS1, ATM, SMC1, 53BP1 and γ-H2AX. These proteins are known to be phosphorylated by ATM. As ATR belongs to the same family of proteins as ATM and shares a consensus phosphorylation motif, it was interesting to investigate how the phosphorylation cascade spreads in response to SSBs and fork

stalling, influencing the phosphorylation status of those proteins. It was also of my interest to investigate whether the depletion of CtIP has an effect on the phosphorylation events in response to UV and replication fork stalling. On the other hand, as it was reported that ATR activates ATM in response to SSBs and replication fork stalling (Stiff et al., 2006), it was of interest to investigate the role of ATR phosphorylation of established ATM targets. Thus, we also investigated whether the depletion of CtIP influences ATR activation and subsequent ATM activation in response to SSBs and replication fork stalling. In addition ATM is responsible for ATR activation in response to DSBs (Yoo et al., 2007) thus it was important to establish whether CtIP also plays role in this process.

4.2. Results.

4.2.1. The in vivo association of CtIP with the DNA damage response proteins before and after DNA damage.

4.2.1.1. The association of CtIP with the DNA damage sensor proteins.

In order to establish CtIP's association *in vivo* with the DNA damage sensor proteins, before and after DNA damage, a co-immunoprecipitation assay was performed. HeLa cells were mock-irradiated, irradiated with 5Gy or with 30J (section 2.1.6.2.) and left for 1 h before harvesting. The co-immunoprecipitation assay was performed as described in the section 2.4.2. A rabbit antibody was used to immunoprecipitate CtIP and the complexes were isolated with protein G-Sepharose beads; the associated proteins were fractionated by the SDS-PAGE and visualized by Western blotting. As shown in the Figure.4.1. CtIP associates with the MRN (Mre11, Rad50, NBS1) complex, which is the main sensor of the double stranded DNA break recognition system. As shown in Figure.4.1. CtIP also associates with RPA70, a main sensor of the single stranded break recognition pathway. Furthermore, none of those interactions are influenced by DNA damage. This may account for CtIP being one of the key

components of these complexes thus co-existing with them despite the damage caused to the DNA.

As shown previously in section 3.1.2.4. CtIP interacts directly with NBS1, which is one of the components of the MRN complex. Here we decided to investigate CtIP's direct interaction with the other components of the MRN complex, namely with Mre11 and Rad50. A GST-pull down assay was performed (section 2.3.5.) using three overlapping GST-CtIP fragments and radioactively labelled (section 2.2.8.) full-length Mre11 and Rad50. Full-length Mre11 or Rad50 were cloned into a pRS314 vector containing a T7 promoter site which enables the expression *in vitro* transcription/translation reaction (section 2.2.8.). Complexes were isolated with glutathione-agarose beads and fractionated by SDS-PAGE. The autoradiographs in Figure.4.2. show the lack of the direct interaction of CtIP with either Mre11 or Rad50.

On the basis of these and previous results we could hypothesise that CtIP forms a complex with the MRN complex via direct interaction with NBS1. It has also been reported that RPA70 binds to Mre11 (Robison et al., 2004) thus we could hypothesise that CtIP-RPA complex formation may be mediated by CtIP-NBS1 direct interaction (Figure.4.3.). On the other hand RPA is known to bind to ATRIP and mediate ATR/ATRIP recruitment to ssDNA (Zou & Elledge, 2003) thus CtIP's association with RPA complex could be mediated via the association of CtIP with TopBP1 which in turn binds to ATR/ATRIP (Figure.4.3.).

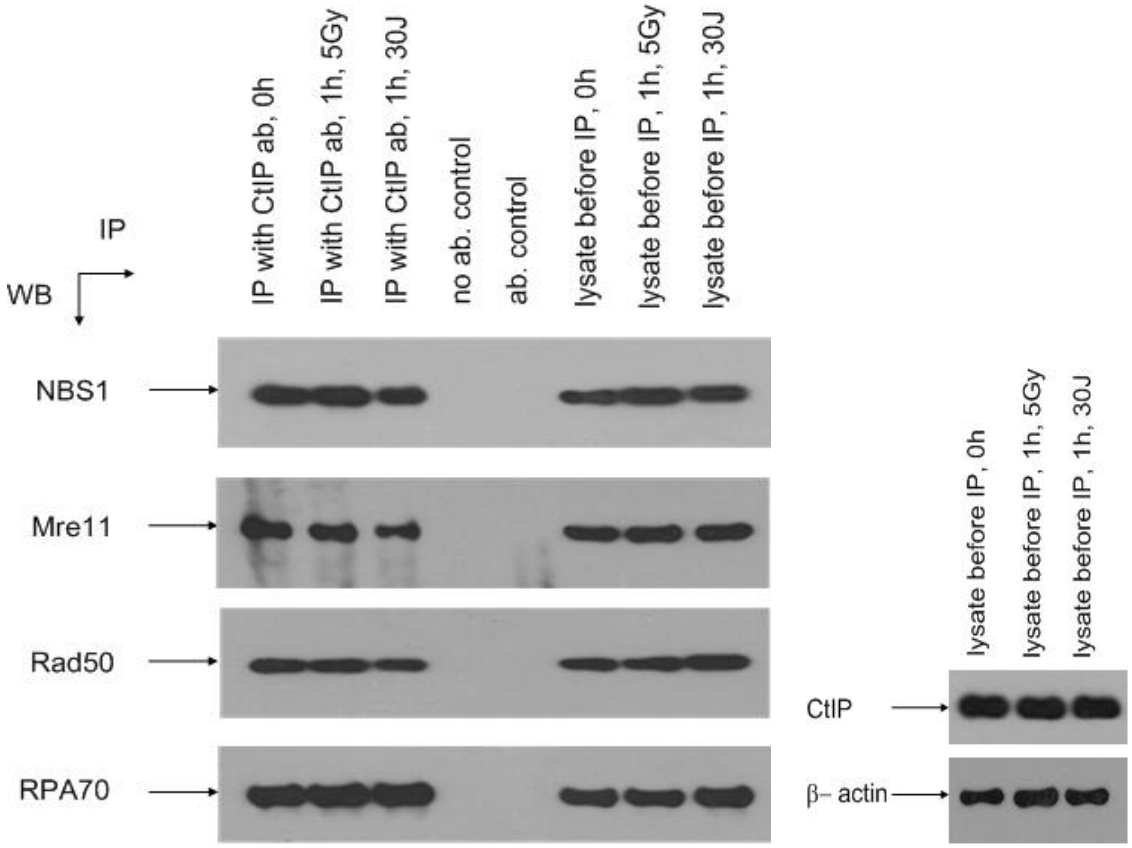

Figure.4.1. The association of CtIP with the DNA damage sensor proteins. HeLa cell lysates were mock-irradiated, irradiated with 5Gy or 30J and harvested 1h post irradiation. CtIP was immunoprecipitated with a rabbit antibody and associated NBS1, Mre11, Rad50 and RPA70 were visualized by Western blotting. In the right hand panel CtIP's basal level is shown before IP and β-actin indicates equal levels of total protein in lysates before IP. This figure is representative of three independent experiments.

a)

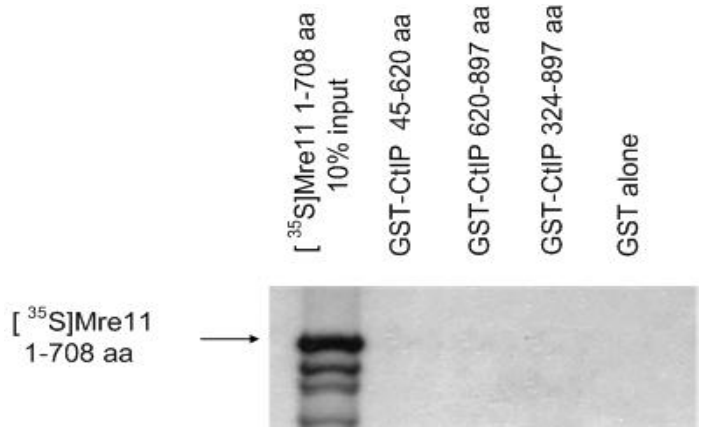

b)

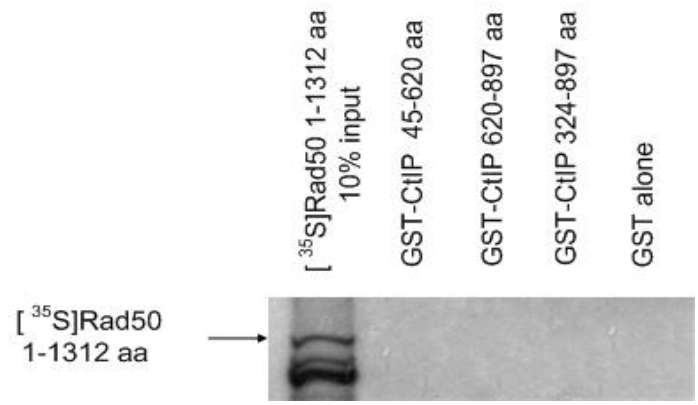

Figure.4.2. CtIP does not interact directly with Mre11 nor Rad50. GST-CtIP polypeptides were incubated with **a)** [^{35}S]Mre11 or **b)** [^{35}S]Rad50 and complexes isolated with the glutathione-agarose beads. Bound proteins were fractionated by SDS-PAGE and visualized by autoradiography. This figure is representative of three independent experiments.

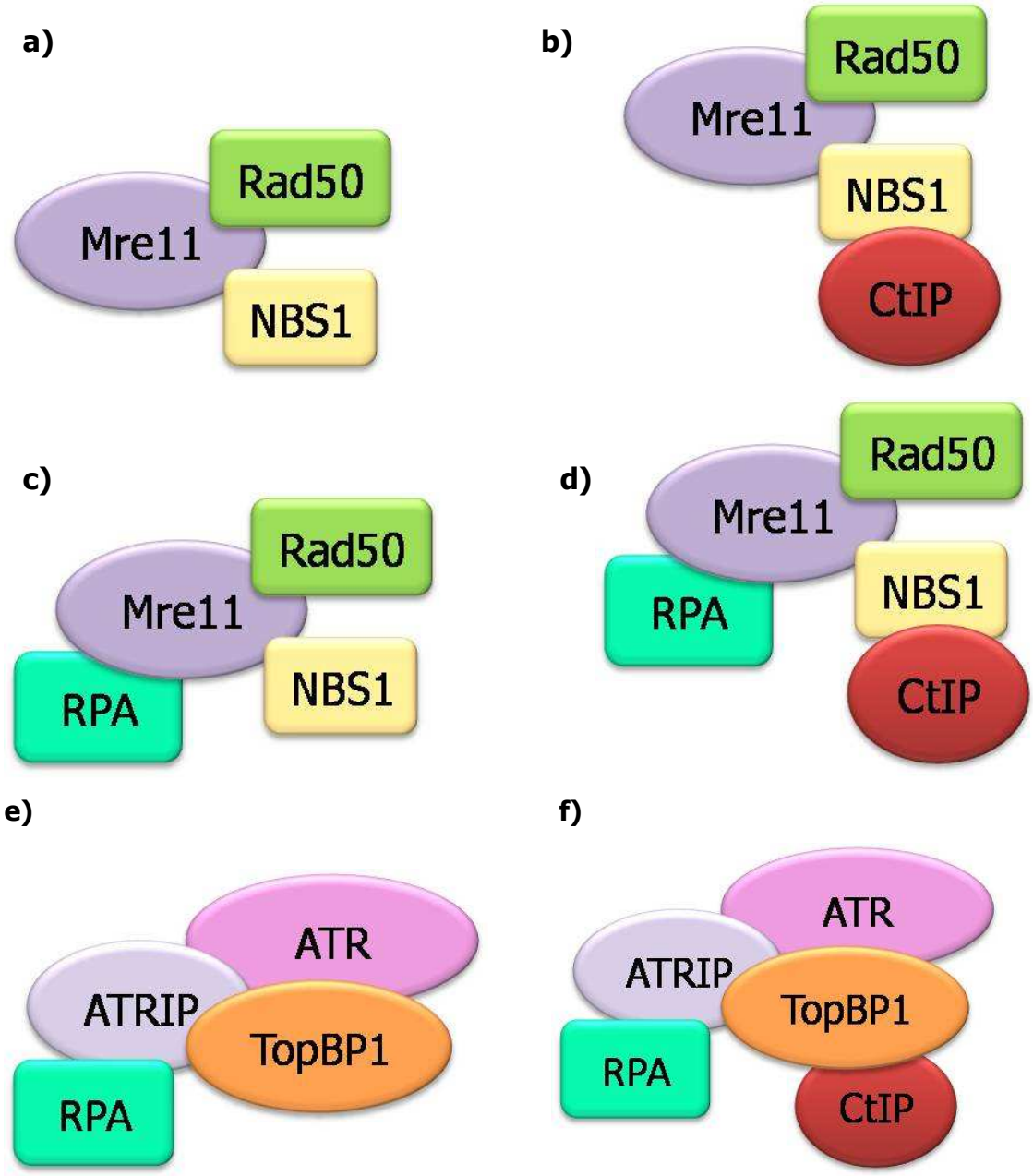

Figure.4.3. Interaction of CtIP with the MRN complex and the RPA complex. **a)** MRN complex, **b)** possible interaction of CtIP with the MRN complex, **c)** MRN and RPA complex, **d)** possible interaction of CtIP with MRN and RPA complexes, **e)** RPA interaction with ATR/ATRIP/TopBP1, **f)** possible interaction of CtIP with RPA and ATR/ATRIP/TopBP1.

4.2.1.2. The association of CtIP with DNA damage transducer proteins.

To assess the *in vivo* interaction of CtIP and DNA damage transducer proteins immunoprecipitation assays were carried out. HeLa cells were mock-irradiated or irradiated with 5Gy or 30J and harvested 1 h post-irradiation. CtIP was immunoprecipitated with a rabbit polyclonal antibody and associated proteins were isolated using protein G-Sepharose beads. Complexes were fractionated by SDS-PAGE and visualized by Western blotting. As shown in Figure.4.4. CtIP associates with the ATM and ATR kinases, the main two kinases transducing the phosphorylation signal to the downstream targets in response to double and single-stranded DNA lesions. The association is not dependent upon DNA damage and occurs with a similar efficiency in irradiated and non-irradiated cells. This result may again suggest that CtIP is a basal component of the complexes formed by ATM and ATR and exists in them on a physiological basis in undamaged cells and that the association is not altered upon the DNA damage.

As shown previously in section 3.1.2.4. CtIP interacts directly with NBS1 which in turn interacts directly with ATM (Falck et al., 2005) thus we could hypothesise that CtIP-ATM interaction in mediated via NBS1 (Figure.4.5.a.).

In section 3.1.2.3. CtIP has been shown to interact directly with TopBP1 which is an activator of ATR. TopBP1 binds to ATR via the PRD domain (Mordes et al., 2008), thus we could hypothesise that association of ATR with CtIP could be mediated by it (Figure.4.5.b.).

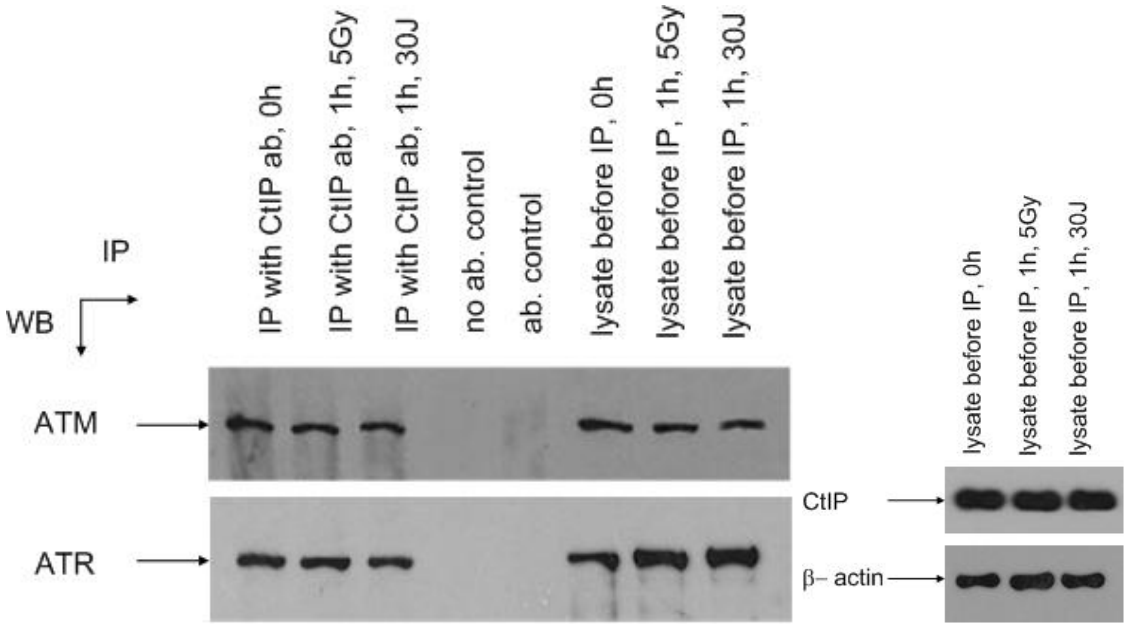

Figure.4.4. The association of CtIP with DNA damage transducer proteins. HeLa cell lysates were mock-irradiated, irradiated with 5Gy or 30J and harvested 1h post irradiation. CtIP was immunoprecipitated with a rabbit antibody and associated ATM and ATR were visualized by Western blotting. In the right hand panel CtIP's basal level is shown before IP and β-actin indicates equal levels of total protein in lysates before IP. This figure is representative of three independent experiments.

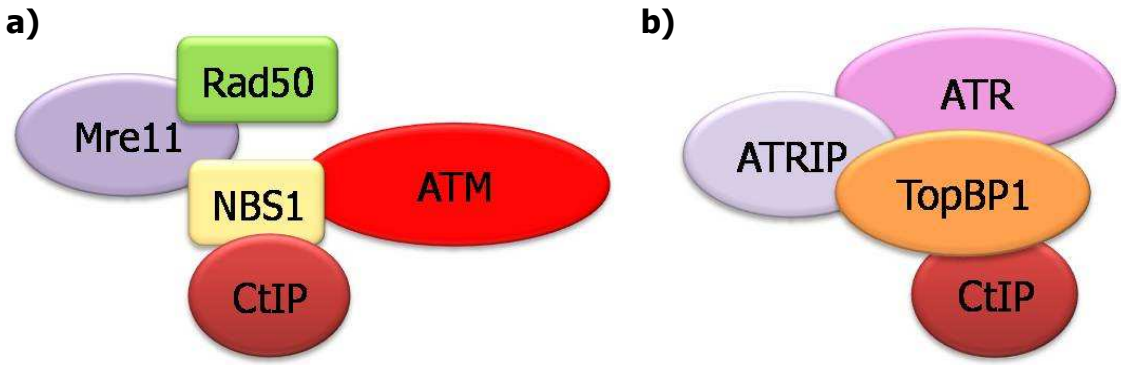

Figure.4.5. Possible CtIP association with ATM and ATR. a) CtIP can associate with ATM via its direct interaction with NBS1, **b)** CtIP can associate with ATR via its direct interaction with TopBP1.

4.2.1.3. The association of CtIP with the DNA damage mediator proteins.

It was shown previously in sections 3.1.2.1. and 3.1.2.2. that CtIP interacts with 53BP1 and MDC1 *in vivo* and *in vitro*. In this section we investigated the influence of DNA damage on those interactions. A co-immunoprecipitation assay was performed (section 2.4.2.) using HeLa cell lysates that were previously mock-irradiated or irradiated with 5Gy or 30J and harvested one hour after irradiation. Rabbit polyclonal antibodies against 53BP1 or MDC1 were used to immunoprecipitate 53BP1 and MDC1 respectively. Complexes were isolated with protein G-Sepharose beads and fractionated with SDS-PAGE. Associated CtIP was detected by Western blotting. As shown in Figure.4.6. CtIP associates with 53BP1 and this interaction is not influenced by the DNA damage as is the case of CtIP's association with MDC1 before and after DNA damage (Figure.4.7.). This result may suggest that those complexes form in normal cells and that the occurrence of the double- or single-stranded DNA lesions does not change them.

As CtIP interacts directly with both 53BP1 and MDC1 and 53BP1 and MDC1 have been reported to interact directly as well (Eliezer et al., 2009) it is possible that CtIP forms a complex involving both of those proteins (Figure.4.8.). MDC1 is also thought to be an indispensible component of the MRN complex thus MDC1, MRN, 53BP1 and CtIP could be involved in a multiprotein complex together with ATM which is known to bind to NBS1 and MDC1 (Stucki & Jackson, 2006).

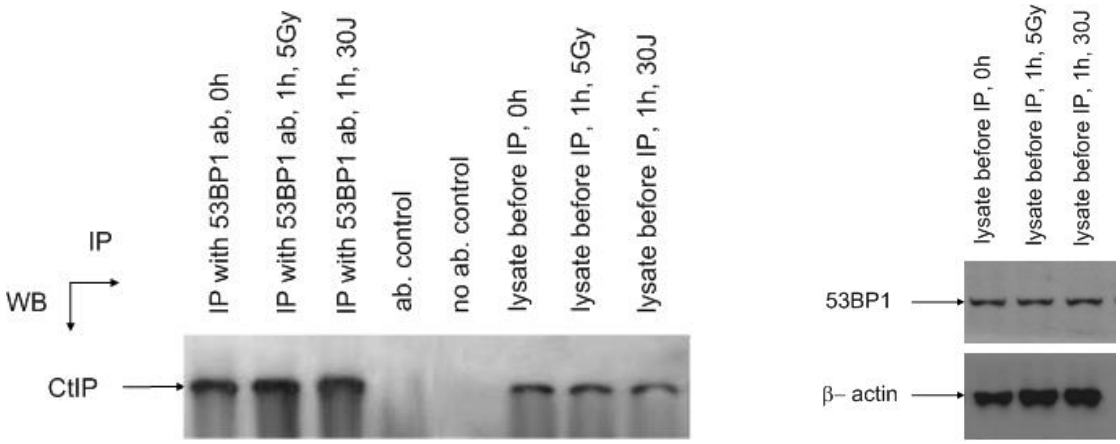

Figure.4.6. The association of CtIP with the DNA damage transducer protein 53BP1. HeLa cell lysates were mock-irradiated, irradiated with 5Gy or 30J and harvested 1h post irradiation. CtIP was immunoprecipitated with a rabbit antibody and associated proteins visualized by Western blotting. In the right hand panel 53BP1's basal level is shown before IP and β-actin indicates equal levels of total protein in lysates before IP. This figure is representative of three independent experiments.

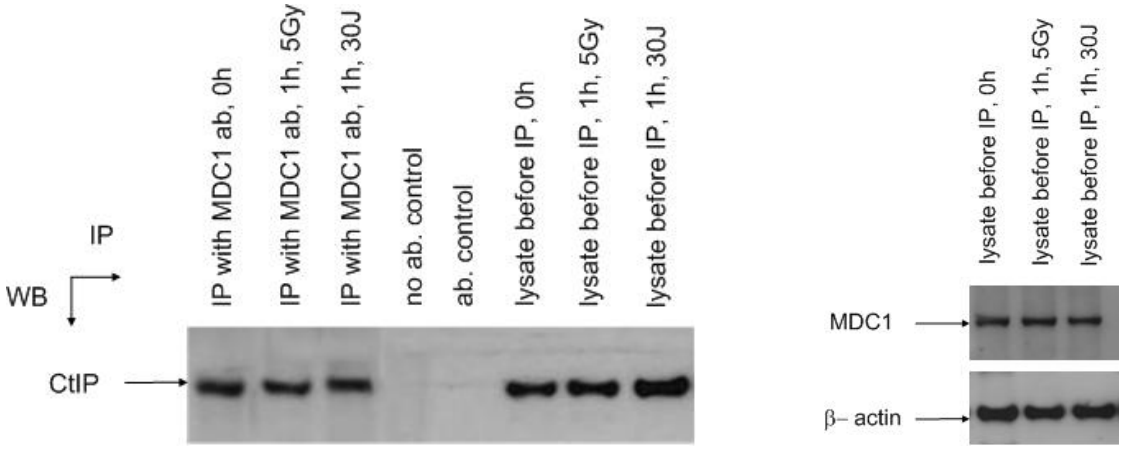

Figure.4.7. The association of CtIP with the DNA damage transducer protein MDC1. HeLa cell lysates were mock-irradiated, irradiated with 5Gy or 30J and harvested 1h post irradiation. CtIP was immunoprecipitated with a rabbit antibody and associated proteins visualized by Western blotting. In the right hand panel MDC1's basal level is shown before IP and β-actin indicates equal levels of total protein in lysates before IP. This figure is representative of three independent experiments.

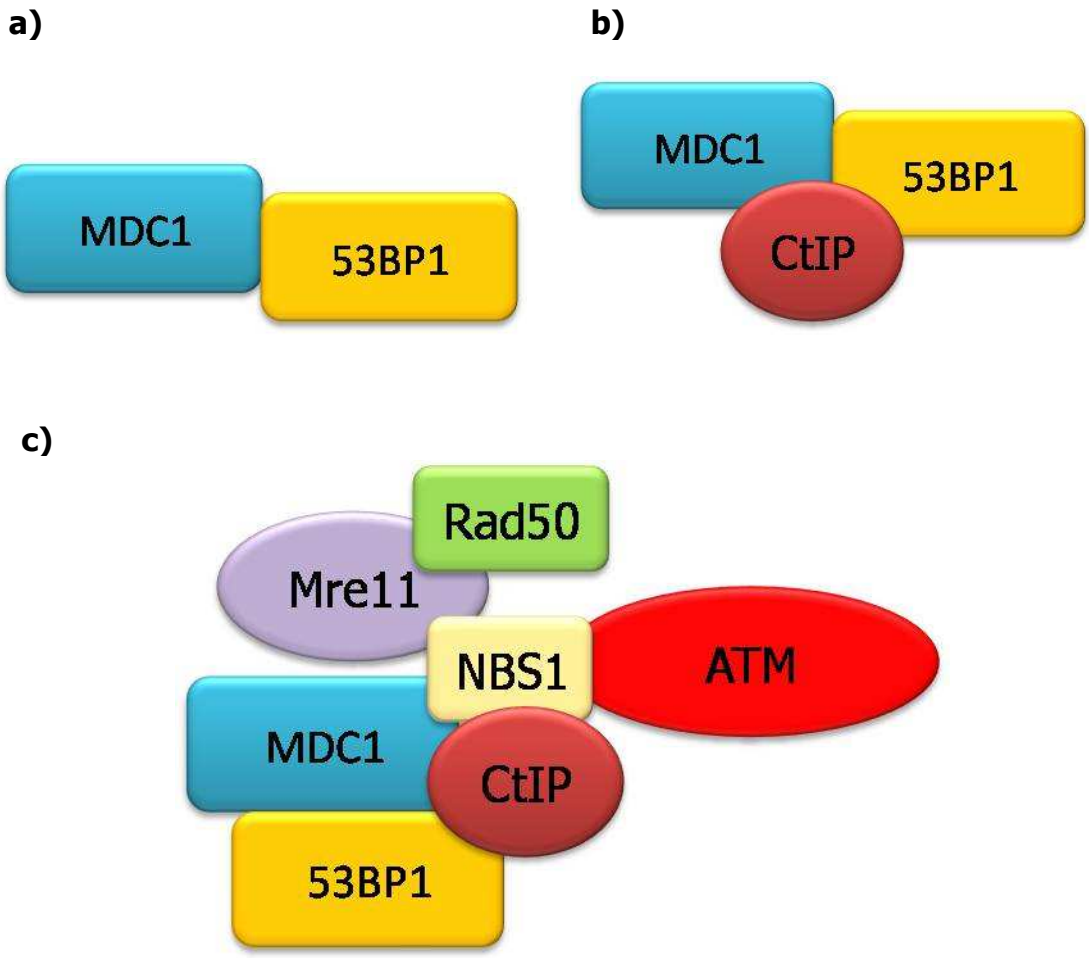

Figure.4.8. Possible CtIP involvement in a multicomplex with the MRN complex, MDC1, 53BP1 and ATM. a) MDC1 and 53BP1 complex formation, **b)** CtIP interaction with MDC1 and 53BP1, **c)** possible complex involving the MRN complex, MDC1, 53BP1, ATM and CtIP.

4.2.2. The interaction of CtIP with ATM and the MRN complex components in patients with ATLD and NBS syndromes.

In order to establish whether CtIP's *in vivo* association with the key factors of the double-stranded DNA damage response pathway differs in genetically pathological backgrounds, a series of co-immunoprecipitation assays (section 2.4.2.) was performed, using LCL cells derived from a healthy donor, ATLD LCLs and NBS LCLs.

The ATLD patient-derived LCLs harbour a truncating mutation, which causes C > T transition at nucleotide 1897, creating an in-frame stop codon and resulting in a premature termination at 571aa instead of 680aa, producing a 65kDa protein in place of a 81kDa one (Figure.4.9; Stewart et al., 1999).

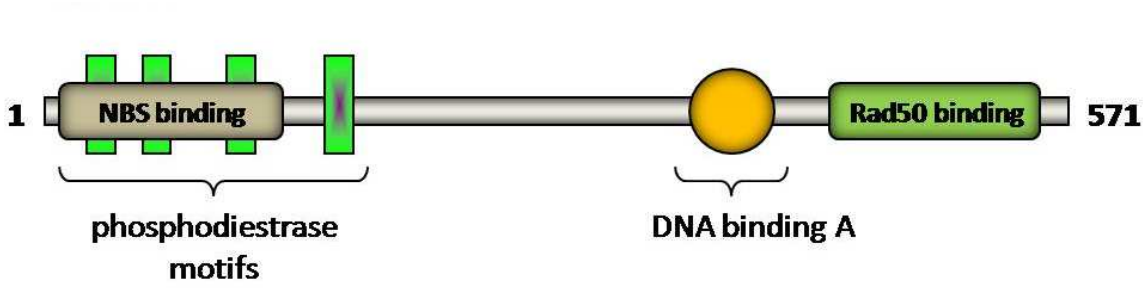

Figure.4.9. The Mre11 protein expressed by the ATLD patient used in this study.

The NBS patient-derived LCLs contain a typical truncation in the *NBS* gene, the 657del5 mutation in exon 6, splitting the protein into a 26K (p26, 1-218aa) and a 70K (p70, 221-754aa) polypeptide (Figure.4.10; Matsura et al., 1998).

CtIP was immunoprecipitated with a rabbit polyclonal antibody from the cell lysates prepared from normal LCL cells, ATLD LCLs and NBS LCLs which were mock-irradiated or irradiated with 5Gy. The complexes were fractionated by SDS-PAGE and associated proteins were visualized by Western blotting. As shown in the Figure.4.11.a.

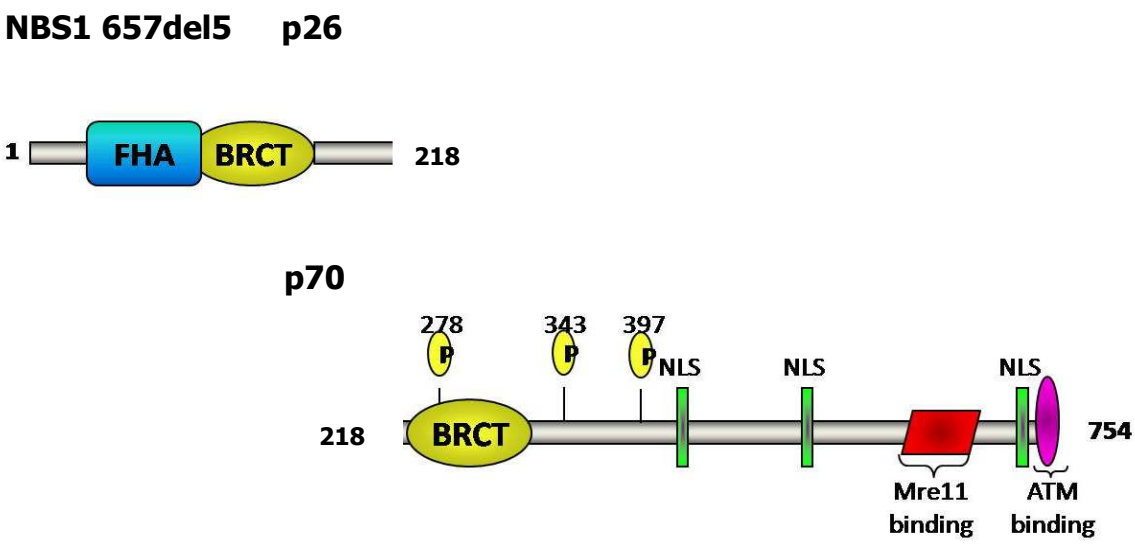

Figure.4.10. The NBS1 proteins expressed by the NBS patient used in this study.

CtIP associates with Mre11 and Rad50 and the efficiency of complex formation corresponds to the basal levels of those proteins in the cell lysates. There is also no change in the association before and after damage caused by 5Gy of irradiation. Mre11 associates with CtIP despite the C-terminal truncation although the complex formation is not as efficient as in the cells with the full-length Mre11. This is possibly due to lower basal levels of mutated protein compared to unmutated one. It has also been reported that despite the truncating mutation NBS1 associates with Mre11 but at lower efficiency (Stewart et al., 1999). This observation is consistent with the observation that the NBS1 binding region on Mre11 is located towards the N-terminus of the protein (Williams et al., 2007) and is unaffected by the truncation.

Mre11 also associates with CtIP in NBS patient LCLs (Figure.4.11.a.) suggesting that the intact NBS1 is not necessary for this interaction and either both of the proteins associate with the p70 protein or these proteins exist in a large complex with other proteins which associate with CtIP and Mre11 separately.

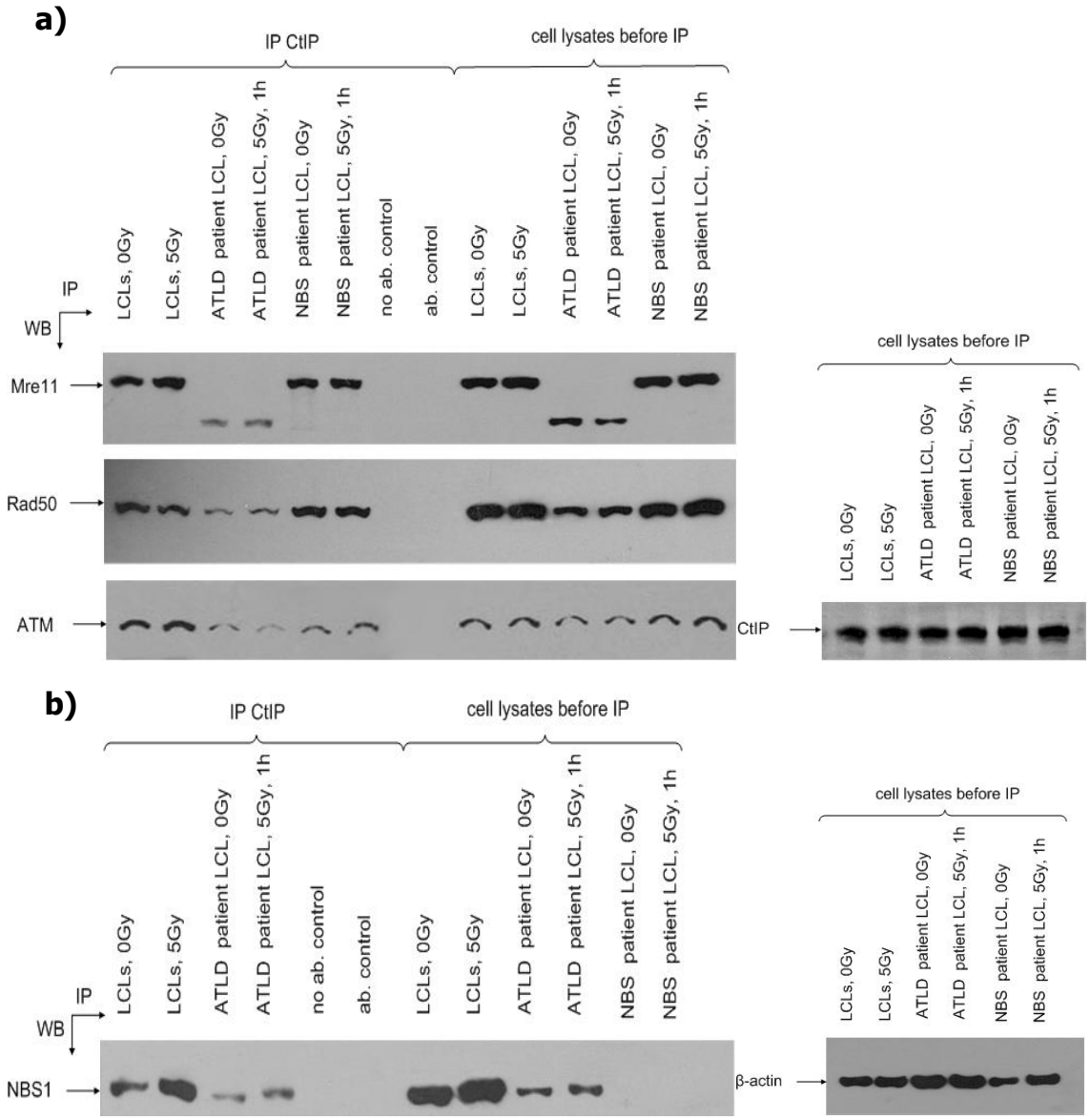

Figure.4.11. The association of CtIP with Mre11, Rad50 and ATM in ATLD and NBS patient derived LCLs and NBS1 in ATLD patient derived LCLs. a) normal LCLs, ATLD LCLs and NBS LCLs or **b)** normal LCLs and ATLD LCLs were mock-irradiated or irradiated with 5Gy and harvested 1 h post irradiation. CtIP was immunoprecipitated with a rabbit antibody and associated **a)** Mre11, Rad50, ATM or **b)** NBS1 were visualized by Western blotting. In the right hand panel CtIP's basal level is shown before IP and β-actin indicates equal levels of total protein in lysates before IP. This figure is representative of three independent experiments.

Rad50 is detected in the CtIP immunoprecipitates as well (Figure.4.11.a.). The interaction in all cell lines appears to be stable and not dependent either upon intact Mre11 nor NBS1. In the ATLD LCLs the association with CtIP is decreased but not abrogated as all of the MRN complex components have decreased levels of expression (Stewart et al., 1999). In the NBS LCLs the interaction is the same as in the normal LCLs, again either due to CtIP's association with p70 NBS1 and Mre11 or due to immunoprecipitation of a complex consisting of more than just the MRN proteins. Rad50's association with CtIP appears to be mediated through other proteins that were immunoprecipitated together with CtIP and MRN complex.

In case of CtIP's association with ATM in normal LCLs and ATLD LCLs the association again does not change after DNA damage and corresponds to the basal levels of ATM before immunoprecipitation (Figure.4.11.a.). However in the NBS LCLs there is a slight reduction in the association of CtIP and ATM in comparison to the basal level of ATM in NBS LCLs which would suggest the same amount of complex formation as in the normal LCLs if the mutation in NBS1 was not affecting the complex formation. Thus we hypothesise that full length NBS1 has influence on ATM and CtIP's complex formation which is disrupted in NBS LCLs which carry a truncating mutation, causing the expression of two NBS1 protein: N-terminal p26 and C-terminal p70. Thus we speculate that the full length NBS1 is necessary for an efficient CtIP and ATM complex formation.

CtIP and ATM's association is also reduced in ATLD LCLs (Figure.4.11.a.) but this is most likely due to lower expression of NBS1 in those cells. This would imply that NBS1 plays a role in efficient formation of CtIP-ATM complex as suggested in the previous section (Figure.4.5.a.).

In order to establish whether NBS1 phosphorylation by ATM influences its association with CtIP a co-immunoprecipitation assay was performed (section 2.4.2.). LCL cells

derived from an A-T patient were mock-irradiated or irradiated with 5Gy and harvested 1h post-irradiation. CtIP was immunoprecipitated with a rabbit antibody and complexes were isolated with protein G-Sepharose beads and fractionated by SDS-PAGE. The associated NBS1 was visualized by Western blotting. As shown in Figure.4.12. NBS1 associates with CtIP in the absence of ATM and the interaction is not dependent upon DNA damage. The association is also unaffected by the phosphorylation status of NBS1, which is seen as a band shift in the presence of ATM following IR (Figure.4.12., top panel, fourth track). Thus we could conclude that association of CtIP and NBS1 is stable and is not affected by the phosphorylation status of NBS1 nor the absence of ATM.

To examine further the interaction of CtIP with the components of the MRN complex an Mre11 knock-down was performed. HeLa cells were incubated twice with an Mre11 siRNA (section 2.1.7.) and 96 h post treatment the cells were mock-irradiated or irradiated with 5Gy. Cell lysates were immunoprecipitated with a rabbit antibody against CtIP, complexes were isolated using protein G-agarose beads (section 2.4.2.), fractionated by SDS-PAGE and associated proteins were visualized by Western blotting. Figure.4.13. shows that Mre11 knock-down causes the down regulation of all of the components of the MRN complex, similarly to mutation in an ATLD patient derived LCLs (Stewart et al., 1999). However the association of CtIP with NBS1 or Rad50 is not abolished in knock-down cells. It is compromised by the down-regulation of expression of NBS1 and Rad50 but not disrupted by Mre11 knock-down. This suggests that Mre11 is not essential for CtIP's association with NBS1 or Rad50.

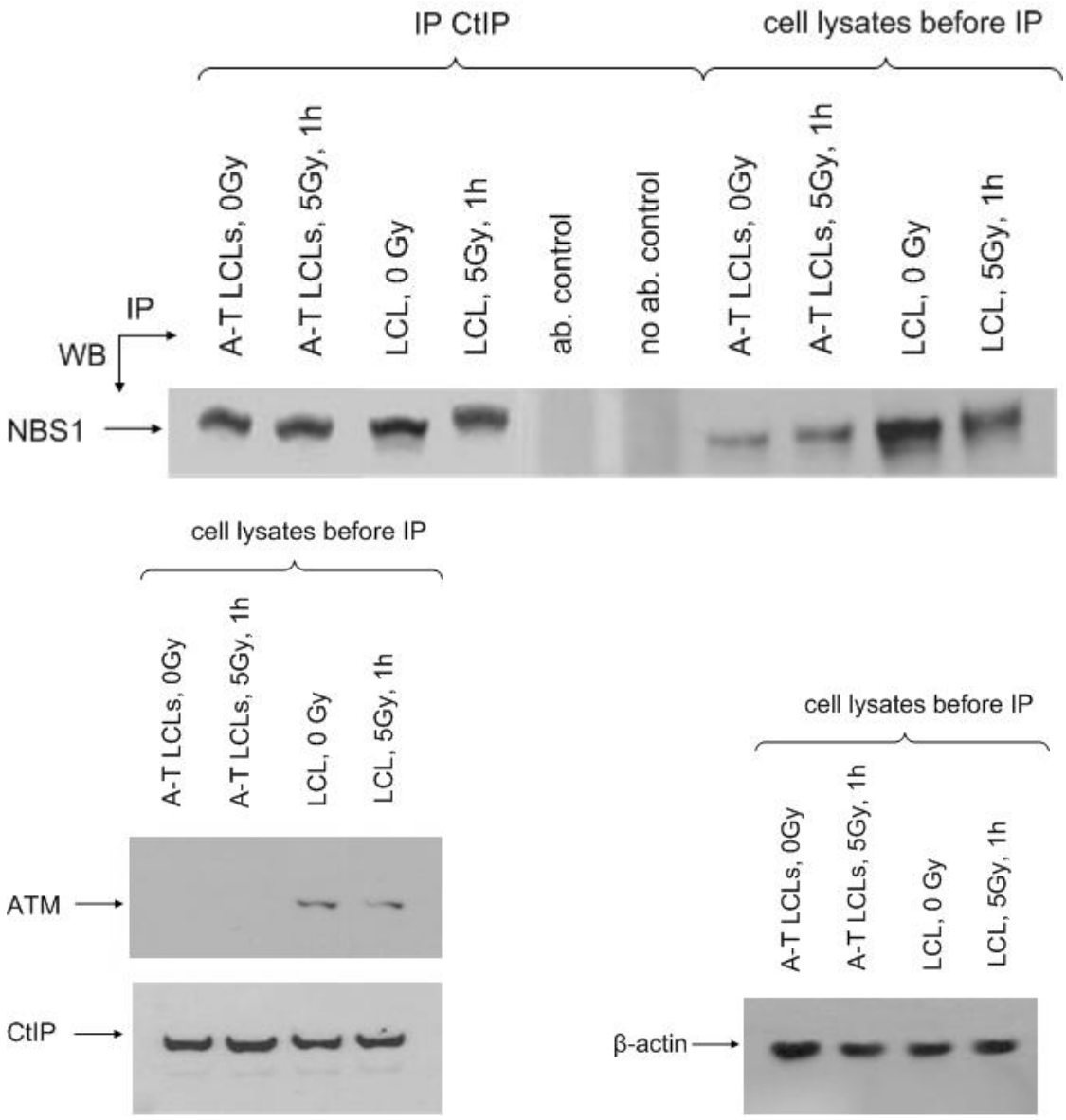

Figure.4.12. The influence of NBS1 phosphorylation on its association with CtIP. Normal LCLs and A-T LCLs were mock-irradiated or irradiated with 5Gy and harvested after 1 h. CtIP was immunoprecipitated with a rabbit antibody and associated NBS1 was visualized by Western blotting. In the lower panels ATM's and CtIP's basal level is shown before IP and β-actin indicates equal levels of total protein in lysates before IP. This figure is representative of three independent experiments.

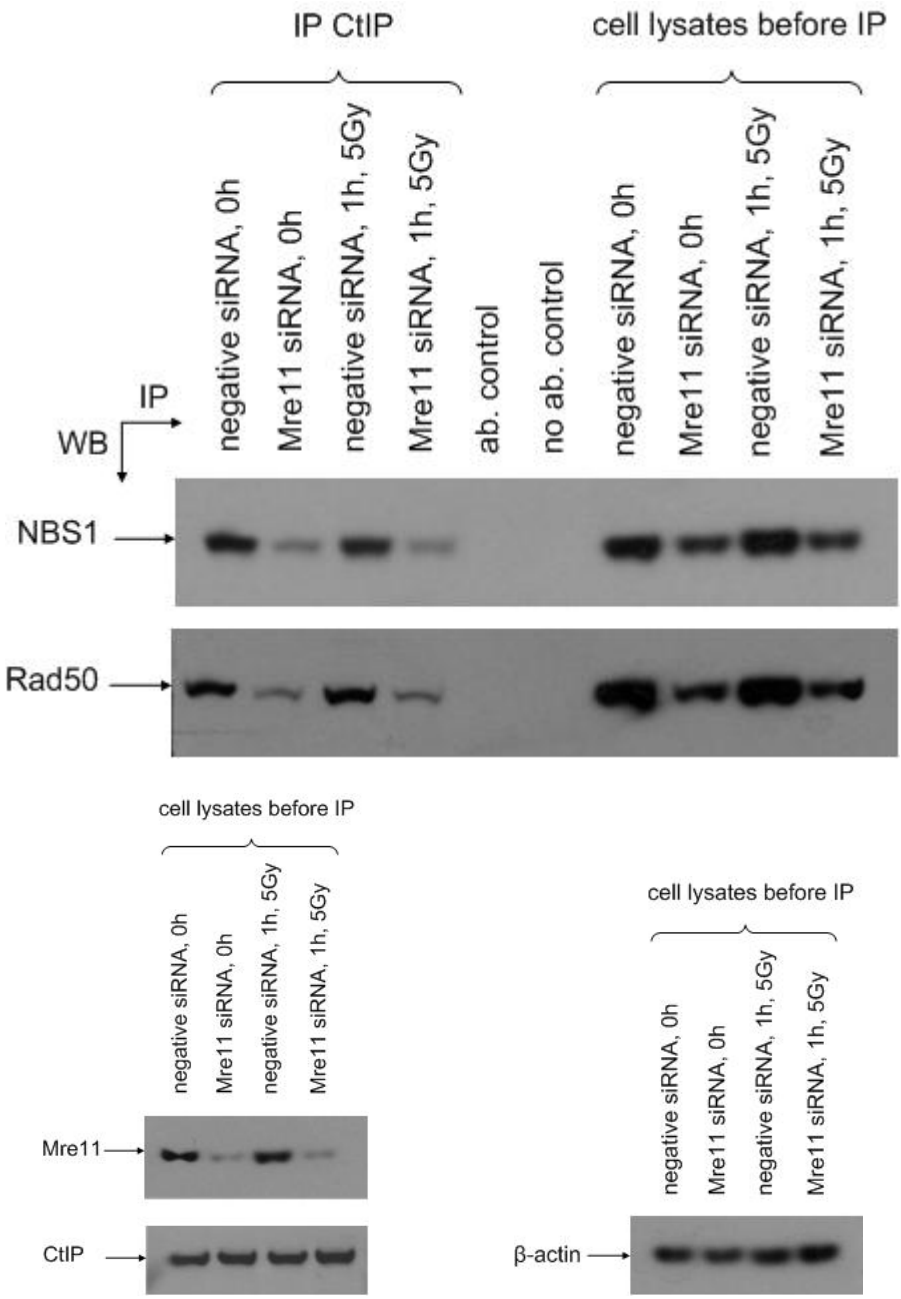

Figure.4.13.The association of CtIP with NBS1 and Rad50 in Mre11 knock-down HeLa cells. HeLa cells were treated with Mre11 siRNA and subsequently mock-irradiated or irradiated with 5Gy. CtIP was immunoprecipitated with a rabbit antibody and associated NBS1 and Rad50 were visualized by Western blotting. In the lower panel Mre11's and CtIP's basal levels are shown and β-actin indicates equal levels of total protein in lysates before IP. This figure is representative of three independent experiments.

As NBS1 was previously shown to bind CtIP directly, mainly through the region containing the Mre11 binding domain and ATM binding site (section 3.1.2.4.), we investigated whether Mre11 can be competed off NBS1 by the addition of excess CtIP. A co-immunoprecipitation assay was performed (section 2.4.2.) using LCL cells which were mock-irradiated or irradiated with 5Gy. A rabbit antibody against NBS1 was used to immunoprecipitate NBS1 in the presence of either 10μg of full length GST-CtIP, no GST-tagged protein or GST protein alone. LCL cell lysates were incubated with the antibody, with or without GST-tagged protein, overnight at 4^{o}C. On the following day complexes were isolated with protein G-Sepharose beads, fractionated by SDS-PAGE and the associated Mre11 was visualized by Western blotting. As shown in Figure.4.14. the association of NBS1 and Mre11 is slightly disrupted by addition of the GST protein alone but is virtually abolished by the addition of the full length GST-CtIP construct. DNA damage caused by 5Gy does not influence that effect.

This result suggests that excess GST-CtIP protein could compete Mre11 off NBS1. We hypothesise that the *in vivo* association of one of the pools of Mre11-NBS1 complexes might be influenced by CtIP as CtIP has been shown to bind to NBS1 via its C-terminal region containing the Mre11-binding site (Chen et al., 2008). This would mean that NBS1 could be competed off Mre11 and directed for association with other proteins and this would be orchestrated by CtIP acting as a mediator protein. Alternatively it is possible that CtIP interacts with a certain pool of NBS1 preventing its binding to Mre11.

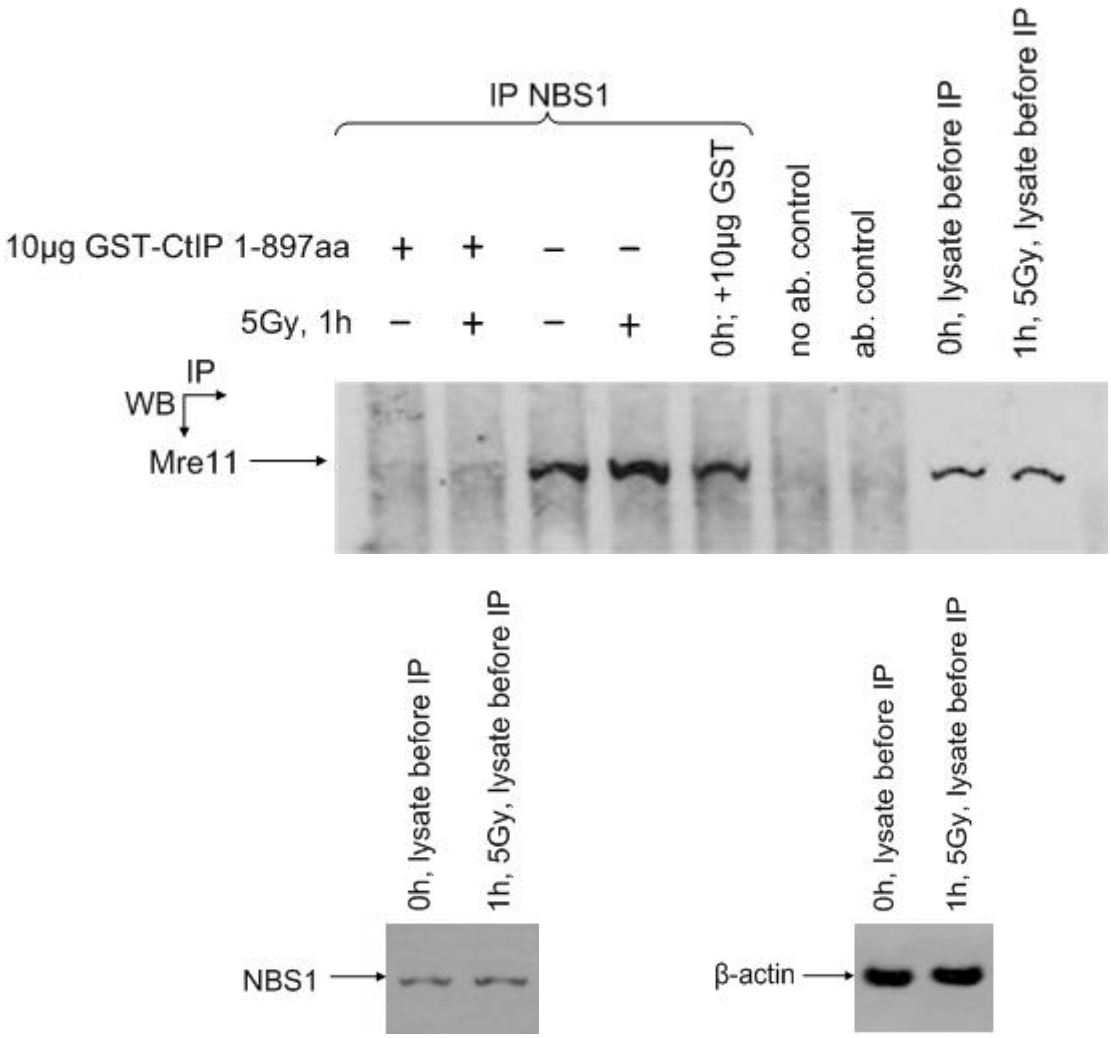

Figure.4.14.CtIP and Mre11 compete for the same binding site on NBS1. LCL cells were mock-irradiated or irradiated with 5Gy and harvested an hour post irradiation. NBS1 was immunoprecipitated with a rabbit antibody in the presence of 10µg of GST-CtIP or 10µg GST protein or without GST-tagged protein. Coimmunoprecipitating Mre11 was identified by Western blotting. In the lower panel NBS1's basal level is shown before IP and β-actin indicates equal levels of total protein in lysates before IP. This figure is representative of three independent experiments.

4.2.2.1. The influence of CtIP's knock-down on the phosphorylation events in response to different DNA damaging agents.

To establish CtIP's influence on phosphorylation events in response to different damaging agents a CtIP knock-down was performed (section 2.1.7.). HeLa cells were mock-treated or treated with the CtIP siRNA and after 72 h they were either mock-irradiated or irradiated with 5Gy or 30J (section 2.1.6.2.) or treated with camptothecin (CPT) at 1μM for 1 h (section 2.1.5.1.). Following treatment, cells were harvested at four time points: before treatment – 0 h and after treatment: 1 h, 5 h and 24 h. The cell lysates were fractionated by SDS-PAGE and proteins were visualized by Western blotting.

Figure.4.15. shows the phosphorylation of five ATM targets after the DNA damage caused by 5Gy. ATM activation is rapid and reaches its maximum 5 min after treatment with 0.5Gy. It has also been shown that ATM stays in a phosphorylated state for at least 24h (Bakkenist & Kastan, 2003). As shown in Figure.4.15. ATM is phosphorylated after exposure to 5Gy at 1h and 5h time point. The absence of phosphorylation after 24h may be due to too short exposure of the X-ray film or the fact that in this study instead of primary fibroblasts HeLa cells were used. However in the absence of CtIP phosphorylation of ATM in HeLa cells persists longer which may be due to DNA damage taking longer time to be repaired in the absence of CtIP. NBS1 is typically phosphorylated by ATM on S343 in response to the DNA double stranded breaks. As shown in Figure.4.15. there is no significant difference in NBS1 phosphorylation on S343 in CtIP-depleted cells. The same result is obtained for autophosphorylation of ATM on S1981, SMC1 phosphorylation on S966 and γ-H2AX on the S139.

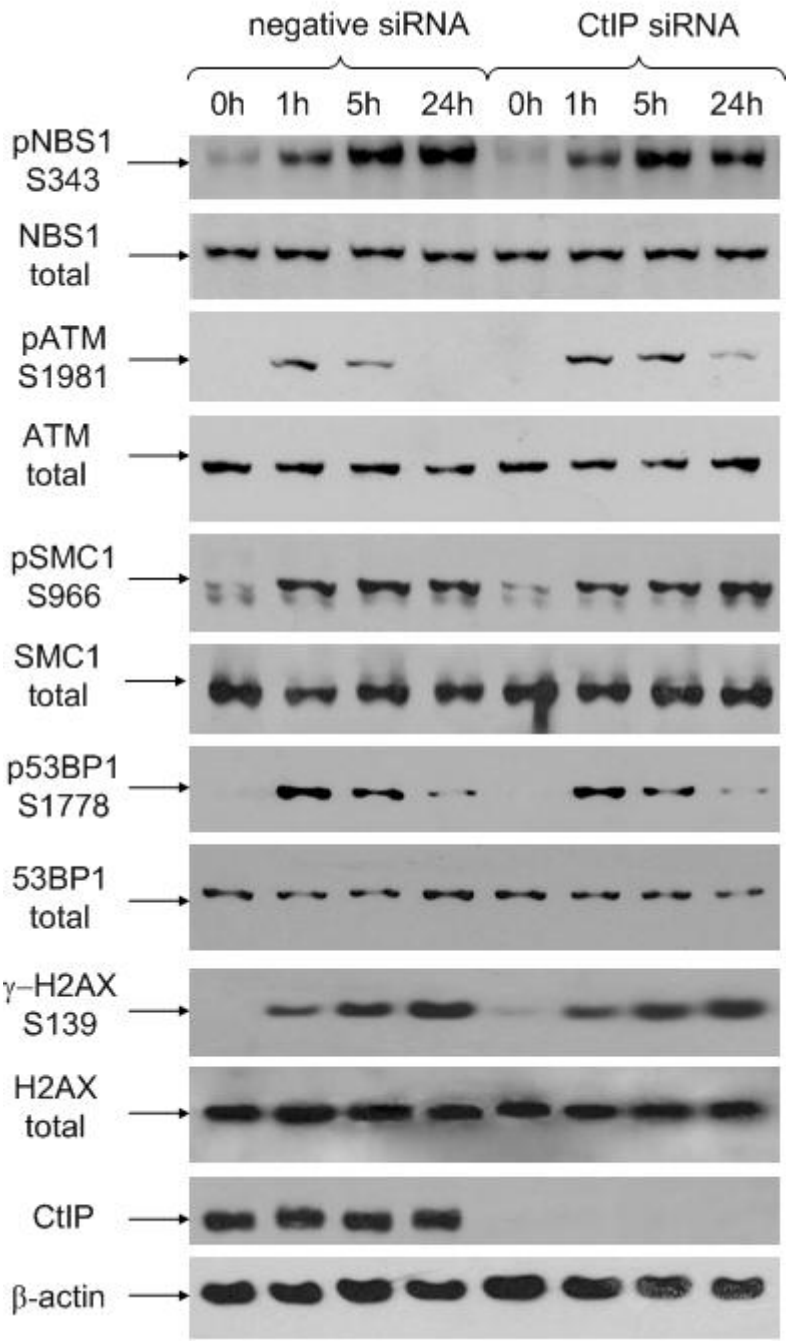

Figure.4.15. The influence of CtIP knock-down on phosphorylation of ATM targets in response to 5Gy of ionizing radiation. HeLa cells were treated with CtIP siRNA and subsequently mock-irradiated or irradiated with 5Gy and harvested at the indicated time points. The cell lysates were fractionated by SDS-PAGE and proteins visualized by Western blotting. This figure represents a result of three independent experiments.

S1778 of 53BP1 has not previously been reported as an ATM phosphorylation site (Jowsey et al., 2007) but it is a consensus site for ATM and ATR and has been shown to be phosphorylated in the response to 3Gy of ionizing radiation by Stewart et al. (Stewart et al., 2007). As shown in Figure.4.15. it is phosphorylated in response to 5Gy and the depletion of CtIP has only a minor effect. As mentioned before, ATM and ATR have a consensus phosphorylation motif and so this phosphorylation may be a joint effort. Thus in CtIP depleted cells 53BP1's phosphorylation on S1778 is not impaired in CtIP knock-down cells. Overall this result suggests that the siRNA depletion of CtIP has a minor effect on the phosphorylation events in response to double-stranded DNA lesions orchestrated by ATM.

To establish if single-stranded DNA lesions and depletion of CtIP have an effect on the phosphorylation cascade, HeLa cells were irradiated with 30J and harvested at the indicated time points. As shown in Figure.4.16. phosphorylation of typical ATR targets such as Chk1 and RPA32 is notably impaired in the CtIP depleted cells suggesting that CtIP facilitates their phosphorylation in response to single-stranded DNA breaks. In Figure.4.17. the influence of CtIP knock-down on previously described ATM targets is shown. As expected there is no significant influence of CtIP depletion on the SMC1 phosphorylation. Its phosphorylation is less in response to UV-irradiation compared with γ-irradiation. The lack of a marked reduction in SMC1 phosphorylation in CtIP-depleted cells may be due to the ATR basal activity that is present in normal cells. As shown by Kim et al. (2002) SMC1 is a major ATM target in response to IR, but it is still phosphorylated in ATM-depleted cells in response to UV and replication fork stalling in an ATR-dependent manner. As has been reported, phosphorylation of SMC1 occurs in cells lacking DNA-PK, thus suggesting that phosphorylation of SMC1 is DNA-PK independent (Kim et al., 2002). Thus one could argue that basal activation of ATR is sufficient to activate a portion of ATM in response to UV and replication fork stalling.

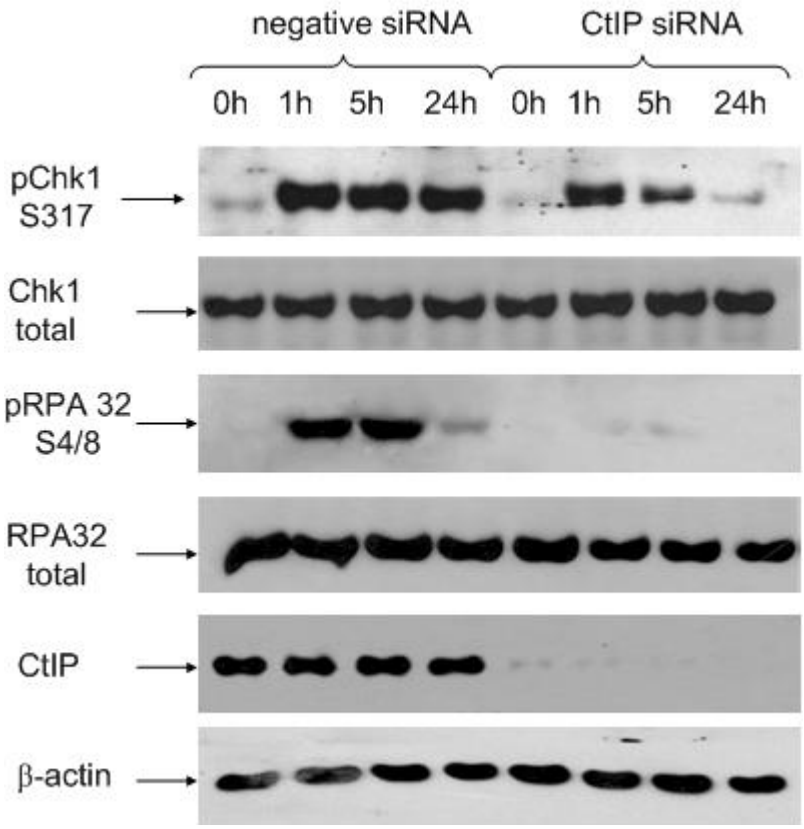

Figure.4.16. The influence of CtIP knock-down on phosphorylation of ATR targets in response to 30J of UV radiation. HeLa cells were treated with CtIP siRNA and subsequently mock-irradiated or irradiated with 30J and harvested at the indicated time points. The cell lysates were fractionated by SDS-PAGE and proteins visualized by Western blotting. This figure is representative of three independent experiments.

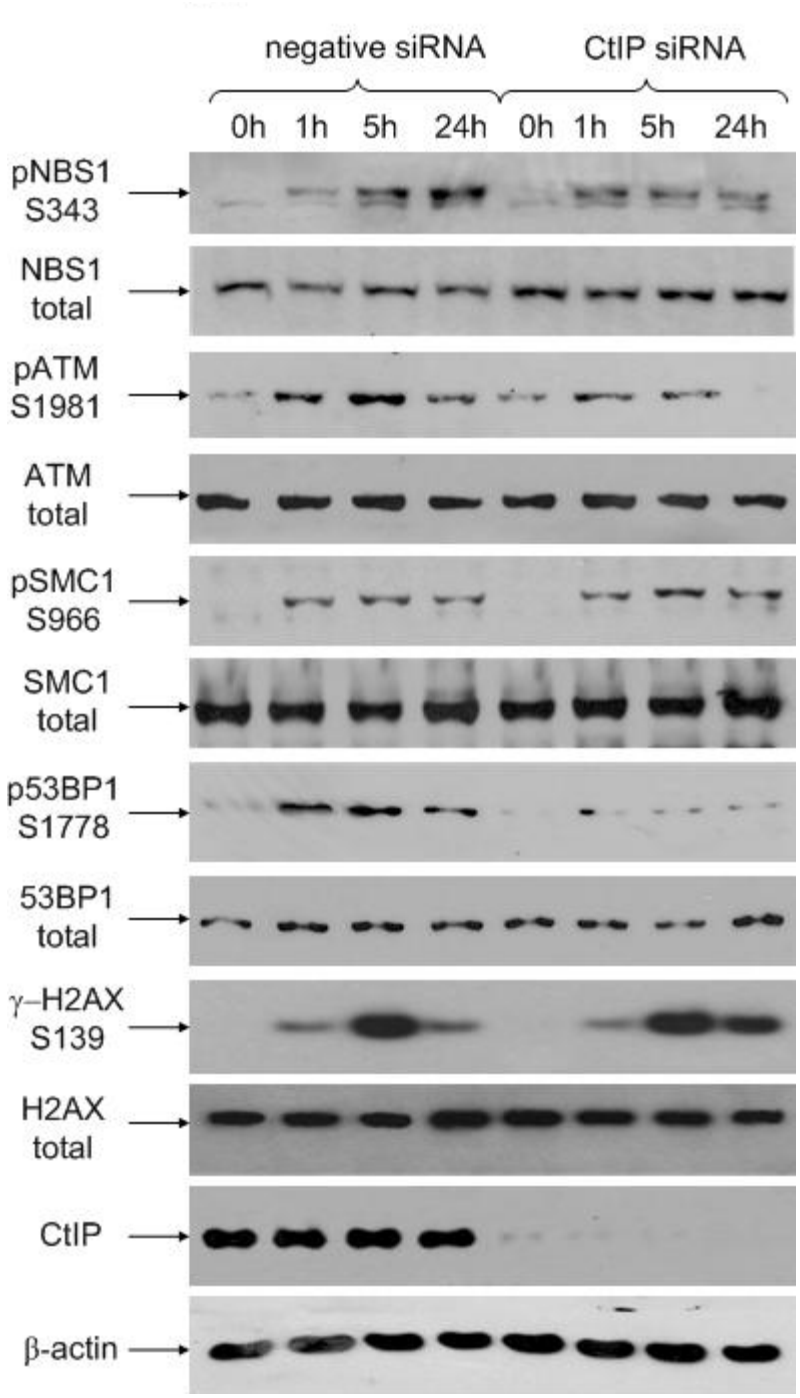

Figure.4.17. The influence of CtIP knock-down on phosphorylation of ATM targets in response to 30J of UV radiation. HeLa cells were treated with CtIP siRNA and subsequently mock-irradiated or irradiated with 30J and harvested at the indicated time points. The cell lysates were fractionated by SDS-PAGE and proteins visualized by Western blotting. This figure is representative of three independent experiments.

However in cells depleted of CtIP, ATR kinase, as it only shows its basal activity, cannot efficiently cooperate with ATM in phosphorylation of such targets as NBS1, ATM itself and 53BP1. This is confirmed by the delayed H2AX phosphorylation (Figure.4.17.). We could speculate, that the basal activity of ATR, observed in cells depleted of CtIP, is sufficient enough to activate only a portion of ATM. This in turn would mean that at the beginning of the ATM phosphorylation cascade H2AX is not phosphorylated efficiently, due to only partial activation of ATM. Which in turn results in prolonged activation of ATM which eventually results in full phosphorylation of H2AX. The process is delayed, however, and it does reach its full potential until 5h post irradiation (Figure.4.17.).

We could hypothesise that ATM in CtIP-depleted cells is active for longer to complete all of its normal tasks and this is seen as prolonged phosphorylation of H2AX and SMC1. On the other hand depletion of CtIP using siRNA seems to create a basal response to DSBs which is seen as appearance of γ-H2AX foci in unirradiated cells treated with CtIP siRNA (data not shown). This could also contribute to ATM's basal activation and its prolonged activity.

However, NBS1 and ATM phosphorylation is impaired in the CtIP knock-down cells, implying its ATR-dependence as reported by Stiff et al. (Stiff et al., 2005 & 2006) who showed that autophosphorylation of ATM in response to SSBs and replication fork stalling is ATR-dependent. 53BP1 phosphorylation is markedly reduced in the CtIP knock-down HeLa cells suggesting that it is mainly phosphorylated by ATR on S1778 and this process is mediated by CtIP.

To investigate further the ATR-dependent phosphorylation events similar experiment was performed using CPT as the DNA damaging agent. CPT is a cytotoxic quinoline alkaloid drug which inhibits DNA topoisomerase I (topo I) and causes replication fork stalling. An acute (1h) drug treatment was applied to previously CtIP siRNA-depleted

cells which were harvested at the indicated time points. As seen in Figure.4.16. phosphorylation of the ATR targets Chk1 and RPA32 is appreciably decreased in CtIP deficient cells as reported previously by Sartori et al. (2007). This suggests CtIP involvement in targeting Chk1 and RPA32 for ATR phosphorylation. Furthermore, phosphorylation of NBS1, ATM, SMC1, 53BP1 and H2XA are considerably reduced suggesting that CtIP plays a major role in ATR signalling in the event of replication fork stalling (Figure.4.19.).

Cells treated with CPT and depleted of CtIP show a greater reduction in phosphorylation of NBS1, ATM, 53BP1 and to lesser extent SMC1, than the cells irradiated with 30J and depleted of CtIP. It may be due to different kinase activation mechanisms. As Yoo et al. report TopBP1 driven activation of ATR has a different route depending on the type of DNA damage (Yoo et al., 2007). In the presence of DSBs ATM phosphorylates TopBP1 on S1131 and this event is required for subsequent ATR activation. But in the case of replication fork stalling that phosphorylation is not necessary and the precise mechanism of the upstream events of that activation remains to be elucidated. The evidence emerging from the CtIP siRNA experiments suggests the existence of three pathways of ATR activation in response to DSBs, SSBs and fork stalling. CtIP would be involved in all three pathways but to different extents and at different levels: post ATR-activation in DSBs and during activation and post activation in SSBs and fork stalling, possibly employing different sets of proteins.

In the response to DSBs, as it is ATM that activates ATR by phosphorylating TopBP1, the impairment of phosphorylation of the downstream targets appears to be minor (Figure.4.15.). Therefore impairment of the actual ATR activation event might be causing phophorylation to be reduced in response to 30J and fork stalling by CPT and

it could be that CtIP has a role in activating ATR in response to the SSBs and the fork stalling.

What is also important to note is that when we compare the difference in phosphorylation of ATR and ATM targets in cells depleted of CtIP in response to UV (Figure.4.16. & 4.17.) and to CPT treatment (Figure.4.18. & 4.19.), CtIP has a major influence on phosphorylation events carried out by ATR alone. And using Chk1 phosphorylation as an example (Figure.4.18.) we can argue that CtIP-depletion causes the most major disruptions in processes carried out by ATR in response to the replication fork stalling.

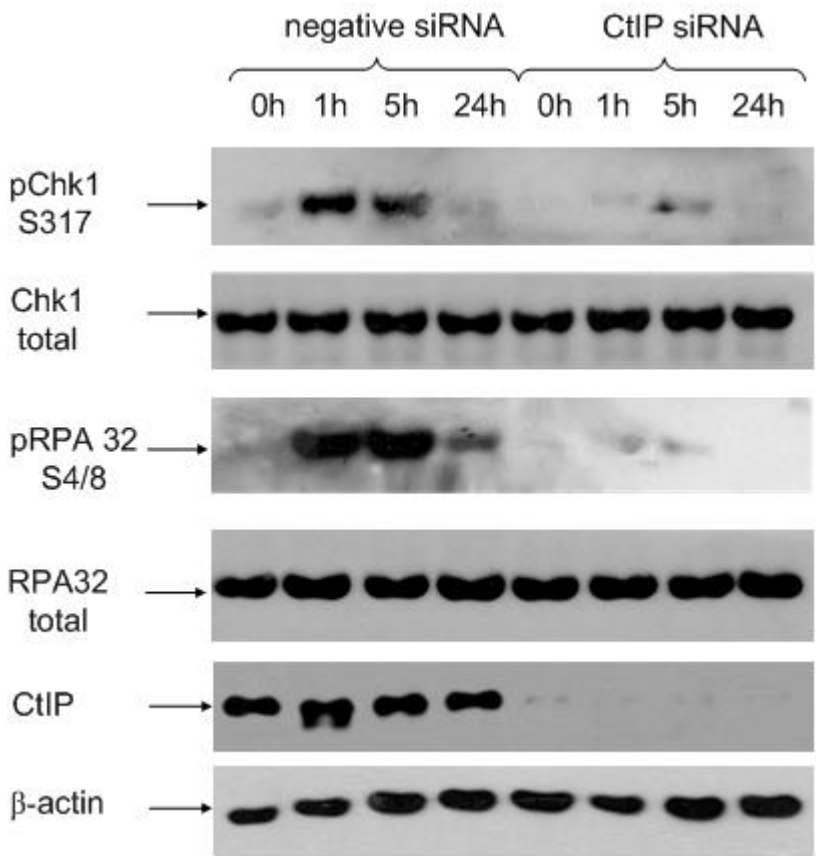

Figure.4.18.The influence of CtIP knock-down on phosphorylation of ATR targets in response to camptothecin (CPT) treatment. HeLa cells were treated with CtIP siRNA and subsequently mock-treated or treated with CPT at 1μM and harvested at the indicated time points. The cell lysates were fractionated by SDS-PAGE and proteins visualized by Western blotting. This figure represents a result of three independent experiments.

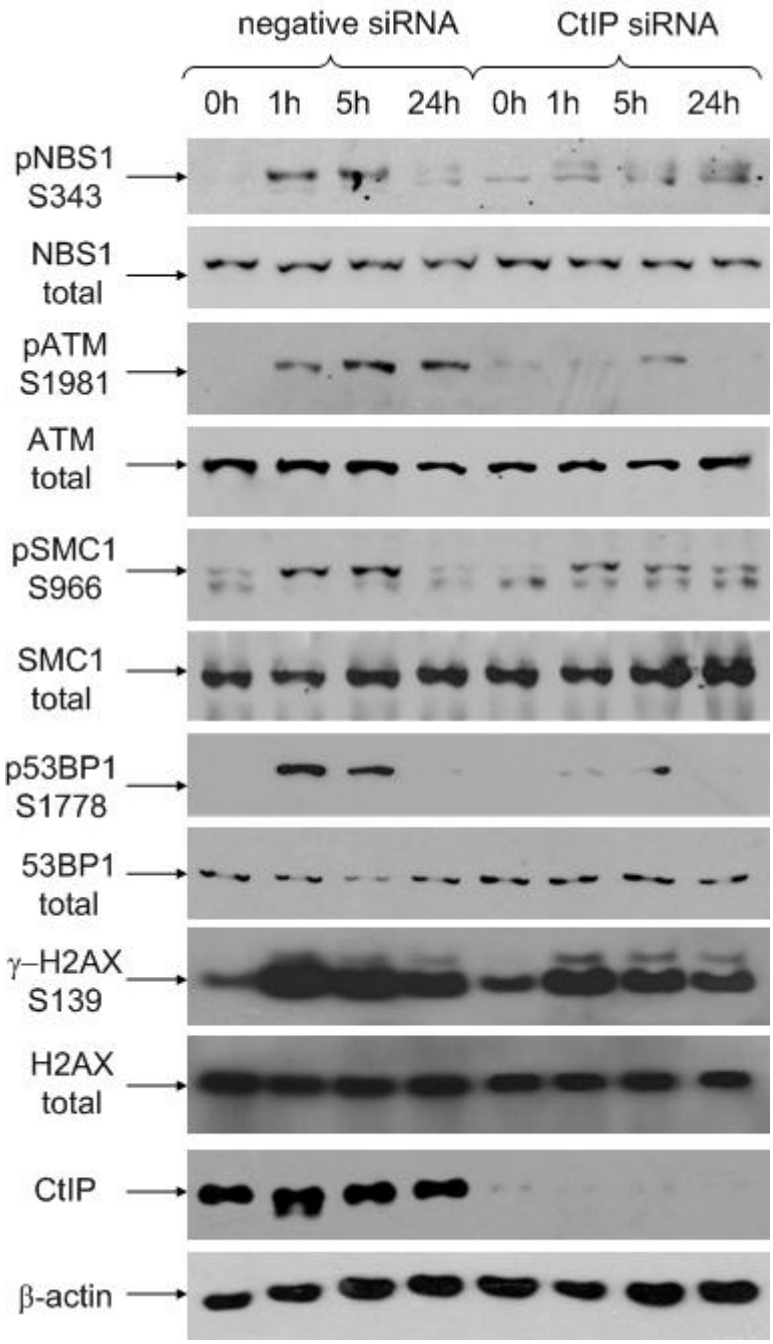

Figure.4.19.The influence of CtIP knock-down on phosphorylation of ATM targets in response to camptothecin (CPT) treatment. HeLa cells were treated with CtIP siRNA and subsequently mock-treated or treated with CPT at 1μM and harvested at the indicated time points. The cell lysates were fractionated by SDS-PAGE and proteins visualized by Western blotting. This figure represents a result of three independent experiments.

4.2.2.2. ATR phosphorylation of 53BP1 in vitro and the influence of CtIP depletion on ATR-53BP1 association in vivo.

To investigate further 53BP1 phosphorylation by ATR a kinase assay was performed (section 2.4.4.). A mouse antibody against ATR was used to immunoprecipitate ATR from HeLa cell lysates. The kinase was isolated with protein G-Sepharose beads and resuspended in kinase buffer. The beads with bound ATR were incubated with either 20μg GST-53BP1 fragment (1584-1972aa) containing the tandem repeats of the BRCT domain and the S1778 site or 20μg GST protein alone and with 1μl of [^{32}P]γ-ATP. As an additional control protein G-Sepharose beads were incubated with the cell lysates alone and then incubated with 1μl of [^{32}P]γ-ATP. The reaction was stopped by addition of Laemmli Sample Buffer, complexes were fractionated by SDS-PAGE, the gel was stained with Coommassie Brilliant Blue, dried and the phosphorylation of the GST-53BP1 fragment was visualized by autoradiography. As shown in Figure.4.20. the GST-53BP1 fragment containing the S1778 site is efficiently phosphorylated by ATR suggesting that this site may be an ATR phosphorylation site in response to DNA damage. This is consistent with previous results where 53BP1 phosphorylation on S1778 is impaired in CtIP siRNA-depleted cells in response to the DNA damage caused by 30J of UV irradiation or the replication fork stalling caused by CPT (Figure. 4.17. & 4.19.). However the GST-53BP1 (1584-1972aa) fragment may contain other, unreported phosphorylation sites that could be potentially phosphorylated by ATR. The non-specific bands in both of the tracks containing the GST-tagged proteins are a possible phosphorylation product of bacterial proteins that are present in the GST-tagged protein eluates.

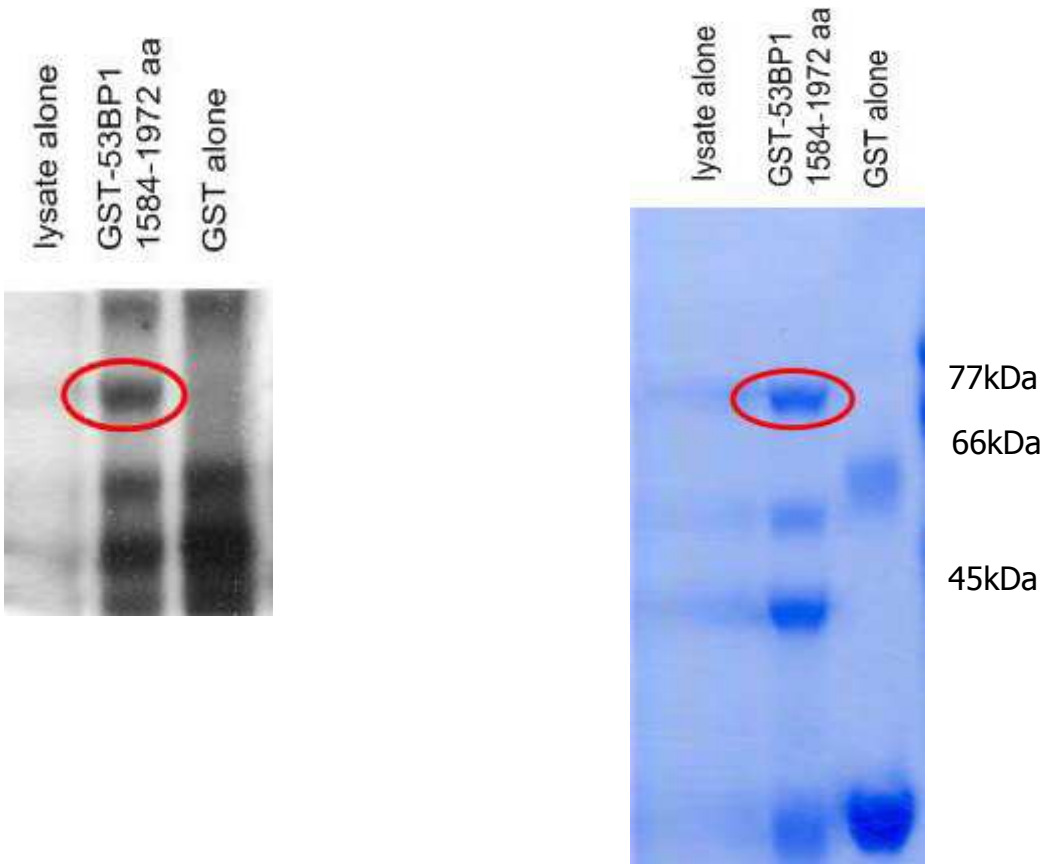

Figure.4.20. The *in vitro* phosphorylation of 53BP1 S1778 by ATR. ATR was immunoprecipitated from HeLa cell lysates and incubated with GST-53BP1 1584-1971aa or with GST alone and with [^{32}P]γ-ATP. Complexes were fractionated by SDS-PAGE and the phosphorylation of the GST-53BP1 fragment was visualized by autoradiography. This figure is representative of three independent experiments.

In order to establish whether the depletion of CtIP has an effect on ATR and 53BP1 association *in vivo* an immunoprecipitation assay was performed. A rabbit antibody against 53BP1 was used to immunoprecipitate 53BP1 from HeLa cell lysates. Complexes were isolated with protein G-Sepharose beads as described in section 2.4.2., fractionated with SDS-PAGE and the associated ATR was visualized by Western blotting. As shown in the Figure.4.21. the 53BP1 and ATR *in vivo* association is impaired in CtIP depleted HeLa cells. This could suggest that CtIP is an important factor in ATR and 53BP1 association and that this association facilitates 53BP1's phosphorylation in response to DNA damage.

4.2.2.3. Association of ATR with 53BP1 in cells depleted of CtIP and CtIP association with BLM after replication stress.

CtIP is a known factor taking part in DNA end resectioning after DNA double strand breaks. This process prepares the DNA ends to be coated with RPA complex and subsequently ATR/ATRIP/TopBP1 complexes are recruited (Figure.1.13.; Sartori et al., 2007). To examine this in more detail, we decided to investigate whether CtIP associates *in vivo* with BLM, a RecQ helicase, which also takes part in DNA end resectioning at DSBs (Gravel et al., 2008).

A co-immunoprecipitation assay was performed (section 2.4.2.). HeLa cell lysates were mock-treated or treated with 1mM Hydroxyurea (HU) as described in section 2.1.5.1. and a goat BLM antibody was used to immunoprecipitate BLM. Complexes were isolated with protein G-Sepharose beads, fractionated with SDS-PAGE and the associated CtIP was visualized by Western blotting. As shown in Figure. 4.22. CtIP and BLM interact *in vivo* in HeLa cells treated with HU. HU is an anti-neoplastic drug and DNA replication inhibitor causing ribonucleotide depletion which results in

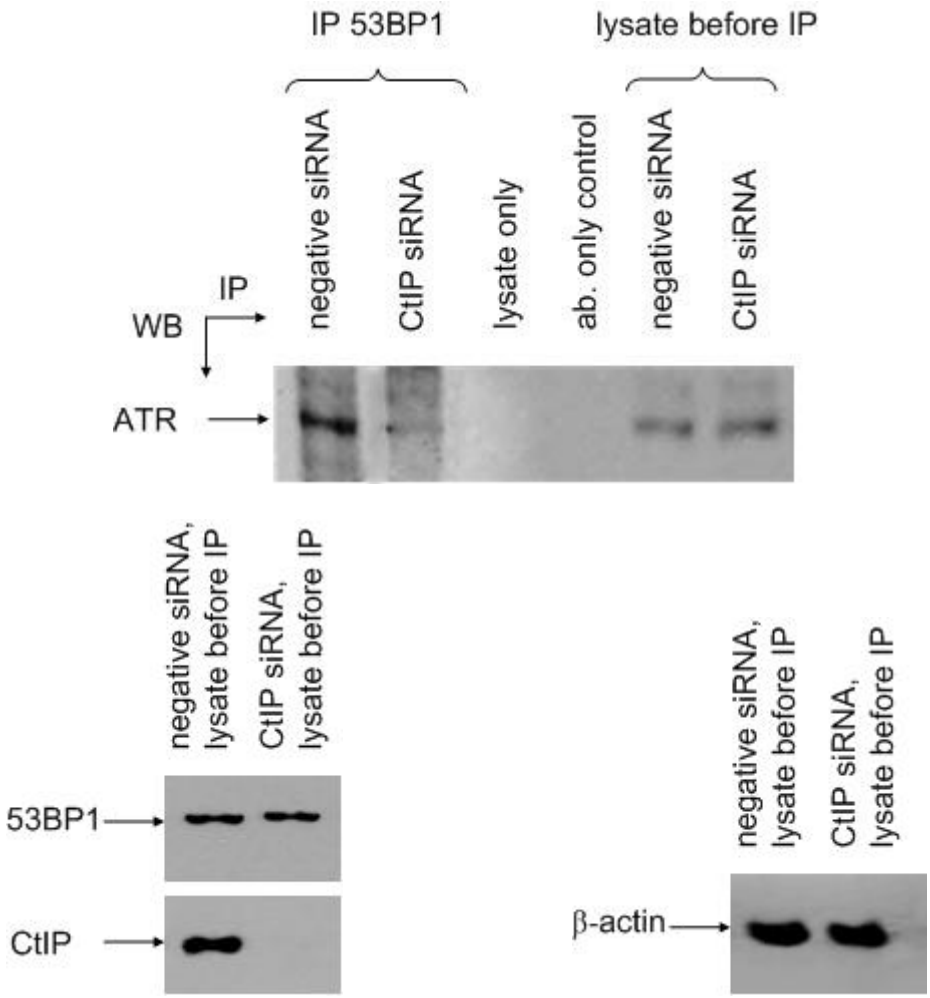

Figure.4.21. The association of 53BP1 and ATR is impaired in CtIP siRNA depleted HeLa cells. HeLa cell lysates were immunoprecipitated with a rabbit 53BP1 antibody and coimmunoprecipitating ATR was visualized by Western blotting. 53BP1's and CtIP's basal level is shown before IP and β-actin indicates equal levels of total protein in lysates before IP. This figure is representative of three independent experiments.

DNA double-stranded breaks near replication forks. CtIP and BLM associated *in vivo* only in the presence of DNA damage. Thus we can speculate that they exist in a complex that assembles to facilitate DNA end resection and subsequent repair of collapsed replication forks.

BLM has been reported to associate with 53BP1 after HU treatment (Sengupta et al., 2004). Thus as a positive control for the previous experiment another co-immunoprecipitation assay was performed using HU-treated HeLa cells. A rabbit antibody against 53BP1 was used to immunoprecipitate 53BP1 and protein G-Sepharose beads were used to isolate formed complexes which were fractionated with SDS-PAGE. Associated BLM was visualized by Western blotting. As shown in Figure.4.23. 53BP1 associates with BLM only after treatment with HU which again suggests its involvement in repairing the collapsed replication fork thus possibly this complex involves amongst other proteins also CtIP, BML and 53BP1.

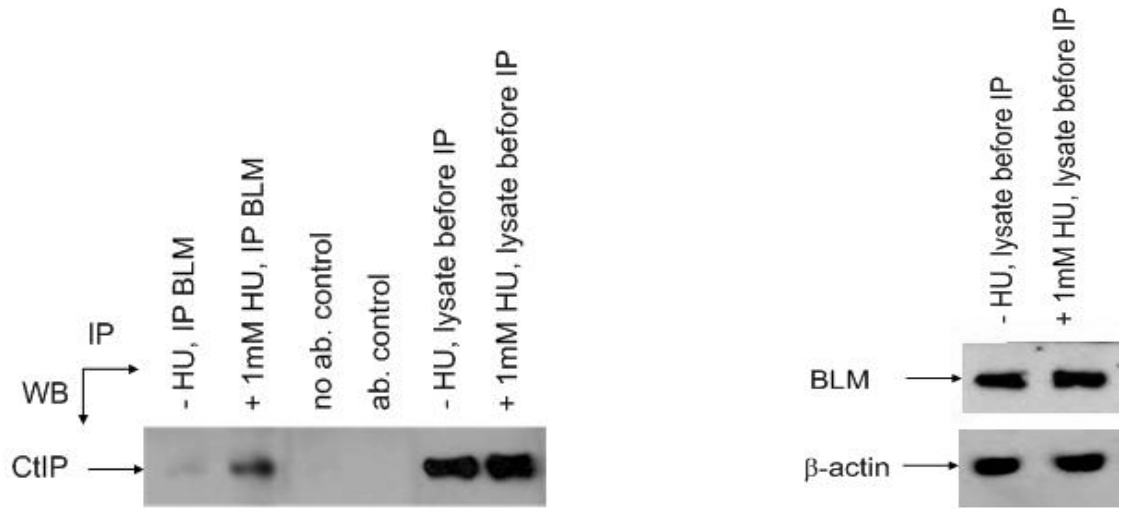

Figure.4.22. The *in vivo* association of CtIP and BLM after hydroxyurea (HU) treatment. HeLa cells were mock-treated or treated with 1mM HU and subsequently a goat antibody against BLM was used to immunoprecipitate BLM. Associated CtIP was visualized by Western blotting. In the right hand panel BLM's basal level is shown and β-actin indicates equal levels of total protein in lysates before IP. This figure is representative of three independent experiments.

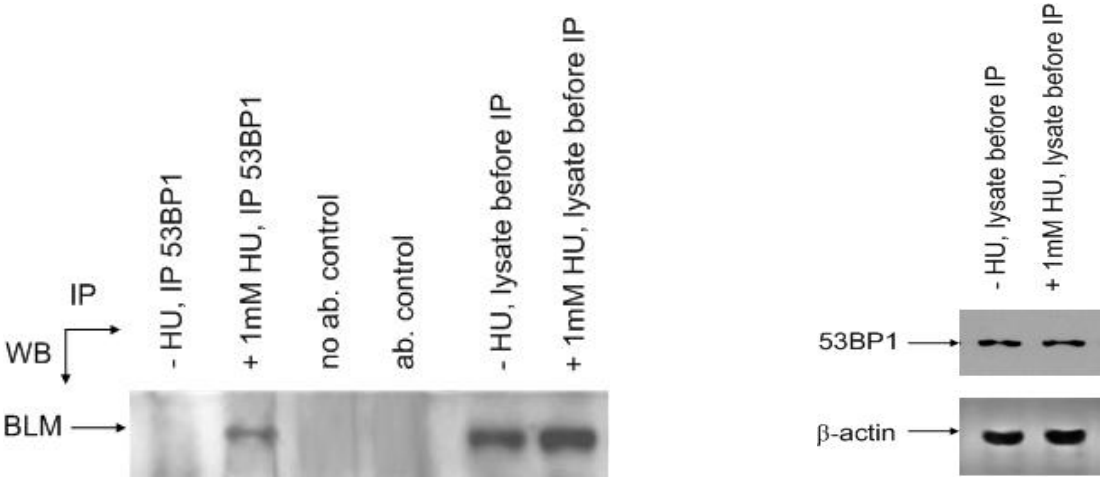

Figure.4.23. The *in vivo* association of BLM and 53BP1 after hydroxyurea (HU) treatment. HeLa cells were mock-treated or treated with 1mM HU and subsequently a rabbit antibody against 53BP1 was used to immunoprecipitate 53BP1. Associated BLM was visualized by Western blotting. In the right hand panel 53BP1's basal level is shown and β-actin indicates equal levels of total protein in lysates before IP. This figure is representative of three independent experiments.

4.3. Discussion.

In the previous chapter, I showed that CtIP binds BRCT domain containing proteins. In this chapter I investigated the influence of γ-irradiation and UV-irradiation on CtIP's ability to interact *in vivo* with these and other proteins involved in DNA damage signalling pathways.

As shown in section 4.2.1.1. CtIP interacts with the components of the MRN complex and with RPA70 (Figure.4.1.) which are sensor proteins of DNA double-stranded breaks and single-stranded breaks, respectively. It also interacts with transducer proteins ATM and ATR (Figure.4.4.) and with mediator proteins 53BP1 (Figure.4.6.) and MDC1 (Figure.4.7.). None of those interactions appear to be influenced by the damage caused to the DNA either in the form of double-stranded breaks nor single-stranded ones. This observation suggests that CtIP is a crucial component of those complexes in normal cells (Figure.4.2., Figure.4.5., Figure.4.8.) It would also imply that for efficient functioning of a viable cell all of these proteins have to stay in close contact. As CtIP interacts with all of these proteins it is likely that it is involved in a multiprotein complex. This hypothesis is based on the findings from the previous chapter, where CtIP interacts directly with 53BP1, MDC1, TopBP1 and NBS1.

On the other hand, BRCA1 is known to form a multicomplex with DNA damage response proteins termed BASC (BRCA1-associated genome surveillance complex; Wang et al., 2000). Amongst the proteins involved in the formation of that complex are ATM, BLM, MRN complex and the mismatch repair genes (MMR): MHS2, MHS6 and MLH1 (Figure.4.24.a.). In the results shown in this chapter CtIP is recognized as an associate of ATM, MRN complex and BLM. CtIP has been also reported to bind directly to the BRCT domains of BRCA1 (Wong et al., 1998).

One CtIP allele is found to be frequently mutated in colon cancer with microsatellite instability and MMR genes are found to be mutated in hereditary colon cancer (Vilkki et

al., 2002). Apart from that finding, genes involved in MMR are frequently mutated in hereditary colon cancer. Thus the hypothesis would suggest that CtIP would take part in MMR, but during malfunctioning MMR it would undergo mutation as well, which would impede its function, which in a feedback loop would cause errors in MMR and consequently lead to the development of the microstability in those cancer tissues.

Exo1 has been reported to play a key role in MMR together with the RPA complex (Modrich, 2006). In recent findings Mre11/Sgs1(BLM)/Sae2(CtIP)/Exo1 have been reported to be involved in DNA end-resectioning in yeast (Mimitou & Symington, 2008). Thus one could hypothesise that CtIP, since it interacts with BRCT domain containing proteins such as 53BP1, MDC1, TopBP1, NBS1 and BRCA1 and associates *in vivo* with a plethora of other DNA damage response proteins and could be a part of the BASC complex (Figure.4.24.a.). The BASC complex could possibly consist of more than just BRCA1 and eight associated proteins and might gather all the proteins necessary to sense DNA damage, to perform the repair processes and modulate their activity by phosphorylation events performed by the PIKK kinases and checkpoint kinases.

By formation of the multi-protein complex CtIP would manage the crucial proteins in a 'ready to react' state in the case of any disruptions caused by internal or external factors. The existence of this multi-protein complex would facilitate a rapid diagnosis followed by response and repair of the damage as soon as it occurs. However CtIP's exact role in the activities of the complex remains to be elucidated (Figure.4.24.b&c).

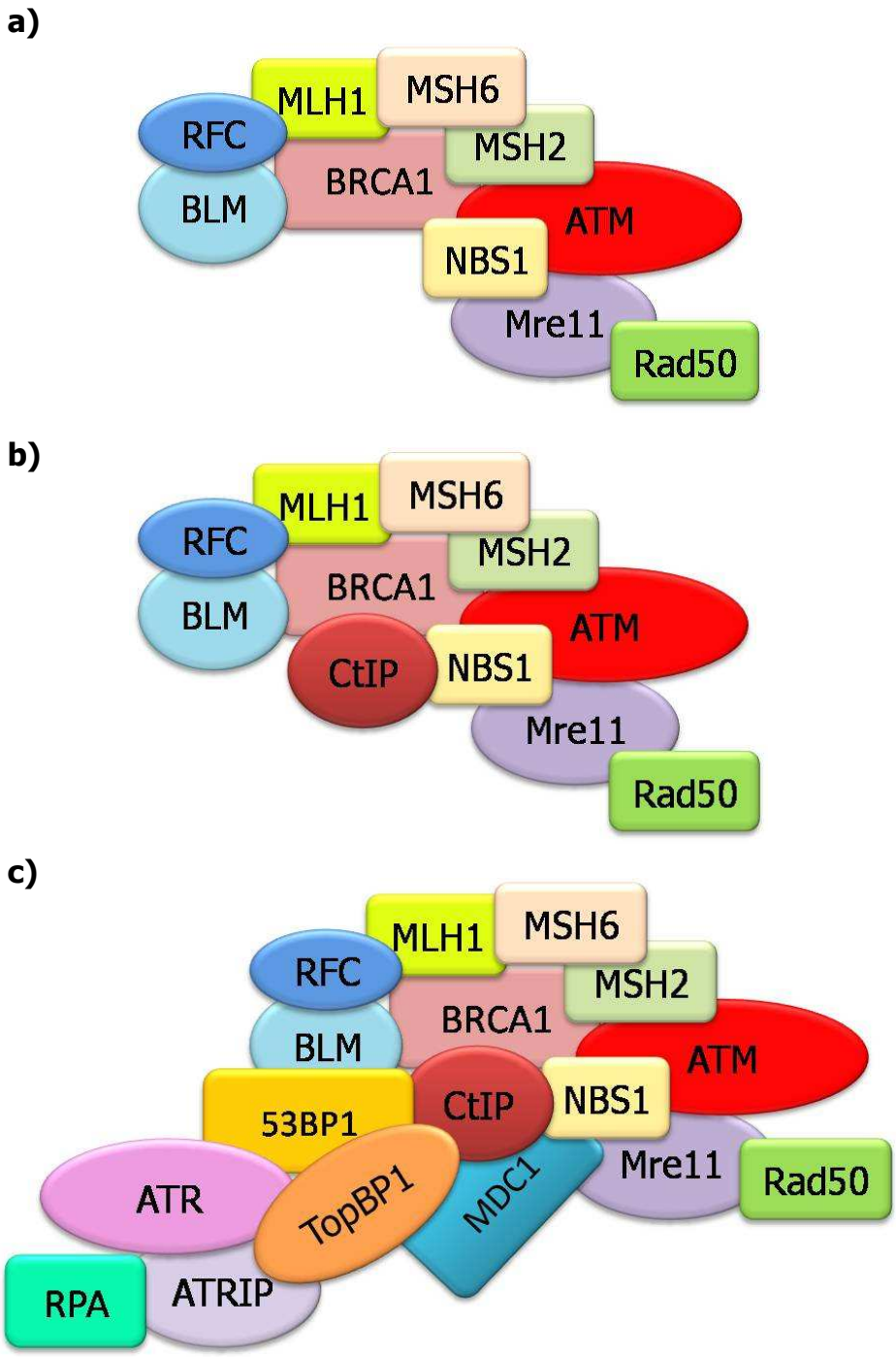

Figure.4.24. The formation of possible multiprotein complex mediated by CtIP. a) the BASC complex, **b)** CtIP's possible association with the BASC complex, **c)** formation of possible multiprotein complex by CtIP.

CtIP's association with the MRN complex and ATM in the inherited disorder backgrounds was also examined. As shown in the Figure.4.11.a. ATM's association with CtIP is not affected by the Mre11 truncating mutation but there is a possibility that the interaction is modified by mutation in NBS1. CtIP's association with ATM appears to be weaker in NBS patient LCLs judged by basal levels of ATM in the cell lysates before IP. Similar weaker association of ATM with CtIP occurs in ATLD LCLs. That would suggest that the interaction, if it was as efficient, should be the same as the CtIP-ATM association in normal LCLs. Thus we could speculate that intact NBS1 is necessary for CtIP-ATM association in the case of NBS LCLs. And the lower level of immunoprecipitated ATM in ATLD LCLs is influenced by lower levels of NBS1 in those cells (Figure.4.11.a.; Stewart et al., 1999).

It appears that truncating mutations in either Mre11 (Figure.4.8.) or NBS1 (Figure.4.9.) do not have a major influence on CtIP's ability to associate with other components of the complex that are intact. Mre11's association with CtIP in the ATLD and NBS cells still appears to be normal (Figure.4.11.a.). There are several possibilities why this may be happening. In the case of ATLD cells, CtIP still associates with Mre11 and this interaction is most likely mediated by NBS1. As described in section 3.1.2.4. NBS1 binds CtIP directly but Mre11 does not. NBS1 also binds Mre11 directly (Carney et al., 1998) and the Mre11 truncating mutation does not affect that interaction (Stewart et al., 1999). The Mre11 and NBS1 association occurs through the N-terminal region of Mre11 (Desai-Mehta et al., 2001) that is left intact by the mutation. As shown in Figure.4.2.a. CtIP does not bind Mre11 directly thus CtIP and Mre11 association must be mediated by NBS1.

As for the CtIP-Rad50 association in ATLD cells, it is compromised by reduced expression levels of Rad50 due to the Mre11 mutation (Stewart et al., 1999) but is not abolished. Rad50 has been reported to bind to Mre11 directly (Dolganov et al., 1996),

although no direct binding to NBS1 has been shown. Thus we suggest that CtIP-Rad50 association again is mediated by NBS1 binding to CtIP such that the whole complex is immunoprecipitated with the CtIP antibody.

The NBS LCLs express two variants of NBS1: p26 and p70 (Maser et al., 2001). CtIP is most likely associated with both of them as the results in the section 3.1.2.4. suggest. The p70 variant and Mre11 would be associated with CtIP so that the whole MRN complex could be immunoprecipitated from the LCL NBS cell lysates using the CtIP antibody. Sartori et al. report the direct binding of CtIP to Mre11 and Rad50 when they are expressed together in a baculovirus system (Sartori et al., 2007). However our results show that CtIP does not interact directly with Mre11 nor Rad50 when they are expressed singly. This difference possibly arises from differences in experimental protocol. Additionally the proteins may fold differently, depending on whether they are expressed together or in isolation. Although CtIP does not bind to Mre11 or Rad50 when they are expressed separately (Figure.4.3.) it may associate with them when they form a complex. As mentioned before this may be due to different folding of the proteins forming a complex. By the way Mre11 and Rad50 associate they may form a binding site for CtIP. Another hypothesis would presume the existence of other proteins in the immunoprecipitated complex such that CtIP could be associated with them and they in turn would bind to Mre11 or Rad50; in which case functional NBS1 would not be necessary for this interaction. Similar explanations could be proposed for the association of CtIP and NBS1 or Rad50 in Mre11 knock-down cells (Figure.4.13.). Another possibility in this case is that the Mre11 depletion is not complete. Thus it could still be expressed in the cell although at lower levels, in that case the MRN complex could still form.

An interesting observation has arisen from the competition experiment where, as shown in the Figure.4.14., the addition of GST-CtIP to the NBS1 immunoprecipitation

reaction abolishes its association with Mre11. This suggests that CtIP and Mre11 may compete *in vivo* for the same binding region on NBS1. Nevertheless, *in vivo*, the affinity of Mre11 for NBS1 must be appreciably greater than that of CtIP or perhaps only a small pool of NBS1 is bound to CtIP and utilized by the cell differently than when it is associated in the MRN complex.

To study the effect of CtIP on phosphorylation events after DNA damage, CtIP knock-down experiments were performed. CtIP-depleted cells were mock-irradiated or irradiated with 5Gy or 30J or treated with CPT and harvested at four different time points. As shown in the Figure.4.15. the depletion of CtIP does not impair the phosphorylation events initiated by DNA DSBs caused by 5Gy. Those phosphorylation events are normally regulated by ATM which has not been reported to be influenced by CtIP. The phosphorylation of the main targets of ATM such as NBS1, ATM, SMC1 or H2AX is not affected by CtIP depletion suggesting a minor role for CtIP in ATM activation. S1778 on 53BP1 has not been reported as an ATM phosphorylation site (Jowsey et al., 2007) and could, thus, be phosphorylated by ATR. As shown in Figure.4.15. the phosphorylation of 53BP1 is only slightly impaired which suggests two possibilities. The first is that ATR is being activated by ATM (as Yoo et al., 2007 report) and in an activated form does not need CtIP as much for the subsequent phosphorylation events. The second option is that in the presence of DSBs the 53BP1 S1778 is phosphorylated by ATM, which in the absence of an ATR activating signal from CtIP, assumes ATR's functions in transducing the signal. In the case of SSBs and replication fork stalling ATR is the activator of ATM (Stiff et al., 2006). If ATR is not activated efficiently, like in the case of CtIP depletion, it cannot efficiently activate ATM. In the Figure.4.17. we can observe an impairment of the phosphorylation of ATM targets, namely NBS1 and ATM, in the absence of CtIP. This suggests that in the cells depleted of CtIP ATR is not effectively activated and in the presence of SSBs caused by

UV irradiation or replication fork stalling ATR is unable to activate ATM efficiently. The same effect, but even more pronounced, could be observed in Figure.4.19. where phosphorylation of these proteins is severely impaired in CtIP-depleted cells. This suggests that CtIP, apart from facilitating phosphorylation performed by ATR, could be an activator of ATR's kinase activity in the presence of SSBs and collapsed replication forks.

Sartori et al. reported that in response to SSBs or replication fork stalling, phosphorylation of RPA32 and Chk1 is impaired in cells lacking CtIP (Sartori et al., 2007). The same results are shown in Figure.4.16. and 4.18., providing confirmation that CtIP is required for efficient phosphorylation of ATR targets.

To assess whether S1778 of 53BP1 is an ATR target a kinase assay was performed. As shown in Figure.4.20. ATR phosphorylates a GST-53BP1 fragment containing that site. We could speculate that it could actually be an ATR dependant phosphorylation site, but that GST-53BP1 fragment may contain other SQ/TQ motifs that could be phosphorylated by ATR. We also established that CtIP depletion reduces the ability of ATR to associate with 53BP1 *in vivo* (Figure.4.21.). One could hypothesise that impaired 53BP1 phosphorylation is due to an inability of ATR to associate with 53BP1 and subsequently efficiently phosphorylate it in the absence of CtIP.

CtIP emerges as an important co-activator and partner of ATR. As CtIP also associates with BLM it could be playing a role in BLM's phosphorylation by ATR but this remains to be elucidated as the antibody that we acquired for pT99 for BLM from Dr. Y. Pommier did not give a clear answer.

CHAPTER V

RESULTS

The phosphorylation of CtIP by members of the PIKK kinase family.

5. The phosphorylation of CtIP by members of the PIKK kinase family.

5.1. Introduction.

Complex organisms have developed many ways to respond to internal and external stimuli. One of the responses is phosphorylation of proteins and lipids. Enzymes that transfer the phosphate group are classed as kinases. At any given time in the cell cycle it has been estimated that one-third of all the proteins exists in a phosphorylated state. The great majority of kinases are serine/threonine kinases that phosphorylate their targets on serine residues and less often on threonine residues. Another, less numerous class, are tyrosine kinases phosphorylating their targets at tyrosine residues (Stryer, 1995). Human genome sequencing has revealed that kinases represent around 2% of the genome (Amit et al., 2007). Phosphorylation is the most wide spread reversible post-translational modification. The process is carried out by hydrolyzing an ATP molecule to transfer its γ phosphate group onto serine, threonine or tyrosine residue. Only intracellular proteins are eligible for phosphorylation unlike extracellular ones (Stryer, 1995).

The kinases involved in the initiation of the DNA damage response are members of the superfamily of PIKK kinases (phosphoinositide 3-kinase (PI3K) – related kinase) including ATM (ataxia telangiectasia-mutated), ATR (ATM and Rad3-related), DNA-PKcs (DNA-dependent protein kinase catalytic subunit), SMG1 (suppressor with morfogenetic effect on genitalia 1, also referred to as ATX), mTOR (mammalian target of rapamycin) and TRRAP (transformation/transcription domain-associated protein) which does not possess kinase activity. They are all large proteins whose domain structure shares similarities (Figure.5.1.).

The N-terminal regions of the PIKK proteins contain HEAT (**H**untingtin, **E**longation factor 3, **A** subunit of protein phosphatase 2A and **T**OR1) repeats that are not very

conserved between these proteins. The C-terminal part contains the kinase domain or kinase-like domain in case of TRRAP. This domain is flanked by two conserved regions, FAT (FRAP, ATM, TRRAP) and FATC (FAT C-terminus). The FATC domain is necessary for the kinase activity of all PIKK family members apart from TRRAP and the precise function of the FAT domain remains to be elucidated (Lovejoy et al., 2009). The members of the family that possess the kinase activity share a common phosphorylation motif: SQ/TQ. The C-terminus of the PIKK kinases also contains the PRD region (PIKK regulatory domain) which is responsible for interaction with activating proteins: ATM-MRN, ATR-TopBP1 and DNA-PKcs-Ku70/80. The PRD region in case of SMG1 is atypically long and the activating protein for SMG1 has not been identified.

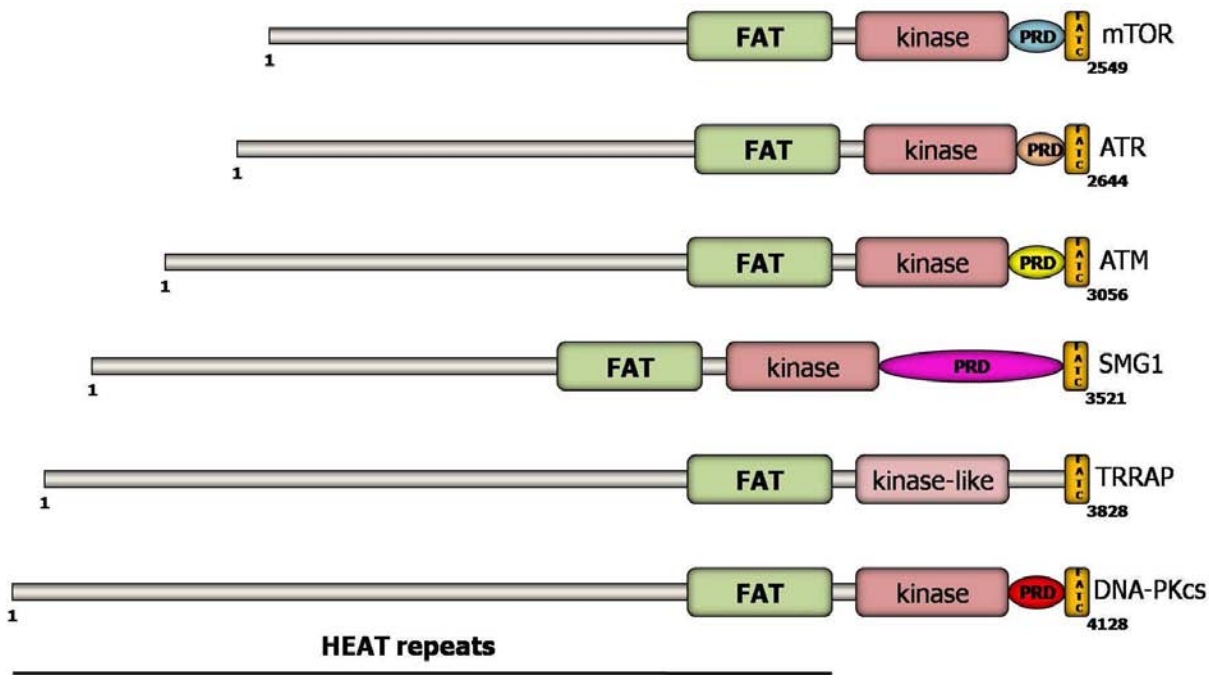

Figure.5.1. The domain structure of the PIKK family members. HEAT repeats - Huntingtin, Elongation factor 3, A subunit of protein phosphatase 2A and TOR1; FAT - FRAP, ATM, TRRAP; PRD - PIKK regulatory domain; FATC - FAT C-terminus.

SMG1 is an essential component of the nonsense-mediated mRNA decay (NMD) pathway which is a surveillance mechanism for malfunctioning mRNAs. In this process mRNAs are checked for premature termination codons (PTCs) and if they are found to possess one, are directed for degradation. This process is orchestrated by SMG1. It has been suggested that SMG1, although involved in NMD, is able to respond to other external stimuli such as growth factors and environmental stress, such as IR or UV. Indeed, Abraham (2004) suggests that SMG1 function developed during metazoan evolution, from a protein with a main function in NMD into a protein that is an integral component of vertebrate stress-response pathways. SMG1 was shown to be activated by IR and UV irradiation (Brumbaugh et al., 2004). The siRNA depletion of SMG1 causes constitutive activation of the Chk2 kinase and appearance of γ-H2AX foci in the absence of DNA damage. These observations suggest that the loss of SMG1 causes an inappropriate detection of genotoxic stress. SMG1 depleted cells also lose the potential to divide which resembles the loss of ATR kinase. These observations suggest a strong involvement of SMG1 in the maintenance of genome stability (Abraham, 2004).

In this chapter I focused on CtIP and its ability to associate with kinases in multiprotein complexes. As shown in this chapter CtIP, when immunoprecipitated from cell lysates, pulls down kinase activity. This suggests that it plays a 'scaffold role' in phosphorylation processes carried out by those kinases. It is also revealed that CtIP associates with SMG1. CtIP's sequence analysis showed two regions of homology with NBS1 C-terminal region, that is found to be responsible for interaction with ATM. This region has also been shown to be conserved among proteins that are activator proteins for other PIKK family members, namely ATRIP for ATR and Ku70/80 for DNA-PKcs (Falk et al., 2005). I suggest that CtIP might be a possible activator protein for the SMG1 kinase although further experiments are required to establish direct binding between CtIP and SMG1.

5.2. Results.

5.2.1. Co-immunoprecipitation of active caffeine-sensitive kinases with CtIP.

To investigate whether CtIP can co-immunoprecipitate with an active kinase and whether that kinase is caffeine sensitive, kinase assays were performed (section 2.4.4.). LCLs were irradiated with 5Gy and harvested 30 min post irradiation or treated with 5mM caffeine for 30 min, subsequently irradiated with 5Gy and harvested 30 min post irradiation. A rabbit antibody was used to immunoprecipitate CtIP and associated kinases. Complexes were isolated with protein G-Sepharose beads which were resuspended in the kinase buffer after the last wash. GST-p53 (aa 1-73), GST-RPA32 (aa 1-270) and GST were used as substrates for the kinase reaction. When GST-CtIP fragments were used as substrates sufficient protein equivalent to 10 μg of non-degraded GST-tagged protein, assessed on the basis of a stained Coomassie blue stained gel (Figure.5.2.b.), was incubated with the protein G-Sepharose beads.

For the kinase assay the protein G-sepharose beads were resuspended, after the last wash, in the kinase buffer with the addition of [^{32}P]γ-ATP and incubated with the GST-tagged protein at 37^{o}C for 15 min. As an additional control protein G-Sepharose beads were incubated with the cell lysates alone, washed and then incubated with [^{32}P]γ-ATP as described previously. The reaction was stopped by addition of Laemmli Sample Buffer, proteins were fractionated by SDS-PAGE and visualized by autoradiography. As shown in red in the Figure.5.2.a. CtIP has the ability to immunoprecipitate active kinases which are caffeine sensitive suggesting that it could be one or more PIKK kinases such as ATM and ATR. The bands in GST-p53 and GST-RPA tracks that are

a) **b)**

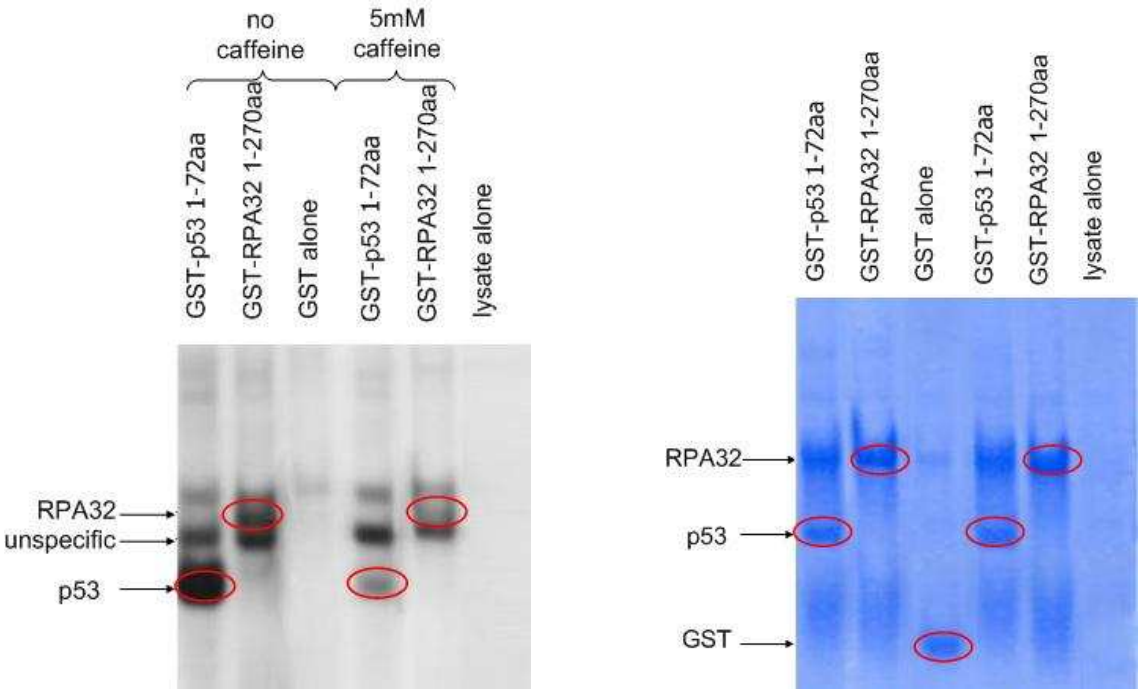

Figure.5.2. CtIP immunoprecipitates kinase activity which is caffeine sensitive. a) LCLs were irradiated with 5Gy and a rabbit antibody was used to immunoprecipitate CtIP. Associated kinase activity was used to phosphorylate GST-p53, GST-RPA32 or GST without or with addition of caffeine. Complexes were fractionated by SDS-PAGE and phosphorylation of the GST-tagged proteins was visualized by audioradiography, **b)** The SDS-PAGE gel stained with Coommassie Brilliant Blue showing the GST-tagged proteins used in this experiment. This figure is representative of three independent experiments.

phosphorylated in the reaction inhibited with caffeine as well as without caffeine are a possible product of nonspecific phosphorylation. The phosphorylation could also be carried out by other kinases, that are not caffeine sensitive, that could be potentially immunoprecipitated with the CtIP antibody. A potential substrate for those kinases could be the differentially spliced variants of GST-p53 and GST-RPA or bacterial proteins.

Additional bands on the Coomassie Brilliant Blue stained gel, not marked by the red circles, are most likely a product of degradation of the originally GST-tagged protein or bacterial-protein contamination (Figure 5.2.b.).

In order to establish whether it is a pool of kinases or just ATM that is the active kinase associated with CtIP, another kinase assay was performed. HeLa cells depleted of ATM (established by stable transfection of shATM construct in a retroviral system resulting in ATM expression silencing, a generous gift from Grant Stewart) were lysed in TGN buffer (section 2.4.4.). A rabbit CtIP antibody was used to immunoprecipitate CtIP and associated kinases. Complexes were isolated with protein G-Sepharose beads and resuspended in the kinase buffer after the last wash. The equivalent of 10 μg of non-degraded GST-tagged protein, assessed on the basis of previously stained Coomassie blue stained gel was used in each reaction. The GST-tagged protein used in the experiment was either GST-p53 (aa 1-73) or GST-RPA32 (aa 1-270) or GST-CtIP (aa 327-897) or GST . As an additional control, protein G-Sepharose beads were incubated with the cell lysates alone and then incubated with [^{32}P]γ-ATP. The kinase reaction was performed at 37^{o}C for 15 min and stopped by addition of the Laemmli Sample Buffer. Complexes were fractionated by SDS-PAGE and the phosphorylation of GST-p53, GST-RPA32 and GST-CtIP was visualized by autoradiography. As shown by the red circles in Figure.5.3.a. CtIP co-immunoprecipitates with active kinases apart from ATM as

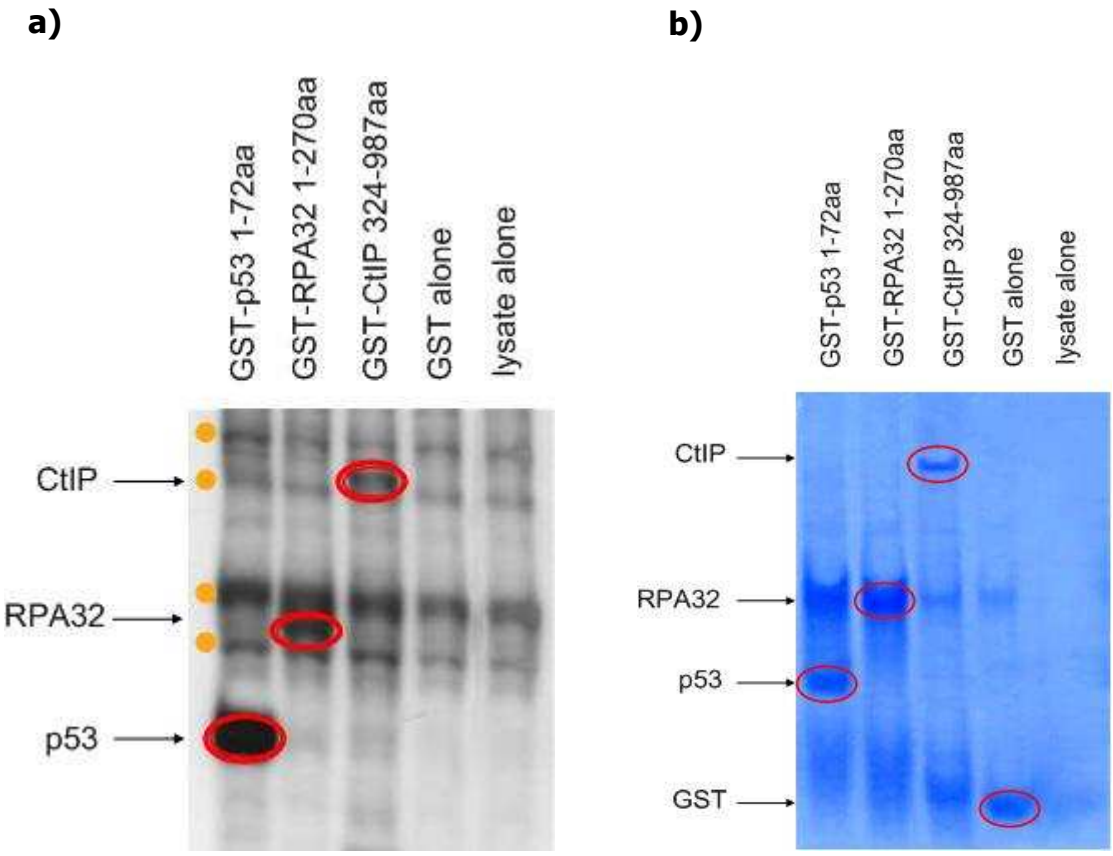

Figure.5.3. CtIP immunoprecipitates active kinases apart from ATM. a) HeLa cells depleted of ATM were harvested and a rabbit antibody against CtIP was used to immunoprecipitate CtIP and associated kinases. The associated kinase activity was used to phosphorylate GST-p53, GST-RPA32, GST-CtIP and GST. Complexes were fractionated by SDS-PAGE and phosphorylation of GST-tagged proteins was visualized by audioradiography, **b)** The SDS-PAGE gel stained with Coommassie Brilliant Blue showing the GST-tagged proteins used in the experiment. This figure is representative of three independent experiments.

indicated by still visible phosphorylation of CtIP as well as p53 and RPA32. Four bands marked with orange dots are results of nonspecific phosphorylation carried out by kinases that bind directly to the protein G-sepharose beads and phosphorylate proteins present in cell lysates used in the experiment.

Additional bands on the Coomassie Brilliant Blue stained gel, not marked by the red circles, are most likely a product of degradation of the originally GST-tagged protein or bacterial-protein contamination (Figure 5.3.b.).

5.2.2. The phosphorylation of CtIP by kinases from the PIKK family and the association of CtIP with SMG1.

To establish whether ATR and ATM phosphorylate CtIP *in vitro* a kinase assay was performed. LCLs were irradiated with 5Gy for the ATM kinase assay and harvested 30 min post irradiation to allow for full ATM activation. LCLs for ATR kinase assay were harvested without irradiation. Mouse anti ATR or ATM antibodies were used to immunoprecipitate ATR or ATM respectively and the kinases were isolated with protein G-Sepharose beads. After the last wash the beads with associated kinase were resuspended in the kinase buffer and for each kinase, ATR or ATM, four different reactions were performed. As positive controls GST-p53 and GST-RPA32 were used as substrates. In each reaction the equivalent of 10 μg of non-degraded GST-tagged protein, assessed on the basis of previously stained Coomassie Brilliant Blue stained gel was used. The GST-tagged proteins used in the experiment were either GST-p53 (aa 1-73), GST-RPA32 (aa 1-270), GST-CtIP (aa 327-897) or GST protein. Each reaction was supplemented with 1μl of [^{32}P]γ-ATP. As an additional control protein G-Sepharose beads were incubated with the cell lysates alone and then incubated with 1μl of [^{32}P]γ-ATP. The kinase reaction was performed at 37^{o}C for 15 min and was stopped with Laemmli Sample Buffer. Proteins were fractionated by SDS-PAGE and visualized by

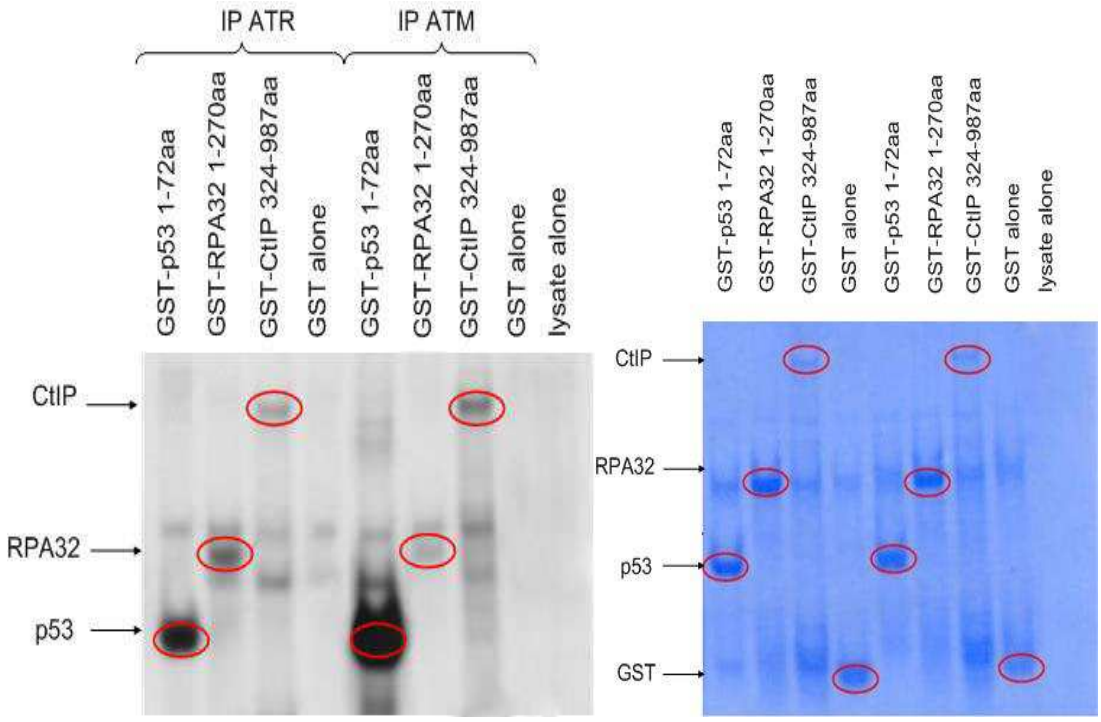

Figure.5.4. ATR and ATM phosphorylate CtIP *in vitro*. a) LCLs were mock-irradiated for ATR kinase assay and irradiated with 5Gy for ATM kinase assay and harvested 30 mins post irradiation. A mouse antibody against ATR or ATM was used to immunoprecipitate ATR or ATM respectively. Each kinase was used to phosphorylate GST-p53, GST-RPA32, GST-CtIP or GST alone. Complexes were fractionated by SDS-PAGE and phosphorylation of GST-tagged proteins was visualized by audioradiography, **b)** The SDS-PAGE gel stained with Coommassie Billiant Blue showing the GST-tagged proteins used in the experiment. This figure is representative of three independent experiments.

autoradiography. As shown in the Figure.5.4.a. ATR and ATM kinases phoshorylate GST-CtIP protein as well as the positive controls: GST-p53 and GST-RPA32. CtIP is phosphorylated more efficiently by ATM rather than ATR, as well as p53. RPA32 is phosphorylated to a greater extent by ATR kinase.

Additional bands on the Coomassie Brilliant Blue stained gel, not marked by the red circles, are most likely a product of degradation of the originally GST-tagged protein, alternatively spliced variants or bacterial-protein contamination (Figure 5.3.b.).

5.2.2.1. CtIP binding to SMG1.

In the previous chapter (section 4.2.1.2.) CtIP was shown to associate *in vivo* with two members of the PIKK kinase family: ATM and ATR (Figure.4.4.). In this section it was decided to establish whether CtIP associates with another member of that family, namely SMG1 also known as ATX.

To establish the possible interaction, co-immunoprecipitation was performed (section 2.4.2.). HeLa cells were mock-irradiated, irradiated with 5Gy or irradiated with 30J and harvested one hour post irradiation. A rabbit antibody was used to immunoprecipitate SMG1. Complexes were isolated with protein G-Sepharose beads, fractionated with SDS-PAGE and associated CtIP or RPA70 was visualized by Western blotting. As shown in the Figure.5.5. SMG1 associates with CtIP and RPA70 before and after DNA damage. The CtIP-SMG1 association appears to be enhanced by single stranded DNA lesions and the RPA70-SMG1 association is enhanced by DNA damage generally. As shown previously CtIP associates with RPA70 before and after DNA damage (Figure.4.1.). This could suggest that a SMG1-CtIP-RPA70 complex is involved in DNA damage sensing and repair alongside ATM and ATR.

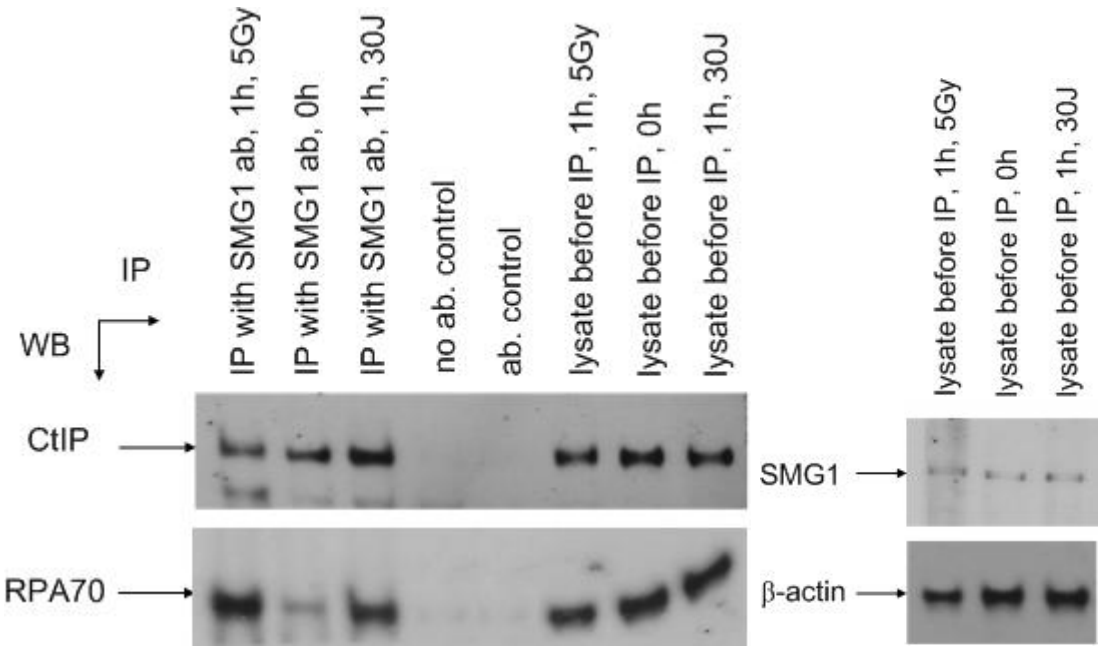

Figure.5.5. The *in vivo* association of SMG1 with CtIP and RPA70. Hela cells were mock-irradiated or irradiated with 5Gy or 30J and harvested at the indicated time points. SMG1 was immunoprecipitated with a rabbit antibody and associated CtIP or RPA70 were visualized by Western blotting. In the right hand panel SMG1's basal level is shown and β-actin indicates equal levels of total protein. This figure is representative of three consecutive repeats.

In order to investigate whether SMG1 phosphorylates CtIP, and whether that process is caffeine sensitive, a kinase assay was performed. LCLs were irradiated with 5Gy and harvested 30 min post irradiation or treated with 5mM caffeine for 30 min, subsequently irradiated with 5Gy and harvested 30 min post irradiation. A rabbit antibody was used to immunoprecipitate SMG1 and the kinase was isolated using protein G-Sepharose beads. The equivalent of 10 μg of non-degraded GST-tagged protein, assessed on the basis of previously stained Coomassie Brilliant Blue stained gel was used in each reaction. The GST-tagged proteins used in the experiment were either GST-p53 (aa 1-73), GST-RPA32 (aa 1-270), or GST-CtIP (aa 327-897).Each reaction was supplemented with 1μl of [^{32}P] γ-ATP. As an additional control protein G-Sepharose beads were incubated with the cell lysates alone and then incubated with 1μl of [^{32}P]γ-ATP. The reactions were stopped after 15 min by addition of Leamelli Sample Buffer. Complexes were fractionated by SDS-PAGE and phosphorylation of the GST-tagged proteins was visualized by autoradiography. As shown in red ovals in Figure.5.6.a. CtIP is phosphorylated by SMG1 to a limited extent compared to p53 and this process is caffeine sensitive. RPA32 does not appear to be an SMG1 phosphorylation substrate. The pronounced band marked by the orange dot is possibly a product of a different kinase than SMG1 binding nonspecifically to the protein G-Sepharose beads and phosphorylating a protein present in the cell lysates used in the experiment.

Additional bands on the Coomassie Brilliant Blue stained gel, not marked by the red circles, are most likely a product of degradation of the originally GST-tagged protein or bacterial-protein contamination (Figure 5.6.b.).

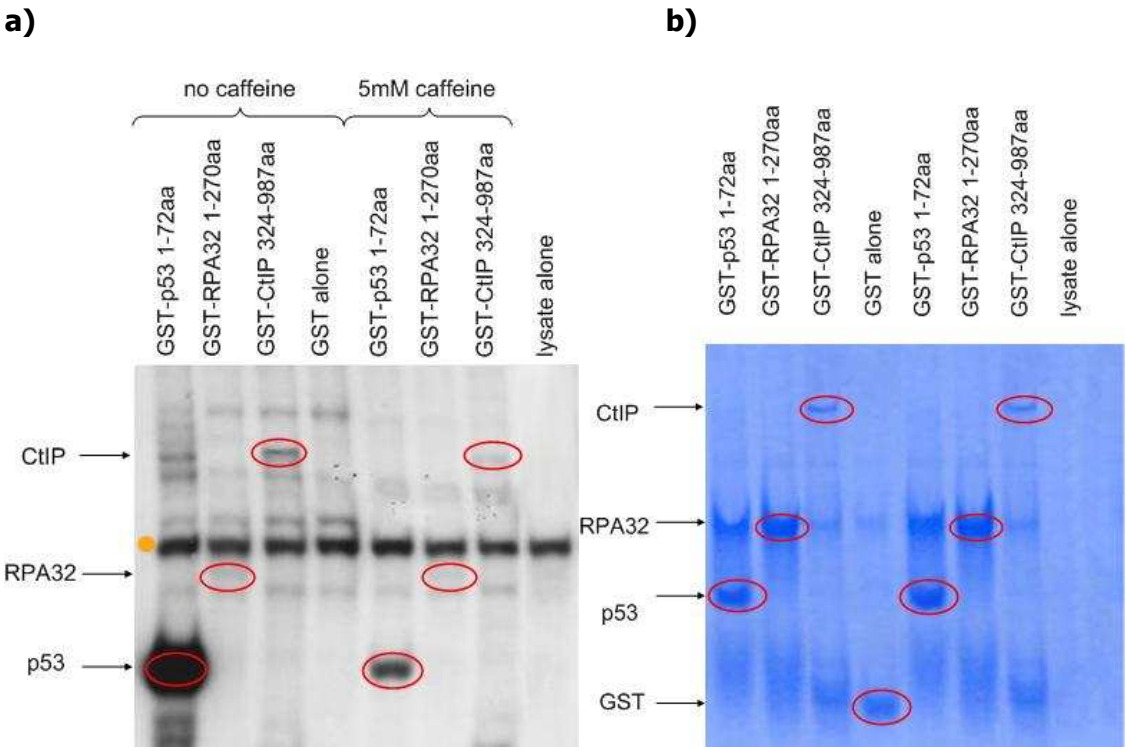

Figure.5.6. CtIP is phosphorylated by SMG1 and the proccess is caffeine sensitive. a) LCLs were mock-treated or treated with 5mM caffeine and harvested 1 h post treatment. A rabbit antibody was used to immunoprecipitate SMG1 and the kinase was used to phosphorylate GST-p53, GST-RPA32, GST-CtIP and GST. Complexes were fractionated by SDS-PAGE and the phosphorylation of GST-tagged proteins was visualized by audioradiography, **b)** The SDS-PAGE gel stained with Coommassie Brilliant Blue showing the GST-tagged proteins used in the experiment. This figure is representative of three independent repeats.

5.2.3. Homology between CtIP and NBS1, ATRIP and Ku80.

It has been reported that NBS1, ATRIP and Ku80 are homologous in their C-terminal regions which bind to ATM, ATR or DNA-PK respectively (Falk et al., 2005). The homologous region and the identical amino acids are shown in the Figure.5.7. As CtIP associates with ATM and ATR *in vivo* we carried out a sequence comparison between CtIP and NBS1 and found that CtIP shares homology with the NBS1 C-terminal region at two sites in the protein. These sites are situated between residues 267 and 284aa and 595 and 603aa, shown in the Figure.5.8.a. The first region is located before the BRCA1 binding site and the second one is located before the pair of ATM phosphorylation sites at S664 and S745 (Figure.5.8.b.). This result raised a possibility that CtIP could be a binding partner for SMG1 or other PIKKs in the same way as NBS1 is to ATM, ATRIP to ATR and Ku70/80 to DNA-PKcs. It would be a very interesting new link in the DNA damage response pathways thus we decided to investigate this further. We obtained SMG1 siRNA and tried to decrease its expression but in the system used the experiment was not successful. As we could not obtain GST-SMG1 constructs or SMG1 constructs that would translate *in vitro*, we could not establish whether CtIP and SMG1 bind directly. I also could not establish optimal phosphorylation conditions for SMG1 antibody in HeLa cell lysates which were used to perform a kinase assay with CtIP knock-down to examine whether knock-down of CtIP influences the kinase activity of SMG1.

Thus the question whether CtIP and SMG1 are direct binding partners taking part in the DNA damage response and CtIP affects SMG1 kinase activity remains to determined.

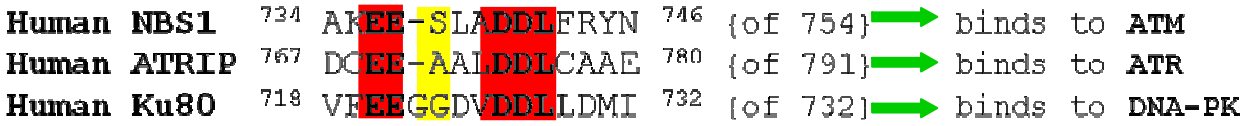

Figure.5.7. The homology between the C-terminal region of NBS1, ATRIP and Ku80. The sequence alignment of the homologous regions of NBS1, ATRIP and Ku80 that bind to ATM, ATR and DNA-PK respectively (Falk et al., 2005).

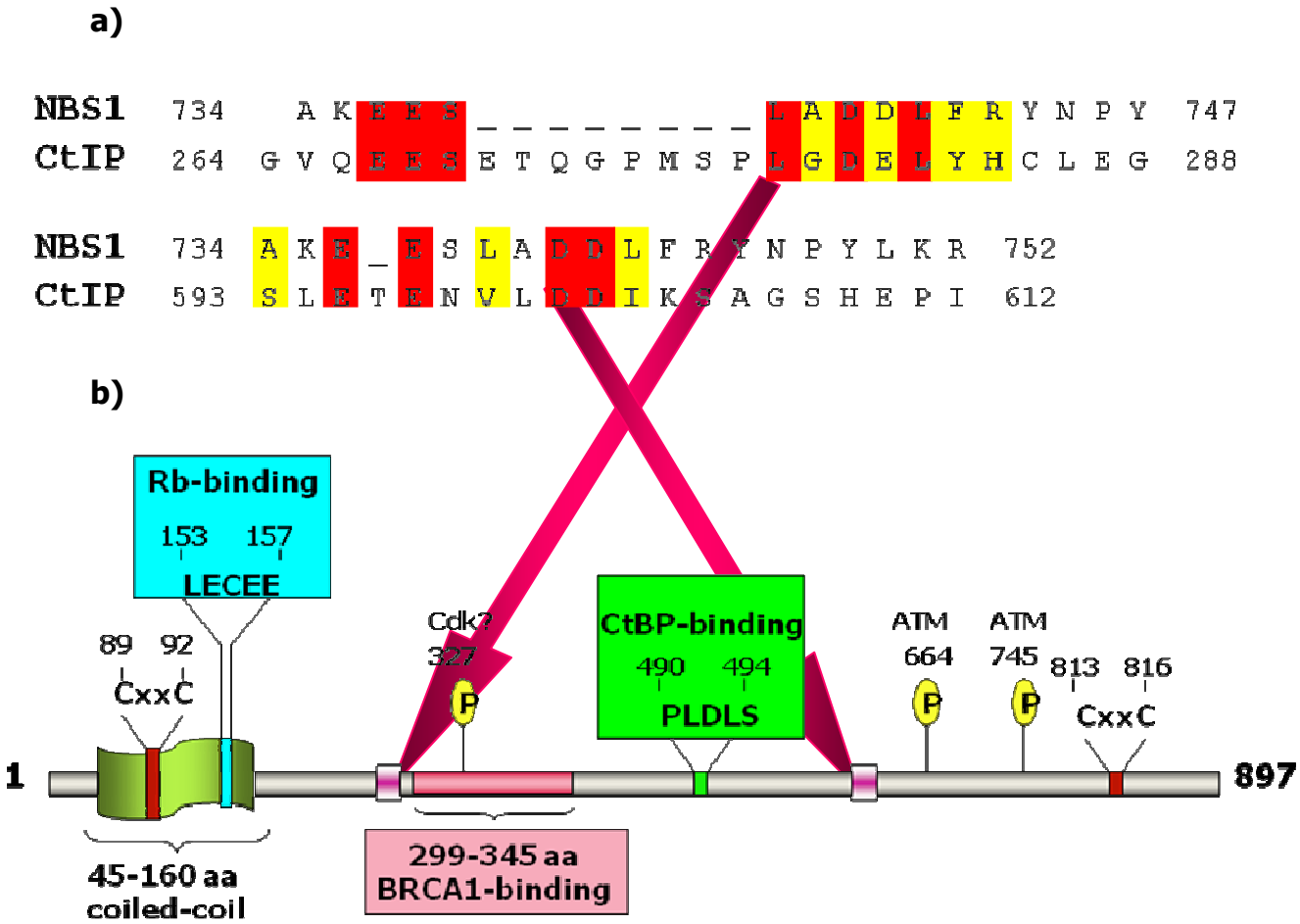

Figure.5.8. The C-terminal region of NBS1 shows homology with two regions of CtIP. a) The sequence alignment the of C-terminal region of NBS1 with two regions of CtIP; residues highlighted in red are identical and residues highlighted in yellow are similar. **b)** A CtIP diagram showing the positions of the aligned sequences.

5.2.4. Establishing new phosphorylation sites on CtIP.

CtIP was reported to be phosphorylated at S664 and S745 by Li S. et al. (Li et al., 2000). Using amino acid sequence analysis it is predicted that there are five more potential phosphorylation sites (Figure.5.9.), which are consensus phosphorylation sites for PIKK kinase family members: SQ/TQ. It was decided to investigate in detail four of them. The investigation was dictated by the fact, that the full length GST-CtIP protein is unstable and the longest GST-CtIP protein available starts at 327aa. Thus to examine the phosphorylation pattern in the most physiologically relevant construct available GST-CtIP 327-897aa was chosen.

To establish the importance of each SQ/TQ site site-directed mutagenesis was performed. DNA encoding CtIP 327-897aa cloned into pGex vector was used. Each serine or threonine followed by a glutamine residue, namely S506, S555, S679 or T859 was mutated into an alanine. The S664 and S745 residues were mutated separately and together to serve as a control for this experiment. In each PCR reaction (section 2.2.9.1.) a set of primers with a point mutation at the appropriate position was used so the PCR product would express an alanine instead of serine or threonine. Each mutated CtIP construct was sequenced (section 2.2.9.2.) and the mutated codons are shown in Figure.5.10. Mutated constructs were used to transform (section 2.2.2.) XL10-Gold Ultracompetent bacteria for small scale DNA preparation (section 2.2.3.2.) and subsequently BL21-CodonPlus (DE3)-RIL bacteria were transformed for mutated GST-CtIP protein production and purification (section 2.2.7.).

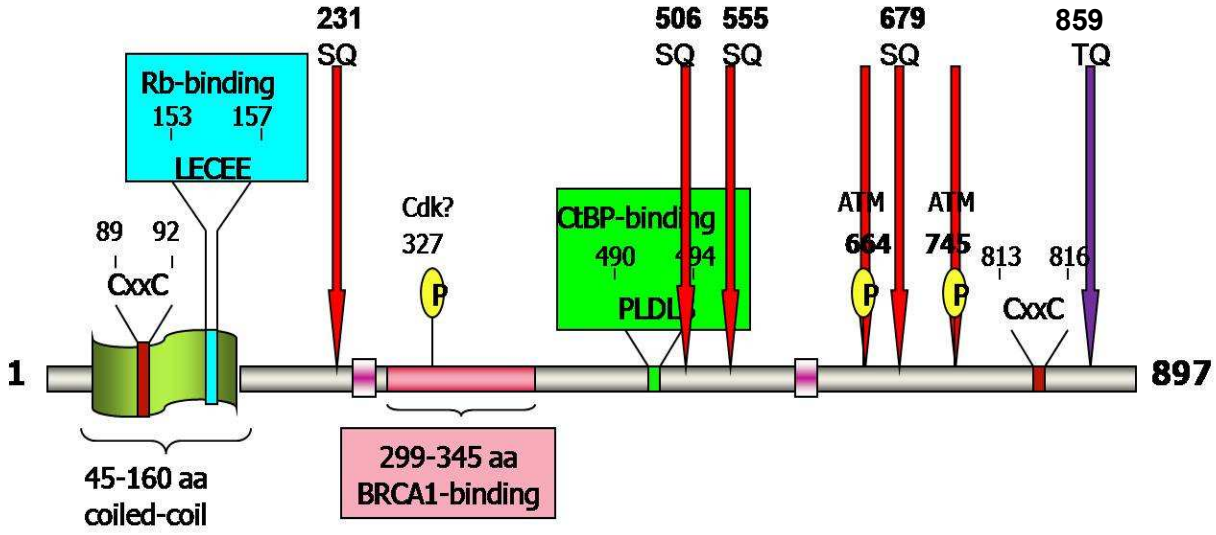

Figure.5.9. The positioning of new and reported phosphorylation sites on human CtIP. The CtIP cartoon showing positions of reported: S664 and S745 and new: S231, S506, S555, S679 and T859 phosphorylation sites.

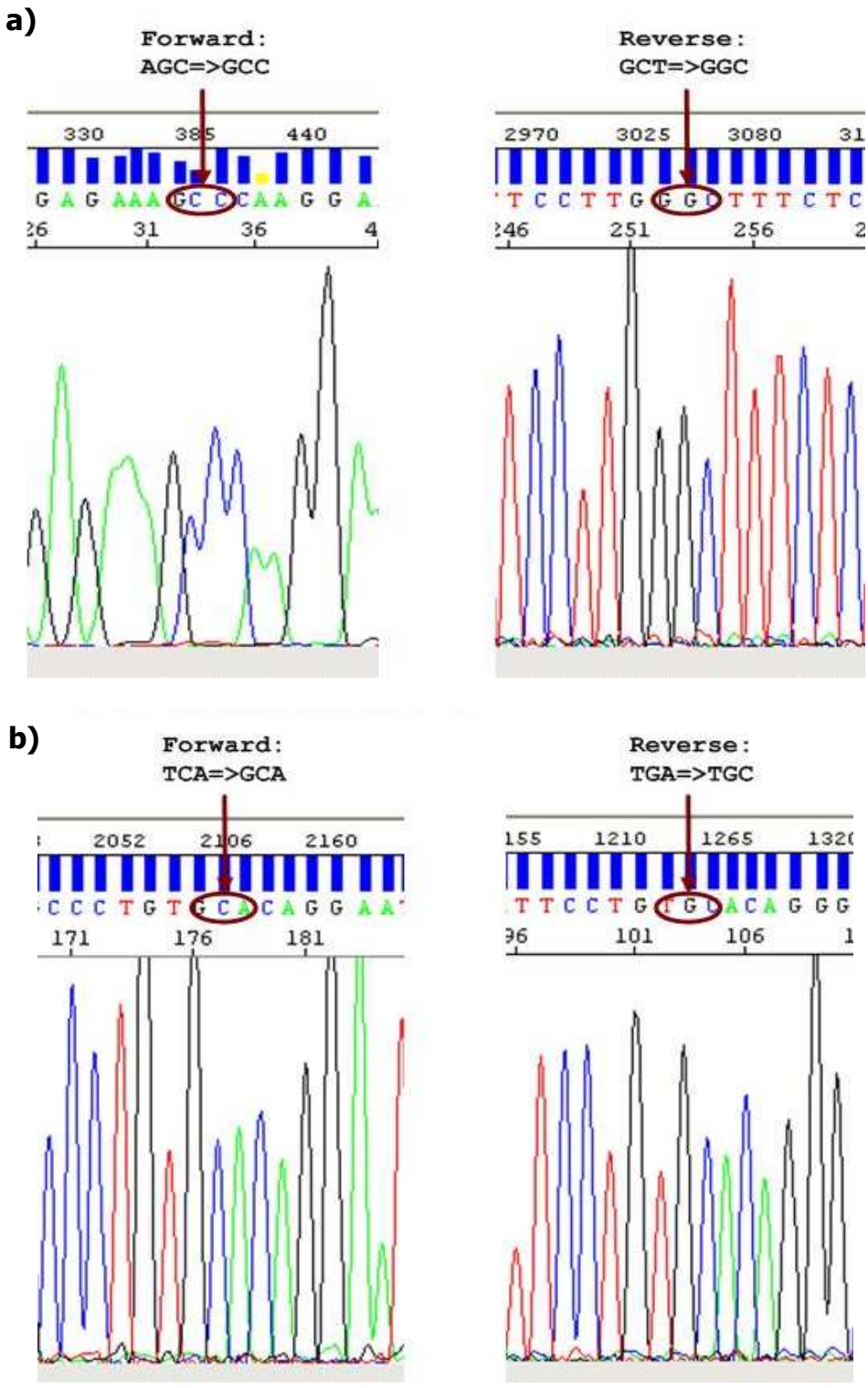

Figure.5.10. The point mutations generated in GST-CtIP 327-897aa construct. CtIP construct cloned into pGex vector was used to generate point mutations of the chosen Serine or Threonine residues. **a)** Point mutation changing S506 into A506. **b)** Point mutation changing S555 into A555.

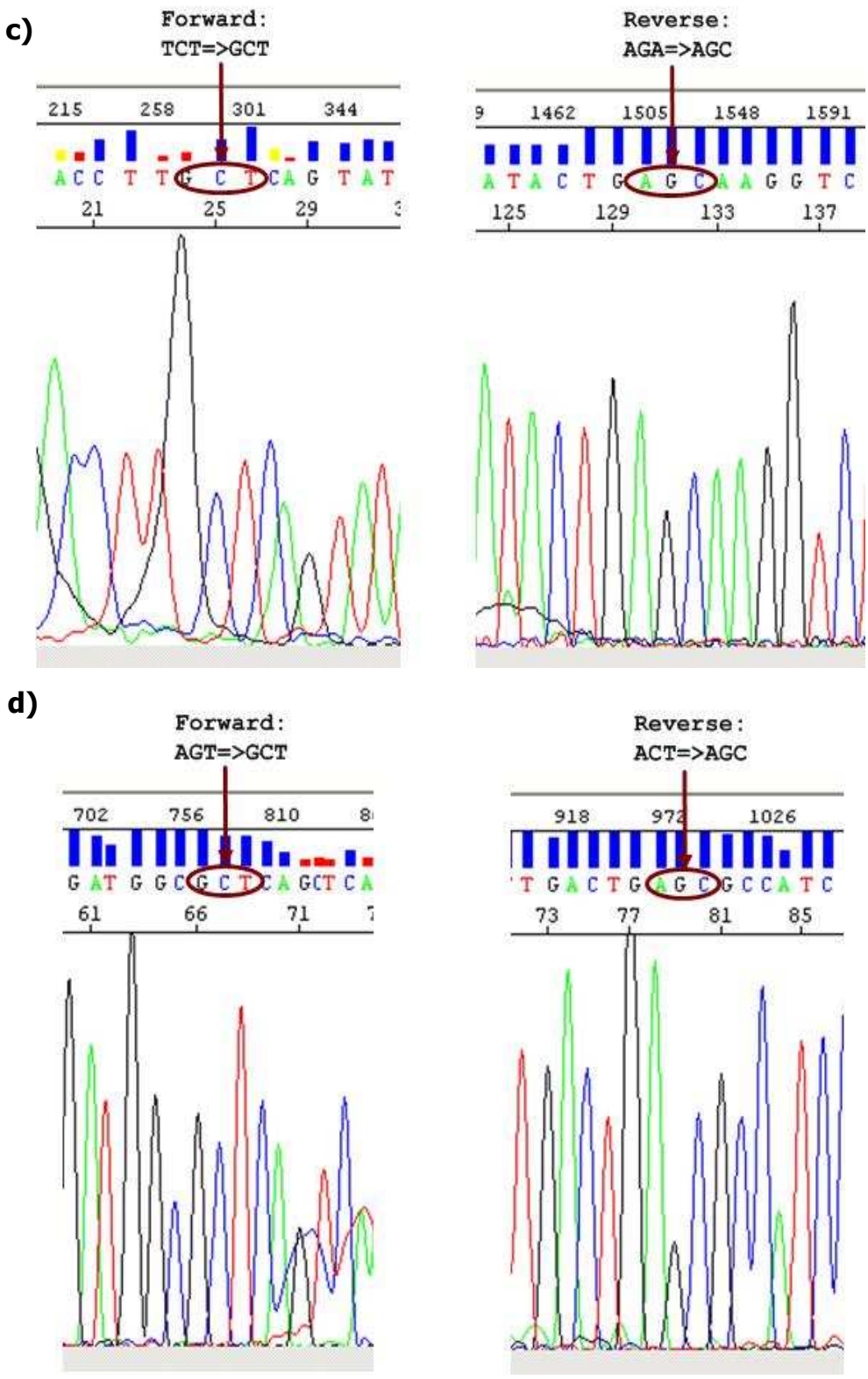

Figure.5.10. The point mutations generated in GST-CtIP 327-897aa construct. CtIP construct cloned into pGex vector was used to generate point mutations of the chosen Serine or Threonine residues. **c)** Point mutation changing S664 into A664. **d)** Point mutation changing S679 into A679.

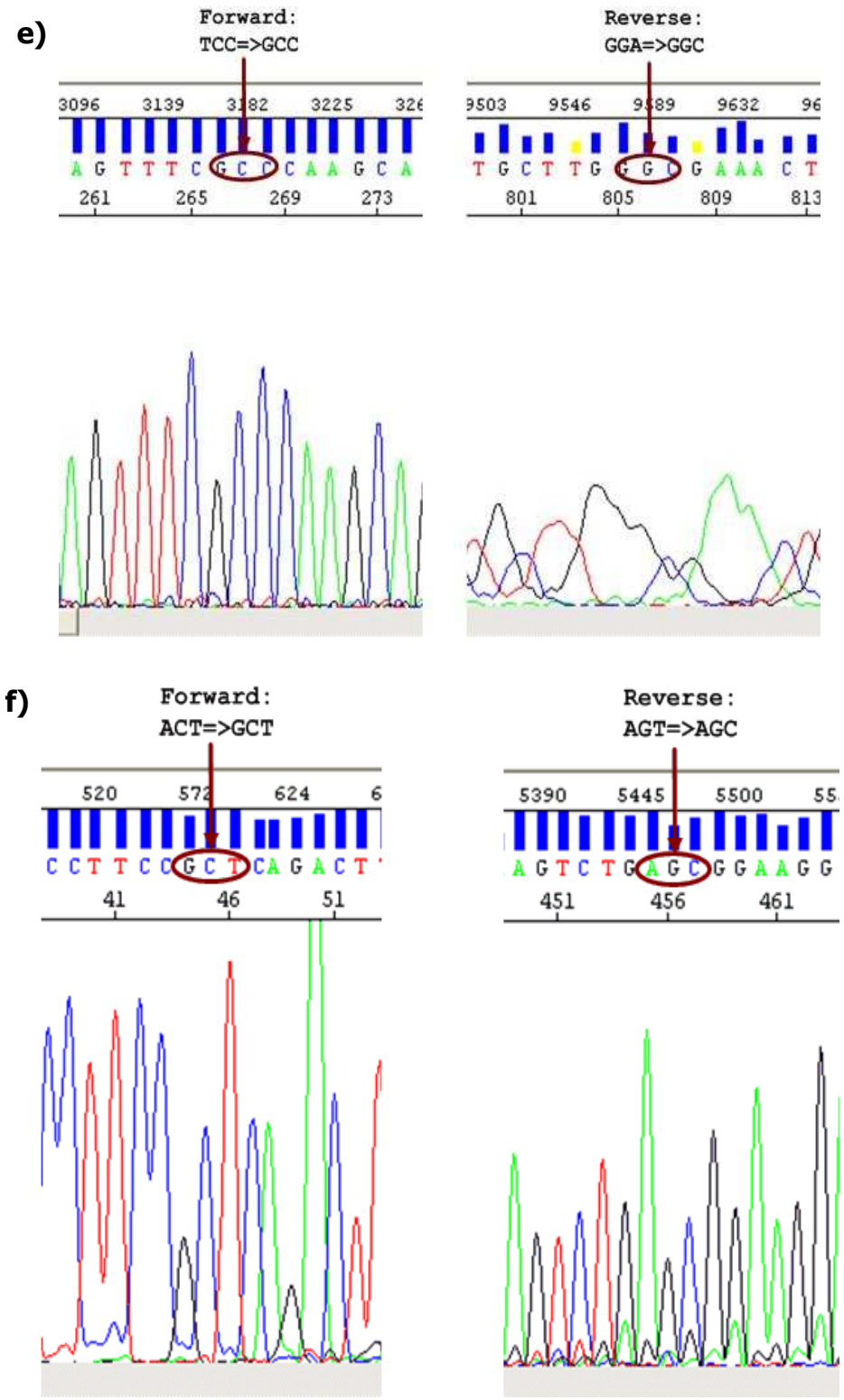

Figure.5.10. The point mutations generated in GST-CtIP 327-897aa construct. CtIP construct cloned into pGex vector was used to generate point mutations of the chosen Serine or Threonine residues. **e)** Point mutation changing S745 into A745. **f)** Point mutation changing T859 into A859.

From the PIKK family ATM was chosen as a model kinase involved in DNA DSBs response. A kinase assay was performed (section 2.4.4.) to investigate the influence of mutation in each SQ/TQ site, or two mutations in the case of S664 and S745, in one construct, on the *in vitro* phosphorylation of CtIP by ATM. LCLs were irradiated with 5Gy and harvested 30 min post irradiation to allow for ATM full activation. A mouse antibody was used to immunoprecipitate ATM and the kinase was isolated using protein G-Sepharose beads. After the last wash the beads with bound ATM were resuspended in kinase buffer and to each portion of beads 10 μg of wild type GST-CtIP 324-897aa or GST-CtIP 324-897aa mutant: S506A, S555A, S664A, S679A, S745A, S859A or S664A and S745A mutations together or GST alone was added and supplemented with 1 μl of [^{32}P]γ-ATP. As an additional control protein G-Sepharose beads were incubated with the cell lysates alone and then incubated with 1μl of [^{32}P]γ-ATP. The kinase reaction was incubated at 37^{o}C for 3 min and stopped by the addition of Laemmli Sample Buffer. Samples were heated to 95 ^{o}C for 5 min, fractionated by SDS-PAGE and phosphorylated GST-tagged proteins were visualized by autoradiography. As shown in the Figure.5.11. the phosphorylation of the wild type GST-CtIP is much more pronounced than phosphorylation of each of the mutated protein. The greatest reduction in phosphorylation was observed for the two previously described phosphorylation sites S664 and S745 mutated together. In the case of the proposed phosphorylation sites mutation in residue S555 gave the greatest reduction in the phosphorylation efficiency.

A greater degree of specificity has been suggested with ATM preferentially phosphorylating LSQE and, to a lesser extent, LTQE (O'Neill et al., 2000). On the other hand the presence of adjacent positively charged residues next to neutral residues reduces the phosphorylation efficiency when the kinase assay is performed using a

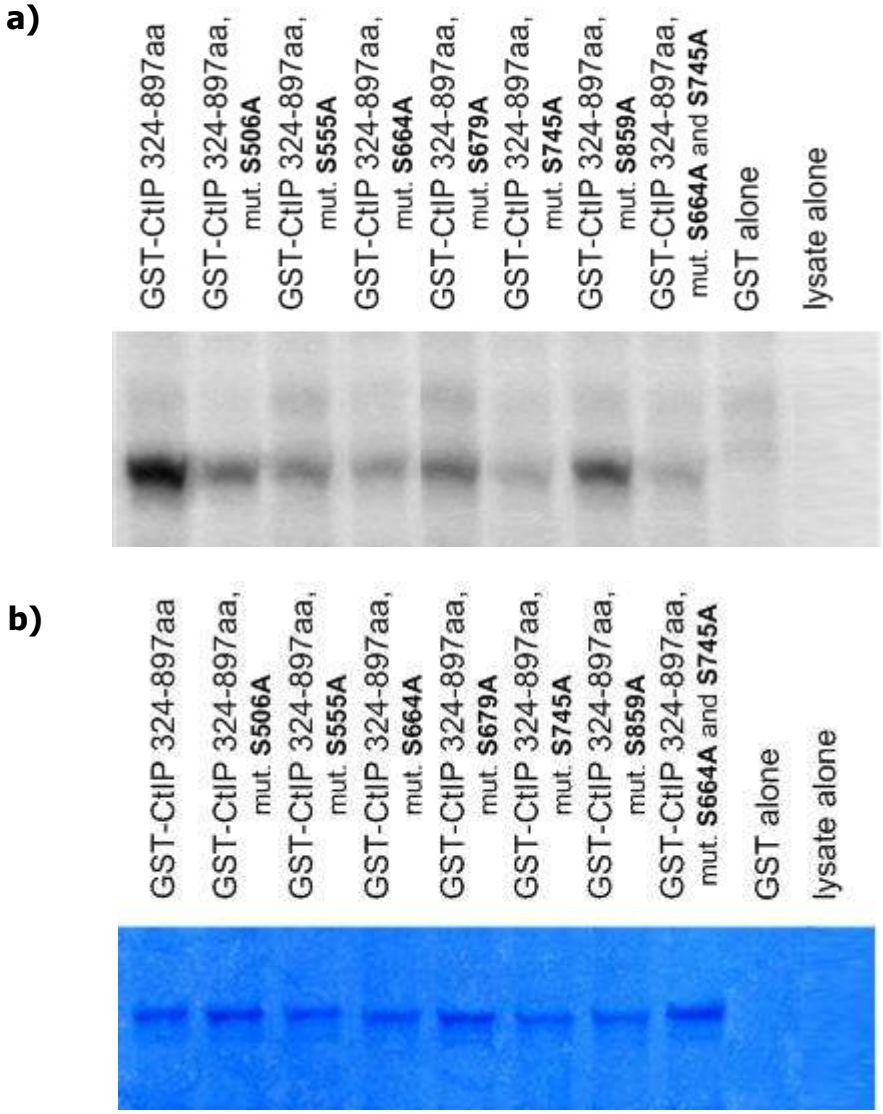

Figure.5.11. The phosphorylation of GST-CtIP 327-897aa mutants. a) LCLs were irradiated with 5Gy and harvested 30 min post irradiation. A mouse antibody was used to immunoprecipitate ATM and the kinase was used to phosphorylate wild type GST-CtIP, GST-CtIP point mutants and GST. Complexes were fractionated by SDS-PAGE and the phosphorylation of GST-tagged proteins was visualized by audioradiography, **b)** The SDS-PAGE gel stained with Coommassie Brilliant Blue showing the GST-tagged proteins used in the experiment. This figure is representative of three independent experiments.

GST-p53 fragment (Table.5.1; Kim et al., 1999). Amino acid sequence examination of residues adjacent to the predicted SQ/TQ phosphorylation sites reveals that these regions have different charges. Table.5.1. shows the amino acid composition of the SQ/TQ sites in the GST-p53 fragment (Kim et al., 1999) and the GST-CtIP fragments (this study), their surrounding residues and their charges.

Table.5.1. Sequence of the p53 fragment used to establish the specificity of ATM kinase and established and predicted SQ/TQ phosphorylation sites in CtIP with their adjacent residues.

GST-protein	amino acid sequence	a.a. charge
p53	P(0)P(0)L(0)**S**(0)**Q**(0)E(-)T(0)F(0)	000**00**-00
CtIP residue no.		
506	Q(0)E(-)K(+)**S**(0)**Q**(0)G(0)S(0)E(-)	0-+**00**00-
555	E(-)P(0)C(0)**S**(0)**Q**(0)E(-)C(0)I(0)	-00**00**-00
664	A(0)D(-)L(0)**S**(0)**Q**(0)Y(0)K(+)M(0)	0-00**00**+0
679	K(+)D(-)G(-)**S**(0)**Q**(0)S(0)K(+)L(0)	+--**00**0+0
745	D(-)S(0)F(0)**S**(0)**Q**(0)A(0)A(0)D(-)	-00**00**00-
859	F(0)P(0)S(0)**T**(0)**Q**(0)T(0)C(0)M(0)	000**00**000

When we compare the charges of the adjacent residues with the phosphorylation efficiency in Figure.5.11. we can hypothesise that if the S residue is adjacent to one or two negatively charged amino acids that are on opposite sides of the S residue we can observe the greatest influence of that sequence on phosphorylation of that S residue. This is seen in Figure.5.11. as the greatest reduction of phosphorylation of S555, S664 and S745. However if a positively charged residue or neutral residues surround the predicted phosphorylation site we do not observe such a great impairment in the phosphorylation. This can be caused by the conformation of the protein enabling efficient phosphorylation of a particular residue. However it seems to be rather

important that the residue before S is hydrophobic (L or F in the case of CtIP; Kim et al., 1999) or that a negatively charged residue should follow the Q residue. Those two configurations give the best possible efficiency of ATM phosphorylation. However as seen in the case of S664 or S745 even the presence of just one of those sequence factors such as a hydrophobic residue (L or F) directs the S residue for efficient ATM phosphorylation. Thus in the case of S555 we could hypothesise that it is the E residue that influences the phosphorylation of this S by ATM. In the case of S506, S679 and T859 the amino acids that surround the phosphorylation site do not share many similarities with the described LSQE/LTQE sequence. For S506 it can be the positively charged K that lowers the efficiency of phosphorylation, S679 is next to two negatively charged residues which could influence the phosphorylation efficiency and T859 would not only have a default lower phosphorylation rate then S residue (Kim et al., 1999; O'Neill et al., 2000) but the adjacent residues are not very similar to the ones in the p53 sequence (Kim et al., 1999). Thus we could expect a smaller reduction in phosphorylation in comparison to non-mutated residues or none at all.

5.3. Discussion.

In the previous chapters CtIP was shown to form novel complexes with proteins involved in the DNA damage response pathways. In this chapter we analysed whether the complexes formed with the PIKK family kinases possess kinase activity when associated with CtIP. As shown in Figure.5.2.a. CtIP antibody co-immunoprecipitates a kinase activity that is able to phosphorylate GST-p53 fragment 1-73 containing three reported PIKK kinase phosphorylation sites (Siliciano et al., 1997) and GST-RPA32 that has been shown to be phosphorylated at several serine and threonine residues by the kinases from the PIKK family (Block et al., 2004; Manthey et al.,2007). The kinase activity immunoprecipitated by CtIP is caffeine sensitive which suggests that it is a member of the PIKK family or all of them complexed together. To establish whether it

is a pool of kinases or just ATM, CtIP was immunoprecitipated from HeLa cells depleted of ATM. As shown in Figure.5.3.a. CtIP associates with other PIKK kinases apart from ATM. This result suggests that CtIP forms complexes with possibly one or more PIKK kinases, apart from ATM, and those complexes have an ability to phosphorylate downstream targets such as p53, RPA32 or CtIP.

CtIP was reported to be phosphorylated on S664 and S745 by ATM (Li et al., 2000). As shown in Figure.5.3.a. GST-CtIP protein is still phosphorylated even in the absence of ATM. Thus we decided to investigate whether it is phophorylated by ATR and SMG1. In Figure. 5.4.a. we can clearly observe phosphorylation of GST-CtIP by ATR and we compare it with almost the same level of phosphorylation performed by ATM. Figure.5.6.a. shows SMG1 phosphorylating GST-p53 and GST-CtIP to a limited extent. This process, as for all other PIKK family members, is caffeine sensitive. This suggests that CtIP can be phosphorylated *in vivo* by all members of the PIKK family. There is a possibility that each of the kinases has a preference for a specific site but this remains to be established.

Protein phosphorylation is known to change protein conformation. The change in conformation may expose regions of the protein previously buried, for example in hydrophobic areas. Phosphorylation also changes the charge of a region of a protein which, in turn changes its folding (secondary/tertiary structure; Krupa et al., 2004). Protein phosphorylation also alters the specificity of protein-protein interactions. A wide range of DNA damage response proteins have domains that are known to specifically bind to phospho-peptides such as the FHA domain or the BRCT domains (Durocher & Jackson, 2002; Manke et al., 2003).

The fact that CtIP is phosphorylated by several kinases may suggest that each of those kinases shows a preference towards a specific site. Thus depending on the type of

DNA damage CtIP could be phosphorylated at different sites, by differet kinases, which would result in different protein folding. Differential folding could effectively enable CtIP to bind different partners, thus it might engage in different cellular processes.

As shown previously CtIP associates with ATM and ATR and the complex formation is not influenced by DNA damage (Figure.4.3). Figure.5.5. demonstrates CtIP's association with SMG1 kinase before and after DNA damage inflicted by 5Gy or 30J. The interaction appears to be stronger after SSBs. However, SMG1 also interacts with RPA70 and this interaction is enhanced by DNA damage, Figure.5.5. As shown previously CtIP interacts stably with RPA70 before and after damage (Figure.4.1.) and we could hypothesise that the SMG1-CtIP-RPA70 complex is involved in DNA damage sensing and repair. It is also possible, therefore, that CtIP does not bind SMG1 directly *in vivo*.

As CtIP associates with SMG1 and SMG1 has not been reported to possess a binding partner that would associate with its PRD (PIKK regulatory domain, Figure.5.1.) motif it was decided to investigate this further. A sequence analysis of NBS1's C-terminal ATM binding region aligned with the CtIP sequence showed two regions of homology. The first one is located between 267 and 284aa and the second is located between 595 and 603aa (Figure.5.7.a.). The first region is located just N-terminal to the BRCA1 binding site and the second is located between two pairs of ATM phosphorylation sites: S506, S555 and S664, S745. If the binding region of CtIP-SMG1 was located between those phosphorylation sites CtIP binding could be modulated depending on which site is phosphorylated. Phosphorylation would change the conformation of the protein thus enhancing or decreasing the interaction, but this remains to be elucidated, as it was impossible to establish the direct interaction of SMG1 and CtIP. This was due to our inability to obtain SMG1 constructs that would either translate *in vitro* or would produce GST-SMG1 protein fragments. Due to lack of time it was also impossible to

create such constructs ourselves. Thus we can only speculate on CtIP being an activator protein for SMG1 kinase activity and binding to its PRD motif. It must also be borne in mind, however, that CtIP could bind primarily to ATM and/or ATR mediating an, as yet, unknown function.

CtIP has been reported to be phosphorylated by ATM on residues S664 and S745 (Li . et al., 2000). Sequence analysis showed that there are five other S-T/Q motifs that could be potentially phosphorylated by members of the PIKK family. It was decided to mutate four of them as the most physiological GST-CtIP construct available did not include the first one, S231. As shown in Figure.5.11. immunoprecipitated ATM kinase phosphorylates the wild type GST-CtIP most effectively and the mutated species are all phosphorylated less efficiently. From the newly recognized phosphorylation sites it appears that S555 shows the greatest decrease in the phosphorylation efficiency after mutation. This may be due to the fact that it is a potential ATM phosphorylation site *in vivo*. On the other hand there is a possibility that if the phosphorylation assay was carried out using other PIKK kinases we would be able to establish phosphorylation sites specific for each kinase, but this remains to be elucidated. As has been reported it is difficult to establish site-specific phosphorylation using a phosphorylation assay, if the site can be recognized by different members of the same family of kinases (Temporini et al., 2008). As O'Neill et al. (2000) and Kim et al. (1999) report ATM, ATR and DNA-PK have different preferences towards SQ/TQ sites depending on the adjacent residues. Thus one could hypothesise that it would be of interest to perform the kinase assay shown in Figure.5.11. with other members of the PIKK family as well. However it seems that the best way to recognize a site and a kinase that phosphorylates it is by carrying out *in vivo* experiments. Possibly introducing mutated proteins into cells and knocking down the kinases and then looking at the phosphorylation profile of the protein either by phosphospecific antibodies or mass

spectrophotometry (Jowsey et al., 2007). This approach was beyond available time for this project.

CHAPTER VI

GENERAL DISCUSSION

Possible roles for CtIP in the cellular DNA damage response.

6.1. Research on CtIP in a historical perspective.

CtIP was first described as a binding partner of CtBP, Rb and BRCA1 (Fusco et al., 1998, Schaeper et al., 1998; Yu et al., 1998). Thus the initial research focused on exploring how CtIP and its binding partners act together to regulate transcription and the cell cycle. The research that we undertook was based on the observation that CtIP binds to the BRCT domains of BRCA1 (Wong et al., 1998, Yu et al., 1998).

BRCA1 was known, not only to be involved in the cell cycle regulation, but also was recognized as a tumour suppressor gene (Hakem et al., 1996; Hall et al., 1990; Miki et al., 1994). It was later shown to be involved in homologous recombination together with Rad51 (Baumann et al. 1996; Scully et al., 1997a) and this has led to investigations into BRCA1's involvement in the DNA damage response (Moynahan et al., 1999). As CtIP was a BRCA1 binding partner investigation was initiated into CtIP's involvement in the DNA damage response and this work has been presented here.

In a review in 2006 Chinnadurai described CtIP as a 'team player with luminaries' such as tumour supressors BRCA1 and Rb. By the middle of 2006 Wu & Lee had described CtIP as a 'multivalent adaptor' taking part in transcriptional regulation, DNA damage response and cell cycle checkpoint regulation. Previous studies had concentrated on the regulation of Rb activity by CtIP. However, also in 2006, a different report appeared, showing BRCA1/BARD1 DNA damage-induced association with the MRN complex and TopBP1 (Greenberg et al., 2006). It was possibly a milestone in the research into CtIP function.

In late 2007 Jackson's lab published a first paper on CtIP's function in the DNA end resectioning (Sartori et al., 2007) and CtIP's importance became apparent to a larger audience. Now CtIP is thought to be indispensible in ssDNA end creation, DSBR, HR and MMEJ.

6.2. CtIP involvement in the initiation of DNA damage response by the MRN complex.

In the course of this study we established, at the same time as Jackson's lab, that CtIP forms a complex and binds directly to the MRN complex. However, our data indicate that CtIP binds directly to NBS1 rather than Mre11 or Rad50 when they are expressed separately (Figure.3.13., Figure.3.14., Figure.4.2.). As Sartori et al. (2007) show, CtIP binds directly to a complex formed by Mre11 and Rad50, which does not exclude the possibility that it does not bind to them separately as they may form a binding site for CtIP by their complex formation. However, considering our data and Sartori's et al. results one could postulate that CtIP is an integral part of the MRN complex. To investigate this matter further, we performed co-immunoprecipitation assays from cells that are defective either in Mre11 (ATLD patient-derived LCLs) or NBS1 (NBS patient-derived LCLs). The ATLD patient-derived LCLs express a truncated version of Mre11, lacking the second DNA binding motif (DNA binding B, Figure.1.6. & Figure.4.9). The NBS patient-derived LCLs express two NBS1 proteins: p26, containing the FHA domain and the first BRCT domain and p70, comprising the C-terminal region of the protein starting with the second BRCT domain (Figure.4.10). The results revealed that CtIP associates with the members of the complex despite mutations in either Mre11 or NBS1, although the level of association of CtIP with NBS1 and Rad50 is compromised by the mutation of Mre11 in ATLD LCLs (Figure.4.11.).

An interesting observation was also made, showing that CtIP's association with ATM is compromised in NBS1 mutated cells and in ATLD cells, which show a lower level of NBS1 expression due to the Mre11 mutation (Figure.4.11.a.; Stewart et al., 1999). This would suggest that ATM associates with CtIP via NBS1 indicating that CtIP would not be necessary for ATM activation by the MRN complex.

In a recent article, Yuan & Chen (2009) demonstrated that the MRN complex is one of the first sensors of DNA damage. They report that, in cells depleted of H2AX, 53BP1 IRIF formation is still present upon DNA damage although retention of those foci is not longer than 120 mins. Further, they have shown that 53BP1 and BRCA1 transient foci formation in H2AX-depleted cells depends on the presence of NBS1 and Mre11.

Yuan & Chen (2009) also point out, that cells depleted of ATM (Barlow et al., 1996), MDC1 (Lou et al., 2006), 53BP1 (Manis et al., 2004; Ward et al., 2004) or H2AX (Celeste et al., 2002) are still viable whereas mice knock-outs of the MRN complex (Luo et al., 1999; Zhu J. et al., 2001; Xiao Y.& Weaver D. T., 1997), CtIP (Chen et al., 2005), ATR (Brown & Baltimore, 2000; de Klein et al., 2000), BRCA1 (Ludwig et al., 1997), BRCA2 (Sharan et al., 1997) and Rad51 (Tsuzuki et al., 1996) show embryonic lethality. However, the key finding in this article is the transient formation of IRIF in the absence of H2AX that is stimulated by the MRN complex. This suggests that the DNA damage response is initiated by the MRN complex protein-protein interaction resulting in foci formation. Yuan & Chen also suggest that NBS1 could be a binding partner for 53BP1 but I would hypothesise that CtIP is the missing link in the transient formation of IRIF at the sites of DNA damage preformed by MRN.

CtIP seems to be a scaffold that binds to a variety of factors and interacts *in vivo* with an even larger number of proteins. It seems reasonable to propose that Mre11 and Rad50 are the factors that bind broken DNA ends. Mre11 also binds to NBS1 which could facilitate complex protein-protein interactions. To enlarge the spectrum of possible interactions NBS1 would bind CtIP, which in this setting, would mainly serve as a docking station for other proteins, that are involved in the DNA damage repair. This transient complex could repair the damage that would arise from low doses of UV before the phosphorylation of H2AX would occur and before ATM or ATR would be recruited to the repair process. Thus we could speculate, on the basis of the Yuan &

Chen (2009) report, that low level DNA damage is readily repaired by MRN/CtIP transient IRIF formation and formation of γ-H2AX/MDC1 dependent foci is the next step in the repair process, that is activated in the case of more severe damage. Those foci are long-lived and also contain 53BP1 and BRCA1 and other proteins that are involved in the transient foci formation. On the basis of this deduction it would be interesting to look at TopBP1 transient foci formation as well as the efficiency of their formation in CtIP-depleted cells.

6.3. Implication of CtIP interaction with the BRCT domain containing proteins in transient IRIF formation.

In support of the hypothesis described above, in chapter III I have shown that CtIP binds directly to a number of BRCT domain-containing proteins involved in the DNA damage response such as MDC1, 53BP1, TopBP1 and NBS1. Thus the model of the transient IRIF formation I would propose is the recruitment of MRN/CtIP to the sites of damage and subsequent concentration of 53BP1, BRCA1 and possibly MDC1 and TopBP1. In the case of more severe damage ATM would be recruited and subsequently phosphorylate H2AX which in turn recruits MDC1 which forms a firm, anchored scaffold with γ-H2AX and MRN/CtIP. This scaffold recruits other DNA repair proteins. The latter process is not CtIP dependent as MDC1 anchors itself to chromatin mainly via γ-H2AX. As shown in Figure.3.24. depletion of CtIP does not interfere with MDC1 γ-H2AX-dependent foci formation and their retention. It is also indicated by normal formation of 53BP1 foci in CtIP-depleted cells (Figure.3.23.).

However, CtIP has been reported to be ubiquitylated by BRCA1/BARD E3 Ub-protein ligase (Yu et al., 2006). This results in CtIP's relocalization to the sites of DNA damage; however further investigations are needed to resolve this pathway of DNA damage recognition and repair (Figure.1.19.).

Furthermore, CtIP in the later stages of the DNA damage response, after the engagement of γ-H2AX and its dependent foci formation, could orchestrate the repair events due to its ability to form protein multicomplexes by its wide range of protein-protein interactions. As it binds directly to TopBP1 we could propose that by this interaction it engages ATR in DSBR. We could also hypothesise that CtIP-TopBP1 interaction could be involved in TopBP1 transient foci formation but this remains to be investigated.

As shown in Figures: 3.18, 3.20 and 3.22. CtIP is a nuclear protein that in normal cells shows a slightly granular distribution which changes after DNA damage caused by IR into distinct structures resembling foci. In those Figures we can observe, in yellow, the overlap of CtIP staining with foci formed by 53BP1, MDC1 and NBS1. We can also conclude that as 53BP1, MDC1 and NBS1 foci colocalize with γ-H2AX (Figures: 3.17, 3.19 and 3.21) CtIP's staining would also overlap γ-H2AX foci. Thus it is possible that CtIP concentrates at the sites of DSBs to facilitate formation of protein complexes by proteins that are involved in the DNA damage repair response. Thus CtIP could be potentially involved in transient foci assembly with the MRN complex as well as facilitating DNA damage repair triggered by phosphorylation of γ-H2AX.

6.4. CtIP involvement in the DNA repair pathway choice.

CtIP has been also shown to be involved in the selection of the appropriate DNA damage repair pathway together with BRCA1 (Yun & Hiom, 2009). That report reveals that CtIP, by interaction with BRCA1 in G2/M, redirects DNA repair towards HR. As CtIP interacts with MDC1, Figure.3.5.b., we could argue that this interaction may favour HR in G2/M as MDC1 is involved in controlling HR, although this pathway is distinct from the BRCA1 pathway. Thus CtIP could redirect repair in G2/M towards HR by two different mechanisms involving either BRCA1 or MDC1. In case of failure one of the pathways the other would still be able to repair the damage.

As mentioned before, CtIP's interaction with both NBS1 and 53BP1 could be involved in the formation of the temporary foci. Furthermore, CtIP could be involved in the DNA damage pathway that those proteins take part in. In the case of NBS1 it could be the MMEJ (Deriano et al., 2009), thus CtIP could potentially redirect the repair in G1 towards MMEJ. NBS1 has also been reported to be involved in phosphorylation events orchestrated by ATR such as phosphorylation of RPA32 (Manthey et al., 2007). As CtIP is involved in phosphorylation events directed by ATR (Figure.4.14, Figure.4.16), NBS1 and CtIP could be potentially cooperating in that repair mechanism.

NBS1 has also been reported to interact with TopBP1 via its N-terminal region containing the FHA and the BRCT domain. This interaction *in vivo* has an irradiation dose-dependent character (Morishima et al., 2007). This would agree with the previous hypothesis that CtIP/MRN could involve TopBP1 in the repair processes, in the transient foci formation, in the case of local DNA damage cause by a low doses of UV. In the case of γ-H2AX foci formation and subsequent IRIF formation of other DNA damage response proteins, like 53BP1, CtIP/MRN would be engaged in the retention of those foci occurring in the presence of severe DNA damage. Secondly, Morishima et al. (2007) report that NBS1 and TopBP1 are involved in HR which would imply that the ATR pathway together with CtIP could be involved in HR as well.

6.5. Influence of CtIP depletion on phosphorylation events caused by DNA damage.

As shown in the Figure.4.16.and Figure.4.18., CtIP is involved in ATR signaling. A major impairment of the phosphorylation of proteins such as RPA32 or Chk1 in response to DNA damage caused by 30J or CPT in CtIP-depleted cells shows that CtIP is either involved in enabling the interaction between ATR and its substrates or it stimulates ATR kinase activity together with TopBP1.

The effect of CtIP depletion on phosphorylation events following DNA damage caused by 5Gy, 30J or CPT is shown in Figures:4.15. to 4.19. As expected CtIP depletion has a minor effect on phosphorylation of such proteins as NBS1, ATM, SMC1 or H2AX which in response to 5Gy of γ-irradiation are regulated by ATM kinase activity initiated by the MRN complex (Lee & Paull, 2005). As mentioned before, CtIP-ATM association is most likely mediated by NBS1 (Figure.4.11.a.), thus we could conclude that CtIP has virtually no effect on ATM's activation and subsequent phosphorylation of ATM targets. In the case of 53BP1 phosphorylation on S1778, which has not been reported as an ATM phosphorylation site (Jowsey et al., 2007), we suggest that it is phosphorylated by ATR. As Yoo et al. (2007) report, ATR is activated in response to IR (but not replication stress) by ATM phosphorylation of S1131 on TopBP1 thus it would not need CtIP for the activation process. If 53BP1 S1778 was a true ATR phosphorylation site it could still be phosphorylated even in the absence of CtIP as ATR would be activated by ATM. The other possibility is that S1778 on 53BP1, in response to IR, is phosphorylated by ATM as ATR and ATM belong to the same kinase family thus share a consensus phosphorylation site. Furthermore ATM is recognized as a main kinase in DSB response thus there is a likelihood that ATM would phosphorylate ATR targets in response to DSBs.

Stiff et al. (2006) report that ATR activates ATM after SSBs and replication fork stalling. If ATR is not activated efficiently in response to UV irradiation, as in the case of CtIP depletion, it cannot efficiently activate ATM. Figure.4.17. shows an impairment of the phosphorylation of ATM targets, namely NBS1 and ATM, in the absence of CtIP. This suggests that in cells depleted of CtIP ATR is not effectively activated, thus in the presence of SSBs caused by UV irradiation or replication fork stalling ATR is unable to activate ATM efficiently. The same effect, but even more pronounced, is observed in Figure.4.19. where those proteins' phosphorylation is severely impaired in CtIP-

depleted cells treated with CPT. This suggests that CtIP, apart from facilitating phosphorylation performed by ATR, could be an enhancer of ATR's kinase activity in the presence of SSBs and collapsed replication forks. Sartori et al., report that after SSBs or replication fork stalling in cells lacking CtIP the phosphorylation of RPA32 and Chk1 is impaired (Sartori et al., 2007). Figure.4.16.&4.18. show the same result. This confirms that CtIP is required for efficient phosphorylation of ATR targets.

Figure.4.17.shows no significant influence of CtIP depletion on SMC1 phosphorylation after UV, which is the target of ATM. SMC1 is also phosphorylated less in response to UV-irradiation as compared to γ-irradiation. We could hypothesise that there is no significant reduction of SMC1 phosphorylation in CtIP-depleted cells and this may be due to ATR's basal activity present in normal cells and in cells depleted of CtIP which would be the major factor phosphorylating SMC1 in response to UV. Kim et al. (2002) show SMC1 as a major ATM target in response to IR (Kim et al., 2002). On the other hand, it is still phosphorylated in ATM-depleted cells in response to UV and replication fork stalling in an ATR-dependent manner. These authors also report that SMC1 is phosphorylated in cells lacking DNA-PK thus suggesting that phosphorylation of SMC1 is DNA-PK independent (Kim et al., 2002). On the basis of this report we suggest that basal activity of ATR is sufficient to activate a portion of ATM in response to UV and replication fork stalling. This would also explain the lack of reduction in H2AX phosphorylation following DNA damage caused by IR, UV and CPT in CtIP depleted cells.

6.6. ATR phosphorylation of the BRCT region of 53BP1 containing S1778.

Figure.4.20. shows that ATR phosphorylates (*in vitro*) a GST-53BP1 fragment containing the S1778 site - thus we could speculate that it actually is an ATR dependent phosphorylation site. On the other hand, that GST-53BP1 fragment contains one more SQ motif, S1943, that could be phosphorylated by ATR. Furthermore I also

established that CtIP depletion reduces the ability of ATR to associate with 53BP1 *in vivo*, Figure.4.21. Thus we could hypothesise that impaired phosphorylation of 53BP1 in cells lacking CtIP is due to a reduced ability of ATR to associate with 53BP1 and subsequently efficiently phosphorylate it in the absence of CtIP.

6.7. CtIP's multiprotein complex formation.

As shown in chapter IV, CtIP associates *in vivo* with the MRN complex, RPA70 (Figure.4.1.), ATM, ATR (Figure.4.4.), 53BP1 (Figure.4.6.) and MDC1 (Figure.4.7.). The interactions are not influenced either by DSBs or SSBs. We conclude that CtIP forms a stable complex with these proteins similarly to BRCA1, which forms a BASC complex (Wang et al., 2000). Alternatively, as CtIP binds directly to BRCA1 (Wong et al., 1998) it is possible that CtIP could broaden the spectrum of activity of the BASC complex by recruiting its other binding partners to it (Figure.4.22.). However further investigation into CtIP's complex formation ability is needed to establish an exact role for CtIP in mediating protein interactions.

Another aspect of this issue is that CtIP is able to form complexes with the MRN complex components even in the case of either NBS1 or Mre11 mutation, Figure.4.11. Furthermore, in excess, CtIP has the ability to compete Mre11 off NBS1, Figure.4.14. This would suggest that this interaction has a dynamic nature and that, depending on the metabolic circumstances of the cell, could change to perform different activities.

CtIP is associated with the MRN complex and appears to be involved in different processes such as DNA end resectioning in DSBR or removing covalently bound Top1 and Top2 from ssDNA ends in SSBR (Hartsuiker et al., 2009; Sartori et al., 2007). Engagement in two such distinct processes suggests that the MRN/CtIP may impinge on both DSBR and SSBR. Thus it could lead us to a conclusion that CtIP could be closely associated with the MRN complex and could be involved in modulating its protein-protein binding ability.

As mentioned before, this could also apply to the MRN transient foci formation and recruitment of 53BP1 or BRCA1 that would be potentially recruited by direct interaction with CtIP (Hartsuiker et al., 2009).

We also investigated CtIP's association with BLM helicase. BLM is known to associate with 53BP1 in response to replication fork collapse caused by HU treatment (Tripathi et al., 2007). BLM is thought to regulate HR by modulating the functions of proteins that are involved in that process as well as being a component of the BASC complex (Wang et al., 2000; Wu et al., 2001). Thus, the fact that it associates with CtIP after HU treatment (Figure.4.20) may suggest another possible mechanism in which CtIP is engaged in HR. Thus, we might speculate, that CtIP takes part in homologous recombination events on several different levels. Firstly being involved in redirecting the repair towards HR together with BRCA1 in S/G2 (Yun & Hiom, 2009) and possibly by similar mechanism with MDC1, as discussed previously. Secondly it could be involved in HR together with BLM enlarging its spectrum of protein-protein interactions. CtIP forms complexes with PIKK kinases as described in chapter V. This suggests that it possibly could orchestrate phosphorylation events by its binding ability with other proteins that are substrates for those kinases. Perhaps by choosing a binding partner and directing it for phosphorylation CtIP would orchestrate the sequence of events during the DNA damage response. However, it seems more likely that CtIP organizes the phosphorylation cascade in response to SSB or replication fork collapse which is indicated by the impairment of the phosphorylation of such proteins as ATM, NBS1 and 53BP1 in response to 30J of UV or CPT treatment (Figure.4.15.&4.16).

6.8. Recognition of new ATM phosphorylation sites on CtIP.

CtIP itself undergoes phosphorylation by members of the PIKK family, namely by ATM, ATR and to less extent, SMG1. Each of those kinases can potentially have a preference for specific SQ/TQ sites on CtIP. If that was the case, CtIP could be phosphorylated by

each of them at a different residue or each of the kinases could phosphorylate a different set of sites at each time. Depending on which residue would be phosphorylated it would differentially change the conformation of CtIP protein. The different folding of the CtIP protein could enable it to interact with a different set of binding partners in response to different genotoxic insults. This ability would be very useful taking into consideration the spectrum of activities that CtIP is involved in. Thus CtIP's activity would depend on the type of damage and the kinase activated by it.

6.9. CtIP sequence homology with the conserved C-terminal region of NBS1.

The C-terminal region of NBS1 that is responsible for interaction with the ATM kinase and its subsequent activation (Falk et al., 2005) has two regions of homology with CtIP, Figure.5.7. Thus it is possible that CtIP might be an activator of SMG1 kinase activity, by binding to its PRD motif, however this remains to be investigated as the kinase assay with CtIP knock-down cells was not optimized to obtain any significant results.

The interplay between the DNA damage response proteins reveals a very complicated network. It seems that most of the proteins involved in the DNA damage response are somehow interlinked with each other. This forms a very sophisticated web of connections where protein posttranslational modifications play a key role.

CHAPTER VII

REFERENCES

Abraham R. T. **(2001)** Cell cycle checkpoint signaling through the ATM and ATR kinases. *Genes Dev.* **15**, 2177–2196.

Abraham R.T. **(2004)** PI 3-kinase related kinases: 'big' players in stress-induced signaling pathways. *DNA Repair* **3**, 883–887.

Adams K. E., Medhurst A. L., Dart D. A. & Lakin N. D. **(2006)** Recruitment of ATR to sites of ionising radiation-induced DNA damage requires ATM and components of the MRN protein complex. *Oncogene* **25**, 3894-3904.

Ahel I., Rass U., El-Khamisy S. F., Katyal S., Clements P. M., McKinnon P. J., Caldecott K. W., West S. C. **(2006)** The neurodegenerative disease protein aprataxin resolves abortive DNA ligation intermediates. *Nature* **443**, 713–716.

Ahmad A., Robinson A. R., Duensing A., van Drunen E., Beverloo H. B., Weisberg D. B., Hasty P., Hoeijmakers J. H. J. & Niedernhofer L. J. **(2008)** ERCC1-XPF endonuclease facilitates DNA double-strand break repair. *Mol. Cell. Biol.* **28**, 5082–5092.

Ahnesorg P., Smith P. & Jackson S. P. **(2006)** XLF interacts with the XRCC4-DNA ligase IV complex to promote DNA nonhomologous end-joining. *Cell* **124**, 301–313.

Aicardi J., Barbosa C, Andermann E., Andermann F., Morcos R., Ghanem Q., Fukuyama Y., Awaya Y. & Moe P. **(1988)** Ataxia-ocular motor apraxia: a syndrome mimicking ataxia-telangiectasia. *Ann. Neurol.* **24**, 497–502.

Alani E., Padmore R. & Kleckner N. **(1990)** Analysis of wild-type and rad50 mutants of yeast suggests an intimate relationship between meiotic chromosome synapsis and recombination. *Cell* **61**, 419–436.

Ali A., Zhang J., Bao S., Irene Liu I., Otterness D., Dean N. M., Abraham R. T. & Wang X.-F. **(2004)** Requirement of protein phosphatase 5 in DNA-damage-induced ATM activation. *Gen. Dev.* **18**, 249-254.

Ame J. C., Rolli V., Schreiber V., Niedergang C., Apiou F., Decker P., Muller S., Hoger T., Menissier-de Murcia J., de Murcia G. **(1999)** PARP-2, a novel mammalian DNA damage-dependent poly(ADP-ribose) polymerase. *J. Biol. Chem.* **274**, 17860–17868.

Amit I., Wides R. & Yarden Y. **(2007)** Evolvable signaling networks of receptor tyrosine kinases: relevance of robustness to malignancy and to cancer therapy. *Mol. Syst. Biol.* **3**, 151.

Anderson D. E., Trujillo K. M., Sung P. & Erickson H. P. **(2001)** Structure of the RAD50 × Mre11 DNA repair complex from Saccharomyces cerevisiae by electron microscopy. *J. Biol. Chem.* **276**, 37027–37033.

Anderson S. F., Schlegel B. P., Nakajima T., Wolpin E. S. & Parvin J. D. **(1998)** BRCA1 protein is linked to the RNA polymerase II holoenzyme complex via RNA helicase A. *Nat. Genet.* **19**, 254–256.

Aravind L., Walker D. R. & Koonin E. V. **(1999)** Conserved domains in DNA repair proteins and evolution of repair systems. *Nucleic Acids Res.* **27**, 1223–1242.

Armitage P. & Doll R. **(1954)** The age distribution of cancer and a multi-stage theory of carcinogenesis. *British J. Can.* **8**, 1-12.

Arthur L. M., Gustausson K., Hopfner K. P., Carson C. T., Stracker T. H., Karcher A., Felton D., Weitzman M. D., Tainer J. & Carney J. P. **(2004)** Structural and functional analysis of Mre11-3. *Nucleic. Acids Res.* **32**, 1886–1893.

Audebert M., Salles B. & Calsou P. **(2004)** Involvement of poly(ADP-ribose) polymerase-1 and XRCC1/DNA ligase III in an alternative route for DNA double-strand breaks rejoining. *J. Biol. Chem.* **279**, 55117–55126.

Bakkenist C. J. & Kastan M. B. **(2003)** DNA damage activates ATM through intermolecular autophosphorylation and dimer dissociation. *Nature* **421**, 499-506.

Ball H. L., Ehrhardt M. R., Mordes D. A., Glick G. G., Chazin W. J. & Cortez D. **(2007)** Function of a conserved checkpoint recruitment domain in ATRIP proteins. *Mol. Cell Biol.* **27**, 3367–3377.

Ball H. L., Myers J. S. & Cortez D. **(2005)** ATRIP binding to Replication Protein A single- stranded DNA promotes ATR-ATRIP localization but is dispensable for Chk1 phosphorylation. *Mol. Biol. Cell.* **16**, 2372–2381.

Banin S., Moyal L., Shieh S., Taya Y., Anderson C. W., Chessa L., Smorodinsky N. I., Prives C., Reiss Y., Shiloh Y. & Ziv Y. **(1998)** Enhanced phosphorylation of p53 by ATM in response to DNA damage. *Science* **281**, 1674-1677.

Barlow C., Hirotsune S., Paylor R., Liyanage M., Eckhaus M., Collins F., Shiloh Y., Crawley J. N., Ried T, Tagle D. & Wynshaw-Boris A. **(1996)** Atm-deficient mice: a paradigm of ataxia telangiectasia. *Cell* **86**, 159-171.

Bartek J. & Lukas J. **(2001)** Mammalian G1- and S-phase checkpoints in response to DNA damage. *Curr. Opin. Cell Biol.* **13**, 738–747.

Bartek J. & Lukas J. **(2003)** Chk1 and Chk2 kinases in checkpoint control and cancer. *Cancer Cell* **3**, 421–429.

Baumann P., Benson F. E. & West S. C. **(1996)** Human Rad51 protein promotes ATP-dependent homologous pairing and strand transfer reactions in vitro. *Cell* **87**, 757–766.

Baumann P. & West S. C. **(1997)** The human Rad51 protein: polarity of strand transfer and stimulation by hRP-A. *EMBO J.* **16**, 5198-5206.

Baumann P. & West S. C. **(1999)** Heteroduplex formation by human Rad51 protein: effects of DNA end-structure, hRP-A and hRad52. *J. Mol. Biol.* **291**, 363-374.

Beamish H., Kedar P., Kaneko H., Chen P., Fukao T., Peng C., Beresten S., Gueven N., Purdie D., Lees-Miller S., Ellis N., Kond N. & Lavin M. F. **(2002)** Functional link between BLM defective in Bloom's syndrome and the ataxia-telangiectasia-mutated protein, ATM. *J. Biol. Chem.* **277**, 30515–30523.

Becker E., Meyer V., Madaoui H. & Guerois R. **(2006)** Detection of a tandem BRCT in Nbs1 and Xrs2 with functional implications in the DNA damage response. *Bioinformatics* **22**, 1289-92.

Bekker-Jensen S., Lukas C., Kitagawa R., Melander F., Kastan M. B., Bartek J. & Lukas J. **(2006)** Spatial organization of the mammalian genome surveillance machinery in response to DNA strand breaks. *J. Cell. Biol.* **173**, 195-206.

Bekker-Jensen S., Lukas C., Melander F., Bartek J. & Lukas J. **(2005)** Dynamic assembly and sustained retention of 53BP1 at the sites of DNA damage are controlled by Mdc1/NFBD1. *J. Cell Biol.* **170**, 201-211.

Bender C. F., Sikes M. L., Sullivan R., Huye L. E., Le Beau M. M., Roth D. B., Mirzoeva O. K., Oltz E. M. & Petrini J. H. **(2002)** Cancer predisposition and hematopoietic failure in RAD50(S/S) mice. *Genes. Dev.* **16**, 2237–2251.

Benjamin R. C. & Gill D. M. **(1980)** Poly(ADP-ribose) synthesis in vitro programmed by damaged DNA. A comparison of DNA molecules containing different types of strand breaks. *J. Biol. Chem.* **255**, 10502–10508.

Bennardo N., Cheng A., Huang N. & Stark J. M. **(2008)** Alternative-NHEJ is a mechanistically distinct pathway of mammalian chromosome break repair. *PLoS Genet.* **4**, e1000110.

Bermudez V. P., Lindsey-Boltz LA, Cesare AJ, Maniwa Y, Griffith JD, Hurwitz J, Sancar A. **(2003)** Loading of the human 9-1-1 checkpoint complex onto DNA by the checkpoint clamp loader hRad17-replication factor C complex in vitro. *Proc. Natl. Acad. Sci. U. S. A.* **100**, 1633–1638.

Bhaskara V., Dupre A., Lengsfeld B., Hopkins B. B., Chan A., Lee J. H., Zhang X., Gautier J., Zakian V. & Paull T. T. **(2007)** Rad50 adenylate kinase activity regulates DNA tethering by Mre11/Rad50 complexes. *Mol. Cell* **25**, 647–661.

Bischof O., Kim S. H., Irving J., Beresten S., Ellis N. A. & Campisi J. **(2001)** Regulation and localization of the Bloom syndrome protein in response to DNA damage. *J. Cell. Biol.* **153**, 367-380.

Blasina A., Price B. D., Turenne G. A. & McGowan C. H. **(1999a)** Caffeine inhibits the checkpoint kinase ATM. *Curr. Biol.* **9**, 1135–1138.

Blasina A., de Weyer I. V., Laus M. C., Luyten W. H., Parker A. E. & McGowan C. H. **(1999b)** A human homologue of the checkpoint kinase Cds1 directly inhibits Cdc25 phosphatase. *Curr. Biol.* **9**, 1-10

Blinov V. M., Koonin E. V., Gorbalenya A. E., Kaliman A. V. & Kryukov V. M. **(1989)** Two early genes of bacteriophage T5 encode proteins containing an NTP-binding sequence motif and probably involved in DNA replication, recombination and repair. *FEBS Lett.* **252**, 47–52.

Block W. D., Yu Y. & Lees-Miller S. P. **(2004)** Phosphatidyl inositol 3-kinase-like serine/threonine protein kinases (PIKKs) are required for DNA damage-induced phosphorylation of the 32 kDa subunit of replication protein A at threonine 21. *Nucl. Acids Res*. **32**, 997-1005.

Bloom D. **(1954)** Congenital telangiectatic erythema resembling lupus erythematosus in dwarfs. *Am. J. Dis. Child.* **88**, 754-758.

Bochkarev A., Bochkareva E., Frappier L. & Edwards A. M. **(1999)** The crystal structure of the complex of replication protein A subunits RPA32 and RPA14 reveals a mechanism for single-stranded DNA binding. *EMBO J.* **18**, 4498-4504.

Bochkareva E., Korolev S., Lees-Miller S. P. & Bochkarev A. **(2002)** Structure of the RPA trimerization core and its role in the multistep DNA binding mechanism of RPA. *EMBO J.* **21**, 1855-1863.

Boder E. & Sedgwick R. P. **(1957)** Ataxia-telangiectasia. A familial syndrome of progressive cerebellar ataxia, oculocutaneous telangiectasia and frequent pulmonary infection. A preliminary report on 7 children, an autopsy, and a case history. *Univ. S. Calif. Med. Bull.* **9**, 15–28.

Borglum A. D., Balslev T., Haagerup A., Birkebaek N., Binderup H., Kruse T. A. & Hertz J. M. **(2001)** A new locus for Seckel syndrome on chromosome 18p11.31-q11.2. *Eur. J. Hum. Genet.* **9**, 753–757.

Bork P., Hofmann K., Bucher P., Neuwald A. F., Altschul S. F. & Koonin E. V. **(1997)** A superfamily of conserved domains in DNA damage-responsive cell cycle checkpoint proteins. *FASEB J.* **11**, 68-76.

Bosotti R., Isacchi A. & Sonnhammer E. L. L. **(2000)** FAT: a novel domain in PIK-related kinases. *Trends Biochem. Sci.* **25**, 225-227.

Bradley M. O. & Kohn K. W. **(1979)** X-ray induced DNA double strand break production and repair in mammalian cells as measured by neutral filter elution. *Nucleic Acids Res.* **7**, 793–804.

Breen A. P. & Murphy J. A. **(1995)** Reactions of oxyl radicals with DNA *Free Radic. Biol. Med.* **18,** 1033–1077

Brosh, Jr. R. M., Li J. L., Kenny M. K., Karow J. K., Cooper M. P., Kureekattil R. P., Hickson I. D. & Bohr V. A. **(2000)** Replication protein A physically interacts with the Bloom's syndrome protein and stimulates its helicase activity. *J. Biol. Chem.* **275**, 23500-23508.

Brown E. J. & Baltimore D. **(2000)** ATR disruption leads to chromosomal fragmentation and early embryonic lethality. *Genes. Dev.* **14**, 397–402.

Brumbaugh K. M., Otterness D. M., Geisen C., Oliveira V., Brognard J., Li X., Lejeune F., Tibbetts R. S., Maquat L. E. & Abraham R. T. **(2004)** The mRNA surveillance protein, hSMG-1, functions in genotoxic stress response pathways in mammalian cells, *Mol. Cell.* **14**, 585-598.

Burma S., Chen B. P. & Chen D. J. **(2006)** Role of non-homologous end joining (NHEJ) in maintaining genomic integrity. *DNA Repair* **5**, 1042–1048.

Byun T. S., Pacek M., Yee M. C., Walter J. C. 7 Cimprich K. A. **(2005)** Functional uncoupling of MCM helicase and DNA polymerase activities activates the ATR-dependent checkpoint. *Genes Dev.* **19**, 1040–1052.

Cadet J., Douki T., Ravanat J.-L. & Di Mascio P. **(2009)** Sensitized formation of oxidatively generated damage to cellular DNA by UVA radiation. *Photochem. Photobiol. Sci.* **8**, 903–911.

Caldecott K. W. **(2006)** Mammalian single-strand break repair: Mechanisms and links with chromatin. *DNA Repair* **6**, 443–453.

Callebaut I. & Mornon J. P. **(1997)** From BRCA1 to RAP1: a widespread BRCT module closely associated with DNA repair. *FEBS Lett.* **400**, 25-30.

Canman C. E., Lim D.-S., Cimprich K. A., Taya Y., Tamai K., Sakaguchi K., Apella E., Kastan M. B. & Siliciano J. D. **(1998)** Activation of the ATM Kinase by Ionizing Radiation and Phosphorylation of p53. *Science* **281**, 1677–1679.

Cantor S. B., Bell D. W., Ganesan S., Kass E. M., Drapkin R., Grossman S., Wahrer D. C., Sgroi D. C., Lane W. S., Haber D. A. & Livingston D. M. **(2001)** BACH1, a novel helicase-like protein, interacts directly with BRCA1 and contributes to its DNA repair function. *Cell* **105**, 149-160.

Carney P. J., Maser R. S., Olivares H., Davis E. M., Le Beau M., Yates J. R. 3rd, Hays L., Morgan W. F. & Pertini J. H. J. **(1998)** The hMre11/hRad50 protein complex and Nijmegen breakage syndrome: linkage of double-strand break repair to the cellular DNA damage response. *Cell* **93**, 477-486.

Celeste A., Fernandez-Capetillo O., Kruhlak M. J., Pilch D. R., Staudt D. W., Lee A., Bonner R. F., Bonner W. M., Nussenzweig A. **(2003)** Histone H2AX phosphorylation is dispensable for the initial recognition of DNA breaks, *Nat. Cell Biol.* **5**, 675-679.

Celeste A., Petersen S., Romanienko P. J., Fernandez-Capetillo O., Chen H. T., Sedelnikova O. A., Reina-San-Martin B., Coppola V., Meffre E., Difilippantonio M. J., Redon C., Pilch D. R., Olaru A., Eckhaus M., Camerini-Otero R. D., Tessarollo L., Livak F., Manova K., Bonner W. M., Nussenzweig M. C. & Nussenzweig A. **(2002)** Genomic instability in mice lacking histone H2AX. *Science* **296**, 922-927.

Cerosaletti K., Wright J. & Concannon P. **(2006)** Active role for nibrin in the kinetics of atm activation. *Mol. Cell Biol.* **26**, 1691-1699.

Chaudhuri J., Basu U., Zarrin A., Yan C., Franco S., Perlot T., Wang J., Phan R. T., Datta A., Manis J. & Alt F. W. **(2007)** Evolution of the immunoglobulin heavy chain class switch recombination mechanism. *Adv. Immunol.* **94**, 157-214.

Chen C. & Kolodner R. D. **(1999)** Gross chromosomal rearrangement in *Saccharomyces cerevisiae* replication and recombination defective mutants. *Nat. Genet*. **23**, 81–85.

Chen J. **(2000)** Ataxia telangiectasia related protein is involved in the phosphorylation of BRCA1 following deoxyribonucleic acid damage. *Cancer Res*. **60**, 5037-5039.

Chen J., Silver D. P., Walpita D., Cantor S. B., Gazdar A. F., Tomlinson G., Couch F. J., Weber B. L., Ashley T., Livingston D. M. & Scully R. **(1998)** Stable interaction between the products of the BRCA1 and BRCA2 tumor suppressor genes in mitotic and meiotic cells. *Mol. Cell.* **2**, 317-328.

Chen L., Nievera C. J., Lee A. Y. & Wu X. **(2008)** Cell cycle-dependent complex formation of BRCA1.CtIP.MRN is important for DNA double-strand break repair. *J. Biol. Chem.* **283**, 7713-7720.

Chen P. L., Liu F., Cai S., Lin X., Li A., Chen Y., Gu B., Lee E. Y. & Lee W. H. **(2005)** Inactivation of CtIP leads to early embryonic lethality mediated by G1 restraint and to tumorigenesis by haploid insufficiency. *Mol. Cell. Biol.* **25**, 3535– 3542.

Chen Y. M., Farmer A. A., Chen C. F., Jones D. C., Chen P. L. & Lee W. H. **(1996)** BRCA1 is a 220-kDa nuclear phosphoprotein that is expressed and phosphorylated in a cell cycle–dependent manner. *Cancer Res.* **56**, 3168–3172.

Chen Z. J. & Sun L. J. **(2009)** Nonproteolytic functions of ubiquitin in cell signaling. *Mol. Cell.* **33**, 275–286.

Cheng W.-H., von Kobbe C., Opresko P. L., Arthur L. M., Komatsu K., Seidman M. M., Carney J. P., Bohr V. A. **(2004)** Linkage between Werner syndrome protein and the Mre11 complex via Nbs1. *J. Biol. Chem.* **279**, 21169–21176.

Chinnadurai G. **(2006)** CtIP, a candidate tumor susceptibility gene is a team player with luminaries. *Biochim. Biophys. Acta* **1765**, 67-73.

Choudhary S. K. & Li R. **(2002)** BRCA1 modulates ionizing radiation-induced nuclear focus formation by the replication protein A p34 subunit. *J. Cell. Biochem.* **84**, 666–674.

Chrzanowska K. H., Kleijer W. J., Krajewska-Walasek M., Białecka M., Gutkowska A., Goryluk-Kozakiewicz B., Michałkiewicz J., Stachowski J., Gregorek H., Lysón-Wojciechowska G, et al. **(1995)** Eleven Polish patients with microcephaly, immunodeficiency and chromosomal instability; the Nijmegen breakage syndrome. *Am. J. Med. Genet.* **57**, 462-471.

Chun H. H. & Gatti R. A. **(2004)** Ataxia-telangiectasia, an evolving phenotype. *DNA Repair* **3**, 1187–1196.

Cimprich K. A. & Cortez D. **(2008)** ATR: An Essential Regulator of Genome Integrity. *Nat. Rev. Mol. Cell. Biol*. **9**, 616–627.

Clarke R., Liu M. C., Bouker K. B., Gu Z., Lee R. Y., Zhu Y., Skaar T. C., Gomez B., O'Brien K., Wang Y. & Hilakivi-Clarke L. A. **(2003)** Antiestrogen resistance in breast cancer and the role of estrogen receptor signaling. *Oncogene* **22,** 7316–7339.

Clements P. M., Breslin C., Deeks E. D., Byrd P. J., Ju L., Bieganowski P., Brenner C., Moreira M. C., Taylor A. M., Caldecott K. W. **(2004)** The ataxia-oculomotor apraxia 1 gene product has a role distinct from ATM and interacts with the DNA strand break repair proteins XRCC1 and XRCC4. *DNA Repair* **3**, 1493–1502.

Connelly J. C., de Leau E. S. & Leach D. R. **(2003)** Nucleolytic processing of a protein-bound DNA end by the E. coli SbcCD (MR) complex. *DNA Repair* **2**, 795–807.

Cooper E. M., Cutcliffe C., Kristiansen T. Z., Pandey A., Pickart C. M. & Cohen R. E. **(2009)** K63-specific deubiquitination by two JAMM/MPN+ complexes: BRISC-associated Brcc36 and proteasomal Poh1. *EMBO J.* **28**, 621–631.

Costanzo V., Robertson K., Ying C. Y., Kim E., Avvedimento E., Gottesman M., Grieco D. & Gautier J. **(2000)** Reconstitution of an ATM-dependent checkpoint that inhibits chromosomal DNA replication following DNA damage. *Mol Cell.* **6**, 649-659.

Cortez D., Guntuku S., Qin J. & Elledge S. J. **(2001)** ATR and ATRIP: partners in checkpoint signaling. *Science* **294**, 1713-1716.

Cortez D., Wang Y., Qin J. & Elledge S. J. **(1999)** Requirement of ATM-dependent phosphorylation of Brca1 in the DNA damage response to double-strand breaks. *Science* **286**, 1162–1166.

Costa R. M. A., Chigançcas V., da Silva Galhardo R., Carvalho H. & Menck C. F. M. **(2003)** The eukaryotic nucleotide excision repair pathway. *Biochimie* **85**, 1083–1099

Cox M. M., Goodman M. F., Kreuzer K. N., Sherratt D. J., Sandler S. J. & Marians K. J. **(2000)** The importance of repairing stalled replication forks. *Nature* **404**, 37–41.

Cuadrado M., Martinez-Pastor B., Murga M., Toledo L. I., Gutierrez-Martinez P., Lopez E. & Fernandez-Capetillo O. **(2006)** ATM regulates ATR chromatin loading in response to DNA double-strand breaks. *J. Exp. Med.* **203**, 297-303.

D'Amours D., Desnoyers S., D'Silva I. & Poirier G. G. **(1999)** Poly(ADP-ribosyl)ation reactions in the regulation of nuclear functions. *Biochem. J.* **342**, 249–268.
D'Amours D. & Jackson S. P. **(2002)** The Mre11 complex: at the crossroads of DNA repair and checkpoint signaling. *Nat. Rev. Mol. Cell. Biol.* **3**, 317–327.

Davalos A. R. & Campisi J. **(2003)** Bloom syndrome cells undergo p53-dependent apoptosis and delayed assembly of BRCA1 and NBS1 repair complexes at stalled replication forks. *J. Cell Biol.* **162**, 1197-1209.

Davies S. L., North P. S., Dart A., Lakin N. D. & Hickson I. D. **(2004)** Phosphorylation of the Bloom's syndrome helicase and its role in recovery from S-phase arrest. *Mol. Cell. Biol.* **24**, 1279–1291.

De A. & Campbell C. **(2007)** A novel interaction between DNA ligase III and DNA polymerase gamma plays an essential role in mitochondrial DNA stability. *Biochem. J.* **402**, 175–186.

de Boer J. & Hoeijmakers J. H. **(2000)** Nucleotide excision repair and human syndromes. *Carcinogenesis* **21**, 453–60.

Decottignies A. **(2007)** Microhomology-mediated end joining in fission yeast is repressed by pku70 and relies on genes involved in homologous recombination. *Genetics* **176**, 1403–1415.

de Jager M., van Noort J., van Gent D. C., Dekker C., Kanaar R. & Wyman C. **(2001)** Human RAD50/Mre11 is a flexible complex that can tether DNA ends. *Mol. Cell.* **8**, 1129–1135.

de Klein A., Muijtjens M., van Os R., Verhoeven Y., Smit B., Carr A. M., Lehmann A. R. & Hoeijmakers J. H. J. **(2000)** Targeted disruption of the cell cycle checkpoint gene ATR leads to early embryonic lethality in mice. *Curr. Biol.* **10**, 479–482.

Delacroix S., Wagner J. M., Kobayashi M., Yamamoto K. & Karnitz L. M. **(2007)** The Rad9-Hus1-Rad1 (9-1-1) clamp activates checkpoint signaling via TopBP1. *Genes Dev.* **21**, 1472–1477.

Deriano L., Stracker T. H., Baker A., Petrini J. H. J. & Roth D. B. **(2009)** Roles for NBS1 in alternative nonhomologous end-joining of V(D)J recombination intermediates. *Mol. Cell* **34**, 13–25.

Desai-Mehta A., Cerosaletti K. M. & Concannon P. **(2001)** Distinct functional domains of nibrin mediate Mre11 binding, focus formation, and nuclear localization. *Mol. Cell. Biol.* **21**, 2184-2191.

DiBiase S. J., Zeng Z. C., Chen R., Hyslop T., Curran W. J. Jr. & Iliakis G. **(2000)** DNA-dependent protein kinase stimulates an independently active, nonhomologous, end-joining apparatus. *Cancer Res.* **60**, 1245-1253.

Dick F. A., Sailhamer E. & Dyson N. J. **(2000)** Mutagenesis of the pRB pocket reveals that cell cycle arrest functions are separable from binding to viral oncoproteins. *Mol. Cell. Biol.* **20**, 3715–3727.

Di Fiore P. P., Polo S. & Hofmann K. **(2003)** When ubiquitin meets ubiquitin receptors: a signalling connection. *Nature reviews* **4**, 491–497.

Digweed M. & Sperling K. **(2004)** Nijmegen breakage syndrome: clinical manifestation of defective response to DNA double-strand breaks. *DNA Repair* **3**, 1207–1217.

DiTullio R. A. Jr., Mochan T. A., Venere M., Bartkova J., Sehested M., Bartek J. & Halazonetis T. D. **(2002)** 53BP1 functions in an ATM-dependent checkpoint pathway that is constitutively activated in human cancer. *Nat. Cell Biol.* **4**, 998–1002.

Doil C., Mailand N., Bekker-Jensen S., Menard P., Larsen D. H., Pepperkok R., Ellenberg J., Panier S., Durocher D., Bartek J., Lukas J. & Lukas C. **(2009).** RNF168 binds and amplifies ubiquitin conjugates on damaged chromosomes to allow accumulation of repair proteins. *Cell* **136**, 435–446.

Dolganov G. M., Maser R. S., Novikov A., Tosto L., Chong S., Bressan D. A. & Petrini J. H. J. **(1996)** Human Rad50 is physically associated with human Mre11: identification of a conserved multiprotein complex implicated in recombinational DNA repair. *Mol. Cell. Biol.* **16**, 4832-4841.

Donzelli M. & Draetta G. F. **(2003)** Regulating mammalian checkpoints through Cdc25 inactivation. *EMBO Rep.* **4**, 671–677.

Dubin M. J., Stokes P. H., Sum E. Y., Williams R. S., Valova V. A., Robinson P. J., Lindeman G. J., Glover J. N., Visvader J. E. & Matthews J. M. **(2004)** Dimerization of CtIP, a BRCA1- and CtBP-interacting protein, is mediated by an N-terminal coiled-coil motif. *J. Biol. Chem.* **279**, 26932–26938.

Dutertre S., Ababou M., Onclercq R., Delic J., Chatton B., Jaulin C. & Amor-Guéret M. **(2000)** Cell cycle regulation of the endogenous wild type Bloom's syndrome DNA helicase. *Oncogene* **19**, 2731-2738.

Dutta A. & Stillman B. **(1992)** cdc2 family kinases phosphorylate a human cell DNA replication factor, RPA, activate DNA replication. *EMBO J.* **11**, 2189–2199.

Dumon-Jones V., Frappart P.-O., Tong W.-M., Sajithlal G., Hulla W., Schmid G., Herceg Z., Digweed M. & Wang Z.-Q. **(2003)** *Nbn* Heterozygosity Renders Mice Susceptible to Tumor Formation and Ionizing Radiation-Induced Tumorigenesis. *Cancer Res.* **63**, 7263–7269.

Durkacz B. W., Omidiji O., Gray D. A. & Shall S. **(1980)** (ADP-ribose)n participates in DNA excision repair. *Nature* **283**, 593–596.

Durocher D. & Jackson S. P. **(2002)** The FHA domain. *FEBS letters* **513**, 58-66.

Durocher D., Smerdon S. J., Yaffe M. B. & Jackson S. P. **(2000)** The FHA Domain in DNA Repair and Checkpoint Signaling. *Cold Spring Harb. Symp. Quant. Biol.* **65**, 423-431.

Early Breast Cancer Trialists' Collaborative Group (EBCTCG) **(2005)** Effects of chemotherapy and hormonal therapy for early breast cancer on recurrence and 15-year survival: an overview of the randomised trials. *Lancet* **365,** 1687–1717

Eliezer Y., Argaman L., Rhie A., Doherty A. J. & Goldberg M. **(2009)** The direct interaction between 53BP1 and MDC1 is required for the recruitment of 53BP1 to sites of damage. *J. Biol. Chem*. **284**, 426-435.

Ellis N. A., Groden J., Ye T. Z., Straughen J., Lennon D. J., Ciocci S., Proytcheva M. & German J. **(1995)** The Bloom's syndrome gene product is homologous to RecQ helicases. *Cell* **83**, 655-666.

Faivre L., Le Merrer M., Lyonnet S., Plauchu H., Dagoneau N., Campos-Xavier A. B., Attia-Sobol J., Verloes A., Munnich A. & Cormier-Daire V. **(2002)** Clinical and genetic heterogeneity of Seckel syndrome. *Am. J. Med. Genet.* **112**, 379–383.

Falck J., Mailand N., Syljuåsen R. G., Bartek J. & Lukas J. **(2001)** The ATM-Chk2-Cdc25A checkpoint pathway guards against radioresistant DNA synthesis. *Nature* **410**, 842-847.

Falk J., Coates J. & Jackson S. P. **(2005)** Conserved modes of recruitment of ATM, ATR and DNA-PKcs to sites of DNA damage. *Nature* **434**, 605-611.

Fang F. & Newport J. W. **(1993)** Distinct roles of cdk2 and cdc2 in RP-A phosphorylation during the cell cycle, *J. Cell Sci.* **106**, 983–994.

Fearon E. R. **(1999)** Cancer progression. *Curr. Biol.* **9**, 873-875.

Feijoo C., Hall-Jackson C., Wu R., Jenkins D., Leitch J., Gilbert D. M. & Smythe C. **(2001)** Activation of mammalian Chk1 during DNA replication arrest: a role for Chk1 in the intra-S phase checkpoint monitoring replication origin firing. *J. Cell Biol.* **154**, 913–923.

Feng L., Huang J. & Chen J. **(2009)** MERIT40 facilitates BRCA1 localization and DNA damage repair. *Genes Dev.* **23**, 719–728.

Fernandes N., Sun Y., Chen S., Paul P., Shaw R. J., Cantley L. C. & Price B. D. **(2005)** DNA Damage-induced Association of ATM with Its Target Proteins Requires a Protein Interaction Domain in the N Terminus of ATM. *J. Biol. Chem.* **280**, 15158–15164.

Fernandez-Capetillo O., Chen H. T., Celeste A., Ward I., Romanienko P. J., Morales J. C., Naka K., Xia Z., Camerini-Otero R.D., Motoyama N., Carpenter P. B., Bonner W. M., Chen J. & Nussenzweig A. **(2002)** DNA damage-induced G2-M checkpoint activation by histone H2AX and 53BP1. *Nat. Cell Biol.* **4**, 993–997.

Fernet M., Gribaa M., Salih M. A., Seidahmed M. Z., Hall J. & Koenig M. **(2005)** Identification and functional consequences of a novel MRE11 mutation affecting 10 Saudi Arabian patients with the ataxia telangiectasia-like disorder. *Hum Mol Genet* **14**, 307-318.

Foray N., Marot D., Gabriel A., Randrianarison V., Carr A. M., Perricaudet M., Ashworth A. & Jeggo P. **(2003)** A subset of ATM- and ATR dependent phosphorylation events requires the BRCA1 protein, *EMBO J.* **22**, 2860–2871.

Franco S., Alt F. W. & Manis J. P. **(2006)** Pathways that suppress programmed DNA breaks from progressing to chromosomal breaks and translocations. *DNA Repair* **5**, 1030-1041.

Furnari B., Rhind N. & Russell P. **(1997)** Cdc25 mitotic inducer targeted by chk1 DNA damage checkpoint kinase. *Science* **277**, 1495–1497.

Fusco C., Reymond A. & Zervos A. S. **(1998)** Molecular cloning and characterization of a novel retinoblastoma-binding protein. *Genomics* **51**, 351-358.

Gatei M., Scott S. P., Filippovitch I., Sorokina N., Lavin M. F., Weber B. & Khanna K. K. **(2000)** Role for ATM in DNA damage-induced phosphorylation of BRCA1. *Cancer Res.* **60**, 3299–3304.

Gatti R. A., Berkel I., Boder E., Braedt G., Charmley P., Concannon P., Ersoy F., Foroud T., Jaspers N. G. J., Lange K., Lathrop G. M., Leppert M., Nakamura Y., O'Connell P., Paterson M., Salser W., Sanal O., Silver J., Sparkes R. S., Susi E., Weeks D. E., Wei S., White R. & Yoder F. **(1988)** Localization of an ataxia-telangiectasia gene to chromosome 11q22–23. *Nature* **336**, 577–580.

German J. **(1993)** Bloom Syndrome, a Mendelian prototype of somatic mutational disease. *Medicine* **71**, 393-406.

German J., Roe A. M., Leppert M. & Ellis N. A. **(1994)** Bloom syndrome: an analysis of consanguineous families assigns the locus mutated to chromosome band 15q26.1. *Proc. Acad. Natl. Sci. USA* **91**, 6669–6673.

Gharibyan V. & Youssoufian H. **(1999)** Localization of the Bloom syndrome helicase to punctate nuclear structures and the nuclear matrix and regulation during the cell cycle: comparison with the Werner's syndrome helicase. *Mol. Carcinog*. **26**, 261-273.

Girard P. M., Riballo E., Begg A.C., Waugh A. & Jeggo P. A. **(2002)** Nbs1 promotes ATM dependent phosphorylation events including those required for G1/S arrest. *Oncogene* **21**, 4191–4199.

Goldberg M., Stucki M., Falck J., D'Amours D., Rahman D., Pappin D., Bartek J. & Jackson S. P. **(2003)** MDC1 is required for the intra-Sphase DNA damage checkpoint. *Nature* **421**, 952–956.

Goodarzi A. A., Jonnalagadda J. C., Douglas P., Young D., Ye R., Moorhead G. B. G., Lees-Miller S. P. & Khanna K. K. **(2004)** Autophosphorylation of ataxia-telangiectasia mutated is regulated by protein phosphatase 2A. *EMBO J.* **23**, 4451–4461.

Goodship J., Gill H., Carter J., Jackson A., Splitt M. & Wright M. **(2000)** Autozygosity mapping of a seckel syndrome locus to chromosome 3q22. 1-q24. *Am. J. Hum. Genet.* **67**, 498–503.

Gorbalenya A. E. & Koonin E. V. **(1990)** Superfamily of UvrA-related NTP-binding proteins. Implications for rational classification of recombination/repair systems. *J. Mol. Biol.* **213**, 583–591.

Grawunder U., Wilm M., Wu X., Kulesza P., Wilson T. E., Mann M. & Lieber M. R. **(1997)** Activity of DNA ligase IV stimulated by complex formation with XRCC4 protein in mammalian cells. *Nature* **388**, 492–495.

Gravel S., Chapman J. R., Magill C. & Jackson S. P. **(2008)** DNA helicases Sgs1 and BLM promote DNA double-strand break resection. *Genes Dev*. **22**, 2767-2772.

Greenberg R. A., Sobhian B., Pathania S., Cantor S. B., Nakatani Y. & Livingston D. M. **(2006)** Multifactorial contributions to an acute DNA damage response by BRCA1/BARD1-containing complexes. *Genes Dev.* **20**, 34-46.

Guirouilh-Barbat J., Huck S., Bertrand P., Pirzio L., Desmaze C., Sabatier L., Lopez B. S. **(2004)** Impact of the KU80 pathway on NHEJ-induced genome rearrangements in mammalian cells. *Mol. Cell* **14**, 611–623.

Haber J. **(2000)** Partner and pathways — repairing of double strand break. *Trends Genet.* **16**, 259–264.

Hakem R., de la Pompa J. L., Sirard C., Mo R., Woo M., Hakem A., Wakeham A., Potter J., Reitmair A., Billia F., Firpo E., Hui C. C., Roberts J., Rossant J. & Mak T. W. **(1996)** The tumor suppressor gene Brca1 is required for embryonic cellular proliferation in the mouse. *Cell* **85**, 1009-1023.

Hall J.M., Lee M. K., Newman B., Morrow J. E., Anderson L. A., Huey B. & King M. C. **(1990)** Linkage of Early-Onset Familial Breast Cancer to Chromosome 17q21. *Science* **250**, 1684-1689.

Hanahan D. & Weinberg R. A. **(2000)** The hallmarks of cancer. *Cell* **100**, 57–70.

Harper J. W., Adami G. R., Wei N., Keyomarsi K. & Elledge S. J. **(1993)** The p21 Cdk-interacting protein Cip1 is a potent inhibitor of G1 cyclin-dependent kinases. *Cell.* **75**, 805-816.

Hartsuiker E., Neale M. J. & Carr AM. **(2009)** Distinct requirements for the Rad32(Mre11) nuclease and Ctp1(CtIP) in the removal of covalently bound topoisomerase I and II from DNA. *Mol. Cell* **33**, 117-123.

Heffernan T. P., Simpson D. A., Frank A. R., Heinloth A. N., Paules R. S., Cordeiro-Stone M., Kaufmann W. K. **(2002)** An ATR- and Chk1-dependent S checkpoint inhibits replicon initiation following UVC-induced DNA damage. *Mol. Cell Biol.* **22**, 8552–8561.

Heppner G. H. **(1984)** Tumor Heterogeneity. *Cancer Res.* **44**, 2259-2265.

Hershko A., Ciechanover A. & Varshavsky A. **(2000)** The ubiquitin system. *Nat. Med.* **6**, 1073–1081.

Hickson I. D. **(2003)** RecQ helicases: caretakers of the genome. *Nat. Rev. Cancer.* **3**, 169–178.

Hickson I. D., Davies S. L., Li J.-L., Levitt N. C., Mohaghegh P., North P. S. & Wu L. **(2001)** Role of the Bloom's syndrome helicase in maintenance of genome stability. *Biochem. Soc. Trans.* **29**, 201-204.

Hofmann K. & Bucher P. **(1995)** The FHA domain: a putative nuclear signalling domain found in protein kinases and transcription factors. *Trends Biochem. Sci.* **20,** 347–349.

Holt J. T., Thompson M. E., Szabo C., Robinson-Benion C., Artteaga C. L., King M. C. & Jensen R. A. **(1996)** Growth retardation and tumor inhibition by BRCA1. *Nat. Genet.* **12**, 298–302.

Hopfner K. P., Karcher A., Shin D., Fairley C., Tainer J. A. & Carney J. P. **(2000a)** Mre11 and RAD50 from *Pyrococcus furiosus*: cloning and biochemical characterization reveal an evolutionarily conserved multiprotein machine. *J. Bacteriol.* **182**, 6036–6041.

Hopfner K. P., Karcher A., Shin D. S., Craig L., Arthur L. M., Carney J. P & Tainer J. A. **(2000b)** Structural biology of RAD50 ATPase: ATP-driven conformational control in DNA double-strand break repair and the ABCATPase superfamily. *Cell* **101**, 789–800.

Hopfner K. P., Karcher A., Craig L., Woo T. T., Carney J. P. & Tainer J. A. **(2001)** Structural biochemistry and interaction architecture of the DNA double-strand break repair Mre11 nuclease and RAD50-ATPase. *Cell* **105**, 473–485.

Hopfner K.-P., Craig L., Moncalian G., Zinkel R. A., Usui T., Owenk B. A. L., Karcher A., Henderson B., Bodmer J.-L., McMurrayk C. T., CarneyJ. P., Petrini J. H J. & Tainer J. A. **(2002)** The Rad50 zinc-hook is a structure joining Mre11 complexes in DNA recombination and repair. *Nature* **418**, 562-566.

Hopfner K. P. & Tainer J. A. **(2003)** Rad50/SMC proteins and ABC transporters: unifying concepts from high-resolution structures. *Curr. Opin. Struct. Biol.* **13**, 249-255.

Horejsi Z., Falck J., Bakkenist C. J., Kastan M. B., Lukas J. & Bartek J. **(2004)** Distinct functional domains of Nbs1 modulate the timing and magnitude of ATM activation after low doses of ionizing radiation. *Oncogene* **23**, 3122–3127.

Huen M. S., Grant R., Manke I., Minn K., Yu X., Yaffe M. B. & Chen J. **(2007)** RNF8 transduces the DNA-damage signal via histone ubiquitylation and checkpoint protein assembly. *Cell.* **131**, 901–914.

Hurley P. J. & Bunz F. **(2007)** ATM and ATR: Components of an Integrated Circuit. *Cell Cycle* **6**, 414-417.

Hurley P. J., Wilsker D. & Bunz F. **(2007)** Human cancer cells require ATR for cell cycle progression following exposure to ionizing radiation. *Oncogene* **26**, 2535-2542.

Huyen Y., Zgheib O., Ditullio R. A. Jr., Gorgoulis V. G., Zacharatos P., Petty T. J., Sheston E. A., Mellert H. S., Stavridi E. S. & Halazonetis T. D. **(2004)** Methylated lysine 79 of histone H3 targets 53BP1 to DNA double-strand breaks. *Nature* **432**, 406–411.

Huyton T., Bates P. A., Zhang X., Sternberg M. J. E. & Freemont P. S. **(2000)** The BRCA1 C-terminal domain: structure and function. *Mut. Res.* **460**, 319–332.

Iftode C. & Borowiec J. A. **(2000)** 5'=>3' molecular polarity of human replication protein A (hRPA) binding to pseudo-origin DNA substrates. *Biochemistry* **39**, 11970-11981.

Iijima K., Komatsu K., Matsuura S. & Tauchi H. **(2004)** The Nijmegen breakage syndrome gene and its role in genome stability. *Chromosoma* **113**, 53-61.

Ito A., Tauchi H., Kobayashi J., Morishima K., Nakamura A., Hirokawa Y., Matsuura S., Ito K. & Komatsu K. **(1999)** Expression of full-length NBS1 protein restores normal radiation responses in cells from Nijmegen breakage syndrome patients. *Biochem. Biophys. Res. Commun.* **265**, 716–721.

Iwabuchi K., Bartel P. L., Li B., Marraccino R. & Fields S. **(1994)** Two cellular proteins that bind to wild-type but not mutant p53. *Proc. Natl. Acad. Sci. U. S. A.* **91**, 6098-6102.

Iwabuchi K., Basu B. P., Kysela B., Kurihara T., Shibata M., Guan D., Cao Y., Hamada T., Imamura K., Jeggo P. A., Date T. & Doherty A. J. **(2003)** Potential role for 53BP1 in DNA end-joining repair through direct interaction with DNA. *J. Biol. Chem.* **278**, 36487-36495.

Iwabuchi K., Hashimoto M., Matsui T., Kurihara T., Shimizu H., Adachi N., Ishiai M., Yamamoto K., Tauchi H., Takata M., Koyama H. & Date T. **(2006)** 53BP1 contributes to survival of cells irradiated with X-ray during G1 without Ku70 or Artemis. *Genes Cells* **11**, 935-948.

Iwabuchi K., Li B., Massa H. F., Trask B. J., Date T., Fields S. **(1998)** Stimulation of p53-mediated transcriptional activation by the p53-binding proteins, 53BP1 and 53BP2. *J. Biol. Chem.* **273**, 26061-26068.

Jacobs D. M., Lipton A. S., Isern N. G., Daughdrill G. W., Lowry D. F., Gomes X. & Wold M. S. **(1999)** Human replication protein A: global fold of the N-terminal RPA-70 domain reveals a basic cleft and flexible C-terminal linker. *J. Biomol. NMR* **14**, 321-331.

Jazayeri A., Falck J., Lukas C., Bartek J., Smith G. C., Lukas J. & Jackson S. P. **(2006)** ATM- and cell cycle-dependent regulation of ATR in response to DNA double-strand breaks. *Nat. Cell Biol.* **8**, 37-45.

Jensen D. R. & Rauscher F. J. 3rd **(1999)** BAP1, a candidate tumor suppressor protein that interacts with BRCA1. *Ann. N. Y. Acad. Sci.* **886**, 1–4.

Jilani A., Ramotar D., Slack C., Ong C., Yang X. M., Scherer S. W. & Lasko D. D. **(1999)** Molecular cloning of the human gene, *PNKP*, encoding a polynucleotide kinase 3′- phosphatase and evidence for its role in repair of DNA strand breaks caused by oxidative damage. *J. Biol. Chem.* **274**, 24176–24186.

Jowsey P., Morrice N. A., Hastie C. J., McLauchlan H., Toth R. & Rouse J. **(2007)** Characterisation of the sites of DNA damage-induced 53BP1 phosphorylation catalysed by ATM and ATR. *DNA Rep.* **6**, 1536-1544.

Jullien D., Vagnarelli P., Earnshaw W. C. & Adachi Y. **(2002)** Kinetochore localisation of the DNA damage response component 53BP1 during mitosis. *J. Cell Sci.* **115**, 71-79.

Karow, J. K., Constantinou, A., Li, J.-L., West, S. C. & Hickson I. D. **(2000a)** The Bloom's syndrome gene product promotes branch migration of Holliday junctions *Proc. Natl. Acad. Sci. U.S.A.* **97**, 6504-6508

Karow J. K., Wu L. & Hickson I. D. **(2000b)** RecQ family helicases: roles in cancer and aging. *Curr. Opin. Genet. Dev.* **10**, 32-38.

Kastan M. B., Zhan Q., el-Deiry W. S., Carrier F., Jacks T., Walsh W. V., Plunkett B. S., Vogelstein B., Fornace A. J. Jr. **(1992)** A mammalian cell cycle checkpoint pathway utilising p53 and GADD45 is defective in ataxia-telangiectasia. *Cell* **71**, 587–597

Keeney S. & Neale M. J. **(2006)** Initiation of meiotic recombination by formation of DNA double-strand breaks: mechanism and regulation. *Biochem. Soc. Trans.* **34**, 523-525.

Khan A. O., Oystreck D. T., Koenig M. & Salih M. A. **(2008)** Ophthalmic features of ataxia telangiectasia-like disorder. *J. A. A. P. O. S.* **12**, 186-189.

Khanna K. K., Keating K. E., Kozlov S., Scott S., Gatei M., Hobson K., Taya Y., Gabrielli B., Chan D., Lees-Miller S. P. & Lavin M. F. **(1998)** ATM associates with and phosphorylates p53: mapping the region of interaction. *Nat. Genet.* **20**, 398–400.

Kilinç M. O., Ninis V. N, Ugur S. A., Tüysüz B., Seven M., Balci S., Goodship J. & Tolun A. **(2003)** Is the novel SCKL3 at 14q23 the predominant Seckel locus? *Eur. J. Hum. Genet.* **11**, 851-857.

Kim H., Huang J. & Chen J. **(2007a)** CCDC98 is a BRCA1-BRCT domain-binding protein involved in the DNA damage response. *Nat. Struct. Mol. Biol.* **14**, 710-715.

Kim H. T., Kim K. P., Lledias F., Kisselev A. F., Scaglione K. M., Skowyra D., Gygi S. P. & Goldberg A. L. **(2007b)** Certain pairs of ubiquitin-conjugating enzymes (E2s) and ubiquitin-protein ligases (E3s) synthesize nondegradable forked ubiquitin chains containing all possible isopeptide linkages. *J. Biol. Chem.* **282**, 17375–17386.

Kim J.-S., Krasieva T. B., Kurumizaka H., Chen D. J., Taylor A. M. R. & Yokomori K. **(2005)** Independent and sequential recruitment of NHEJ and HR factors to DNA damage sites in mammalian cells. *J. Cell Biol.* **170**, 341-347.

Kim S. T., Lim D. S., Canman C. E. & Kastan M. B. **(1999)** Substrate specificities and identification of putative substrates of ATM kinase family members. *J. Biol. Chem*. **274**, 37538-37543.

Kim S.-T., Xu B. & Kastan M. B. **(2002)** Involvement of the Cohesin Protein, Smc1, in Atm-Dependent and Independent Responses to DNA Damage. *Genes Dev.* **16**, 560-570.

Kinner A., Wu W., Staudt C. & Iliakis G. **(2008)** γ-H2AX in recognition and signaling of DNA double-strand breaks in the context of chromatin. *Nucl. Acids Res.* **36**, 5678–5694.

Kinzler K. W. & Vogelstein B. **(1997)** Cancer-susceptibility genes. Gatekeepers and caretakers. *Nature* **386**, 761–763.

Kishi S., Zhou X. Z., Ziv Y., Khoo C., Hill D. E., Shiloh Y. & Lu K. P. **(2001)** Telomeric protein Pin2/TRF1 as an important ATM target in response to double strand DNA breaks. *J. Biol. Chem.* **276**, 29282-29291.

Kitao S., Ohsugi I., Ichikawa K., Goto M., Furuichi Y. & Shimamoto A. **(1998)** Cloning of two new human helicase genes of the RecQ family: biological significance of multiple species in higher eukaryotes. *Genomics* **54**, 443-452.

Kitao S., Shimamoto A., Goto M., Miller R. W., Smithson W. A., Lindor N. M. & Furuichi Y. **(1999)** Mutations in RECQL4 cause a subset of cases of Rothmund-Thomson syndrome. *Nat. Genet*. **22**, 82-84.

Kobayashi J., Tauchi H., Sakamoto S., Nakamura A., Morishima K., Matsuura S., Kobayashi T., Tamai K., Tanimoto K. & Komatsu K. **(2002)** NBS1 localizes to gamma-H2AX foci through interaction with the FHA/BRCT domain. *Curr. Biol.* **12** 1846–1851.

Kolas N. K., Chapman J. R., Nakada S., Ylanko J., Chahwan R., Sweeney F. D., Panier S., Mendez M., Wildenhain J., Thomson T. M, Pelletier L., Jackson S. P. & Durocher D. **(2007)** Orchestration of the DNA-damage response by the RNF8 ubiquitin ligase. *Science.* **318**, 1637–1640.

Koonin V. F., Altschul S. F. & Bork P. **(1996)** BRCA1 proten products: functional motifs. *Nat. Genet.* **13**, 266-267.

Kotnis A., Du L., Liu C., Popov S. W. & Pan-Hammarström Q. **(2009)** Non-homologous end joining in class switch recombination: the beginning of the end. *Phil. Trans. R. Soc. B* **364**, 653–665.

Kowalczykowski S. C. **(2002)** Molecular mimicry connects BRCA2 to Rad51 and recombinational DNA repair. *Nat. Struct. Biol.* **9**, 897-899.

Kozlov S. V., Graham M. E., Peng C., Chen P., Phillip J Robinson P. J. & Lavin M. F. **(2006)** Involvement of novel autophosphorylation sites in ATM activation. *EMBO J.* **25**, 3504–3514

Krupa A., Preethi G. & Srinivasan N. **(2004)** Structural modes of stabilization of permissive phosphorylation sites in protein kinases: distinct strategies in Ser/Thr and Tyr kinases. *J. Mol. Biol.* **339**, 1025-1039.

Kubota Y., Nash R. A., Klungland A., Schär P., Barnes D. E. & Lindahl T. **(1996)** Reconstitution of DNA base excisionrepair with purified human proteins: interaction between DNA polymerase beta and the XRCC1 protein. *EMBO J.* **15**, 6662–6670.

Kumagai A. & Dunphy W. G. **(2000)** Claspin, a novel protein required for the activation of Chk1 during a DNA replication checkpoint response in Xenopus egg extracts. Mol. Cell **6**, 839–849.

Kumagai A. & Dunphy W. G. **(2006)** How cells activate ATR. *Cell Cycle* **5**, 1265-1268.

Kumagai A., Lee J, Yoo H. Y. & Dunphy W. G. **(2006)** TopBP1 activates the ATR-ATRIP complex. *Cell* **124**, 943-955.

Kurz E.U. & Lees-Miller S. P. **(2004)** DNA damage-induced activation of ATM and ATM-dependent signaling pathways. *DNA Repair* **3**, 889-900.
Lane T. F. **(2004)** BRCA1 and Transcription. *Cancer Biol. Ther.* **3**, 528-533.

Lavin M. F. **(2008)** Ataxia-telangiectasia: from a rare disorder to a paradigm for cell signaling and cancer. *Mol. Cell Biol.* **9**, 759-769.

Lee J., Kumagai A. & Dunphy W. G. **(2007)** The Rad9-Hus1-Rad1 checkpoint clamp regulates interaction of TopBP1 with ATR. *J. Biol. Chem.* **282**, 28036–28044.

Lee J.-H., Ghirlando R., Bhaskara V., Hoffmeyer M. R., Gu J. & Paull T. T. **(2003)** Regulation of Mre11/Rad50 by Nbs1: effects on nucleotide-dependent DNA binding and association with ATLD mutant complexes. *J. Biol. Chem.* **278**, 45171–45181.

Lee J.-H. & Paull T. T. **(2005)** ATM Activation by DNA Double-Strand Breaks Through the Mre11-Rad50-Nbs1 Complex. *Science* **308**, 551-554

Lee J. S., Collins K. M., Brown A. L., Lee C. H. & Chung J. H. **(2000)** hCds1-mediated phosphorylation of BRCA1 regulates the DNA damage response. *Nature* **404**, 201–204.

Lee J. W., Blanco L., Zhou T., Garcia-Diaz M., Bebenek K., Kunkel T. A., Wang Z. & Povirk L. F. **(2004)** Implication of DNA polymerase lambda in alignment-based gap filling for nonhomologous DNA end joining in human nuclear extracts. *J. Biol. Chem.* **279**, 805–811.

Li C., Heidt D. G., Dalerba P., Burant C. F., Zhang L., Adsay V., Wicha M., Clarke M. F. & Simeone D M. **(2007)** Identification of pancreatic cancer stem cells. *Cancer Res.* **67**, 1030-1037.

Li S., Chen P. L., Subramanian T., Chinnadurai G., Tomlinson G., Osborne C. K., Sharp Z. D. & Lee W. H. **(1999)** Binding of CtIP to the BRCT repeats of BRCA1 involved in the transcription regulation of p21 is disrupted upon DNA damage. *J. Biol. Chem.* **274**, 11334-11338.

Li S., Ting N. S. Y., Zheng L., Chen P.-L., Ziv Y., Shiloh Y., Lee E. Y. – H. P. & Lee. W.-H. **(2000)** Functional link of BRCA1 and ataxia telangiectasia gene product in DNA damage response. *Nature* **406**, 210-215.

Liang F., Romanienko P. J. & Jasin M. **(1998)** Homology-directed repair is a major double-strand break repair pathway in mammalian cells. *Proc. Natl. Acad. Sci. U. S. A.* **95**, 5172–5177.

Liang L., Deng L., Chen Y., Li G. C., Shao C. & Tischfield J. A. **(2005)** Modulation of DNA end joining by nuclear proteins. *J. Biol. Chem.* **280**, 31442–31449.

Liang L., Deng L., Nguyen S. C., Zhao X., Maulion C. D., Shao C., Tischfield J. A. **(2008)** Human DNA ligases I and III, but not ligase IV, are required for microhomology-mediated end joining of DNA doublestrand breaks. *Nucleic Acids Res.* **36**, 3297–3310

Lim D.-S., Kim S. T., Xu B., Maser R. S., Lin J., Petrini J. H. & Kastan M. B. **(2000)** ATM phosphorylates p95/nbs1 in an S-phase checkpoint pathway. *Nature* **404**, 613-617.

Lim D.-E., Kirsch D. G., Canman C. E., Ahn J.-H., Ziv Y., Newman L. S., Darnell R. B., Shiloh Y. & Kastan M. B. **(1998)** ATM binds to β-adaptin in cytoplasmic vesicles. *PNAS* **95**, 10146–10151.

Lindahl T **(1993)** Instability and decay of the primary structure of DNA. *Nature* **362**, 709–715.

Liu J.-S., Kuo S.-R. & Melendy T. **(2006)** Phosphorylation of replication protein A by S-phase checkpoint kinases. *DNA Repair* **5**, 369-380.

Liu Q., Guntuku S., Cui X. S., Matsuoka S., Cortez D., Tamai K., Luo G., Carattini-Rivera S., DeMayo F., Bradley A., Donehower L. A & Elledge S. J. **(2000)** Chk1 is an essential kinase that is regulated by Atr and required for the G(2)/M DNA damage checkpoint. *Genes Dev.* **14**, 1448–1459.

Loizou J. I., El-Khamisy S. F., Zlatanou A., Moore D. J., Chan D. W., Qin J., Sarno S., Meggio F., Pinna L. A., Caldecott K. W. **(2004)** The protein kinase CK2 facilitates repair of chromosomal DNA single-strand breaks. *Cell* **117**, 17–28.

Lombard D. B. & Guarente L. **(2000)** Nijmegen breakage syndrome disease protein and MRE11 at PML nuclear bodies and meiotic telomeres. *Cancer Res.* **60**, 2331–2334.

Lou Z., Chen B. P.-C., Asaithamby A., Minter-Dykhouse K., Chen D. J. & Chen J. **(2004)** MDC1 Regulates DNA-PK Autophosphorylation in Response to DNA Damage. *J. Biol. Chem.* **279**, 46359–46362.

Lou Z., Chini C. C. S., Minter-Dykhouse K. & Chen J. **(2003a)** Mediator of DNA damage checkpoint protein 1 regulates BRCA1 localization and phosphorylation in DNA damage checkpoint control. *J. Biol. Chem.* **278**, 13599–13602.

Lou Z., Minter-Dykhouse K., Franco S., Gostissa M., Rivera M. A., Celeste A., Manis J. P., van Deursen J., Nussenzweig A., Paull T. T., Alt F. W. & Chen J. **(2006)** MDC1 maintains genomic stability by participating in the amplification of ATM-dependent DNA damage signals. *Mol. Cell* **21**, 187–200.

Lou Z., Minter-Dykhouse K., Wu X. & Chen J. **(2003b)** MDC1 is coupled to activated CHK2 in mammalian DNA damage response pathways. *Nature* **421**, 957-961.

Lovejoy C. A. & Cortez D. **(2009)** Common mechanisms of PIKK regulation. *DNA Repair* **8**, 1004–1008.

Ludwig T., Chapman D. L., Papaioannou V. E. & Efstratiadis A. **(1997)** Targeted mutations of breast cancer susceptibility gene homologs in mice: lethal phenotypes of Brca1, Brca2, Brca1/Brca2, Brca1/p53, and Brca2/p53 nullizygous embryos. *Genes Dev.* **11**, 1226-1241.

Lukas C., Melander F., Stucki M., Falck J., Bekker-Jensen S., Goldberg M., Lerenthal Y., Jackson S. P., Bartek J. & Lukas J. **(2004)** Mdc1 couples DNA double-strand break recognition by Nbs1 with its H2AX-dependent chromatin retention. *EMBO J.* **23**, 2674–2683.

Luo G., Yao M. S., Bender C. F., Mills M., Bladl A. R., Bradley A. & Petrini J. H. **(1999)** Disruption of mRad50 causes embryonic stem cell lethality, abnormal embryonic development, and sensitivity to ionising radiation. *Proc. Natl. Acad. Sci. U.S.A.* **96**, 7376–7381.

Ma Y., Lu H., Tippin B., Goodman M. F., Shimazaki N., Koiwai O., Hsieh C. L., Schwarz K. & Lieber M. R. **(2004)** A biochemically defined system for mammalian nonhomologous DNA end joining. *Mol. Cell* **16**, 701–713.

Mailand N., Bekker-Jensen S., Faustrup H., Melander F., Bartek J., Lukas C. & Lukas J. **(2007)** RNF8 ubiquitylates histones at DNA double-strand breaks and promotes assembly of repair proteins. *Cell* **131**, 887–900.

Mailand N., Podtelejnikov A. V., Groth A., Mann M., Bartek J. & Lukas J. **(2002)** Regulation of G(2)/M events by Cdc25A through phosphorylation-dependent modulation of its stability. *EMBO J.* **21**, 5911–5920.

Majewski F. & Goecke T. **(1982)** Studies of microcephalic primordial dwarfism I: approach to a delineation of the Seckel syndrome. *Am. J. Med. Genet*. **12**, 7-21.

Majka J., Binz S. K., Wold M. S. & Burgers P. M. **(2006)** Replication protein A directs loading of the DNA damage checkpoint clamp to 5′-DNA junctions. *J. Biol Chem.* **281**, 27855–27861.

Makiniemi M., Hillukkala T., Tuusa J., Reini K., Vaara M., Huang D., Pospiech H., Majuri I., Westerling T., Makela T. P. & Syvaoja J. E. **(2001)** BRCT Domain-containing Protein TopBP1 Functions in DNA Replication and Damage Response *J. Biol. Chem.* **276,** 30399–30406

Manis J. P., Morales J. C., Xia Z., Kutok J. L., Alt F. W. & Carpenter P. B. **(2004)** 53BP1 links DNA damage-response pathways to immunoglobulin heavy chain class-switch recombination. *Nat. Immunol.* **5**, 481-487.

Manke I. A., Lowery D. M., Nguyen A. & Yaffe M. B. **(2003)** BRCT repeats as phosphopeptide-binding modules involved in protein targeting. *Science* **302**, 636–639

Manthey K. C., Opiyo S., Glanzer J. G., Dimitrova D., Elliott J. & Oakley G. G. **(2007)** NBS1 mediates ATR-dependent RPA hyperphosphorylation following replication-fork stall and collapse. *J. Cell Sci.* **120**, 4221-4229.

Marshall C. J. **(1991)** Tumor suppressor genes. *Cell* **64**, 313–326.

Martinez-Climent J. A., Andreu E. J. & Prosper F. **(2006)** Somatic stem cells and the origin of cancer. *Clin. Transl. Oncol.* **8**, 647–663.

Maser R. S., Zinkel R. & Petrini J. H. **(2001)** An alternative mode of translation permits production of a variant NBS1 protein from the common Nijmegen breakage syndrome allele. *Nat. Gen.* **27**, 417-421.

Massarweh S. & Schiff R. **(2006)** Resistance to endocrine therapy in breast cancer: exploiting estrogen receptor/growth factor signaling crosstalk. *Endocr.-Relat. Cancer.* **13**, Suppl. 1, S15–S24.

Matsumoto M., Yaginuma K., Igarashi A., Imura M., Hasegawa M., Iwabuchi K., Date T., Mori T., Ishizaki K., Yamashita K., Inobe M. & Matsunaga T. **(2007)** Perturbed gap-filling synthesis in nucleotide excision repair causes histone H2AX phosphorylation in human quiescent cells. *J. Cell Sci.* **120**, 1104-1112.

Matsuoka S., Ballif B. A., Smogorzewska A., McDonald E. R. 3rd, Hurov K. E., Luo J., Bakalarski C. E., Zhao Z., Solimini N., Lerenthal Y., Shiloh Y., Gygi S. P. & Elledge S. J. **(2007)** ATM and ATR Substrate Analysis Reveals Extensive Protein Networks Responsive to DNA Damage. *Science* **316**, 1160-1166.

Matsuoka S., Rotman G., Ogawa A., Shiloh Y., Tamai K. & Elledge S. J. **(2000)** Ataxia telangiectasia-mutated phosphorylates Chk2 in vivo and in vitro. *Proc. Natl. Acad. Sci. U. S. A.* **97**, 10389-10394.

Matsuura S., Tauchi H., Nakamura A., Kondo N., Sakamoto S., Endo S., Smeets D., Solder B., Belohradsky B. H., Der Kaloustian V. M., Oshimura M., Isomura M., Nakamura Y. & Komatsu K. **(1998)** Positional cloning of the gene for Nijmegen breakage syndrome. *Nature Genetics* **19**, 179-181.

McVey M. & Lee S. E. **(2008)** MMEJ repair of double-strand breaks (director's cut): deleted sequences and alternative endings. *Trends Genet.* **24**, 529–538.

Melo J. A., Cohen J. & Toczyski D. P. **(2001)** Two checkpoint complexes are independently recruited to sites of DNA damage in vivo. *Genes. Dev.* **15**, 2809–2821.

Melo J. & Toczyski D. **(2002)** A unified view of the DNA-damage checkpoint. *Curr. Opin. Cell Biol.* **14**, 237–245.

Mer G., Bochkarev A., Chazin W. J. & Edwards A. M. **(2000)** Three-dimensional structure and function of replication protein A. *Cold Spring Harb. Symp. Quant. Biol*. **65**, 193-200.

Messick T. E. & Greenberg R. A. **(2009)** The ubiquitin landscape at DNA double-strand breaks. *J. Cell Biol.* **187**, 319-326.

Miki Y., Swensen J., Shattuck-Eidens D., Futreal P. A., Harshman K., Tavtigian S., Liu Q., Cochran C., Bennett L. M., Ding W., Bell R., Rosenthal J., Hussey C., Tran T., McClure M., Frye C., Hattier T., Phelps R., Haugen-Strano A., Katcher H., Yakumo K., Gholami Z., Shaffer D., Stone S., Bayer S., Wray C., Bogden R., Dayananth P., Ward J., Tonin P., Narod S., Bristow P. K., Norris F. H., Helvering L., Morrison P., Rosteck P., Lai M., Barrett J. C., Lewis C., Neuhausen S., Cannon-Albright L., Goldgar D., Wiseman R., Kamb A. & Skolnick M. H. **(1994)** A strong candidate for the breast and ovarian cancer susceptibility gene BRCA1. *Science* **266**, 66-71.

Mimitou E. P. & Symington L. S. **(2008)** Sae2, Exo1 and Sgs1 collaborate in DNA double-strand break processing. *Nature* **455**, 770-775.

Mirzoeva O. K. & Petrini J. H. **(2001)** DNA damage-dependent nuclear dynamics of the Mre11 complex. *Mol. Cell. Biol.* **21**, 281–288, (Erratum in *Mol. Cell. Biol.* **21**, 1898).

Modrich P. **(2006)** Mechanisms in Eukaryotic Mismatch Repair. *J. Biol. Chem.* **281**, 30305–30309.

Moens P. B., Freire R., Tarsounas M., Spyropoulos B. & Jackson S. P. **(2000)** Expression and nuclear localization of BLM, a chromosome stability protein mutated in Bloom's syndrome, suggest a role in recombination during meiotic prophase. *J. Cell Sci.* **113**, 663-672.

Mohammad D. H. & Yaffe M. B. **(2009)** 14-3-3 proteins, FHA domains and BRCT domains in the DNA damage response. *DNA Rep.* **8**, 1009-1017.

Mordes D. A., Glick G. G., Zhao R. & Cortez D. **(2008)** TopBP1 activates ATR through ATRIP and a PIKK regulatory domain. *Genes. Dev.* **22**, 1478-89.

Moreno-Herrero F., de Jager M., Dekker N. H., Kanaar R., Wyman C. & Dekker C. **(2005)** Mesoscale conformational changes in the DNA-repair complex Rad50/Mre11/Nbs1 upon binding DNA. *Nature* **437**, 440-443.

Morishima K., Sakamoto S., Kobayashi J., Izumi H., Suda T., Matsumoto Y., Tauchi H., Ide H., Komatsu K. & Matsuura S. **(2007)** TopBP1 associates with NBS1 and is involved in homologous recombination repair. *Biochem. Biophys. Res. Commun.* **362**, 872-879.

Mortensen U. H., Bendixen C., Sunjevaric I. & Rothstein R. **(1996)** DNA strand annealing is promoted by the yeast Rad52 protein. *Proc. Natl. Acad. Sci. U. S. A.* **93**, 10729-10734.

Mortusewicz O., Rothbauer U., Cardoso M. C. & Leonhardt H. **(2006)** Differential recruitment of DNA ligase I and III to DNA repair sites. *Nucleic Acids Res.* **34**, 3523–3532.

Moynahan M. E., Chiu J. W., Koller B. H. & Jasin M. **(1999)** Brca1 controls homology-directed DNA repair. *Mol. Cell.* **4**, 511-518.

Moynahan M. E., Cui T. Y. & Jasin M. **(2001)** Homology-directed DNA repair, mitomycin-c resistance, and chromosome stability is restored with correction of a Brca1 mutation. *Cancer Res.* **61**, 4842-4850.

Murr R., Loizou J. I., Yang Y. G., Cuenin C., Li H., Wang Z. Q. & Herceg Z. **(2006)** Histone acetylation by Trrap-Tip60 modulates loading of repair proteins and repair of DNA double-strand breaks. *Nat. Cell Biol.* **8**, 91-99.

Myers J. S. & Cortez D. **(2006)** Rapid activation of ATR by ionizing radiation requires ATM and Mre11. *J. Biol. Chem.* **281**, 9346-9350.

Nagase T., Seki N., Ishikawa K., Tanaka A. & Nomura N. **(1996)** Prediction of the coding sequences of unidentified human genes. V. The coding sequences of 40 new genes (KIAA0161-KIAA0200) deduced by analysis of cDNA clones from human cell line KG- 1. *DNA Res.* **3**, 17–24.

Nakanishi K., Taniguchi T., Ranganathan V., New H. V., Moreau L. A., Stotsky M. , Mathew C. G., Kastan M. B., Weaver D. T. & D'Andrea A. D. **(2002)** Interaction of FANCD2 and NBS1 in the DNA damage response. *Nat. Cell. Biol.* **4**, 913–920.

Nedelcheva M. N., Roguev A., Dolapchiev L. B., Shevchenko A., Taskov H. B., Shevchenko A., Stewart A. F. & Stoynov S. S. **(2005)** Uncoupling of unwinding from DNA synthesis implies regulation of MCM helicase by Tof1/Mrc1/Csm3 checkpoint complex. *J. Mol. Biol.* **347**, 509–521.

Nelms B. E., Maser R. S., MacKay J. F., Lagally M. G. & Petrini J. H. **(1998)** In situ visualization of DNA double-strand break repair in human fibroblasts. *Science* **280**, 590–592.

Nishikawa H., Ooka S., Sato K., Arima K., Okamoto J., Klevit R. E., Fukuda M. & Ohta T. **(2004)** Mass spectrometric and mutational analyses reveal Lys-6-linked polyubiquitin chains catalyzed by BRCA1-BARD1 ubiquitin ligase. *J. Biol. Chem.* **279**, 3916–3924.

Nuss, J. E., Patrick, S. M., Oakley, G. G., Alter, G. M., Robison, J. G., Dixon, K. & Turchi J. J. **(2005)** DNA damage induced hyperphosphorylation of replication protein A. 1. Identification of novel sites of phosphorylation in response to DNA damage. *Biochemistry* **44**, 8428-8437.

Nyberg K. A., Michelson R. J., Putnam C. W. & Weinert T. A. **(2002)** Toward maintaining the genome: DNA damage and replication checkpoints. *Annu. Rev. Genet.* **36**, 617–656.

O'Driscoll M., Cerosaletti K. M., Girard P.-M., Dai Y., Stumm M., Kysela B., Hirsch B., Gennery A., Palmer S. E., Seidel J., Gatti R. A., Varon R., Oettinger M. A., Sperling K., Jeggo P. A. & Concannon P. **(2001)** DNA ligase IV mutations identified in patients exhibiting development delay and immunodeficiency. *Mol. Cell* **8**, 1175–1185.

O'Driscoll M., Gennery A. R., Seidel J., Concannon P. & Jeggo P. A. **(2004)** An overview of three new disorders associated with genetic instability: LIG4 syndrome, RS-SCID and ATR-Seckel syndrome. *DNA Repair* **3**, 1227–1235.

O'Driscoll M., Ruiz-Perez V. L., Woods C. G., Jeggo P. A. & Goodship J. A. **(2003)** A splicing mutation affecting expression of ataxia-telangiectasia and Rad3-related protein (ATR) results in Seckel syndrome. *Nat. Genet.* **33**, 497-501.

Olson E., Nievera C. J., Klimovich V., Fanning E. & Wu X. **(2006)** RPA2 is a direct downstream target for ATR to regulate the S-phase checkpoint. *J. Biol. Chem*. **281**, 39517-39533.

Olson E., Nievera C. J., Liu E., Lee A. Y., Chen L. & Wu X. **(2007)** The Mre11 complex mediates the S-phase checkpoint through an interaction with RPA. *Mol. Cell. Biol*. **27**, 6053-6067.

O'Neill T., Dwyer A. J., Ziv Y., Chan D. W., Lees-Miller S. P., Abraham R. H., Lai J. H., Hill D., Shiloh Y., Cantley L. C. & Rathbun G. A. **(2000)** Utilization of oriented peptide libraries to identify substrate motifs selected by ATM*. J. Biol. Chem.* **275**, 22719-22727.

Ortega S., Malumbres M. & Barbacid M. **(2002)** Cyclin D-dependent kinases, INK4 inhibitors and cancer. *Biochim. Biophys. Acta* **1602**, 73–87.

Osborn A. J., Elledge S. J. & Zou L. **(2002)** Checking on the fork: The DNA-replication stress-response pathway. Trends Cell Biol. 12, 509-516.

Ozaki T., Nagase T., Ichimiya S., Seki N., Ohiri M., Nomura N., Takada N., Sakiyama S., Weber B. L. & Nakagawara A. **(2000)** NFBD1/KIAA0170 is a novel nuclear transcriptional transactivator with BRCT domain. *DNA Cell Biol.* **19**, 475–485.

Park M. S., Ludwig D. L., Stigger E. & Lee S. H. **(1996)** Physical interaction between human Rad52 and RPA is required for homologous recombination in mammalian cells. *J. Biol. Chem.* **271**, 18996-19000.

Pathak S. **(2002)** Organ- and tissue-specific stem cells and carcinogenesis. *Anticancer Res.* **22**, 1353–1356.

Paull T. T. & Gellert M. **(1998)** The 3′ to 5′ exonuclease activity of Mre 11 facilitates repair of DNA double-strand breaks. *Mol. Cell.* **1**, 969–979.

Paull T. T. & Gellert M. **(1999)** Nbs1 potentiates ATP-driven DNA unwinding and endonuclease cleavage by the Mre11/Rad50 complex. *Genes. Dev.* **13**, 1276–1288.

Peng A. & Chen P. L. **(2003)** NFBD1, like 53BP1, is an early and redundant transducer mediating Chk2 phosphorylation in response to DNA damage. *J. Biol. Chem.* **278**, 8873–8876.

Perrault R., Wang H., Wang M., Rosidi B. & Iliakis G. **(2004)** Backup pathways of NHEJ are suppressed by DNA-PK. *J. Cell. Biochem.* **92**, 781–794.

Perry J. & Kleckner N. **(2003)** The ATRs, ATMs, and TORs Are Giant HEAT Repeat Proteins. *Cell* **112**, 151-155.

Petrini J. H. & Stracker T. H. **(2003)** The cellular response to DNA double-strand breaks: defining the sensors and mediators. *Trends Cell. Biol.* **13**, 458–462.

Pfeifer G. P., You Y.-H. & Besaratinia A. **(2005)** Mutations induced by ultraviolet light. *Mut. Res.* **571**, 19–31

Pichierri P., Rosselli F. & Franchitto A. **(2003)** Werner's syndrome protein is phosphorylated in an ATR/ATMdependent manner following replication arrest and DNA damage induced during the S phase of the cell cycle. *Oncogene* **22**, 1491–1500.

Pickart C. M. **(2001)** Mechanisms underlying ubiquitination. *Annu. Rev. Biochem.* **70**, 503–533.

Pickart C. M. & Cohen R. E. **(2004)** Proteasomes and their kin: proteases in the machine age. *Nat. Rev. Mol. Cell Biol.* **5**, 177–187.

Pitts S. A., Kullar H. S., Stankovic T., Stewart G. S., Last J. I., Bedenham T., Armstrong S. J., Piane M., Chessa L., Taylor A. M. & Byrd P. J. **(2001)** hMRE11: genomic structure and a null mutation identified in a transcript protected from nonsense-mediated mRNA decay. *Hum. Mol. Genet.* **10**, 1155-1162.

Plo I., Liao Z. Y., Barceló J. M., Kohlhagen G., Caldecott K. W., Weinfeld M., Pommier Y. **(2003)** Association of XRCC1 and tyrosyl DNA phosphodiesterase (Tdp1) for the repair of topoisomerase I-mediated DNA lesions. *DNA Repair* **2**, 1087–1100.

Pohl A., Lurje G., Kahn M. & Lenz H. J. **(2008)** Stem cells in colon cancer. *Clin. Colorectal Cancer*. **7**, 92-8.

Pommier Y. (2006) Topoisomerase I inhibitors: camptothecins and beyond. *Nat. Rev. Cancer* **6**, 789–802.

Pouliot J. J., Yao K. C., Robertson C. A. & Nash H. A. **(1999)** Yeast gene for a Tyr-DNA phosphodiesterase that repairs topoisomerase I complexes. *Science* **286**, 552–555.

Ranganathan V., Heine W. F., Ciccone D. N., Rudolph K. L., Wu X., Chang S., Hai H., Ahearn I. M., Livingston D. M., Resnick I., Rosen F., Seemanova E., Jarolim P., DePinho R. A. & Weaver D. T. **(2001)** Rescue of a telomere length defect of Nijmegen breakage syndrome cells requires NBS and telomerase catalytic subunit. *Curr. Biol.* **11**, 962–966.

Reya T., Morrison S. J., Clarke M. F. & Weissman I. L. **(2001)** Stem cells, cancer, and cancer stem cells. *Nature* **414**, 105-111.

Robison J. G., Elliott J., Dixon K. & Oakley G. G. **(2004)** Replication protein A and the Mre11.Rad50.Nbs1 complex co-localize and interact at sites of stalled replication forks. *J. Biol. Chem.* **279**, 34802-34810.

Rodriguez M., Yu X., Chen J. & Songyang Z. **(2003)** Phosphopeptide Binding Specificities of BRCA1 COOH-terminal (BRCT) Domains. *J. Biol. Chem.* **278**, 52914–52918.

Rogakou E. P., Boon C., Redon C. & Bonner W. M. **(1999)** Megabase chromatin domains involve in DNA double-strand breaks in vivo. *J Cell Biol.* **146**, 905-916.

Rogakou E.P., Pilch D.R., Orr A.H., Ivanova V.S. & Bonner W.M. **(1998)** DNA double-stranded breaks induce histone H2AX phosphorylation on serine 139. *J. Biol. Chem.* **273**, 5858–5868.

Rupnik A., Grenon M. & Lowndes N. **(2008)** The MRN complex. *Curr. Biol.* **18**, 455-457.

Sanchez Y., Wong C., Thoma R. S., Richman R., Wu Z., Piwnica-Worms H. & Elledge S. J. **(1997)** Conservation of the Chk1 checkpoint pathway in mammals: linkage of DNA damage to Cdk regulation through Cdc25. *Science* **277**, 1497–1501.

Sanders S. L., Portoso M., Mata J., Bähler J., Allshire R. C., Kouzarides T. **(2004)** Methylation of histone H4 lysine 20 controls recruitment of Crb2 to sites of DNA damage. *Cell* **119**, 603-614.

Sartori A. A., Lukas C., Coates J., Mistrik M., Fu S., Bartek J., Baer R., Lukas J. & Jackson S. P. **(2007)** Human CtIP promotes DNA end resection. *Nature* **22**, 509-514.

Savitsky K., Bar-Shira A., Gilad S., Rotman G., Ziv Y., Vanagaite L., Tagle D. A., Smith S., Uziel T., Sfez S., Ashkenazi M., Pecker I., Fryman M., Harnik R., Patanjali S. R., Simmons A., Clines G. A., Sartiel A., Gatti R. A., Chessa L., Sanal O., Lavin M. F., Jaspers N. G. J., Taylor A. M. R., Arlett C. F., Miki T., Weissman S. M., Lovett M., Collins F. S., Shiloh Y. **(1995a)** A single ataxia-telangiectasia gene with a product similar to Pl-3 kinase. *Science* **268**, 1749–1753.

Savitsky K., Sfez S., Tagle D. A., Ziv Y., Sartiel A., Collins F. S., Shiloh Y. & Rotman G. **(1995b)** The complete sequence of the coding region of the *ATM* gene reveals similarity to cell cycle regulators in different species. *Hum. Mol. Genet.* **4**, 2025–2032.

Schaeper U., Boyd J. M., Verma S., Uhlmann E., Subramanian T. & Chinnadurai G. **(1995)** Molecular cloning and characterization of a cellular phosphoprotein that interacts with a conserved C terminal domain of adenovirus E1A involved in negative modulation of oncogenic transformation. *Proc. Natl. Acad. Sci. USA* **92**, 10467–10471.

Schaeper U., Subramanian T., Lim L., Boyd J. M. & Chinnadurai G. **(1998)** Interaction between a cellular protein that binds to the C-terminal region of adenovirus E1A (CtBP) and a novel cellular protein is distrupted by E1A through a conserved PLDLS motif. *J. Biol. Chem.* **273**, 8549–8552.

Scully R., Anderson S. F., Chao D. M., Wei W., Ye L., Young R. A. & Livingston D. M. **(1997a)** BRCA1 is a component of the RNA polymerase II holoenzyme. *Proc. Nat. Acad. Sci. U.S.A.* **94**, 5605–5610.

Scully R., Chen J., Plug A., Xiao Y., Weaver D., Feunteun J., Ashley T., Livingston D. M. **(1997b)** Association of BRCA1 with Rad51 in mitotic and meiotic cells. *Cell* **88**, 265-275.

Seckel H. P. G. **(1960)** Bird-headed Dwarfs: Studies in Developmental Anthropology Including Human Proportions. Springfield, IL, Charles C Thomas.

Seki M, Miyazawa H, Tada S, Yanagisawa J, Yamaoka T, Hoshino S, Ozawa K, Eki T, Nogami M, Okumura K, Taguchi H, Hanaoka F & Enomoto T. **(1994)** Molecular cloning of cDNA encoding human DNA helicase Q1 which has homology to Escherichia coli Rec Q helicase and localization of the gene at chromosome 12p12. *Nucleic Acids Res*. **22**, 4566- 4573.

Sengupta S., Linke S. P., Pedeux R., Yang Q., Farnsworth J., Garfield S. H., Valerie K., Shay J. W., Ellis N. A., Wasylyk B. & Harris C. C. **(2003)** BLM helicase-dependent transport of p53 to sites of stalled DNA replication forks modulates homologous recombination. *EMBO J.* **22**, 1210–1222.

Sengupta S., Robles A. I., Linke S. P., Sinogeeva N. I., Zhang R., Pedeux R., Ward I. M., Celeste A., Nussenzweig A., Chen J., Halazonetis T. D. & Harris C. C. **(2004)** Functional interaction between BLM helicase and 53BP1 in a Chk1-mediated pathway during S-phase arrest. *J. Cell Biol.* **166**, 801–813.

Shao G., Lilli D. R., Patterson-Fortin J., Coleman K. A., Morrissey D. E. & Greenberg R. A. **(2009a)** The Rap80-BRCC36 de-ubiquitinating enzyme complex antagonizes RNF8-Ubc13-dependent ubiquitination events at DNA double strand breaks. *Proc. Natl. Acad. Sci. USA.* **106**, 3166–3171.

Shao G., Patterson-Fortin J., Messick T. E., Feng D., Shanbhag N., Wang Y. & Greenberg R. A. **(2009b)** MERIT40 controls BRCA1-Rap80 complex integrity and recruitment to DNA double-strand breaks. *Genes Dev.* **23**, 740–754.

Sharan S. K., Morimatsu M., Albrecht U., Lim D. S., Regel E., Dinh C., Sands A., Eichele G., Hasty P. & Bradley A. **(1997)** Embryonic lethality and radiation hypersensitivity mediated by Rad51 in mice lacking Brca2. *Nature* **386**, 804-810.

Shechter D., Costanzo V. & Gautier J. **(2004)** Regulation of DNA replication by ATR: signaling in response to DNA intermediates. *DNA Repair* **3**, 901–908.
Sherr C. J. **(1996)** Cancer cell cycles. *Science* **274**, 1672–1677.

Sherr C. J. & McCormick F. **(2002)** The Rb and p53 pathways in cancer. *Cancer Cell* **2**, 103–112.

Shiloh Y. **(1997)** Ataxia-telangiectasia and the Nijmegen breakage syndrome: related disorders but genes apart. *Annu. Rev. Genet.* **31**, 635–662

Shiloh Y. **(2003)** ATM and related protein kinases: safeguarding genome integrity. *Nat. Rev. Cancer.* **3**, 155–168.

Shinohara A. & Ogawa T. **(1998)** Stimulation by Rad52 of yeast Rad51-mediated recombination. *Nature* **391**, 404-407.

Shinohara A., Shinohara M., Ohta T., Matsuda S. & Ogawa T. **(1998)** Rad52 forms ring structures and co-operates with RPA in single-strand DNA annealing. *Genes Cells* **3**, 145-156.

Schultz L. B., Chehab N. H., Malikzay A. & Halazonetis T. D. **(2000)** p53 binding protein 1 (53BP1) is an early participant in the cellular response to DNA double-strand breaks. *J. Cell Biol.* **151**, 1381-1390.

Shull E. R., Lee Y., Nakane H., Stracker T. H., Zhao J., Russell H. R., Petrini J. H. & McKinnon P. J. **(2009)** Differential DNA damage signaling accounts for distinct neural apoptotic responses in ATLD and NBS. *Genes Dev.* **23**, 171-180.

Siliciano J. D., Canman C. E., Taya Y., Sakaguchi K., Appella E. & Kastan M. B. **(1997)** DNA damage induces phosphorylation of the amino terminus of p53 *Gen. & Dev.* **11**, 3471–3481.

Sobhian B., Shao G., Lilli D. R., Culhane A. C., Moreau L. A., Xia B., Livingston D. M. & Greenberg R. A. **(2007)** RAP80 targets BRCA1 to specific ubiquitin structures at DNA damage sites. *Science.* **316**, 1198–1202.

Sobol R. W., Prasad R., Evenski A., Baker A., Yang X. P., Horton J. K. & Wilson S. H. **(2000)** The lyase activity of the DNA repair protein beta-polymerase protects from DNA-damage-induced cytotoxicity. *Nature* **405**, 807–810.

Stewart G. S., Maser R. S., Stankovic T., Bressan D. A., Kaplan M. I., Jaspers N. G., Raams A., Byrd P. J., Petrini J. H. & Taylor A. M. **(1999)** The DNA double-strand break repair gene hMRE11 is mutated in individuals with an ataxia-telangiectasia-like disorder. *Cell* **99**, 577-587.

Stewart G. S., Panier S., Townsend K., Al-Hakim A. K., Kolas N. K., Miller E. S., Nakada S., Ylanko J., Olivarius S., Mendez M., Oldreive C., Wildenhain J., Tagliaferro A., Pelletier L., Taubenheim N., Durandy A., Byrd P. J., Stankovic T., Taylor A. M. & Durocher D. **(2009)** The RIDDLE syndrome protein mediates a ubiquitin-dependent signaling cascade at sites of DNA damage. *Cell* **136**, 420-434.

Stewart G. S., Wang B., Bignell C. R., Taylor A. M. R. & Elledge S. J. **(2003)** MDC1 is a mediator of the mammalian DNA damage checkpoint. *Nature* **421**, 961–966.

Stiff T., Cerosaletti K., Concannon P., O'Driscoll M. & Jeggo P. A. **(2008)** Replication independent ATR signalling leads to G2/M arrest requiring Nbs1, 53BP1 and MDC1. *Hum. Mol. Gen.* **17**, 3247–3253.

Stiff T., Reis C., Alderton G. K., Woodbine L., O'Driscoll M. & Jeggo P. A. **(2005)** Nbs1 is required for ATR-dependent phosphorylation events. *EMBO J.* **24**, 199–208.

Stiff T., Walker S. A., Cerosaletti K., Goodarzi A. A., Petermann E., Concannon P., O'Driscoll M. & Jeggo P. A. **(2006)** ATR-dependent phosphorylation and activation of ATM in response to UV treatment or replication fork stalling. *EMBO J.* **25**, 5775-5782.

St Onge R. P., Besley B. D., Pelley J. L. & Davey S. **(2003)** A role for the phosphorylation of hRad9 in checkpoint signaling. *J. Biol. Chem.* **278**, 26620–26628.

Stryer L. **(1995)** *Biochemistry* PWN, Warszawa 2000, Fourth Polish edition, 258-259.

Stucki M., Clapperton J. A., Mohammad D., Yaffe M. B., Smerdon S. J. & Jackson S. P. **(2005)** MDC1 directly binds phosphorylated histone H2AX to regulate cellular responses to DNA double-strand breaks. *Cell* **123**, 1213-1226.

Stucki M. & Jackson S. P. **(2004)** MDC1/NFBD1: A key regulator of the DNA damage response in higher eukaryotes. *DNA Repair* **3**, 953–957.

Stucki M. & Jackson S. P. **(2006)** γ-H2AX and MDC1: anchoring the DNA-damage-response machinery to broken chromosomes. *DNA Repair* **5**, 534-543.

Sun Y., Xu Y., Roy K., & Price B. D. **(2007)** DNA Damage-Induced Acetylation of Lysine 3016 of ATM Activates ATM Kinase Activity. *Mol. Cell. Biol.* **27**, 8502–8509.

Sung P., Krejci L., Van Komen S. & Sehorn M. G. **(2003)** Rad51 recombinase and recombination mediators. *J. Biol. Chem.* **278**, 42729–42732.

Syllaba, K. & Henner, K. **(1926)** Contribution a l'independencede l'athetose double idiopathique et congenitale. Atteinte familiale, syndrome dystrophique, signe de reseau vasculaire conjonctival, integrite psychique. *Rev. Neurol.* **1**, 541–562 (in French).

Symington L. S. **(2002)** Role of RAD52 epistasis group genes in homologous recombination and double-strand break repair. *Microbiol. Mol. Biol. Rev.* **66**, 630-670.

Takashima H., Boerkoel C. F., John J., Saifi G. M., Salih M. A., Armstrong D., Mao Y., Quiocho F. A., Roa B. B., Nakagawa M., Stockton D. W. & Lupski J. R. **(2002)** Mutation of TDP1, encoding a topoisomerase I-dependent DNA damage repair enzyme, in spinocerebellar ataxia with axonal neuropathy. *Nature Genet.* **32**, 267–272.

Taniguchi T., Garcia-Higuera I., Xu B., Andreassen P. R., Gregory R. C., Kim S. T., Lane W. S., Kastan M. B. & D'Andrea A. D. **(2002)** Convergence of the fanconi anemia and ataxia telangiectasia signaling pathways. *Cell* **109**, 459-472.

Tarsounas M., Davies D. & West S. C. **(2003)** BRCA2-dependent and independent formation of RAD51 nuclear foci. *Oncogene* **22**, 1115-1123.

Tauchi H., Kobayashi J., Morishima K., van Gent D., Shiraishi T., Verkaik N. S., van Heems D., Ito E., Nakamura A., Sonoda E., Takata M., Takeda S., Matsuura S. & Komatsu K. **(2002)** Nbs1 is essential for DNA repair by homologous recombination in higher vertebrate cells. *Nature* **420**, 93–98.

Tavtigian S. V. ., Simard J., Rommens J., Couch F., Shattuck-Eidens D., Neuhausen S., Merajver S., Thorlacius S., Offit K., Stoppa-Lyonnet D., Belanger C., Bell R., Berry S., Bogden R., Chen Q., Davis T., Dumont M., Frye C., Hattier T., Jammulapati S., Janecki T., Jiang P., Kehrer R., Leblanc J. F., Mitchell J. T., McArthur-Morrison J., Nguyen K., Peng Y., Samson C., Schroeder M., Snyder S. C., Steele L., Stringfellow M., Stroup C., Swedlund B., Swense J., Teng D., Thomas A., Tran T., Tranchant M., Weaver-Feldhaus J., Wong A. K., Shizuya H., Eyfjord J. E., Cannon-Albright L., Tranchant M., Labrie F., Skolnick M. H., Weber B., Kamb A., Goldgar D. E. **(1996)** The complete BRCA2 gene and mutations in chromosome 13q-linked kindreds. *Nat. Genet.* **12**, 333-337

Taya Y. **(1997)** RB kinases and RB binding proteins: New points of view. *Trends Biochem. Sci.* **22**, 14–17.

Taylor A. M. R. & Byrd P. J. **(2005)** Molecular pathology of ataxia telangiectasia. *J. Clin. Pathol.* **58**, 1009–1015.

Taylor A. M, Groom A. & Byrd P. J. **(2004)** Ataxia-telangiectasia-like disorder (ATLD)-its clinical presentation and molecular basis. *DNA Rep.* **3**, 1219-1225.

Temporini C., Calleri E., Massolini G. & Caccialanza G. **(2008)** Integrated analytical strategies for the study of phosphorylation and glycosylation in proteins. *Mass Spectrom. Rev.* **27**, 207-236.

Tercero J. A. & Diffley J. F. **(2001)** Regulation of DNA replication fork progression through damaged DNA by the Mec1/Rad53 checkpoint. *Nature* **412**, 553–557.

Tibbetts R. S., Brumbaugh K. M., Williams J. M., Sarkaria J. N., Cliby W. A., Shieh S. Y., Taya Y., Prives C. & Abraham R. T. **(1999)** A role for ATR in the DNA damage-induced phosphorylation of p53. *Genes Dev.* **13**, 153-157.

Tibbetts R. S., Cortez D., Brumbaugh K. M., Scully R., Livingston D., Elledge S. J. & Abraham R. T. **(2000)** Functional interactions between BRCA1 and the checkpoint kinase ATR during genotoxic stress. *Genes Dev.* **14**, 2989–3002.

Thompson M. E., Jensen R. A., Obermiller P. S., Page D. L., Holt J. T. **(1995)** Decreased expression of *BRCA1* accelerates growth and is often present during sporadic breast progression. *Nat. Genet.* **9**, 444–450.

Tripathi V., Nagarjuna T. & Sengupta S. **(2007)** BLM helicase–dependent and –independent roles of 53BP1 during replication stress–mediated homologous recombination. *J. Cell Biol.* **178**, 9-14.

Trujillo K. M., Roh D. H., Chen L., Van Komen S., Tomkinson A. & Sung P. **(2003)** Yeast xrs2 binds DNA and helps target rad50 and mre11 to DNA ends. *J. Biol. Chem.* **278**, 48957–48964.

Trujillo K. M., Yuan S. S., Lee E. Y. & Sung P. **(1998)** Nuclease activities in a complex of human recombination and DNA repair factors Rad50, Mre11, and p95. *J. Biol. Chem.* **273**, 21447–21450.

Tsuzuki T., Fujii Y., Sakumi K., Tominaga Y., Nakao K., Sekiguchi M., Matsushiro A., Yoshimura Y. & MoritaT. **(1996)** Targeted disruption of the Rad51 gene leads to lethality in embryonic mice. *Proc. Natl. Acad. Sci. U. S. A.* **93**, 6236-6240.

Turrene G. A., Paul P., Laflair L. & Price B. D. **(2001)** Activation of p53 transcriptional activity requires ATM's kinase domain and multiple N-terminal serine residues of p53, *Oncogene* **20**, 5100–5110.

Uziel T., Savitsky K., Platzer M., Ziv Y., Helbitz T., Nehls M., Boehm T., Rosental A., Shiloh Y. & Rotman G. **(1996)** Genomic Organization of the ATM Gene. *Genomics* **2**, 317–320.

van Attikum H. & Gasser S. M. **(2005)** The histone code at DNA breaks: a guide to repair? *Nat. Rev. Mol. Cell Biol.* **6**, 757–765.

van der Burgt I., Chrzanowska K. H., Smeets D. & Weemaes C. **(1996)** Nijmegen breakage syndrome. *J. Med. Genet.* **33**, 153-156.

van Komen S., Petukhova G., Sigurdsson S. & Sung P. **(2002)** Functional cross-talk among Rad51, Rad54, and replication protein A in heteroduplex DNA joint formation. *J. Biol. Chem.* **277**, 43578–43587.

van Vugt M. A., Bràs A. & Medema R. H. **(2005)** Restarting the Cell Cycle When the Checkpoint Comes to a Halt. *Cancer Res.* **65**, 7037-7040.

Varon R., Vissinga C., Platzer M., Cerosaletti K. M., Chrzanowska K. H., Saar K., Beckmann G., Seemanová E., Cooper P. R., Nowak N. J., Stumm M., Weemaes C. M., Gatti R. A., Wilson R. K., Digweed M., Rosenthal A., Sperling K., Concannon P. & Reis A. **(1998)** Nibrin, a novel DNA double-strand break repair protein, is mutated in Nijmegen breakage syndrome. *Cell* **93**, 467-476.

Venkitaraman A. R. **(2002)** Cancer Susceptibility and the Functions of BRCA1 and BRCA2. *Cell* **108**, 171–182.

Vilkki S., Launonen V., Karhu A., Sistonen P., Vastrik I. & Aaltonen L. A. **(2002)** Screening for microsatellite instability target genes in colorectal cancers. *J. Med. Genet.* **39**, 785–789.

Waltes R., Kalb R., Gatei M., Kijas A. W., Stumm M., Sobeck A., Wieland B., Varon R., Lerenthal Y., Lavin M. F., Schindler D. & Dörk T. **(2009)** Human RAD50 deficiency in a

Nijmegen breakage syndrome-like disorder. *Am J Hum Genet.* **84**, 605-616.

Wang B., Hurov K., Hofmann K. & Elledge S. J. **(2009)** NBA1, a new player In the Brca1 A complex, is required for DNA damage resistance and checkpoint control. *Genes Dev.* **23**, 729–739.

Wang B., Matsuoka S., Carpenter P. B. & Elledge S. J. **(2002)** 53BP1, a mediator of the DNA damage checkpoint. *Science* **298**, 1435–1438.
Wang M., Wu W., Wu W., Rosidi B., Zhang L., Wang H. & Iliakis G. **(2006a)** PARP-1 and Ku compete for repair of DNA double strand breaks by distinct NHEJ pathways. *Nucleic Acids Res.* **34**, 6170–6182

Wang X. W., Tseng A., Ellis N. A., Spillare E. A., Linke S. P., Robles A. I., Seker H., Yang Q., Hu P., Beresten S., Bemmels N. A, Garfield S. & Harris C. C. **(2001)** Functional interaction of p53 and BLM DNA helicase in apoptosis. *J. Biol. Chem.* **276**, 32948–32955.

Wang X., Zou L., Lu T., Bao S., Hurov K. E., Hittelman W. N., Elledge S. J. & Li L. **(2006b)** Rad17 phosphorylation is required for claspin recruitment and Chk1 activation in response to replication stress. *Mol. Cell* **23**, 331-341.

Wang Y., Cortez D., Yazdi P., Neff N., Elledge S. J. & Qin J. **(2000)** BASC, a super complex of BRCA1-associated proteins involved in the recognition and repair of aberrant DNA structures. *Genes Dev.* **14**, 927–939.

Ward I. M., Minn K., Jorda K. G. & Chen J. **(2003)** Accumulation of checkpoint protein 53BP1 at DNA breaks involves its binding to phosphorylated histone H2AX. *J. Biol. Chem.* **278**, 19579-19582.

Ward I. M., Reina-San-Martin B., Olaru A., Minn K., Tamada K., Lau J. S., Cascalho M., Chen L., Nussenzweig A., Livak F., Nussenzweig M. C. & Chen J. **(2004)** 53BP1 is required for class switch recombination. *J. Cell Biol.* **165**, 459-464.

Watters D., Kedar P., Spring K., Bjorkman J., Chen P., Gatei M., Birrell G., Garrone B., Srinivasa P., Crane D. I. & Lavin M. F. **(1999)** Localization of a Portion of Extranuclear ATM to Peroxisomes. *J. Biol. Chem.* **274**, 34277-34282.

Weemaes C. M., Hustinx T. W., Scheres J. M., van Munster P. J., Bakkeren J. A. & Taalman R. D. **(1981)** A new chromosomal instability disorder: the Nijmegen breakage syndrome. *Acta Paediatr. Scand.* **70**, 557-564.

Weinberg R. A. **(1995)** The retinoblastoma protein and cell cycle control. *Cell* **81**, 323–330.
Weinberg R. A. **(2006)** The Biology of Cancer. *Garland Science*.

West S. C. **(2003)** Molecular views of recombination proteins and their control. *Mol. Cell Biol*. **4**, 1-11.

Whitehouse C. J., Taylor R. M., Thistlethwaite A., Zhang H., Karimi-Busheri F., Lasko D. D., Weinfeld M. & Caldecott K. W. **(2001)** XRCC1 stimulates human polynucleotide kinase activity at damaged DNA termini and accelerates DNA single-strand break repair. *Cell* **104**, 107–117.

Williams R. S., Williams J. S. & Tainer J. A. **(2007)** Mre11-Rad50-Nbs1 is a keystone complex connecting DNA repair machinery, double-strand break signaling, and the chromatin template. *Biochem. Cell Biol.* **85**, 509-520.

Winters T. A., Henner W. D., Russell P. S., McCullough A. & Jorgensen T. J. **(1994)** Removal of 3'-phosphoglycolate from DNA strand-break damage in an oligonucleotide substrate by recombinant human apurinic/apyrimidinic endonuclease 1. *Nucleic Acids Res.* **22**, 1866–1873.

Wold M. S. **(1997)** Replication protein A: a heterotrimeric, singlestranded DNA-binding protein required for eukaryotic DNA metabolism. *Annu. Rev. Biochem.* **66**, 61-92.

Wong A. K., Ormonde P. A., Pero R., Chen Y., Lian L., Salada G., Berry S., Lawrence Q., Dayananth P., Ha P., Tavtigian S. V., Teng D. H. & Bartel P. L. **(1998)** Characterization of a carboxy-terminal BRCA1 interacting protein. *Oncogene* **17,** 2279–2285.

Wong A. K. C., Pero R., Ormonde P. A., Tavtigian S. V. & Bartel P. L. **(1997)** RAD51 interacts with the evolutionarily conserved BRC motifs in the human breast cancer susceptibility gene brca2. *J. Biol. Chem.* **272**, 31941–31944.

Wong J. M, Ionescu D. & Ingles C. J. **(2003)** Interaction between BRCA2 and replication protein A is compromised by a cancer-predisposing mutation in BRCA2. *Oncogene* **22**, 28-33.

Wooster R., Bignell G., Lancaster J., Swift S., Seal S., Mangion J., Collins N., Gregory S., Gumbs C. & Micklem G. **(1995)** Identification of the breast cancer susceptibility gene BRCA2. *Nature* **378**, 789-792, (Erratum in: 1996, *Nature* **379**, 749).

Wooster R., Neuhausen S. L., Mangion J., Quirk Y., Ford D., Collins N., Nguyen K., Seal S., Tran T., Averill D., Fields P., Marshall G., Narod S., Lenoir G. M., Lynch H., Feunteun J., Devilee P., Cornelisse C. J., Menko F. H., Daly P. A., Ormiston W., McManus R., Pye C., Lewis C. M., Cannon-Albright L. A., Peto J., Ponder B. A. J., Skolnick M. H., Easton D. F., Goldgar D. E. & Stratton M. R. **(1994)** Localization of a breast cancer susceptibility gene, BRCA2, to chromosome 13q12-13. *Science* **265**, 2088-2090.

Wright R. H., Dornan E. S., Donaldson M. M. & Morgan I. M. **(2006)** TopBP1 contains a transcriptional activation domain suppressed by two adjacent BRCT domains. *Biochem. J.* **400**, 573-582.

Wu G. & Lee W. H. **(2006)** CtIP a multivalent adaptor connecting transcriptional regulation, checkpoint control and tumor suppression. *Cell Cycle* **5**, 1592-1596.

Wu L., Davies S. L., Levitt N. C. & Hickson I. D. **(2001)** Potential role for the BLM helicase in recombinational repair via a conserved interaction with RAD51. *J. Biol. Chem.* **276**, 19375–19381.

Wu L., Davies S. L., North P. S., Goulaouic H., Riou J. F., Turley H., Gatter K. C. & Hickson I. D. **(2000a)** The Bloom's syndrome gene product interacts with topoisomerase III. *J. Biol. Chem.* **275**, 9636-9644.

Wu L., Luo K., Lou Z. & Chen J. **(2008)** MDC1 regulates intra-S-phase checkpoint by targeting NBS1 to DNA double-strand breaks. *Proc. Natl. Acad. Sci. U. S. A.* **105**, 11200-11205.

Wu L. C., Wang Z. W., Tsan J. T., Spillman M. A., Phung A., Xu X. L., Yang M. C., Hwang L. Y., Bowcock A. M. & Baer R. **(1996)** Identification of a RING protein that can interact in vivo with the BRCA1 gene product. *Nat. Genet.* **14**, 430–440.

Wu M., Soler D. R., Abba M. C., Nunez M. I., Baer R., Hatzis C., Llombart-Cussac A., Llombart-Bosch A. & Aldaz C. M. **(2007)** CtIP silencing as a novel mechanism of tamoxifen resistance in breast cancer. *Mol. Cancer Res.* **5**, 1285-1295.

Wu X., Ranganathan V., Weisman D. S., Heine W. F., Ciccone D. N., O'Neill T. B., Crick K. E., Pierce K. A., Lane W. S., Rathbun G., Livingston D. M. & Weaver D. T. **(2000b)** ATM phosphorylation of Nijmegen breakage syndrome protein is required in a DNA damage response. *Nature* **405**, 477-482.

Wu-Baer F. & Baer R. **(2001)** Effect of DNA damage on a BRCA1 complex. *Nature* **414**, 36.

Wu-Baer F., Lagrazon K., Yuan W. & Baer R. **(2003)** The BRCA1/BARD1 heterodimer assembles polyubiquitin chains through an unconventional linkage involving lysine residue K6 of ubiquitin. *J. Biol. Chem.* **278**, 34743–34746.

Xiao Y.& Weaver D. T. **(1997)** Conditional gene targeted deletion by Cre recombinase demonstrates the requirement for the double-strand break repair Mre11 protein in murine embryonic stem cells. *Nucleic Acids Res.* **25**, 2985–2991.

Xie A., Hartlerode A., Stucki M., Odate S., Puget N., Kwok A., Nagaraju G., Yan C., Alt F. W., Chen J., Jackson S. P. & Scully R. **(2007)** Distinct roles of chromatin-associated proteins MDC1 and 53BP1 in mammalian double-strand break repair. *Mol. Cell.* **28**, 1045-1057.

Xu B., Kim S. & Kastan M. B. **(2001)** Involvement of Brca1 in S-phase and G(2)-phase checkpoints after ionizing irradiation. *Mol. Cell. Biol.* **21**, 3445–3450.

Xu X. & Stern D. F. **(2003)** NFBD1/MDC1 regulates ionizing radiation induced focus formation by DNA checkpoint signaling and repair factors. *FASEB J.* **17**, 1842–1848.

Yamane K., Chen J. & Kinsella T. J. **(2003)** Both DNA Topoisomerase II-binding Protein 1 and BRCA1 Regulate the G2-M Cell Cycle Checkpoint. *Cancer Res.* **63**, 3049–3053.

Yang D. Q. & Kastan M. B. **(2000)** Participation of ATM in insulin signalling through phosphorylation of eIF-4E-binding protein 1. *Nat. Cell. Biol.* **2**, 893-898.

Yang H., Jeffrey P. D., Miller J., Kinnucan E., Sun Y., Thoma N. H., Zheng N., Chen P. L., Lee W. H. & Pavletich N. P. **(2002)** BRCA2 Function in DNA Binding and Recombination from a BRCA2-DSS1-ssDNA Structure. *Science* **297**, 1837-1848.

Yang S. W. Burgin A. B. Jr, Huizenga B. N., Robertson C. A., Yao K. C. & Nash H. A. **(1996)** A eukaryotic enzyme that can disjoin dead-end covalent complexes between DNA and type I topoisomerases. *Proc. Natl. Acad. Sci. USA* **93**, 11534–11539.

Yang X. & Lippman M. E. **(1999)** *BRCA1* and *BRCA2* in breast cancer. *Breast Can. Res. Treat.* **54**, 1–10.
Yarbro J. W. **(1992)** Mechanism of action of hydroxyurea. *Semin. Oncol.* **19**, (3 Suppl. 9) 1–10

Yazdi P. T., Wang Y., Zhao S., Patel N., Lee E. Y. & Qin J. **(2002)** SMC1 is a downstream effector in the ATM/NBS1 branch of the human S-phase checkpoint. *Genes Dev.* **16**, 571-582.

Yoo E., Kim B. U., Lee S. Y., Cho C. H., Chung J. H. & Lee C. H. **(2005)** 53BP1 is associated with replication protein A and is required for RPA2 hyperphosphorylation following DNA damage. *Oncogene* **24**, 5423-5430.

Yoo H. Y., Kumagai A., Shevchenko A., Shevchenko A. & Dunphy W. G. **(2007)** Ataxia-telangiectasia mutated (ATM)-dependent activation of ATR occurs through phosphorylation of TopBP1 by ATM. *J. Biol. Chem.* **282**, 17501-17506.

You Z., Chahwan C., Bailis J., Hunter T. & Russell P. **(2005)** ATM Activation and Its Recruitment to Damaged DNA Require Binding to the C Terminus of Nbs1. *Mol. Cell. Biol.* **25**, 5363- 5379.

Yu C.-E., Oshima J., Fu Y.-H., Wijsman E. M., Hisama F., Alisch R., Matthews S., Nakura J., Miki T., Ouais S, Martin G. M., Mulligan J. & Schellenberg G. D. **(1996)** Positional cloning of the Werner's syndrome gene. *Science* **272**, 258- 262.

Yu X. & Chen J. **(2004)** DNA damage-induced cell cycle checkpoint control requires CtIP, a phosphorylation-dependent binding partner of BRCA1 C-terminal domains. *Mol. Cell. Biol.* **24**, 9478– 9486.

Yu X., Chini C. C., He M., Mer G. & Chen J. **(2003)** The BRCT domain is a phospho-protein binding domain. *Science* **302**, 639-642.

Yu X., Fu S., Lai M., Baer R. & Chen J. **(2006)** BRCA1 ubiquitinates its phosphorylation-dependent binding partner CtIP. *Genes Dev.* **20**, 1721–1726.

Yu X., Wu L. C., Bowcock A. M., Aronheim A. & Baer R. **(1998)** The C-terminal (BRCT) domains of BRCA1 interact in vivo with CtIP, a protein implicated in the CtBP pathway of transcriptional repression. *J. Biol. Chem.* **273**, 25388–25392.

Yuan J. & Chen J. **(2009)** MRE11/RAD50/NBS1 complex dictates DNA repair independent of H2AX. *J. Biol. Chem.* [Nov 12. - Epub ahead of print].

Yun M. H. & Hiom K. **(2009)** CtIP-BRCA1 modulates the choice of DNA doublestrand-break repair pathway throughout the cell cycle. *Nature* **459**, 460-464.

Zahradka P. & Ebisuzaki K. **(1982)** A shuttle mechanism for DNA–protein interactions. The regulation of poly(ADP-ribose) polymerase. *Eur. J. Biochem.* **127**, 579–585.

Zernik-Kobak M., Vasunia K., Connelly M., Anderson C. W. & Dixon K. **(1997)** Sites of UV-induced phosphorylation of the p34 subunit of replication protein A from HeLa cells. *J. Biol. Chem.* **272**, 23896–23904.

Zhang H. B., Somasundaram K., Peng Y., Tian H., Zhang H. X., Bi D. Weber B. L. & El-Deiry W. S. **(1998)** BRCA1 physically associates with p53 and stimulates its transcriptional activity. *Oncogene* **16**, 1713–1721.

Zhang J., Ma Z., Treszezamsky A. & Powell S. N. **(2005)** MDC1 interacts with Rad51 and facilitates homologous recombination. *Nat. Struct. Mol. Biol.* **12**, 902–909.

Zhang Y., Zhou J. & Lim C. U. **(2006)** The role of NBS1 in DNA double strand break repair, telomere stability, and cell cycle checkpoint control *Cell Res.* **16**, 45-54.

Zhao S., Weng Y. C., Yuan S. S., Lin Y. T., Hsu H C., Lin S. C., Gerbino E., Song M. H., Zdzienicka M. Z., Gatti R. A., Shay J. W., Ziv Y., Shiloh Y. & Lee E. Y. **(2000)** Functional link between ataxia-telangiectasia and Nijmegen breakage syndrome gene products. *Nature* **405**, 473-477.

Zhong Q., Chen C. F., Chen P. L., & Lee W. H. **(2002)** BRCA1 facilitates microhomology-mediated end joining of DNA double strand breaks. *J. Biol. Chem.* **277,** 28641–28647

Zhong Q., Chen C. F., Li S., Chen Y., Wang C. C., Xiao J., Chen P. L., Sharp Z. D. & Lee W. H. **(1999)** Association of BRCA1 with the hRad50-hMre11-p95 complex and the DNA damage response. *Science* **285**, 747-750.

Zhou B. B. & Elledge S. J. **(2000)** The DNA damage response: putting checkpoints in perspective. *Nature* **408**, 433–439.

Zhu J., Petersen S., Tessarollo L. & Nussenzweig A. **(2001)** Targeted disruption of the Nijmegen breakage syndrome gene *NBS1* leads to early embryonic lethality in mice. *Curr. Biol.* **11**, 105–109.

Ziv Y., Bielopolski D., Galanty Y., Lukas C., Taya Y., Schultz D. C., Lukas J., Bekker-Jensen S., Bartek J. & Shiloh Y. **(2006)** Chromatin relaxation in response to DNA double-strand breaks is modulated by a novel ATM- and KAP-1 dependent pathway. *Nat. Cell Biol*. **8**, 870-876.

Zou L., Cortez D. & Elledge S. J. **(2002)** Regulation of ATR substrate selection by Rad17-dependent loading of Rad9 complexes onto chromatin. *Genes. Dev.* **16**, 198–208.

Zou L. & Elledge S. J. **(2003)** Sensing DNA damage through ATRIP recognition of RPA-ssDNA complexes. *Science* **300**, 1542-1548.

Zou L., Liu D. & Elledge S. J. **(2003)** Replication protein A-mediated recruitment and activation of Rad17 complexes. *Proc. Natl. Acad. Sci. U. S. A.* **100**, 13827–13832.

Zou Y., Liu Y., Wu X. & Shell S. M. **(2006)** Functions of human replication protein A (RPA): from DNA replication to DNA damage and stress responses. *J. Cell. Physiol.* **208**, 267-273.